UNIVERSITY OF BELGRADE,
FACULTY OF BIOLOGY

UNIVERSITY OF CLERMONT AUVERGNE,
DOCTORAL SCHOOL OF BIOLOGICAL SCIENCE,
HEALTH, AGRICULTURE AND ENVIRONMENT

Irena S. Krga

EFFECTS OF ANTHOCYANINS AND THEIR METABOLITES ON THE FUNCTION OF HUMAN ENDOTHELIAL CELLS AND PLATELETS *in vitro*

Doctoral Dissertation

Belgrade, 2018

UNIVERZITET U BEOGRADU,
BIOLOŠKI FAKULTET

UNIVERZITET KLERMON OVERNJA,
DOKTORSKA ŠKOLA BIOLOŠKIH NAUKA,
ZDRAVSTAVA, POLJOPRIVREDE I ŽIVOTNE SREDINE

Irena S. Krga

UTICAJ ANTOCIJANA I NJIHOVIH METABOLITA NA FUNKCIJU ENDOTELNIH ĆELIJA I TROMBOCITA ČOVEKA *in vitro*

Doktorska Disertacija

Beograd, 2018

Université Clermont Auvergne
ECOLE DOCTORALE DES SCIENCES DE LA VIE, SANTE, AGRONOMIE, ENVIRONNEMENT

Université de Belgrade
FACULTE DE BIOLOGIE

Thèse

Présentée à l'Université de Belgrade pour l'obtention du grade de

DOCTEUR d'UNIVERSITE, Spécialité : Nutrition (Biologie Santé) à l'Université Clermont Auvergne
DOCTEUR ES SCIENCES, sciences biologiques, à l'Université de Belgrade

en 2018 par

Irena S. KRGA

RÔLE DES ANTHOCYANES ET CES METABOLITES SUR LA FONCTION DES CELLULES ENDOTHELIALES ET PLAQUETTES HUMAINE *in vitro*

Rapporteurs :
Pr Claude Beaudoin, Université Clermont Auvergne, France
Dr Sophie Layé, INRA**,** UMR 1286, Université de Bordeaux, France
Pr Ljuba Mandić, Faculté de chimie, Université de Belgrade, Serbie
Dr Tanja Jevđović, Faculté de Biologie, Université de Belgrade, Serbie

Membres :
Dr Dragan Milenkovic, INRA, UMR 1019, Université Clermont Auvergne, France
Dr Marija Glibetić, Institut de Recherche médicale, Université de Belgrade, Serbie

THESIS DEFENCE COMMITTEE MEMBERS

Dr Marija Glibetić, Principal Research Fellow, PhD co-supervisor
Centre of Research Excellence in Nutrition and Metabolism, Institute for Medical Research, University of Belgrade, Belgrade, Serbia

Dr Dragan Milenkovic, Senior Research Scientist, PhD co-supervisor,
National Institute for Agricultural Research, Human Nutrition Unit, University Clermont Auvergne, Clermont-Ferrand, France

Dr Ljuba Mandić, Full professor,
Faculty of Chemistry, University of Belgrade, Belgrade, Serbia

Dr Tanja Jevđović, Assistant professor
Faculty of Biology, University of Belgrade, Belgrade, Serbia

Dr Claude Beaudoin, Full professor,
University of Clermont Auvergne, CNRS UMR6293-GReD/INSERM U1103, Clermont-Ferrand, France

Dr Sophie Layé, Research director
University of Bordeaux, National Institute for Agricultural Research, UMR 1286, Nutrition and integrative neurology, Bordeaux, France.

Date of the thesis defence _____

This PhD thesis was prepared under joint international supervision according to the International Agreement on Joint Supervision of Doctoral Thesis (Cotutelle) signed between the University of Belgrade in Serbia and the University of Clermont Auvergne in France. The experiments were conducted in the Centre of Research Excellence in Nutrition and Metabolism of the Institute for Medical Research, the University of Belgrade, Serbia and the National Institute of Agricultural Research in Theix, France.

ACKNOWLEDGMENTS

First and foremost, I would like to express my most profound gratitude to my supervisors, Dr Dragan Milenkovic and Dr Marija Glibetić, without whose commitment, enthusiasm and immense knowledge this doctoral project would not have been possible. I thank you for your patience, support and guidance during all stages of this thesis. It was a privilege to be your student.

My sincere thanks also go to Dr Christine Morand for giving me the opportunity to work in her lab at the INRA institute and for all of her help and advice as well as to Dr Aleksandra Konic Ristic, for her guidance and friendly support during this thesis.

I am also grateful to Dr Nevena Vidović for her assistance in experimental work and data analysis, suggestions and comments during the preparation of thesis manuscript as well as for her encouragements and friendly advice.

I thank my colleagues, Dr Lauren-Emmanuel Monfoulet, Sylvie Mercie, Filip Stojanović, Celine Bobby and Dominique Bayer for sheering their time and knowledge and their invaluable assistance in the experimental work.

I would also like to thank Dr Radu Tamaian from the National Institute for Research and Development for Cryogenic and Isotopic Technologies in Râmnicu Vâlcea, Romania for his guidance and indispensable help with the docking analyses.

My sincere thanks also go to the thesis comity members: Dr Ljuba Mandić, Dr Tanja Jevđović, Dr Claude Beaudoin and Dr Sophie Layé for their time and insightful comments that contributed to the quality of this thesis.

Finally, I express my sincere gratitude to my family and friends for their love, support and continuous encouragement throughout this thesis. I thank my Kristijan for his devotion, understanding and selfless love. You are my rock. Thank you.

EFFECTS OF ANTHOCYANINS AND THEIR METABOLITES ON THE FUNCTION OF HUMAN ENDOTHELIAL CELLS AND PLATELETS *in vitro*

ABSTRACT

Increasing number of scientific evidence suggests the beneficial role of dietary anthocyanins, phytochemicals mainly present in berries and derived products, in cardiovascular health. These anthocyanin health benefits may be attributed to their effect on endothelial cells or platelets that represent the key players in the development of cardiovascular diseases (CVD). However, the exact molecular mechanisms underlying anthocyanin cardioprotective effects are not fully understood. The aim of this thesis was to investigate the effect of anthocyanins and their metabolites *in vitro* on endothelial and platelet function and identify the underlying mechanisms of their action using physiologically relevant conditions.

Results from this thesis showed that the pretreatment of endothelial cells with physiologically relevant concentrations of circulating anthocyanins and their metabolites attenuated monocyte adhesion to activated endothelial cells as well as their transendothelial migration, which are the initial steps in the development of atherosclerosis that precede CVD. In agreement with these results, gene expression analysis revealed that the treatment of endothelial cells with these compounds modulated the expression of genes involved in regulation of cell-cell adhesion, actin cytoskeleton reorganisation, focal adhesion and leukocyte transmigration. Bioinformatics analyses of gene expression data allowed the identification of potential transcription factors involved in the observed nutrigenomic effects and cell signalling proteins regulating their activity. Molecular docking analyses further revealed cell signalling proteins to which these bioactives may bind to and potentially affect their activity and the activation of downstream signalling proteins and transcription factors, effects that were in agreement with the results of Western blot analyses. Anthocyanins and their metabolites also modulated the expression of microRNAs, especially those involved in regulation of endothelial cell permeability, contributing to the observed changes in endothelial cell function.

In addition to their effects on endothelial cells, anthocyanins and their metabolites displayed the capacity to modulate platelet function by decreasing platelet activation and their aggregation with leukocytes, the processes that are important contributors to CVD development.

In conclusion, results from this thesis revealed the positive effects of anthocyanins and their metabolites, at physiologically relevant concentrations, on endothelial and platelet function and provided new insights into the mechanisms underlying their cardioprotective effects.

Keywords: anthocyanins, metabolites, endothelial dysfunction, monocyte-endothelial cell adhesion, monocyte transendothelial migration, platelet activation, platelet-leukocyte aggregation

Scientific field: Biological Sciences
Scientific subfield: Human nutrition
UDC number: [547.62+581.574]:[611.018.74:611.018.52] (043.3)

UTICAJ ANTOCIJANA I NJIHOVIH METABOLITA NA FUNKCIJU ENDOTELNIH ĆELIJA I TROMBOCITA ČOVEKA *in vitro*

SAŽETAK

Kardiovaskularne bolesti predstavljaju oboljenja koja zahvataju srce i krvne sudove i najčešći su uzrok obolevanja i umiranja u svetu. Prema mestu javljanja mogu se podeliti na bolesti srca, cerebrovaskularne bolesti i bolesti perifernih krvnih sudova. Osnovni uzročnik kardiovaskularnih bolesti je ateroskleroza, hronično zapaljensko oboljenje velikih i srednje velikih arterijskih krvnih sudova koje se karakteriše aterosklerotičnim lezijama koje nastaju nakupljanjem lipida, ćelija i proteina vezivnog tkiva unutar zida krvnog suda. Ove patološke promene krvnih sudova ometaju normalan protok krvi, a u kasnijim stadijumima bolesti mogu dovesti i do pucanja plaka i aterotromboze, što za posledicu može imati infarkt miokarda ili šlog. Sam nastanak ateroskleroze povezan je sa poremećenom funkcijom endotela krvnog suda koja podstiče adheziju leukocita za aktivirane endotelne ćelije i njihovu transendotelnu migraciju. Unutar zida krvnog suda monociti se diferenciraju u makrofage, vrše ingestiju oksidovanog LDL holesterola i formiraju penušave ćelije čije nakupljanje vremenom dovodi do formiranja aterosklerotičnih lezija. Važnu ulogu u nastanku ateroskleroze imaju i trombociti. Interakcija aktiviranih trombocita sa leukocitima i endotelnim ćelijama podstiče adheziju leukocita i njihovu transendotelnu migraciju i time dodatno podstiče zapaljenski proces i razvoj ateroskleroze. Stoga, ispitivanje uzajamnog delovanja endotelnih ćelija, leukocita i trombocita predstavlja značajno područje istraživanja u cilju prevencije i kontrole kardiovaskularnih bolesti.

Ishrana ima važnu ulogu, kako u nastanku i razvoju kardiovaskularnih bolest, tako i u njihovoj prevenciji i lečenju. Rezultati brojnih epidemioloških i kliničkih studija pokazuju povoljno delovanje ishrane bogate voćem i povrćem na kardiovaskularno zdravlje. Ovo pozitivno delovanje namirnica biljnog porekla pripisuje se delom njihovom niskom energetskom vrednošću, visokom sadržaju vlakana i esencijalnih mikronutrijenata, ali pre svega nenutritivnim, biološki aktivnim sastojcima, poput

polifenola. Polifenoli predstavljaju najbrojniju i najzastupljeniju grupu sekundarnih metabolita biljaka. Ova strukturno veoma raznolika grupa jedinjenja je široko zastupljena u namirnicama biljnog porekla, poput voća, povrća i žitarica, čineći najznačajniju grupu nenutritivnih sastojaka namirnica. Antocijani predstavljaju podgrupu polifenolnih jedinjenja koja je u ljudskoj ishrani prevashodno zastupljena preko unosa bobičastog voća i proizvoda dobijenih njegovom preradom. Tokom protekle dve decenije ova jedinjenja su se našla u žiži interesovanja i naučne zajednice i javnosti, zbog pokazane veze između ishrane bogate namirnicama sa visokim sadržajem antocijana i raznovrsnih pozitivnih efekata na zdravlje. Sve veći broj naučnih dokaza ukazuje na važnu ulogu antocijana u prevenciji i lečenju kardiovaskularnih bolesti. Rezultati epidemioloških studija pokazali su inverznu korelaciju između dijetarnog unosa antocijana i rizika od hipertenzije, infarkta miokarda ili stope smrtnosti od kardiovaskularnih bolesti. Takođe, povoljne promene u funkciji endotela i trombocita, kao i poboljšanje krvnog pritiska i lipidnog statusa, uočeni su u brojnim kliničkim studijama nakon konzumacije antocijana ili namirnica bogatih ovim jedinjenjima. Studije na miševima sa nedostatkom apolipoproteina E, koji predstavljaju životinjski model za proučavanje ateroskleroze, pokazale su da suplementacija ekstraktima bogatim antocijanima dovodi do značajnog smanjenja nastanka arteriosklerotičnih lezija. Takođe, poboljšano preživljavanje nakon infarkta miokarda, sprečavanje nastanka tromba kao i poboljšanje krvnog pritiska, lipidnog statusa i endotel-zavisne vazorelaksacije, zabeleženi su u različitim životinjskim modelima za proučavanje kardiovaskularnih bolesti, nakon suplementacije namirnicama bogatim antocijanima. Veliki broj *in vitro* studija sproveden je u cilju identifikacije mehanizama kardioprotektivnog delovanja antocijana. Opisano pozitivno delovanje ovih jedinjenja ranije se pripisivalo njihovim antioksidativnim svojstvima, dok novije studije ukazuju na složene molekularne mehanizme delovanja poput modulacije ekspresije gena, aktivacije signalnih puteva i ekspresije mikro-RNK. Međutim, dostupne *in vitro* studije uglavnom poseduju nekoliko ograničenja. Jedan od nedostataka jeste da većina studija prilikom ispitivanja biološkog dejstva antocijana ne uzima u obzir njihovu apsorpciju, distribuciju, metabolizam i ekskreciju iz ljudskog organizma. U namirnicama biljnog porekla ova jedinjenja su uglavnom prisutna u obliku glikozida. Nakon ingestije, antocijani mogu biti apsorbovani u želucu (uz pomoć nosača) i u neizmenjenom obliku dospeti u krvotok. Njihova apsorpcija se nastavlja u tankom crevu, nakon čega portalnom

venom dospevaju u jetru gde se metabolišu do metilovanih proizvoda, i konjugata sa glukuronskom i sumpornom kiselinom. Zajedno sa neizmenjenim antocijanima, ovi metaboliti dostižu maksimalnu koncentraciju u plazmi od oko 0.1 μM u roku od 2 sata, pri dijetarnom unosu ≤2400 mg antocijana. Iz cirkulacije se eliminišu, prevashodno renalnom ekskrecijom, u roku od 6 sati. Deo antocijana, koji se ne apsorbuje u tankom crevu, dospeva u debelo crevo gde podleže delovanju mikroflore debelog creva, usled čega dolazi do stvaranja fenolnih kiselina poput protokatehuinske, vanilinske ili ferulinske. Ova jedinjenja dostižu maksimalnu koncentraciju u plazmi (0.2 -2 μM) u roku od 15 sati nakon ingestije, a prisutna su u cirkulaciji i do 48 sati. Fenolne kiseline se u cirkulaciji takođe mogu javiti u obliku sulfata, glukuronida ili proizvoda metilovanja. Na osnovu svega navedenog može se zaključiti da se antocijani intenzivno metabolišu u ljudskom organizmu. Međutim, u većini *in vitro* studija korišćeni su ekstrakti ili jedinjenja koja nisu zastupljena u cirkulaciji, u koncentracijama daleko većim od fizioloških (i do 200 μM) i sa dugim vremenom ekspozicije ćelija, dajući rezultate koji nisu fiziološki relevantni. Pored ovoga, još jedan nedostatak *in vitro* studija jeste ispitivanje delovanja antocijana na pojedine, ciljane gene ili proteine, što ne predstavlja pogodan pristup za procenu njihovog plejotropnog delovanja koje je pokazano *in vivo*. Takođe, za razliku od relativno velikog broja studija koje prikazuju dejstvo antocijana na funkciju endotelnih ćelija, broj studija koje ispituju njihovo delovanje na funkciju trombocita je ograničen. Ove *in vitro* studije se uglavnom zasnivaju na ispitivanju dejstva antocijana i ekstrakata bogatih antocijanima na aktivaciju trombocita i njihovu agregaciju sa endotelnim ćelijama i drugim trombocitima. Sa druge strane, dejstvo antocijanina i njihovih metabolita na agregaciju trombocita sa leukocitima nije ispitivano u *in vitro* uslovima. Stoga, uprkos sve većem broju epidemioloških, kliničkih i pretkliničkih dokaza o kardioprotektivnom dejstvu antocijana, tačni mehanizmi njihovog delovanja i dalje nisu u potpunosti razjašnjeni. Shodno navedenom, cilj ove doktorske disertacije bio je da se ispita uticaj antocijana i njihovih metabolita na funkciju endotelnih ćelija i trombocita, kao i da se identifikuju mehanizmi njihovog delovanja u fiziološki relevantnim uslovima *in vitro*.

Jedinjenja, čiji je efekat ispitivan u ovoj tezi, uključivala su antocijane: cijanidin-3-glukozid, cijanidin-3-arabinozid, cijanidin-3-galaktozid, delfinidin-3-glukozid i peonidin-3-glukozid, kao i metabolite antocijana: 4-hidroksibenzaldehid,

protokatehuinsku, vanilinsku, ferulinsku i hipurnu kiselinu. Pomenuti antocijani prisutni su u značajnim koncentracijama u različitom voću (posebno bobičastom) i proizvodima dobijenim njegovom preradom (poput vina i sokova), dok se svih pet antocijana mogu naći u borovnicama, koje predstavljaju najčešće konzumiran izvor antocijana. Metaboliti ispitivani u ovoj doktorskoj disertaciji, prisutni su u cirkulaciji nakon konzumiranja različitih namirnica bogatih antocijanima. Takođe, ovi metaboliti su nedavno identifikovani kao proizvodi razgradnje antocijana u tankom i debelom crevu, u studiji koja je ispitivala biološku raspoloživost radioizotopski obeleženog cijanidin-3-glukozida u ljudskom organizmu.

Uticaj ispitivanih jedinjenja na funkciju endotelnih ćelija određivan je merenjem adhezije monocita za aktivirane endotelne ćelije, kao i njihove transendotelijalne migracije, procesa koji predstavljaju početne korake u nastanku ateroskleroze i prethode razvoju kardiovaskularnih bolesti. U ovim istraživanjima korišćene su primarne kulture humanih endotelnih ćelija pupčane vene (HUVEC), koje predstavljaju pogodan *in vitro* ćelijski model za proučavanje vaskularne inflamacije u aterosklerozi. Ove ćelije tretirane su ispitivanim jedinjenjima u rasponu koncentracija od 0.1 μM do 2 μM, odnosno u koncentracijama koje se u krvi mogu postići dijetarnim unosom antocijana. Podaci iz studija biološke raspoloživosti antocijana pokazuju da su ova jedinjenja kratko prisutna u cirkulaciji za razliku od njihovih metabolita (fenolnih kiselina i njihovih derivata) koji se u cirkulaciji mogu zadržati i do 48 sati nakon ingestije. Takođe, značajna koncentracija 4-hidroksibenzaldehida uočena je u cirkulaciji ubrzo nakon ingestije radioizotopski obeleženog cijanidin-3-glukozida, što ukazuje na to da ovo jedinjenje verovatno nastaje razgradnjom antocijana u gornjem delu gastrointestinalnog trakta. U skladu sa navedenim, endotelne ćelije tretirane su antocijanima ili 4-hidroksibenzaldehidom tokom 3 sata, a metabolitima mikroflore debelog creva (protokatehuinskom, ferulinskom, hipurnom i vanilinskom kiselinom) tokom 18 sati. Nakon pomenutih tretmana, inflamacija i aktivacija endotelnih ćelija indukovana je pomoću proinflamatornog citokina, faktora nekroze tumora alfa (TNFα). Po dodavanju monocita, njihova adhezija za endotelne ćelije merena je metodom protočne citometrije. Rezultati ovih ispitivanja pokazali su da je, sa izuzetkom 4-hidroksibenzaldehida, tretman endotelnih ćelija

antocijanima i njihovim metabolitima doveo do značajnog smanjenja adhezije monocita za TNFα-aktivirane endotelne ćelije. Odnos doze i efekta ispitivanih jedinjenja uglavnom nije bio linearan, što je u skladu sa prethodno opisanim dejstvom polifenola na endotelne i druge tipove ćelija. Među ispitivanim antocijanima, delfinidin-3-glukozid doveo je do najvećeg smanjenja adhezije monocita za aktivirane endotlene ćelije, dok je među metabolitima najizraženiji efekat zabeležen nakon tretmana protokatehuinskom kiselinom. Uočeno dejstvo metabolita debelog creva bilo je slično dejstvu antocijana, što ukazuje na to da delovanjem bakterijske flore nastaju metaboliti koji mogu ispoljiti podjednako povoljan uticaj na endotelne ćelije kao i jedinjenja od kojih su potekli. Dodatno, ovi rezultati ukazuju na to da pored antocijana i njihovi metaboliti mogu doprineti kardioprotektivnom delovanju namirnica bogatih antocijanima. Pozitivno dejstvo antocijana na adheziju monocita za endotelne ćelije opisano je u ranijim istraživanjima. Ipak, ova istraživanja su koristila ekstrakate bogate antocijanima, ili aglikone i glikozide u visokim, fiziološki irelevantnim koncentracijama, sa dugim tretmanima ćelijama. Shodno tome, rezultati ove doktorske disertacije predstavljaju prve fiziološki relevantne podatke o uticaju ispitivanih antocijana na adheziju monocita za aktivirane endotelne ćelije. Uočeno pozitivno dejstvo protokatehuinske i ferulinske kiseline u skladu je sa prethodno opisanim uticajem ovih jedinjenja na adheziju monocita, dok je dejstvo hipurinske i vanilinske kiseline uočeno po prvi put.

U cilju ispitivanja mogućeg kumulativnog delovanja jedinjenja istovremeno prisutnih u cirkulaciji, pripremljene su dve smeše jedinjenja: smeša A (jedinjenja kratko prisutna u cirkulaciji) i smeša B (jedinjenja dugo prisutna u cirkulaciji). Smeša A sadržala je cijanidin-3-glukozid, cijanidin-3-arabinozid, cijanidin-3-galaktozid, delfinidin-3-glukozid, peonidin-3-glukozid i 4-hidroksibenzaldehid. Finalna koncentracija jedinjenja smeše koja je dodavana endotelnim ćelijama iznosila je 0.1 μM za antocijane i 0.5 μM za 4-hidroksibenzaldehid. Smeša B sadržala je protokatehuinsku, vanilinsku, ferulinsku i hipurnu kiselinu u finalnoj koncentraciji od 0.2 μM, 2 μM, 1 μM i 2 μM, redom. Koncentracije komponenata ovih smeša izabrane su tako da najbliže odgovaraju koncentracijama ovih jedinjenja zabeleženim u plazmi u studijama biološke raspoloživosti antocijana u ljudskom organizmu. Dodatno, tretman endotelnih ćelija

smešom A, a potom smešom B (nazvan smeša A+B) kreiran je kako bi se što verodostojnije oponašali uslovi kojima su endotelne ćelije izložene tokom dužeg vremena nakon dijetarnog unosa antocijana. Rezultati ispitivanja dejstva smeša jedinjenja na adheziju monocita za aktivirane endotelne ćelije pokazali su takođe smanjenje adhezije. Ipak, aditivni efekat pojedinačnih komponenata smeša nije uočen. Ovi rezultati su u skladu sa prethodno opisanim odsustvom aditivnog efekta različitih polifenola i mogu se objasniti kompeticijom između komponenata smeše za isto mesto delovanja.

Smeše antocijana i njihovih metabolita su potom korišćene za ispitivanje uticaja ovih jedinjenja na transendotelijalnu migraciju monocita. Rezultati ovih istraživanja pokazali su da je tretman endotelnih ćeilija pomenutim smešama jedinjenja doveo do značajnog smanjenja transendotelijalne migracije monocita indukovane hemoatraktantom, monocitinim hemotaksnim proteinom 1 (MCP-1). Ovi rezultati predstavljaju prve fiziološki relevantne dokaze pozitivnog dejstva antocijana i njihovih crevnih metabolita na transendotelijalnu migraciju monocita.

Shodno navedenom, rezultati istraživanja dejstva antocijana i njihovih metabolita na adheziju i transendotelijalnu migraciju monocita ukazuju na to da ova jedinjenja mogu uticati na početne faze razvoja ateroskleroze. Ovo potencijalno anti-aterogeno dejstvo ispitivanih jedinjenja podržano je rezultatima studija na animalnim modelima ateroskleroze u kojima je uočeno smanjenje formiranja aterosklerotičnih lezija nakon suplementacije antocijanima bogatim ekstraktima.

U cilju razmatranja mehanizama u osnovi uočenog pozitivnog dejstva antocijana i njihovih metabolita na adheziju monocita i njihovu transedneotelijalnu migraciju, ispitan je uticaj smeša ovih jedinjenja na ekspresiju gena u endotelnim ćelijama. Ova ispitivanja podrazumevala su upotrebu makroareja (engl. Taqman Low Density Array) koji su omogućili istovremenu analizu nivoa ekspresije 93 različita gena. Analiza genske ekspresije u endotelnim ćelijama tretiranim navedenim smešama jedinjenja pokazala je promene u ekspresiji gena uključenih u regulaciju adhezije ćelija, reorganizacije aktinskog citoskeleta, fokalne adhezije i transmigracije leukocita. Stoga, zabeležena modulacija ekspresije gena u endotelnim ćelijama može predstavljati jedan od

mehanizama preko kojih ispitivana jedinjenja ispoljavaju pozitivno dejstvo na procese adhezije i transendotelijalne migracije monocita.

Ekspresija gena može biti regulisana transkripcionim faktorima čija je aktivnost pod uticajem signalnih puteva. Bioinformatička analiza rezultata genske ekspresije sprovedena je kako bi se otkrili transkripcioni faktori koji bi mogli doprineti uočenom delovanju ispitivanih jedinjenja na ekspresiju gena, kao i signalni proteini koji regulišu aktivnost ovih transkripcionih faktora. Dodatno, *in silico* analiza molekulskog uklapanja (molekulski doking) izvedena je kako bi se ispitale moguće interakcije antocijana i njihovih metabolita (liganada) sa ovim signalnim proteinima i transkripcionim faktorima. Molekulski doking predstavlja kompjutersku metodu koja se sve češće primenjuje u ispitivanju molekularnih mehanizama delovanja biološki aktivnih jedinjenja. U ovoj disertaciji izvedeno je molekulsko uklapanje liganada sa 62 makromolekula koji su uključeni u regulaciju različitih ćelijskih procesa poput inflamacije, ćelijske proliferacije, migracije i preživljavanja. Rezultati ovih analiza pokazali su da antocijanini i njihovi metaboliti mogu ostvariti interakcije sa signalnim proteinima. Takođe, pokazano je da antocijani mogu ostvariti snažnije interakcije sa ispitivanim signalnim proteinima nego njihovi metaboliti. U okviru grupe ispitivanih antocijana ili njihovih metabolita uočen je sličan afinitet vezivanja za ciljane makromolekule, što ide u prilog hipotezi da je nedostatak aditivnog efekta pojedinačnih jedinjenja smeša rezultat njihove kompeticije za isto mesto delovanja. Rezultati molekulskog dokinga ukazuju na to da antocijani i njihovi metaboliti mogu ostvariti interakcije sa katalitičkim domenom nekoliko proteinskih kinaza (npr. FAK1, MEK2, IKKα, JAK3, p38β) i da potencijalno mogu uticati na njihovu kinaznu aktivnost i aktivaciju nishodnih signalnih molekula. Podaci iz literature pokazuju da vezivanje različitih inhibitora za katalitički domen ovih proteinskih kinaza dovodi do inhibicije njihove aktivnosti koja potom može dovesti do smanjenja adhezije i transendotelijalne migracije leukocita za endotelne ćelije. U cilju potvrde rezultata molekulskog dokinga u *in vitro* uslovima, uticaj antocijana i njihovih metabolita na signalne puteve ispitan je imunobloting (engl. Western blot) analizom. Tretman endotelnih ćelija smešom A doveo je do smanjenja fosforilacije signalnog proteina ERK1/2 kao i transkripcionog faktora NF-κB-p65, dok je smeša B uticala na smanjenje

fosforilacije NF-κB-p65. Shodno navedenom, rezultati istraživanja uticaja antocijana i njihovih metabolita na signalne puteve ukazuju na to da ova jedinjenja vezivanjem za različite signalne proteine mogu uticati na njihovu aktivnost, i aktivaciju nishodnih signalnih molekula i transkripcionih faktora, dovodeći do promena u nivou ekspresije gena koje mogu uticati na procese adhezije i transedotelne migracije monocita.

Pored regulacije na transkripcionom nivou, ekspresija gena može biti regulisana i na posttranskripcionom nivou pomoću mikro-RNK. Ovi nekodirajući molekuli RNK uključeni su u kontrolu različitih ćelijskih procesa, a promene profila njihove ekspresije uočavaju se kod različitih oboljenja, uključujući kardiovaskularne bolesti. Sposobnost antocijana ili njihovih metabolita da utiču na ekspresiju mikro-RNK uočena je u nekoliko *in vivo* studija, dok su *in vitro* ispitivanja i dalje ograničena. U ovoj doktorskoj disertaciji dejstvo antocijana i njihovih metabolita na ekspresiju mikro-RNK ispitano je pomoću mikro-RNK mikroareja. Rezultati ovih ispitivanja pokazali su, po prvi put, sposobnost antocijana i njihovih metabolita da, pri fiziološki relevantnim koncentracijama, moduliraju ekspresiju mikro-RNK u aktiviranim endotelnim ćelijama. Ispitivana jedinjenja posebno su uticala na promenu ekspresije mikro-RNK povezanih sa nastankom endotelne disfunkcije i ateroskleroze (npr. let-7f, miR-181b, miR-125a i miR-26a), doprinoseći uočenim promenama endotelne funkcije. Stoga, navedeni rezultati ukazuju na to da modulacija ekspresije mikro RNK predstavlja još jedan mehanizam pomoću kog ova jedinjenja mogu ispoljiti svoje povoljno dejstvo na kardiovaskularno zdravlje.

Pored ispitivanja uticaja antocijana i njihovih metabolita na funkciju endotelnih ćelija, u okviru ove doktorske disertacije, istraženo je i njihovo dejstvo na funkciju trombocita. Ova istraživanja imala su zadatak da ispitaju uticaj pomenutih jedinjenja na aktivaciju trombocita i njihovu agregaciju sa leukocitima, indukovanu dodavanjem adenozin-difosfata. Adenozin-difosfat je fiziološki agonist deponovan u gustim granulama trombocita iz kojih se oslobađa po njihovoj aktivaciji. Rezultati prospektivnih studija ukazuju na vezu između stepena reaktivnosti trombocita kao odgovora na niske koncentracije adenozin-difosfata i kardiovaskularnog rizika. Ovim se racionalizuje ispitivanje uticaja antocijana i njihovih metabolita na aktivaciju i agregaciju trombocita indukovanu ovim agonistom kao potencijalnog ciljanog mehanizma za prevenciju

kardiovaskularnih bolesti. Uzorci pune krvi dobijene venepunkcijom sedam zdravih volontera muškog pola inkubirani su sa antocijanima u finalnoj koncentraciji od 0.1μM, kao i 4-hidroksibenzaldehidom, protokatehuinskom, vanilinskom, ferulinskom ili hipurnom kiselinom u finalnoj koncentraciji od 0.5 μM, 0.2 μM, 2 μM, 1 μM i 2 μM, redom. Nakon ovoga, uzorci su aktivirani dodavanjem adenozin-difosfata, obeležavani odgovarajućim antitelima i analizirani primenom protočne citometrije. Uticaj navedenih jedinjenja na funkciju trombocita određivan je merenjem ekspresije aktivacionih markera P-selektina i GPIIb/IIIa, kao i agregata trombocita sa neutrofilima i monocitima. P-selektin je adhezioni molekul, prisutan u alfa granulama trombocita, koji nakon aktivacije trombocita dospeva na njihovu površinu i posreduje u agregaciji sa neutrofilima i monocitima vezivanjem za svoj ligand PSGL-1 na površini ovih ćelija. Aktivacija trombocita povezana je i sa konformacionom aktivacijom GPIIb/IIIa, receptora za glikogen, koji osim što ima važnu ulogu u agregaciji trombocita sa drugim trombocitima, doprinosi i formiranju agregata sa leukocitima. Primena protočne citometrije u analizi uzoraka pune krvi omogućila je visok stepen osetljivosti u merenju pomenutih markera, te dobijanje pouzdanih rezultata koji se mogu isključivo pripisati direktnom dejstvu ispitivanih jedinjenja na funkciju trombocita. Rezultati ovih istraživanja pokazali su da sa izuzetkom vanilinske kiseline, kako antocijani tako i njihovi metaboliti ispoljavaju značajno dejstvo na bar jedan od ispitivanih parametara tj. aktivaciju trombocita ili njihovu agregaciju sa leukocitima. Ovi rezultati ukazuju na to da prethodno opisani, povoljni efekti namirnica bogatih antocijanima mogu biti posledica zajedničkog delovanja antocijana i njihovih metabolita na funkciju trombocita. Među ispitivanim antocijanima, najizraženije delovanje na funkciju trombocita ispoljio je cijanidin-3-arabinozid, koji je značajno smanjio procenat trombocita koji eksprimiraju P-selektin, gustinu ovog receptora na trombocitima, kao i agregaciju trombocita sa neutrofilima. Nasuprot ovome, peonidin-3-glukozid, delfinidin-3-glukozid i cijanidin-3-glukozid ispoljili su značajano dejstvo na aktivaciju trombocita preko smanjenja ekspresije P-selektina ili GPIIb/IIIa, dok je cijanidin-3-galaktozid značajno uticao samo na agregaciju leukocita sa trombocitima. Među metabolitima antocijana, 4-hidroksibenzaldehid delovao je na najveći broj ispitivanih parametara, izazivajući značajno smanjenje

aktivacije trombocita i njihove agregacije sa neutrofilima i monocitima. Ovaj metabolit predstavlja jedino ispitivano jedinjenje koje nije ispoljilo značajano dejstvo na adheziju monocita za aktivirane endotelne ćelije. Shodno tome, ovi rezultati ukazuju na to da, iako ne utiče na funkciju endotelnih ćelija, 4-hidroksibenzaldehid preko delovanja na trombocite može indirektno uticati na smanje interakcija leukocita sa endotelnim ćelijama i na taj način štititi od razvoja ateroskleroze. Ograničen broj dostupnih literaturnih podataka o dejstvu antocijana i njihovih metabolita na aktivaciju trombocita i njihovu agregaciju sa leukocitima u *in vitro* uslovima doprinosi značaju rezultata dobijenih u ovoj doktorskoj disertaciji. Delovanje antocijana poput peonidin-3-glukozida, cijanidin-3-galaktozida i cijanidin-3-arabinozida, kao i metabolita 4-hidroksibenzaldehida i vanilinske kiseline na aktivaciju trombocita, nije ranije ispitivano. Pored ovoga, posebno je značajno što je u okviru ovih istraživanja po prvi put pokazano dejstvo antocijana i njihovih metabolita na agregaciju trombocita sa leukocitima, koja u odnosu na aktivaciju trombocita predstavlja još osetljiviji pokazatelj rizika od nastanka kardiovaskularnih bolesti.

Na osnovu izloženih rezultata ove disertacije može se doneti nekoliko zaključaka. Antocijani i njihovi metaboliti dovode do značajnog smanjenja adhezije monocita i njihove transendotelijalne migracije, procesa koji predstavljaju inicijalne korake u nastanku ateroskleroze, na taj način doprinoseći održanju integriteta endotela prilikom zapaljenskog procesa. Uočeno dejstvo na funkciju endotelnih ćelija posledica je složenih molekularnih mehanizmima delovanja, poput sposobnosti ispitivanih jedinjenja da utiču na ekspresiju mikro RNK, kao i da se vežu za ćelijske signalne proteine i utiču na njihovu aktivnost i aktivaciju transkripcionih faktora, dovodeći do promena na nivou ekspresije gena. Pored efekta na endotelne ćelije, ispitivana jedinjenja ispoljavaju povoljno dejstvo i na funkciju trombocita, izraženo smanjenjem aktivacije trombocita i njihove agregacije sa leukocitima, kao procesa koji značajno doprinose nastanku kardiovaskularnih bolesti. U skladu sa izloženim, ova doktorska disertacija pokazala je pozitivan uticaj antocijana i njihovih metabolita, u fiziološki relevantnim koncentracijama, na funkciju endotelinih ćelija i trombocita, i time, pružila nova saznanja o mehanizmima njihovog kardioprotektivnog delovanja.

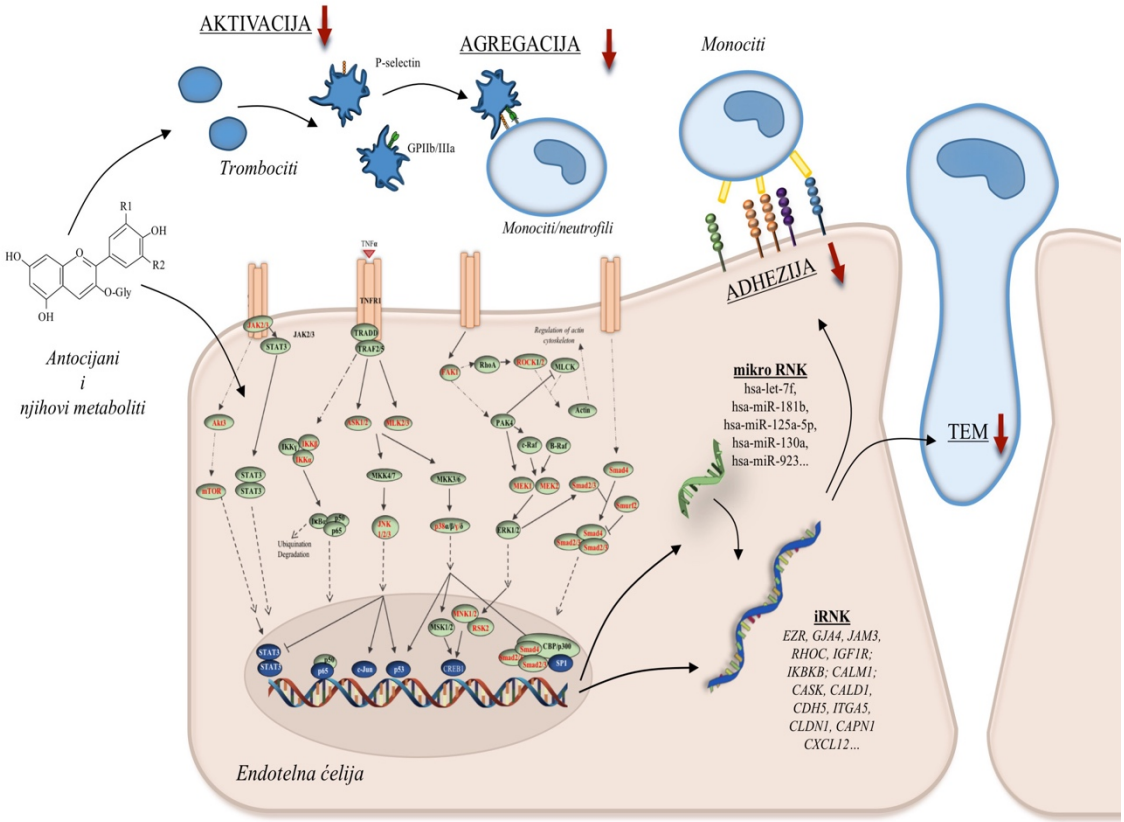

Ključne reči: antocijani, metaboliti, endotelna disfunkcija, adhezija monocita za endotelne ćelije, transendotelna migracija, aktivacija trombocita, agregacija trombocita sa leukocitima.

Naučna oblast: Biologija

Uža naučna oblast: Integrisane nauke o ishrani

UDK broj: [547.62+581.574]:[611.018.74:611.018.52] (043.3)

RÔLE DES ANTHOCYANES ET CES METABOLITES SUR LA FONCTION DES CELLULES ENDOTHELIALES ET PLAQUETTES HUMAINE *in vitro*

RESUME

Les maladies cardiovasculaires sont un groupe de troubles qui affectent le cœur et les vaisseaux sanguins et qui représentent la principale cause de morbidité et de mortalité dans le monde. Ils comprennent les maladies coronariennes, les maladies cérébrovasculaires et les maladies artérielles périphériques, avec l'athérosclérose étant le principal processus pathologique sous-jacent de leur développement. L'athérosclérose, une maladie inflammatoire chronique des artères de gros et moyen calibre, est caractérisée par des lésions athéromateuses qui sont formées par l'accumulation de lipides, des éléments cellulaires et fibreux dans la paroi artérielle. Ces lésions perturbent le flux sanguin et dans les cas les plus graves tel que la rupture de la plaque et la thrombose peuvent entraîner un infarctus du myocarde ou accident vasculaire cérébral. L'athérosclérose est initiée par des altérations de la fonction endothéliale qui favorisent le recrutement et l'adhérence des leucocytes circulants et leur migration transendothéliale dans la paroi du vaisseau sanguin. Dans l'espace sous-endothélial, les leucocytes se différencient en macrophages activés, prennent lipoprotéine oxydée et forme les cellules spumeuses, ce qui conduit à à la formation de lésions athéromateuses. Les plaquettes contribuent également au développement de ce trouble par leurs interactions avec les leucocytes et les cellules endothéliales qui se produisent lors de l'activation plaquettaire. Ces interactions favorisent l'adhésion leucocytaire et la migration transendothéliale, augmentant ainsi les réponses inflammatoires et la progression de l'athérosclérose. Par conséquent, l'interaction entre les cellules endothéliales, les plaquettes et les leucocytes représentent une cible intéressante pour la prévention des maladies cardiovasculaires.

L'alimentation est un facteur important dans la promotion et le maintien de la santé.

Il joue un rôle majeur dans le développement et la progression des maladies cardiovasculaires, mais peut également présenter une importante modification de style de vie pour la prévention et la gestion des maladies cardiovasculaires. De nombreuses études épidémiologiques et cliniques ont suggéré des effets bénéfiques des régimes riches en fruits et légumes sur la santé cardiovasculaire. Ces propriétés favorisant les effets bénéfiques des fruits et légumes ont été attribués non seulement à leur faible valeur en calories, les niveaux élevés de fibres et oligo-éléments essentiels, mais aussi à leur composition en micronutriements, comme les polyphénols. Les polyphénols constituent le groupe phyto-chimique le plus important et le plus largement distribué. Ces composés structurellement très divers sont largement présents dans les aliments végétaux tels que les fruits, les légumes et les céréales, présentant le groupe le plus important de composants alimentaires non nutritifs.

Les anthocyanes représentent un sous-groupe de composés polyphénoliques qui sont abondants dans l'alimentation humaine en raison de leur forte présence dans les baies et les produits dérivés de baies. L'intérêt en anthocyanes a considérablement augmenté au cours des deux dernières décennies, en raison de divers effets bénéfiques pour la santé associée à la consommation d'aliments d'origine végétale riches en anthocyanes. Un nombre croissant de preuves suggère le rôle important des anthocyanes alimentaires dans la prévention et le traitement des maladies cardiovasculaires. Les données des études épidémiologiques ont montré une relation inverse entre la consommation d'anthocyanes et risque d'hypertension artérielle, le risque d'infarctus du myocarde et de mortalité due aux maladies cardiovasculaires. Plusieurs études cliniques avec des anthocyanines ou des aliments riches en anthocyanes ont montré des changements favorables dans l'endothélium et la fonction plaquettaire, la pression artérielle et le taux de cholestérol. Plusieurs interventions nutritionnelles réalisées avec des souris déficientes en apolipoprotéine E, qui développent spontanément l'athérosclérose, ont rapportées que des extraits riches en anthocyanes ou des composés purs, administrés à des doses pertinentes sur le plan nutritionnel, réduit la formation de lésions athéromateuses dans l'aorte de ces

souris. De plus, la supplémentation en anthocyanes augmente la survie après un infarctus du myocarde induit, diminue le développement de thrombus et améliore la tension artérielle, les profils lipidiques et vasorelaxation dépendante de l'endothélium dans plusieurs études utilisant différents modèles animaux de maladies cardiovasculaires. Un certain nombre d'études in vitro ont été réalisées pour identifier les mécanismes par lesquels les anthocyanines exercent leurs effets cardio-protecteurs. Ces avantages pour la santé ont été précédemment associés à leurs propriétés antioxydantes directes, tandis que des études plus récentes ont suggéré l'implication de mécanismes moléculaires plus complexes d'action, y compris la modulation de l'expression génique, la signalisation cellulaire et l'expression de micro-ARN. Cependant, la majorité des études in vitro disponibles présentent plusieurs limitations.

L'une des limites est que dans la recherche sur les effets biologiques des anthocyanines, ces études ne prennent généralement pas en compte l'absorption, la distribution, le métabolisme et l'élimination de ces composés dans le corps humain. Dans les aliments, ces composés sont principalement présents sous forme de glycosides. Une fois ingérées, les anthocyanes sont absorbés par l'estomac et sont présentes rapidement dans la circulation sanguine sous forme inchangée. Leur absorption se poursuit dans l'intestin grêle, suivie de leur conjugaison dans le foie pour donner des métabolites méthylés, glucuronidés et sulfatés. Les anthocyanines inchangées et ces métabolites atteignent une concentration plasmatique maximale d'environ 0.1 μM vers 2 heures, après un apport alimentaire de 2400 mg d'anthocyanines. Ces composés sont éliminés de la circulation dans les 6 heures, principalement par excrétion rénale. Les anthocyanes qui passent la partie supérieure du tractus gastro-intestinal sont dégradés par la microflore de l'intestin dans le côlon, ce qui donne lieu à des acides phénoliques, tels que protocatéchique, vanillique ou l'acide férulique. Ces composés atteignent la concentration plasmatique maximale (0.2 μM-2 μM) dans les 15 heures post ingestion, et sont présents dans la circulation jusqu'à 48 heures. Les acides phénoliques peuvent également se

trouver dans la circulation sous la forme de sulfate, de glucuronide ou de produits de méthylation. De plus, il a été suggéré que la dégradation des anthocyanes ne nécessite pas nécessairement l'action du microbiote colique et qu'une certaine dégradation chimique est susceptible de se produire dans la partie supérieure du tractus gastro-intestinal et de la circulation. Pris ensemble, les métabolites anthocyanes apparaissent rapidement dans le sérum, présentent des profils biphasiques, avec le pic initial dans les 2 heures, suivi par un second pic entre 6 et 48 heures post ingestion. Malgré les preuves d'un métabolisme important des anthocyanines dans le corps humain, les études *in vitro* disponibles utilisent principalement des composés parents ou des extraits plutôt que des métabolites circulants, à des concentrations élevées et supra-physiologiques (jusqu'à 200 μM) et de longues périodes d'exposition des cellules (jusqu'à 24 heures), produisant ainsi des résultats sans pertinence physiologique.

Une autre limitation des études mécanistes *in vitro* est qu'ils utilisent le plus souvent des approches ciblées pour étudiant l'effet sur l'expression des gènes, mettant l'accent sur l'impact sur quelques cibles spécifiques, qui ne convient pas pour les évaluations du mode multicible et complexe d'action attribués aux polyphénols. En outre, contrairement au nombre relativement important d'études portant sur l'effet des anthocyanes sur la fonction des cellules endothéliales, le nombre d'études examinant leurs effets sur la fonction plaquettaire est limité. Ces études *in vitro* se concentrent principalement à étudier l'effet des extraits riches en anthocyanes ou composés purs sur activation des plaquettes et l'agrégation des plaquettes avec des cellules endothéliales ou entre elles, généralement dans les conditions non-physiologiques. En outre, l'effet des anthocyanes et de leurs métabolites sur l'agrégation plaquettaire avec des leucocytes doit encore être mis en place. Ainsi, en dépit du nombre croissant de données épidémiologiques, cliniques et préclinique des effets cardio-protectrices anthocyanes, leurs mécanismes exacts d'actions ne sont pas encore pleinement compris.

L'objectif principal de cette thèse était d'étudier l'impact des anthocyanes et de leurs métabolites sur la fonction endothéliale et des plaquettes et d'identifier les mécanismes

moléculaires sous-jacents de l'action, en utilisant des conditions physiologiques, c'est a dire forme, dose et dure d'exposition des cellules aux formes et métabolites circulants des anthocyanes.

Les composés examinés sont les anthocyanines : cyanidine-3-glucoside, cyanidine-3-arabinoside, la cyanidine-3-galactoside, delphinidine-3-glucoside et péonidine-3-glucoside, et leurs métabolites : 4-hydroxybenzaldéhydes, les acides protocatéchiques, vanilliques, féruliques et hippuriques. Les anthocyanines testées sont présentes en grande quantité dans divers fruits, notamment dans les baies, dans divers produits dérivés des fruits (par exemple les jus et les vins) et dans certains légumes et céréales. En outre, ils peuvent être trouvés dans les bleuets qui sont les sources d'anthocyanes les plus couramment consommés. De plus, les métabolites d'anthocyanes qui ont été examinés auparavant dans la circulation sanguine après la consommation de divers aliments riches en anthocyanes et ont été confirmés comme des produits de dégradation anthocyane issue de petit intestin et du côlon dans une étude de biodisponibilité anthocyanes relativement récente avec cyanidine-3-glucoside marquent isotopiquement.

L'impact des composés testés sur la fonction des cellules endothéliales a été évalué par la mesure de l'adhérence des monocytes aux cellules endothéliales activées et leur migration transendothéliale ultérieure qui représentent les principales étapes initiales du développement de l'athérosclérose. Ces investigations ont été réalisées en utilisant des cellules endothéliales primaires, des cellules endothéliales de veine ombilicale humaine (HUVECs), un système de modèle *in vitro* couramment utilisé pour explorer l'inflammation vasculaire dans l'athérosclérose. Ces cellules ont été traitées avec des composés testés sur une gamme de concentration allant de 0.1 μM à 2 μM, ce qui correspondait à leurs taux plasmatiques circulant après la prise d'aliments riches en anthocyanes. Les résultats des études de biodisponibilité anthocyanes montrent que les anthocyanes sont présents dans le sang pendant une courte période, contrairement à leurs métabolites de l'intestin qui sont détectables jusqu'à 48 heures suivant la consommation. En outre, dans deux études récentes qui ont utilisé les baies de sureau ou cyanidine-3-

glucoside marqué isotopiquement, une quantité importante de 4-hydroxybenzaldéhyde a été observé dans plasma peu de temps après l'ingestion de cyanidine-3-glucoside, ce qui suggère que ce composé est probablement un produit de dégradation de l'anthocyanine produite dans la partie supérieure de tractus gastro-intestinal. Par conséquent, des longueurs différentes de traitement des cellules endothéliales avec des anthocyanes et de leurs métabolites ont été utilisés, à savoir un traitement de 3 heures pour anthocyanes et 4-hydroxybenzaldéhyde et de 18 heures pour les métabolites. Pour créer un environnement pro-athérogène, les cellules ont été stimulées avec une cytokine, facteur de nécrose tumorale alpha (TNFα), qui représente une régulatrice clé de l'inflammation et provoque un dysfonctionnement endothélial. Par la suite, les cellules endothéliales ont été co-incubées avec les monocytes et l'adhésion des monocytes a été mesurée par cytométrie en flux. L'activation des cellules endothéliales avec TNFα a induit l'adhésion des monocytes à la monocouche endothéliale. Les résultats des tests d'adhésion de monocytes ont montré que, à l'exception de 4-hydroxybenzaldéhyde, le prétraitement de cellules HUVEC avec des anthocyanes et de leurs métabolites, avant l'activation du TNFα, a entraîné une réduction significative de l'adhérence des monocytes aux cellules endothéliales. Cet effet a été observé en particulier à des concentrations des composés qui sont les plus proches de leurs niveaux plasmatiques circulants précédemment rapportés. L'effet dose-réponse de composés testés sur les interactions cellulaires de monocytes endothéliaux est essentiellement non linéaire, qui est en ligne avec l'absence d'un effet dose-réponse rapportée pour d'autres polyphénols dans cellules endothéliales ou d'autres types de cellules. Parmi les anthocyanines examinées, le delphinidine-3-glucoside présentait la plus grande capacité à atténuer l'adhésion des monocytes. Les résultats des essais d'adhérence ont également révélé l'activité de métabolites de l'intestin à réduire l'adhérence des monocytes aux cellules endothéliales activées, avec l'effet le plus fort observé pour l'acide protocatéchique. L'impact de ces composés est similaire à celle des anthocyanes, ce qui suggère que la transformation microbienne intestinale produit des métabolites qui peuvent avoir des effets bénéfiques sur la fonction endothéliale que leurs

composés parents. Ces résultats impliquent que, en plus des anthocyanes, leurs métabolites qui sont détectables dans la circulation pour beaucoup plus longtemps que leurs formes mères, peuvent exercer une activité biologique dans les cellules endothéliales et contribuent probablement aux effets cardio protecteurs associés à la consommation habituelle d'aliments riches en anthocyanes. L'influence des anthocyanines sur l'adhésion des monocytes aux cellules endothéliales activées a été précédemment rapportée. Cependant, ces effets ont été observés en utilisant des extraits à base d'anthocyanes et des aglycones ainsi que des concentrations supra-physiologiques de glycosides, avec de longues périodes d'exposition cellulaire. Ainsi, les résultats de cette thèse présentent les premières preuves physiologiquement pertinentes de l'impact des anthocyanes testées sur l'adhésion des cellules endothéliales des monocytes. Les effets précédemment évalués d'acides protocatéchique et férulique sont conformes aux résultats de cette thèse, tandis que les effets des acides hippuriques et vanilliques sur l'adhérence des monocytes aux cellules endothéliales activées sont rapportés pour la première fois.

Pour étudier davantage l'effet potentiel synergique de composés qui sont simultanément présents dans la circulation après l'ingestion d'aliments riches en anthocyanes, deux mélanges de composés qui sont présents dans la circulation pendant un court (mélange A) ou pendant une longue période (mélange B) ont été créés. Le mélange A contient cyanidine-3-glucoside, cyanidine-3-arabinoside, la cyanidine-3-galactoside, delphinidine-3-glucoside, péonidine-3-glucoside et de 4-hydroxybenzaldéhyde. La concentration finale des composés dans ce mélange qui a été ajouté aux cellules endothéliales était de 0.1 μM pour les anthocyanines et de 0.5 μM pour le 4-hydroxybenzaldéhyde. Le mélange B est composé de l'acide protocatéchique, l'acide vanillique, l'acide férulique et l'acide hippurique, administré aux cellules endothéliales à la concentration finale de 0.2 μM, 2 μM, 1 μM et 2 μM, respectivement. Les concentrations de composés dans ces mélanges étaient les plus proches de celles

précédemment identifiées dans le plasma humain dans les études de biodisponibilité des anthocyanes. En outre, la condition appelée mélange A+B a été créé pour imiter le plus fidèlement possible la pharmacocinétique anthocyanes suite à l'ingestion de sources riches en anthocyanes en traitant les cellules endothéliales avec le mélange de composés qui apparaissent rapidement dans la circulation sanguine, puis avec le mélange de métabolites de l'intestin qui apparaissent plus tard et sont présents dans la circulation plus longtemps. Les résultats de ces tests d'adhésion ont révélé la capacité des mélanges à réduire significativement l'adhérence des monocytes aux HUVEC activés par TNFα. Cependant, aucun effet additif des composés individuels des mélanges n'a été observé. L'absence d'effet additif a déjà été observée avec différents mélanges de polyphénols et peut être expliquée par la compétition possible entre les composés du mélange pour la même cible d'action.

Les mélanges d'anthocyanes et de leurs métabolites ont ensuite été utilisés pour étudier l'effet de ces composés sur la migration transendothéliale des monocytes, étape qui suit l'adhésion. Les résultats de ces expériences ont montré une réduction significative de la migration des monocytes induite par la protéine chimiotactique monocytaire 1 (MCP-1) à travers de monocouche endothéliale prétraitée avec les mélanges. Ces résultats représentent le premier rapport sur la capacité des anthocyanes et de leurs métabolites intestinaux à réduire la migration transendothéliale des monocytes à des conditions physiologiquement pertinentes. Ces résultats suggèrent que les anthocyanes et leurs métabolites peuvent affecter les premières étapes du développement de l'athérosclérose en diminuant la perméabilité des cellules endothéliales aux leucocytes. Cette hypothèse peut être étayée par les résultats d'études animales qui a rapporté la réduction de lésions athéromateuses chez des souris déficientes en apolipoprotéine E qui ont consommé un régime alimentaire complété avec des extraits riches en anthocyanes ou des composés purs.

Pour identifier les mécanismes moléculaires sous-jacents aux effets observés sur l'adhésion des monocytes et la migration transendothéliale, l'impact de ces composés sur

l'expression des gènes dans les cellules endothéliales a ensuite été évaluée. Ces expériences ont été réalisées à l'aide macroarray (cartes TaqMan Low Density Array) qui ont permis d'évaluer simultanément les niveaux d'expression de 93 gènes impliqués dans la régulation de la fonction endothéliale. L'analyse de l'expression génique a révélé que le traitement des cellules endothéliales avec les mélanges d'anthocyanes et de leurs métabolites module l'expression des gènes impliqués dans la régulation de l'adhésion cellule-cellule, réorganisation du cytosquelette d'actine, l'adhésion focale, jonctions serrées et transmigration leucocytaire. Ainsi, ces modulations de l'expression des gènes dans les cellules endothéliales par des mélanges peuvent être associés à une diminution de l'adhérence des monocytes et la migration transendothéliale, présentant des cibles moléculaires sous-jacents l'effet observé sur les cellules endothéliales.

L'expression génique est contrôlée au niveau transcriptionnel par des facteurs de transcription dont l'activité est régulée par des voies de signalisation. Les résultats des d'expression génique ont été analysés avec différents outils bio-informatiques pour identifier les facteurs de transcription et des protéines de signalisation qui pourraient être impliquée dans l'effet nutrigénomique observé des composés testés. L'amarrage moléculaire, i-silico docking analyzes, a été utilisé pour prédire si anthocyanes et leurs métabolites peuvent se lier à ces protéines de signalisation cellulaire et les facteurs de transcription et exercer leur activité biologique. Cette technique de calcul est de plus en plus utilisée comme instrument d'identification de cibles moléculaires de composés bioactifs naturels. Dans cette thèse, l'amarrage moléculaire a été réalisée avec 62 protéines de signalisation identifiées et facteurs de transcription qui sont impliqués dans la régulation de différents processus cellulaires tels que l'inflammation, la prolifération cellulaire, la migration et la survie. Les résultats de ces analyses suggèrent que les anthocyanines et leurs métabolites présentent la capacité de se lier aux certaines protéines de signalisation cellulaire. Les anthocyanes se sont avérés être des ligants plus forts que leurs métabolites. De plus, les affinités de liaison similaires pour les mêmes cibles ont été observés lorsque l'on compare les composées anthocyanes au sein des groupes et des

métabolites, ce qui contribue à l'hypothèse que l'absence d'effet cumulatif des composés dans les mélanges est le résultat de leur competition pour la même cible d'action. Des données bibliographiques suggèrent que les anthocyanes et leurs métabolites peuvent se lier à des domaines de la protéine kinase de plusieurs protéines de signalisation cellulaire (par exemple FAK1, MEK2, IKKα, JAK3, p38β) et éventuellement affecter leur activité kinase et la phosphorylation des protéines de signalisation en aval. Les résultats de la littérature disponible ont montré que la liaison de différents inhibiteurs aux domaines de kinase de ces protéines de signalisation cellulaire conduit à réduition de leur activité, ce qui a été associée à la reduction de perméabilité endothéliale, c'est-à-dire l'adhérence et la migration transendothéliale des leucocytes.

Pour associer des résultats obtenus par amarrage moléculaire avec l'effet possible *in vitro* sur des voies de signalisation cellulaire, l'impact des anthocyanes et de leurs métabolites sur l'activation des protéines de signalisation cellulaire et des facteurs de transcription ont été étudiée. Les résultats des analyses par Western blot ont montré que le traitement des cellules endothéliales avec le mélange A réduit la phosphorylation de d'ERK1/2 et de NF-κB-p65, alors que mélange B a diminué la phosphorylation de NF-κB-p65. Ces résultats suggèrent que les anthocyanes et leurs métabolites en se liant à différentes protéines de signalisation cellulaire peuvent affecter leur activité et par conséquent celle des facteurs de transcription ce qui affect la perméabilité endothéliale, présentant les mécanismes possibles d'action sous-jacents aux leurs propriétés cardioprotecteurs.

Outre la réglementation par des protéines de signalisation cellulaire et les facteurs de transcription, l'expression des gènes peut également être réglée au niveau post-transcriptionnel par les micro-ARNs. Ces ARN non codants contrôlent divers processus cellulaires, et des changements dans leurs profils d'expression ont été décrits dans diverses maladies, y compris CVD. La capacité des anthocyanines ou leurs métabolites à moduler l'expression de micro-ARN a été décrite cependant, les études sont encore

limitées. Dans cette thèse, l'effet des anthocyanines et de leurs métabolites sur l'expression du micro-ARN a été examiné en utilisant les puces à micro-ARN. Les résultats de l'analyse d'expression de micro-ARN ont montré pour la première fois la capacité des anthocyanes et de leurs métabolites aux conditions physiologiquement pertinentes à moduler l'expression de micro-ARN et des cellules endothéliales stimulée par le TNFα. Les composés testés particulièrement touchaient l'expression des micro-ARNs impliqués dans la régulation de la perméabilité des cellules endothéliales (par example let-7f, miR-181b, miR-125a et miR-26a), ce qui contribue aux changements observés dans la fonction des cellules endothéliales. Ainsi, ces résultats ont montré que la modulation de l'expression du micro-RNA présente également un mécanisme par lequel ces composés peuvent exercer leurs effets bénéfiques.

En plus des investigations de l'effet des anthocyanes et de leurs métabolites sur la fonction des cellules endothéliales comme l'une des cibles importantes dans la prévention des maladies cardiovasculaires, cette thèse visait également à évaluer l'impact de ces composés sur la fonction plaquettaire. Ces études comprenaient les évaluations de l'effet des anthocyanes et de leurs métabolites sur l'activation des plaquettes et l'agrégation plaquettaire leucocytaire en réponse à adénosine diphosphate exogène. L'adénosine diphosphate est un agoniste plaquettaire qui est stocké dans leurs granules denses et libéré après leur activation. Réponse plaquettaire à de faibles niveaux de cette molécule a été rapporté comme un paramètre avec une valeur prédictive des événements cardiovasculaires et présente donc une cible rationnelle pour l'évaluation des effets bénéfiques de ces composés sur la santé cardiovasculaire. Pour ces études, des échantillons de sang prélevés chez sept sujets de sexe masculin en bonne santé apparente ont été incubées avec des anthocyanines à une concentration de 0.1 μM ou 4-hydroxybenzaldéhyde, protocatéchique, vanillique, l'acide férulique et hippurique à 0.5 μM, 0.2 μM, 2 μM, 1 μM et une concentration de 2 μM, respectivement. Par la suite, les échantillons ont été stimulés avec de l'adénosine diphosphate, marqués et analysés par

cytométrie de flux. L'impact des composés testés sur la fonction plaquettaire a été évaluée en mesurant l'expression des marqueurs d'activation surface P-sélectine et GPIIb/IIIa, ainsi que des plaquettes monocytes et des agrégats de plaquettes-neutrophiles. P-sélectine présente une molécule d'adhésion cellulaire qui est stocké dans les granules alpha des plaquettes et une translocation à la surface des plaquettes a lieu seulement lors de leur activation. Il assure l'adhésion avec les neutrophiles et les monocytes par liaison à son ligand PSGL-1 exprimé sur la surface des leucocytes. L'activation des plaquettes est également associée à une activation conformationnelle de GPIIb/IIIa, un récepteur de fibrinogène qui assure la médiation de l'agrégation plaquettaire avec d'autres plaquettes, mais contribue également à l'agrégation des plaquettes avec des leucocytes. L'utilisation de cytométrie de flux avec les échantillons de sang total a permis non seulement de mesurer avec sensibilité ces marqueurs qui sont très pertinents pour la prévention des maladies cardiovasculaires, mais aussi de diminuer l'activation extracorporelle plaquettaire et de produire des résultats fiables qui peuvent être attribués exclusivement à un effet direct des composés testés sur la fonction plaquettaire. Les résultats de ces expériences ont montré que, sauf l'acide vanillique, les anthocyanes et leurs métabolites affectés de manière significative au moins l'un des paramètres étudiés, activation plaquettaire ou agrégation plaquettaire avec des leucocytaire. Ces résultats impliquent que les effets antiplaquettaires bénéfiques associés à la consommation d'aliments riches en anthocyanines pourraient aussi être une conséquence de l'action combinée des anthocyanes et de leurs métabolites sur la fonction plaquettaire. Les composés testés ont un effet variable sur la fonction plaquettaire. Parmi les anthocyanines testées, cyandin-3-arabinoside affiche la plus grande capacité à moduler la fonction des plaquettes, car il réduit le pourcentage de plaquettes positives P-sélectine, ainsi que la densité de ce récepteur de surface qui se traduit par une formation nettement réduite des agrégats plaquettes-neutrophiles. En revanche, péonidine-3-glucoside, delphinidine-3-glucoside ou cyanidine-3-glucoside affectés l'activation des plaquettes en atténuant la P-sélectine ou de l'expression de surface GPIIb/IIIa, tandis que la cyanidine-3-glucoside ne met en

évidence l'effet sur l'agrégation plaquettaire avec des neutrophiles. 4-hydroxybenzaldéhyde a été le plus efficace entre les métabolites, car il induit une réduction significative de l'activation plaquettaire, ainsi que dans leur agrégation avec les neutrophiles et les monocytes. Fait intéressant, 4-hydroxybenzaldéhyde était le seul composé testé qui ne montre pas l'effet significatif sur l'adhésion des monocytes aux cellules endothéliales activées comme observé dans les expériences d'adhésion cellulaire. Ces résultats suggèrent qu'en agissant sur les plaquettes et non sur les cellules endothéliales, ce métabolite pourrait potentiellement encore plus réduire les interactions entre les leucocytes et les cellules endothéliales et exercer un effet protecteur contre le développement de l'athérosclérose. Un nombre limité de données publiées sont disponibles sur les effets des anthocyanines et de leurs métabolites sur l'activation plaquettaire et leur agrégation avec les leucocytes dans les conditions *in vitro* soulignent l'importance des résultats obtenus dans cette thèse. L'impact des anthocyanes peonidine-3-glucoside, cyanidine-3-galactoside et cyanidine-3-arabinoside, ainsi que des métabolites 4-hydroxybenzaldéhyde et acide vanillique sur l'activation des plaquettes, n'a pas été évalué auparavant. En outre, cette thèse rapporte pour la première fois la capacité des anthocyanes et de leurs métabolites à affecter l'agrégation plaquettaire avec les leucocytes, un marqueur qui s'est avéré être un indicateur encore plus sensible du risque de maladie cardiovasculaire que l'activation plaquettaire.

Sur la base de tous les résultats de cette thèse, plusieurs conclusions peuvent être tirées. Les anthocyanines et leurs métabolites, dans des conditions physiologiquement pertinentes, peuvent réduire l'adhésion des monocytes et la migration transendothéliale, étapes initiales du développement de l'athérosclérose, en maintenant l'intégrité et la fonction des cellules endothéliales. Ces effets semblent être exercés par des mécanismes d'action moléculaires complexes de ces composés. Ces mécanismes incluent la capacité des anthocyanines et de leurs métabolites à interagir avec les protéines de signalisation cellulaire et à moduler leur activité et par conséquent l'activité des facteurs de transcription, conduisant à des changements dans l'expression des gènes ainsi que leur

capacité à moduler l'expression des micro-ARNs. En outre, les résultats de cette thèse ont également montré la puissance d'anthocyanes circulantes et de leurs métabolites aux conditions physiologiques pour atténuer l'activation plaquettaire et l'agrégation avec les leucocytes, les processus qui sont des contributeurs clés au développement des maladies cardiovasculaires. Ainsi, cette thèse a révélé les effets positifs des anthocyanines et de leurs métabolites sur la fonction endothéliale et plaquettaire et a fourni de nouvelles informations sur les mécanismes sous-jacents de leurs effets cardio-protecteurs.

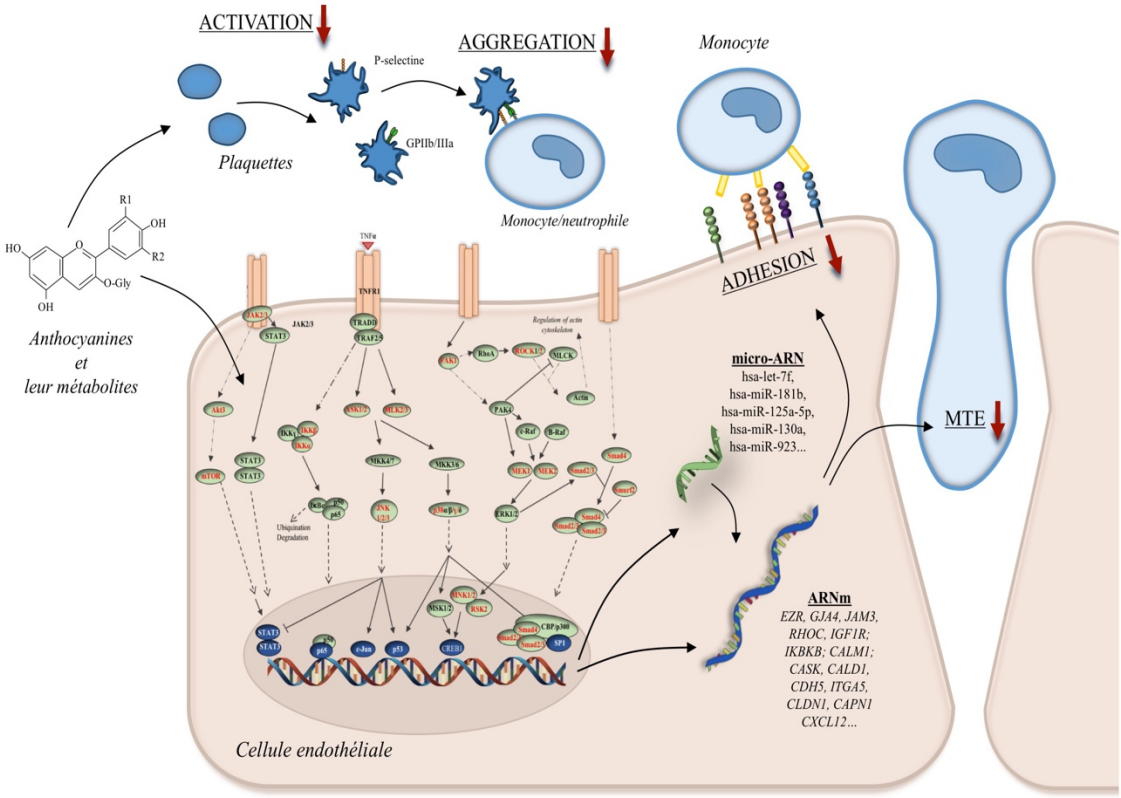

Mots clés : anthocyanes, métabolites, dysfonction endothéliale, adhésion des monocytes, transmigration endothéliale, activation plaquettaire, agrégation plaquettes-leucocytes

Domaine scientifique : Sciences biologiques

Sous-domaine scientifique : Nutrition humaine

Numéro CDU : [547.62+581.574]:[611.018.74:611.018.52] (043.3)

ABBREVIATIONS

AA	Amino acid
ADME	Absorption, distribution, metabolism and excretion
ADP	Adenosine diphosphate
Ala	Alanine
ALT	Alanine transaminase
ANOVA	Analysis of variance
AP-1	Activator protein 1
ApoE−/−	Apolipoprotein E knockout
APS	Ammonium persulfate
Asn	Asparagine
Asp	Aspartic acid
AST	Aspartate transaminase.
ATP	Adenosine triphosphate
b-Raf	Serine/threonine-protein kinase B-raf
BA	Binding affinity
BCA	Bicinchoninic acid
BMI	Body mass index
BSA	Bovine serum albumin
C	Crossover design
c-Raf	RAF proto-oncogene serine/threonine-protein kinase
CALD1	Caldesmon 1
CALM1	Calmodulin 1
CAPN1	Calpain 1
CASK	Calcium/calmodulin-dependent serine protein kinase
CAV1	Caveolin 1
CCL5	C-C Motif Chemokine Ligand
CDH5	Cadherin 5
CHD	Coronary heart disease
CLDN1	Claudin 1
Cmax	Maximal plasma concentration
COMT	Catechol-O-methyltransferase
CREB1	Cyclic AMP-responsive element-binding protein 1
CREBBP	CREB binding protein
Ct	Comparative threshold cycle
CVD	Cardiovascular diseases
CXCL12	C-X-C motif chemokine ligand 12
Cy-3-arab	Cyanidin-3-O-arabinoside
Cy-3-gal	Cyanidin-3-O-galactoside
Cy-3-glc	Cyanidin-3-O-glucoside
Cys	Cysteine
DB	Double-blinded studies
DBP	Diastolic blood pressure
Del-3-glc	Delphinidin-3-O-glucoside
DMSO	Dimethyl sulfoxide
EDTA	Trypsin/ethylenediaminetetraacetic acid
NOS3	Nitric oxide synthase 3
ERK	Extracellular signal-regulated kinase

ERK1	Mitogen-activated protein kinase 3
ESL1	Glycosylated E-selectin ligand 1
EDN1	Endothelin 1
EZR	Ezrin
F11R	F11 receptor
FABP4	Fatty acid binding protein 4
FAK	Focal adhesion kinase
FAK1	Focal Adhesion Kinase 1
FBS	Fetal bovine serum
FITC	Fluorescein isothiocyanate
FMD	Flow-mediated vasodilatation
FW	Fresh weight
GAPDH	Glyceraldehyde-3-phosphate dehydrogenase
GIT	Gastrointestinal tract
GJA4	Gap junction protein alpha 4
Glu	Glutamic acid
GLUT1	Glucose transporter 1
GLUT2	Glucose transporter 2
Gln	Glutamine
Gly	Glycine
GPIIb/IIIa	Glycoprotein IIb/IIIa
HCT	Hematocrit
HDL	High density lipoprotein
HGB	Hemoglobin
His	Histidine
hsCRP	High-sensitivity C reactive protein
HTB	Modified HEPES-Tyrode's buffer
HUVECs	Human umbilical vein endothelial cells
ICAM-1	Intercellular adhesion molecule 1
IGF1R	insulin-like growth factor 1 receptor
IKBKB	inhibitor of nuclear factor kappa B kinase subunit beta
IKK	Inhibitor of kappa B kinase
IKKα	Inhibitor of nuclear factor kappa-B kinase subunit beta
Ile	Isoleucine
ITGA5	integrin subunit alpha 5
IκB	Inhibitor of kappa B
JAK3	Tyrosine-protein kinase JAK3
JAM	Junctional adhesion molecule
JAM3	Junctional adhesion molecule 3
JNK	c-Jun N-terminal kinase
JNK1	Mitogen-activated protein kinase 8
KEGG	Kyoto encyclopedia of genes and genomes
LBRC	Lateral border recycling compartment
LDL	Low-density lipoprotein
Leu	Leucine
LFA-1	Lymphocyte function-associated antigen 1
Lys	Lysine
MAEC	Mouse aortic endothelial cells

MAPK	Mitogen-activated protein kinases
MCP-1	Monocyte chemoattractant protein-1
MEK2	Dual Specificity Mitogen-Activated Protein Kinase Kinase 2
Met	Methionine
MFI	Mean fluorescence intensity
MI	Myocardial infarction
miRNA	microRNA
MLCK	Myosin light chain kinase
MPV	Mean platelet volume
MtS	Metabolic syndrome
NADPH	Nicotinamide adenine dinucleotide phosphate
NF-κB	Nuclear factor kappa B
NO	Nitric oxide
ox-LDL	Oxidized low-density lipoprotein
p38β	Mitogen-activated protein kinase 11
PBS	Phosphate buffered saline
P	Parallel design
PC	Placebo-controlled trial
PCA	Protocatechuic acid
PCT	Plateletcrit
PE	Phycoerythrin
PECAM-1	Platelet endothelial cell adhesion molecule
PerCP	Peridinin chlorophyll protein complex
PF-4	Platelet factor 4
PFA	Paraformaldehyde
Phe	Phenylalanine
PKC	Protein kinase C
PLA	Platelet-leukocyte aggregates
PLT	Platelet count
PMA	Platelet-monocyte aggregates
PNA	Platelet-neutrophil aggregates
Pn-3-glc	Peonidin-3-O-glucoside
Pro	Proline
PSGL1	P-selectin glycoprotein ligand 1
PVDF	Hybond-P polyvinylidene difluoride
PWV	Pulse wave velocity
RAC1	Rac family small GTPase 1
RBC	Red blood cells
RCT	Randomised controlled trial
RHOA	Ras homolog gene family member A
RHOC	Ras homolog gene family member C
RIPA	Radio-immunoprecipitation assay
ROCK2	Rho-associated protein kinase 2
ROS	Reactive oxygen species
RQ	Relative quantitation
SB	Single blinded studies
SBP	Systolic blood pressure
SD	Standard deviation

SDS	Sodium dodecyl sulphate
SDS-PAGE	Sodium dodecyl sulphate polyacrylamide gel electrophoresis
Ser	Serine
SGLT1	Sodium-dependent glucose transporter 1
SOD	Superoxide dismutase
SRC	SRC proto-oncogene, non-receptor tyrosine kinase
SULT	Sulfotransferase
T2D	Type 2 diabetes
TC	Total cholesterol
TEMED	Tetramethylethylenediamine
TG	Triglycerides
TLDA	TaqMan array micro fluidic cards
TLN1	Talin 1
Tmax	Time to reach maximal plasma concentration
TNFα	Tumour necrosis factor alpha
Trp	Tryptophan
Tyr	Tyrosine
UGT	Uridine-5'-diphospho-glucuronosyltransferase
Val	Valine
VCAM-1	Vascular cell adhesion molecule 1
VLA-4	Very late antigen 4
vWF	Von Willebrand factor
WBC	White blood cells
3D	Three-dimensional
4-HBAL	4-hydroxybenzaldehyde

LIST OF TABLES AND FIGURES

LIST OF TABLES

LIST OF FIGURES

LIST OF SUPPLEMENTARY TABLES AND FIGURE

TABLE OF CONTENTS

1. INTRODUCTION

1.1. Cardiovascular diseases

Cardiovascular diseases (CVD) are a group of disorders that affect heart and blood vessels. They include coronary heart disease, cerebrovascular disease and peripheral artery disease and represent the leading cause of mortality worldwide (Mendis et al. 2011). The latest statistics show that in Europe CVD account for 3.9 million deaths each year or 45% of the total number of deaths. The incidence and prevalence of CVD are significant with around 11 million new cases per year and more than 85 million CVD cases reported in European population in 2015 (Wilkins et al. 2017). There are several risk factors connected with the development of CVD. They include non-modifiable risk factors such as age, sex, ethnicity and genetic background, and factors that can be treated or changed such as high blood pressure (hypertension), high cholesterol levels (dyslipidemia), diabetes, obesity, smoking, harmful use of alcohol, physical inactivity and unhealthy diet (Mendis et al. 2011). Of these risk factors, modifiable factors such as hypertension and dietary factors make the most significant contribution to CVD morbidity and mortality (Yusuf et al. 2004; Cassidy et al. 2016; Wilkins et al. 2017).

Atherosclerosis presents the common underlying pathology for most of the CVD. This chronic inflammatory condition is characterised by atherosclerotic lesions formed by accumulation of lipids, cellular and fibrous elements in the wall of large and medium-sized arteries. The early atherosclerotic lesions (i.e. fatty streak) consist of subendothelial accumulations of cholesterol-loaded macrophages, named foam cells, while more advanced lesions are composed of smooth muscle cells and lipid-rich necrotic debris (i.e. fibrous lesions). Over the years, these lesions can become increasingly complex, disturbing the blood flow and in the most severe cases, the plaque rupture and thrombosis can result in myocardial infarction (MI) or stroke (Lusis 2000; Libby et al. 2011).

The development of atherosclerosis is the result of the complex interplay between the endothelium of the blood vessel wall and circulating leukocytes and platelets. The role of these cells and their interactions will be detailed in the following sections.

1.1.1. The role of endothelium in CVD

Endothelium presents a single layer of endothelial cells lining the blood vessels and maintaining vascular homeostasis. It plays a pivotal role in preserving the vascular tone

by balancing the release of vasodilators (e.g. nitric oxide) and vasoconstrictors (e.g. endothelins) and regulates blood flow and coagulation process by secreting factors that affect platelet activity, blood clotting and fibrinolysis (Widlansky et al. 2003). It also controls inflammatory processes through the expression of various cytokines and adhesion molecules that mediate the recruitment of circulating inflammatory cells. This endothelial activation is required for adequate neutralisation of pathogens. Under homeostatic conditions, vascular endothelium provides a non-adhesive and non-coagulant blood-tissue barrier and secrets no or little proinflammatory molecules. However, during chronic inflammation and oxidative stress (i.e. the imbalance between reactive oxygen species (ROS) production and antioxidant defence) that are initiated by cardiovascular risk factors such as dyslipidemia, hypertension, or hyperglycemia, the endothelium becomes continuously activated. This activated endothelium is characterised by reduced vasodilatation (decrease in nitric oxide), prothrombic and proinflammatory properties and altered permeability (Bonetti et al. 2003; Brevetti et al. 2008). Increased endothelial permeability promotes the entry and retention of cholesterol-containing low-density lipoprotein (LDL) particles in the vessel wall, where they can undergo chemical modification (oxidation) and further stimulate endothelial cells to express proinflammatory factors (Osterud & Bjorklid 2003; Libby et al. 2011). Activated endothelium expresses inflammatory cytokines such as monocyte chemoattractant protein-1 (MCP-1), tumour necrosis factor alpha (TNFα) and interleukins (e.g. IL-1β, IL-6) as well as the adhesion molecules that promote the adhesion of circulating leukocytes and their subsequent transmigration into the blood vessel wall (Figure 1). In the subendothelium, monocytes (the most numerous recruited leukocytes) differentiate into macrophages, take up modified LDL and form foam cells. These cells also release proinflammatory agents that additionally promote leukocyte recruitment, transmigration, and foam cell formation, subsequently leading to the development of early atherosclerotic lesions (Libby et al. 2011).

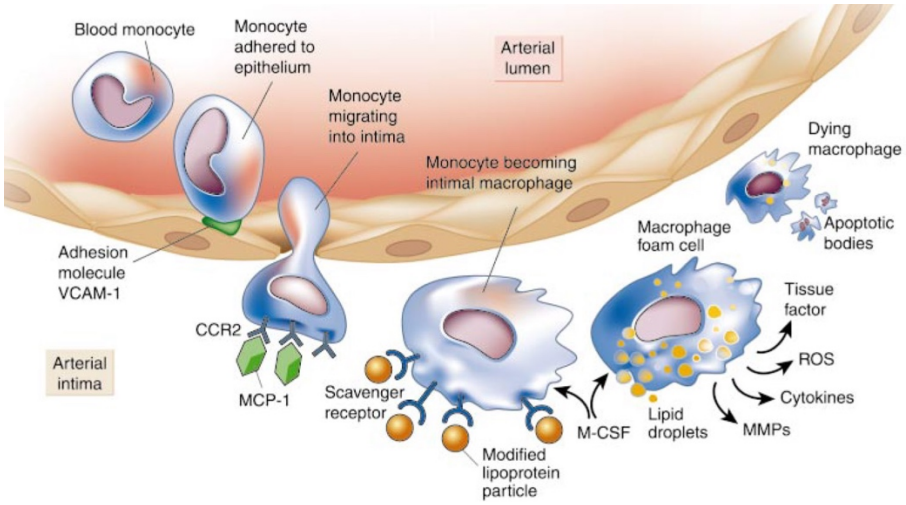

Figure 1. *Early events in the development of atherosclerosis, from Libby et al. 2002.*

These data show that the alteration of endothelial cell function and the consequent repetitive recruitment of circulating leukocytes into the vascular wall are the dominant features of atherosclerosis development that contribute to the progression of CVD. Due to their unique role as sensors and contributors to disturbed vascular homeostasis and associated diseases, the endothelial cells present the interesting target for exploring prevention of CVD.

1.1.1.1. Leukocyte adhesion and transendothelial migration

The processes of adhesion of leukocytes to activated endothelial cells and their transmigration into the subendothelial space are mediated by different adhesion molecules and cytokines. They begin with the capture of circulating white blood cells and their subsequent rolling on the endothelium of the vascular wall, both mediated by selectins (Figure 2). The inflamed endothelium expresses P-selectin and E-selectin, the most significant capture and rolling adhesion molecules, while most of the leukocytes express L-selectin. All of these molecules bind to glycosylated P-selectin glycoprotein ligand 1 (PSGL1), and E-selectin can additionally bind to glycosylated E-selectin ligand 1 (ESL1) and CD44 glycoprotein on leukocytes. Binding interactions between selectins and their ligands have remarkably fast on and off rates (i.e. bond association and dissociation rates) that allow the initial capture of circulating leukocytes and their labile rolling interactions with the endothelium (Ley et al. 2007). The purpose of rolling is to bring leukocyte in contact with the different chemotactic cytokines (chemokines) such as MCP-1 and IL-8, associated with proteoglycans located on the surface of endothelial cells

(Gerszten et al. 1999; Muller 2013). Binding of chemokines to their receptors on the leukocyte surface (G protein-coupled receptors) triggers the complex intracellular signalling that leads to rapid activation of leukocyte integrins and subsequent arrest of leukocyte rolling. Integrins belonging to the β1-integrin and β2-integrin subfamilies, such as the late antigen 4 (VLA-4) and lymphocyte function-associated antigen 1 (LFA-1) are the most relevant for the leukocyte arrest. Their intracellular activation results in a conformational change that favours tight binding of their ligands, i.e. immunoglobulin superfamily members such as vascular cell adhesion molecule 1 (VCAM-1) and intercellular adhesion molecule 1 (ICAM-1) that are expressed in a significant number on the surface of activated endothelial cells (Ley et al. 2007). The tight binding of VCAM-1 to VLA-4 and ICAM-1 to LFA-1, arrests monocytes on the endothelial surface, allowing them to subsequently spread, polarise and move laterally to find preferred sites of transmigration (Gerhardt & Ley 2015).

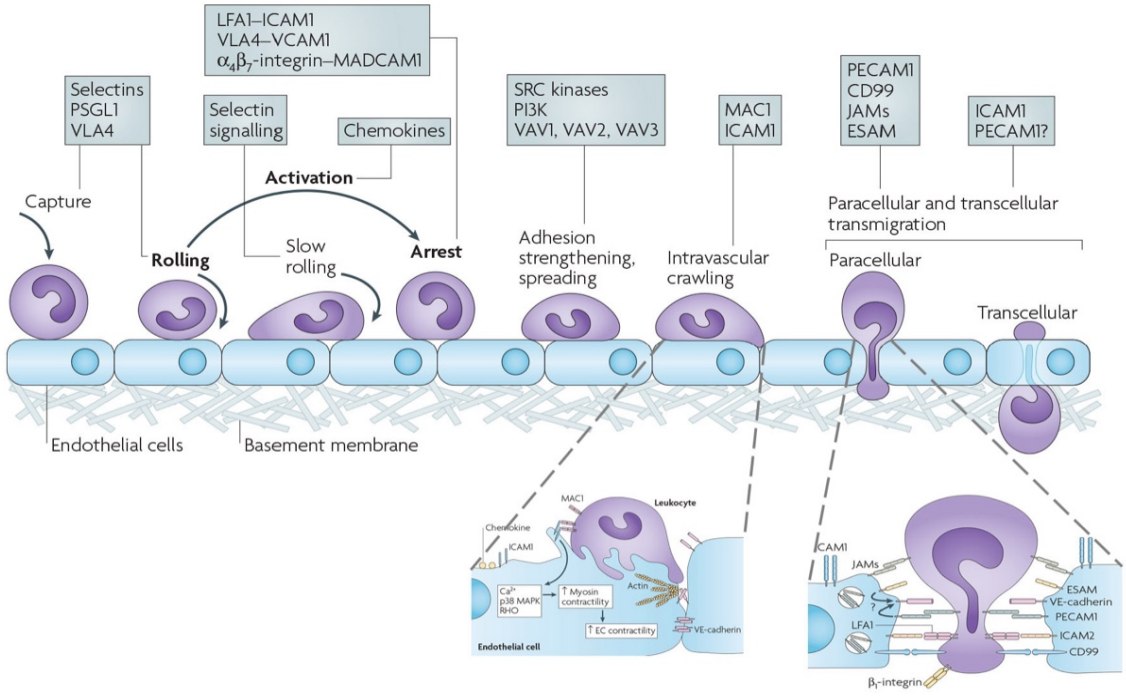

Figure 2. *Multistep process of leukocyte adhesion and transendothelial migration. Adapted from Ley et al. 2007.*

Transmigration can occur either through the cytoplasm of endothelial cells (transcellular transmigration) or between endothelial cells (paracellular transmigration), with the majority of transmigration events happening paracellularly. Unique finger-like endothelial cell projections, rich in clustered ICAM-1 and VCAM-1 adhesion molecules,

actin and actin-binding proteins, are believed to strengthen leukocyte-endothelial interactions and play a guiding role in leukocyte transmigration (Schnoor 2015). These structures named docking structures or transmigratory cups are created in response to initial endothelial binding to LFA-1 and VLA-4, partially wrapping the migrating leukocytes. Binding of leukocytes to clustered ICAM-1 and VCAM-1 activates several cell signalling proteins involved in cytoskeleton reorganisation such as Rac family small GTPase 1 (RAC1), SRC proto-oncogene, non-receptor tyrosine kinase (SRC) and Ras homolog gene family member A (RHOA) that promote loosening of endothelial cell junctions and paracellular transmigration (van Buul & Hordijk 2004; Hordijk 2006).

Endothelial junctions include tight junctions, adherens junctions and gap junctions that are crucial for maintaining the endothelial integrity and regulation of vascular permeability. Gap junctions mediate the direct exchange of ions and small molecules between two cells, while tight and adherens junctions, formed by a complex and dynamic network of transmembrane proteins, allow the regulated leukocyte passage (Bazzoni 2004). On its paracellular transmigration route leukocyte first faces tight junctions formed by transmembrane proteins like claudins, occludins and proteins belonging to a family of junctional adhesion molecules (JAM) that establish close contact between cells. Activation of RHOA, induced by ICAM-1 and VCAM-1 interactions with their leukocyte ligands, leads to the formation of actin-myosin fibres (stress fibres) and cell contraction that loosens cell junctions, increases inter-cellular space and promotes transmigration. The family of JAM proteins have been shown to actively participate in the leukocyte transendothelial migration by interacting with corresponding integrins on the leukocyte surface. Furthermore, vascular endothelial cadherin also known as cadherin 5 (CDH5), a transmembrane protein of adherens junction, is shown to be highly important for leukocyte transmigration by acting as a gatekeeper. This protein interacts in a homophilic way (i.e. the molecule on one cell interacts with the identical molecule on the other cell) attaching the cell membranes to intracellular networks of catenins and actin microfilaments. Activation of RAC1 and SRC signalling proteins leads to phosphorylation of CDH5, its subsequent dissociation from catenins and removal from the junction allowing leukocyte passage. Other junctional molecules such as platelet endothelial cell adhesion molecule (PECAM-1) and CD99 glycoprotein have also been shown to participate in transmigration. These proteins, enriched at endothelial cell

junctions and expressed diffusely on the leukocyte surface, facilitate transmigration by homophilic binding between the molecules on the two cells (Muller 2011; Muller 2013; Gerhardt & Ley 2015). It was recently shown that binding of PECAM-1 could also activate a unique transmigration complex that is actively transported to the site of transmigration by kinesin-microtubule motors. This transmigration complex named the lateral border recycling compartment (LBRC) is composed of subjunctional, intracellular endothelial membrane reticulum, rich in PECAM-1, CD99 and JAM proteins, surrounding the transmigrating cell. Homophilic binding of PECAM-1 triggers rapid, recycling of PECAM-1-bearing membrane to the transmigration site, supplying the migrating cell with functional molecules required to allow its transmigration (Gerhardt & Ley 2015). However, the physiological relevance of LBRC still needs to be shown *in vivo*.

Cell-cell interactions play an essential role in transendothelial migration. Specialized structures named focal adhesions are formed at these contact points. In these structures, actin filaments attach to integrin transmembrane receptors through a complex of various junctional proteins. Some of the proteins of focal adhesions present the structural connections between membrane receptors and the actin cytoskeleton, such as vinculin, talin, tensin, and paxillin, while others are signalling molecules like focal adhesion kinase (FAK) and protein kinase C (PKC). Binding to cell integrins results in a conformational change in their extracellular domains and activation of associated signalling molecules that lead to reorganisation of the actin cytoskeleton and consequent changes in the cell shape that allow cell movement (van Buul & Hordijk 2004; Hordijk & van Buul 2009).

Taken together, the recruitment of circulating monocytes, their adhesion to activated endothelium and subsequent transendothelial migration present the complex multistep processes that involve various adhesion molecules, chemokines, and signalling pathways and constitute the initial, key steps in the atherosclerosis development.

1.1.2. The role of platelets in CVD

Platelets are anuclear, discoid cell fragments formed from the cytoplasm of bone marrow megakaryocytes that in the resting state circulate in the bloodstream with the lifespan of seven to ten days. They contribute to the preservation of vascular integrity through their essential role in hemostasis, i.e. a natural process of preventing blood loss

at sites of mechanical blood vessel injury. This process involves rapid adhesion of platelets to the exposed endothelial cell matrix of an injured blood vessel, their activation and aggregation and a formation of a platelet plug that seals the damaged vessel wall. By contrast, in pathological conditions, such as atherosclerosis, platelet activity can lead to thrombosis, an exaggerated hemostatic response that obstructs the blood flow and can lead to stroke and myocardial infarction (Willoughby et al. 2002). In addition to the late stage thrombotic complications of atherosclerosis, platelets also play a key role as inflammatory mediators in the development of early atherosclerotic lesions. This function is achieved by interactions of activated platelets with monocytes, neutrophils, and endothelial cells, either directly, through their surface adhesion molecules, or indirectly, through various proinflammatory factors secreted from activated platelets (van Gils et al. 2009; Aukrust et al. 2010).

Platelet function in physiological and pathological conditions is based on their specific morphological characteristics. As anuclear cell fragments, platelets possess a large number of pre-synthesised molecules and some specialised structures that allow them to respond to altered environmental conditions and achieve their function rapidly. These molecules of high importance for hemostatic and inflammatory processes are stored in platelets' alpha and dense granules. Alpha granules are rich in membrane glycoproteins (e.g. P-selectin, integrin αIIb3, PECAM-1), adhesion molecules (e.g. Von Willebrand factor (vWF), fibrinogen, fibronectin), various chemokines and cytokines (e.g. MCP-1, platelet factor 4 (PF-4), macrophage inflammatory protein 1α, C-C Motif Chemokine Ligand 5 (CCL5), IL-1 and IL-8), clotting and fibrinolytic factors and their inhibitors (e.g. factor V, plasminogen and plasminogen activator inhibitor 1) as well as growth factors (e.g. platelet-derived growth factor, transforming growth factor β1, insulin-like growth factor-1, and vascular endothelial growth factor), while dense granules contain platelet agonist adenosine diphosphate (ADP), other nucleotides and calcium ions (Nurden 2011; Schnoor 2015). Binding of platelet agonist such as ADP, thrombin, prostaglandins or chemokines to their receptors on the surface of resting platelets triggers cell signalling that leads to platelet activation characterised by changes in platelet shape (formation of multiple pseudopodia), expression of specific surface receptors and release of platelet granule content. The specific receptors such as P-selectin or an active form of glycoprotein IIb/IIIa (GPIIb/IIIa, synonym integrin αIIbβ3) appear

on the surface of activated platelets and allow their direct interactions with leukocytes and endothelium. P-selectin is a glycoprotein that is stored in the α granules of resting platelets. Upon platelet activation, P-selectin is translocated from α granules to the platelet surface where it binds to its ligand PSGL-1 expressed on leukocytes and endothelial cells, thus mediating the initial contact with these cells. Additionally, platelet activation is associated with a conformational change in the GPIIb/IIIa, an integrin family member exclusively expressed by platelets. On the surface of resting (non-activated) platelets, this protein is present in the inactive state. However, binding of platelet agonist induces cell signalling that leads to its activation and increased affinity and avidity for its ligands fibrinogen and vWF. Aside from its role in platelet-platelet aggregation during hemostasis, this protein is also important in mediating the firm platelet adhesion to leukocytes and endothelial cells (Jennings 2009; Aukrust et al. 2010).

In inflammatory conditions, the interaction between platelets and activated endothelium is usually initiated by the endothelial release of platelet binding and stimulating agents, such as ADP and vWF that promote platelet activation and adhesion to endothelium. Stable complex of platelets and activated endothelial cells stimulates secretion of platelet-derived molecules such as PF4, CCL5 and IL-1β. These molecules further induce the inflammatory responses in endothelial cells such as the expression of adhesion molecules (e.g. E-selectin, VCAM-1, ICAM-1) and various chemokines and cytokines (e.g. MCP-1, IL-8 and IL-6) that promote leukocyte adhesion to endothelium and their transmigration (Gawaz et al. 2000; Gawaz et al. 2005; Yu et al. 2005). Additionally, adhered platelets contribute to these processes by their direct involvement in leukocyte rolling and arrest. This is achieved by binding of P-selectin on the adhered platelets with its leukocyte ligand PSGL-1 (Kuijper et al. 1998) as well as by deposing platelet-derived chemokines on the endothelial cell surface, which induces leukocyte arrest and strengthens its adhesion to endothelium (von Hundelshausen et al. 2001).

Inflammatory conditions also promote aggregation of activated platelets with circulating leukocytes. The extent of formation of these aggregates is dependent on the extent of platelet activation. The platelet-leukocyte aggregates (PLA) have been reported in clinical conditions such as hypertension, acute or stable coronary syndromes, MI, stroke and diabetes (Furman et al. 2001; Nomura et al. 2002; McCabe et al. 2004; Elalamy et al. 2008). They present a sensitive marker for *in vivo* platelet activation and are

increasingly considered as the biomarker of CVD (van Gils et al. 2009). The binding of activated platelets to leukocytes as well as the deposition of platelet-derived molecules on leukocyte surface leads to increased expression and activation of leukocyte integrins (CD11b/CD18 and VLA-1) and secretion of proinflammatory agents like TNFα, IL-8, and MCP-1, further promoting inflammation and leukocyte recruitment (van Gils et al. 2009). Binding of platelets to leukocytes decreases the velocity of rolling on activated endothelium thus increasing the probability of leukocyte arrest and firm adhesion. These aggregates also show increased transmigration when compared to platelet-free leukocytes (Martins 2005; van Gils et al. 2008). During the transmigration, platelets are removed from leukocytes by mechanical stress and deposed on the endothelium, suggesting that the lifespan of PLA is at least partly associated with the leukocyte adhesion and transmigration process.

These data show that platelet activation and aggregation are important features of the development of atherosclerosis and CVD (Figure 3). Therefore, in addition to endothelial cells, platelets present the attractive targets for exploring susceptibility to CVD and their prevention.

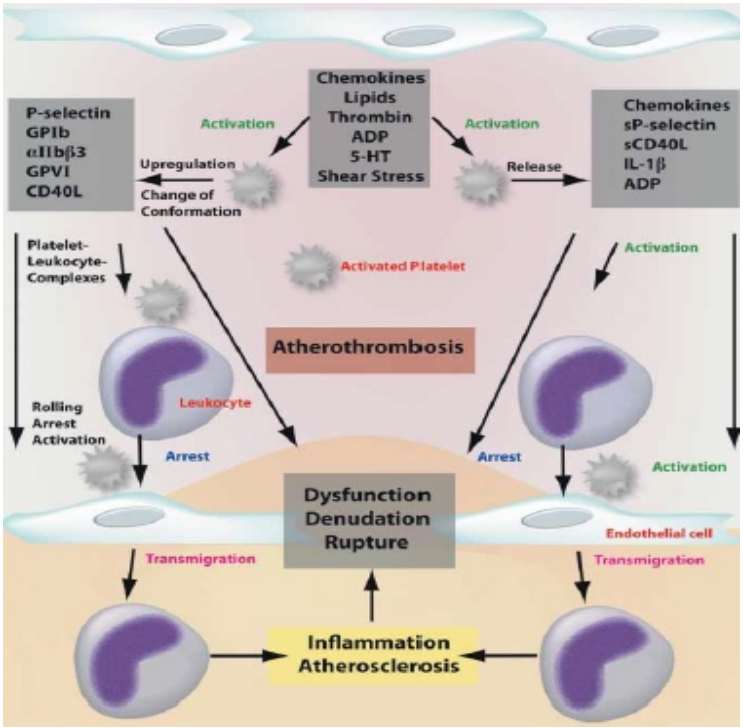

Figure 3. *A summary of platelet effects that contribute to the development of atherosclerosis, from Lievens and von Hundelshausen 2011.*

1.2. Diet and cardiovascular health

Diet is an important factor in the promotion and maintenance of health. It plays a major role in the development and progression of CVD, but can also, together with physical activity, present an important lifestyle modification for the prevention and management of CVD (Perk et al. 2012; Eckel et al. 2014). The evidence on the association between diet and CVD arises mainly from epidemiological cohort studies investigating the relationship between dietary patterns (overall diet) or specific foods and CVD outcomes, as well as from randomised controlled trials (RCT) usually assessing the effect on surrogate markers of CVD risk (e.g. endothelial dysfunction, hypertension, lipid profiles). Results from two recent meta-analyses of prospective cohort studies have shown an increased risk of CVD for a Western-type diet, i.e. a diet characterised by high intake of red and processed meat, refined grains, salty snacks, sweets and high-fat dairy products (Hou et al. 2015; Zhang et al. 2015). Also, these studies showed an inverse association between CVD risk and a healthy diet, i.e. a diet rich in fruit, vegetables and fish, moderate in alcohol and low in meat and dairy products (Figure 4).

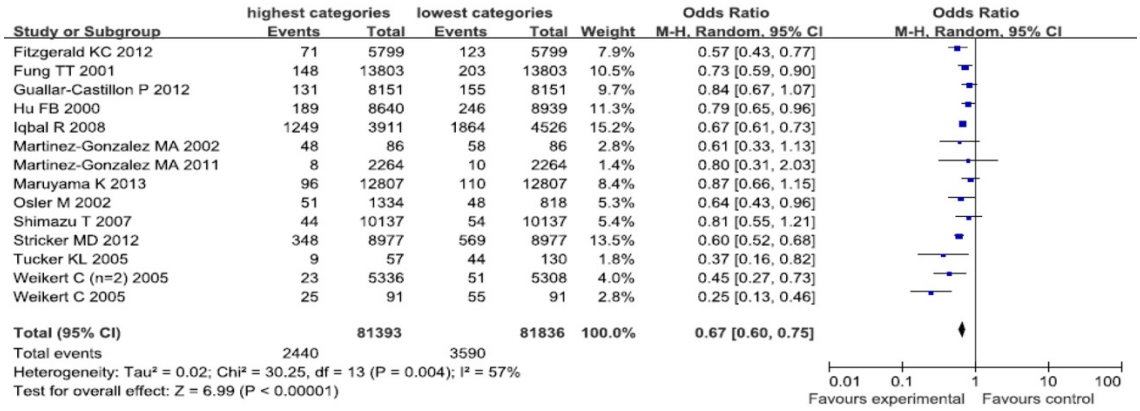

Figure 4. *Meta-analysis of studies examining the associations of healthy diet with CVD risk, from Zhang et al. 2015.*

Regarding healthy diets, the Mediterranean diet (i.e. characterised by high intake of fruits, vegetables, vegetable oils, whole grains, moderate alcohol consumption and low intake of animal products) has been associated with a reduced risk of cardiovascular mortality and decreased endothelial dysfunction and inflammation (Schwingshackl & Hoffmann 2014; Grosso et al. 2017). Furthermore, other healthy diets such as the Nordic diet, based on bilberries, whole grains, and fish, have also been reported to improve endothelial function and decrease inflammation (De Mello et al. 2011).

The important constituents of these healthy diets are fruits and vegetables. The consumption of these foods has been associated with the lower incidence of CVD and stroke based on evidence from numerous epidemiological studies and several meta-analyses (Dauchet et al. 2006; Gan et al. 2015; Sala-Vila et al. 2015). Two recent meta-analyses of cohort studies (Hu et al. 2014; X. Wang et al. 2014) reported a 5% and 4% reduction in risk of CVD mortality for each additional serving/day of fruits and vegetables, respectively, as well as the reduced risk of stroke by 32% for each 200 g/day increase in fruit consumption or by 11% for the same increase in vegetable consumption. Also, several dietary interventions have shown that specific fruits, vegetables and derived products such as berries, citrus fruits, cocoa, leafy vegetables, juices and wine, may exert beneficial effects on different markers of CVD (Dohadwala & Vita 2009; Galleano et al. 2009; Basu, Rhone, et al. 2010; Zheng et al. 2017). These observations underline the general recommendations for consuming at least 400 g of fruits and vegetables per day (FAO/WHO 2004).

Despite convincing evidence of beneficial health effects of fruits and vegetables, their key constituents and the precise mechanisms by which these foods exert health effects are still not well established. Health-promoting properties of fruits and vegetables could be attributed not only to their low-calorie value but also to the high levels of fibre, essential micronutrients and bioactive compounds like polyphenols. Increasing body of evidence suggests that polyphenols can indeed underlie or contribute to cardiovascular health benefits associated with diets rich in fruits and vegetables (Morand et al. 2011; Rodriguez-Mateos et al. 2014; Medina-Remón et al. 2017).

1.2.1. Dietary polyphenols

Polyphenols are the biggest and widely distributed group of phytochemicals, abundantly present in the human diet. In plants, these molecules are involved in pollination and seed dispersal as well as protection against herbivores, microorganisms and ultraviolet radiation (Chalker-Scott 1999). In plant-food, polyphenols contribute to organoleptic characteristics, such as smell, taste (e.g. bitterness, astringency) and colour (Pandey & Rizvi 2009). They are regularly consumed in fruits, vegetables, cereals and plant-derived beverages such as wine, fruit juices, herbal tea, and coffee, with an

estimated intake of more than 1 g/day (Pérez-Jiménez et al. 2011; Zamora-Ros et al. 2016).

Polyphenols are structurally highly diverse compounds, with more than 8000 different phenolic structures identified in plants. They are characterised by the presence of phenolic rings, i.e. aromatic rings with one or more hydroxyl groups attached (Tsao 2010). Depending on the number of phenolic rings and structural elements connecting these rings, polyphenols are classified into four major groups: phenolic acids, lignans, stilbenes, and flavonoids (Figure 5). Of these, phenolic acids and flavonoids are the most abundant polyphenols in the human diet, accounting for almost one-third and two-thirds of total polyphenol intake, respectively (Scalbert & Williamson 2000). By contrast, stilbenes and lignans are in the human diet present only in low quantities, due to their low contents in foods or a limited number of food sources.

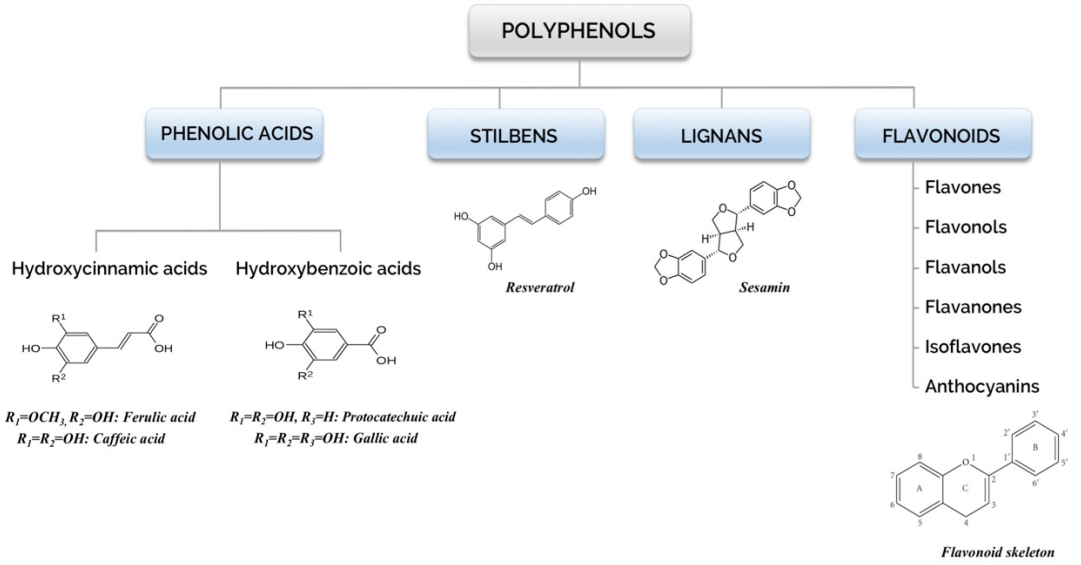

***Figure 5**. Major polyphenol groups*

Phenolic acids are a polyphenol group that includes hydroxybenzoic and hydroxycinnamic acids and their derivatives (Figure 5). Hydroxycinnamic acids (e.g. caffeic, ferulic and p-coumaric acids) occur in high quantities in many regularly consumed foods (0.5- 2.2 g/kg FW), such as fruits, especially pomes and berries, coffee and cereals, therefore presenting the most abundant polyphenols in the human diet (El-Seedi et al. 2012). Hydroxybenzoic acids (e.g. gallic, vanillic, protocatechuic acid (PCA)), both free and esterified, are in plant foods present in low quantities, except in

certain berry fruits (e.g. raspberries, blackberries and blackcurrants), black radish and onions (Del Rio et al. 2013).

Flavonoids present the largest and most studied polyphenol group, widely distributed in plants. Chemically these compounds are characterised by two benzene rings (rings A and B) linked with a heterocyclic pyrane ring (ring C) (Figure 5). Depending on the level of oxidation and substitution pattern of the C-ring these compounds can be further classified as isoflavones (abundant in cereal grains), flavones (parsley, celery, broccoli), flavonols (broccoli, onion, tomato, tea), flavanones (citrus fruits and beverages), flavanols (cocoa, tea, fruits, wine) and anthocyanins (berry fruits and wines) (Figure 6).

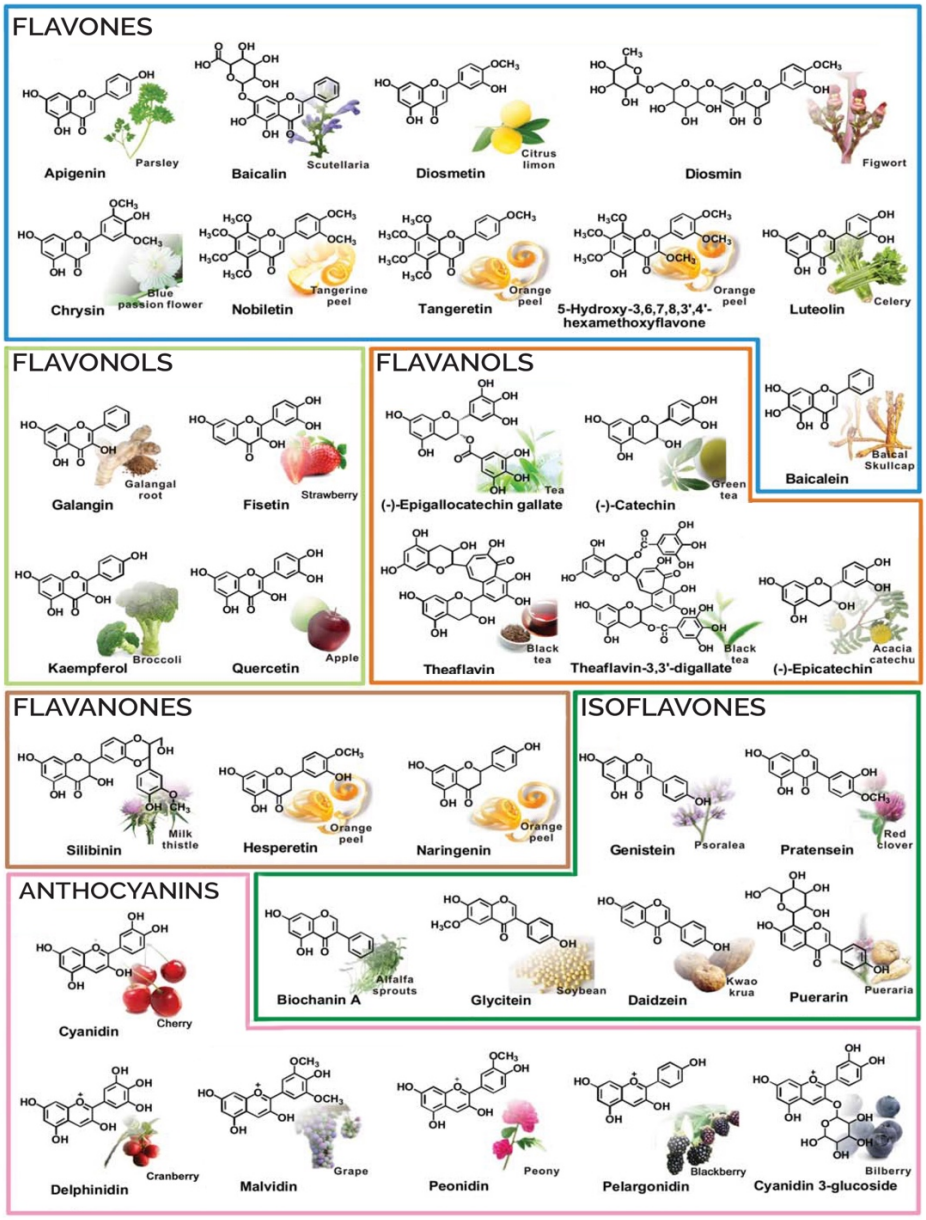

***Figure 6**. Flavonoids and their dietary sources, from Pan et al. 2010.*

1.2.2. Dietary polyphenols and CVD

The effects of polyphenols, especially flavonoids, on cardiovascular health have been intensively studied, and still present an active field of scientific research. Data from numerous epidemiological, clinical, animal and mechanistic *in vitro* studies support the protective role of these compounds against the development of CVD (Chanet et al. 2012; Del Rio et al. 2013; Rodriguez-Mateos et al. 2014). It has been shown that polyphenols can exert anti-inflammatory, antioxidant and antithrombic activates that can contribute to their cardioprotective effects (Pandey & Rizvi 2009; A.N. Li et al. 2014). This range of polyphenol biological activities could be explained by their ability to act trough different complex non-specific and/or specific mechanisms. First are based on the ability of polyphenols to interact with plasma membranes, leading to changes in their structure and physical characteristics that could affect cell function. Second concern the particular structural and conformational characteristics of specific polyphenols and their biological targets, including their ability to modulate enzyme activities and interact with receptors or transcription factors affecting gene expressions (Fraga et al. 2010; Krga et al. 2016).

Since this thesis focuses on anthocyanins, the characteristics of this group of polyphenols and their effects on cardiovascular health are further detailed.

1.3. Anthocyanins and cardiovascular health

Anthocyanins (of the Greek *anthos* = flower and *kyáneos* = blue) are water-soluble plant pigments, responsible for the red, purple and blue colouration of many fruits, flowers and leaves. Additionally, they can be found in other plant tissues such as stems, roots, bulbs and tubers (Andersen & Jordheim 2010).

The interest in these compounds has dramatically increased over the past two decades due to diverse health-promoting effects associated with the consumption of anthocyanin-rich plant foods. Anthocyanins have been associated with the prevention of CVD, neurodegenerative diseases and cancer as well as vision improvements (Jing et al. 2008; Wallace 2011; Arfan et al. 2012; Subash et al. 2014).

Good knowledge of anthocyanin chemistry, dietary sources and fate in the human body (i.e. absorption, distribution, and metabolism) is a prerequisite for understanding the role of anthocyanins in the prevention of CVD, their biological effects and underlying mechanisms of action. An overview of these aspects is given in the following sections.

1.3.1. Chemical structure and characteristics of anthocyanins

Anthocyanins are glycosylated, polyhydroxy or polymetoxy derivatives of flavylium cation (2-phenylchromenylium). To date, there are 702 different anthocyanins and 27 anthocyanidins (the sugar-free, aglycone forms of anthocyanins) identified in nature. However, only six anthocyanidins: cyanidin, delphinidin, pelargonidin, peonidin, malvidin and petunidin are widely distributed, accounting for more than 90% of all known anthocyanins (Andersen & Jordheim 2013) (Figure 7).

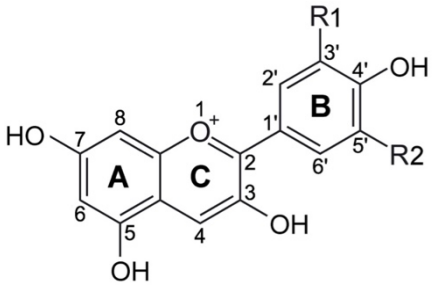

Anthocyanidin	R1	R2	Distribution
Pelargonidin	- H	- H	12%
Cyanidin	- OH	- H	50%
Delphinidin	- OH	- OH	12%
Peonidin	- OCH_3	- H	12%
Petunidin	- OH	- OCH_3	7%
Malvidin	- OCH_3	- OCH_3	7%

***Figure** 7. Structure and approximate distribution of six main anthocyanidins. Adapted from Fang 2014.*

The diversity of anthocyanin structure is achieved by differences in 1) the number and position of hydroxy groups and a degree of their methylation, 2) the nature, number and position of sugar attached to the aglycone and 3) the nature and number of aliphatic and aromatic acids linked to these sugars (Kong et al. 2003). Glucose, galactose, rutinose (rhamnosyl-glucose), rhamnose, arabinose and xylose are commonly found attached to anthocyanidins as mono-, di-, or trisaccharide forms. They are mainly bound to C3-position on the C-ring or C5 or C7-position on the A-ring (Fang 2014). These attached sugars can also be acylated with aromatic acids such as p-coumaric, ferulic, caffeic and p-hydroxybenzoic acids and/or aliphatic acids like malonic, acetic, malic and oxalic acids (Francis & Markakis 1989).

Anthocyanins are highly soluble in water and alcoholic solutions due to the presence of phenolic hydroxyl groups (de Pascual-Teresa & Sanchez-Ballesta 2008). They are reactive and very unstable compounds, which stability can be affected by pH, temperature, light, as well as the presence of oxygen, enzymes, other flavonoids, proteins and metal ions (Castañeda-Ovando et al. 2009). In aqueous solution, anthocyanins can form several structural isoforms, which relative abundance at equilibrium varies with pH

and anthocyanidin structure (Mazza & Brouillard 1987). Anthocyanins are the most stable at low pH (1-3) where they occur as flavylium cations that are red coloured. As the pH increases, the most of the flavylium cations transform to blue quinoidal forms (pH 2-4) or colourless carbinol pseudo-base and pale yellow chalcone (pH 5-6) (Fossen et al. 1998). The stability of glycosylated and acylated forms is significantly increased over aglycones (Zhao et al. 2014).

1.3.2. Dietary consumption of anthocyanins

Anthocyanins are important constituents of the human diet. They are regularly consumed in many fruits and fruit-derived products (e.g. wines, juices and jams) and some dark-coloured vegetables and cereals (e.g. eggplant, red onion, red cabbage, black rice). Furthermore, they are present in the diet as the colouring agent E163 that is increasingly used as an additive in the food industry for various foods and beverages (Heinonen 2001). Among fruits, the most commonly eaten anthocyanin sources are berry fruits belonging to *Vitaceae* family (species *Vitis vinifera*), *Rosaceae* family (e.g. strawberries, raspberries, blackberries, cherries, apples, plums) and genera Ribes (e.g. blackcurrants) and Vaccinium (e.g. bilberries, blueberries, cranberries) of *Ericaceae* family (Andersen & Jordheim 2013). In these dietary sources anthocyanin concentration usually reaches several hundreds of mg in 100 g of fresh weight (FW), providing substantial anthocyanin doses in a single serving (Table 1). In several foods such as elderberry, chokeberry and purple corn anthocyanin concentrations are even higher, reaching up to 1816, 1480 and 1642 mg/100 g FW, respectively (de Pascual-Teresa & Sanchez-Ballesta 2008) (Table 1). However, it should be noted that in foods anthocyanin concentrations can vary considerably as a consequence of genetic, environmental and agronomic factors such as light, temperature, humidity, fertilisation, but also on conditions of processing and storage (Biesiada & Tomczak 2012).

***Table 1**. Anthocyanin concentrations in foods. Adapted from de Pascual-Teresa and Sanchez-Ballesta 2008.*

Food	Content (mg/100g f.w.)
Elderberry	200–1816
Chokeberry	410–1480
Red grape	30–750
Bilberry	300–698
Raspberry	20–687
Black currant	130–476
Cherry	2–450
Blackberry	82.5–325.9
Blueberry	25-495
Cranberry	67–140
Red currant	22
Strawberry	19–55
Plum	2–25
Apple, Red delicious	1.7
Pomegranate (juice)	600–765
Port Wine	14–110
Red Wine	16.4–35
Purple corn	1642
Black rice	10–493
Red cabbage	322
Black olives	42–228
Red radish	100–154
Eggplant	8–85
Red onion, processed	23.3–48.5
Black bean	24.1–44.5

The daily anthocyanin intakes vary greatly depending on dietary habits of the studied population that are influenced by socioeconomic, demographic and lifestyle factors (Burton-Freeman 2010). They are still poorly established, mainly due to the absence of available information in food composition databases and variations in results depending on the used dietary assessment. They range from 2.7 to 82 mg/day, with estimated habitual anthocyanin intake of 58 mg/day in France (Pérez-Jiménez et al. 2011), 82 mg/day in Finland (Heinonen 2001), 12.5 mg/day in the US (Wu et al. 2006), 7.6 mg/day in Belgium (Mullie et al. 2007), 5-9 mg/day in the UK (Clifford & Brown 2006) and 2.7 mg/day in Germany (Watzl et al. 2002).

1.3.3. Anthocyanin bioavailability

To be able to exert their effect in the human body, ingested dietary anthocyanins need to be available in the circulation and tissues. Bioavailability is defined as a portion of the ingested dose of a compound that reaches the general circulation and specific sites where

it can exert its action (Porrini & Riso 2008). Anthocyanin bioavailability has been previously reported to be very low, with the recovery of less than 1% of the ingested anthocyanin dose (Kay et al. 2005). However, recent human bioavailability study, using isotope-labelled anthocyanin cyanidin-3-glucoside (cy-3-glc), has reported the extensive anthocyanin metabolism and a recovery of 12.4% (Czank et al. 2013). This suggests that the anthocyanin bioavailability is much greater than previously thought due to their new identified metabolites. Therefore, a good understanding of the faith of dietary anthocyanins in the human body following their intake, i.e. their absorption, distribution, metabolism and excretion (ADME) is of great importance for assessing their possible biological effects. However, there are still gaps in the knowledge concerning this topic.

In foods, anthocyanins are present as glycosides. Following the consumption, they enter and move through different regions of the gastrointestinal tract (GIT) (Figure 8). There, the specific pH, composition of the dissolved gases and metabolic activity can lead to anthocyanin degradation and metabolism (He et al. 2005). Anthocyanins that are absorbed along GIT are transported through the portal vein into the liver, where they can be further metabolised. Subsequently, these compounds can return to the GIT through the bile (enterohepatic-recycling) or enter the general circulation before being eliminated from the body by the urinary route (Lila et al. 2016). Anthocyanins that are not absorbed in the GIT are eliminated through faeces.

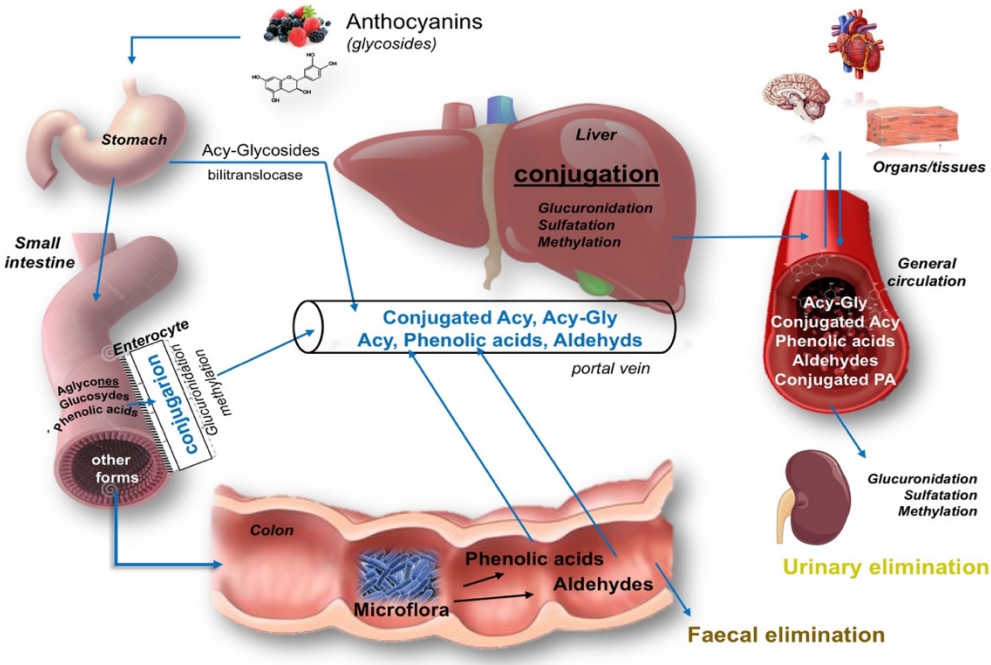

Figure 8. *Scheme of anthocyanin absorption and metabolism*

1.3.3.1. Anthocyanin absorption and metabolism

In the stomach, the low pH (1.5-4) provides favourable conditions for the anthocyanin stability, allowing them to persist in glycoside form. The presence of anthocyanin glycosides in the circulation within minutes of consumption in humans (Matsumoto et al. 2001; Rechner et al. 2002; Frank et al. 2003) suggests that the ingested anthocyanins, unlike other flavonoids, can be absorbed intact from the stomach (Talavéra et al. 2004). Since anthocyanins cannot pass the cell membranes by passive diffusion, a transporter system needs to be involved. An organic anion membrane carrier named bilitranslocase, expressed in the gastric mucosa, as well as in the liver, kidneys and vascular endothelium (Passamonti et al. 2002; Passamonti et al. 2005; Vanzo et al. 2008; Maestro et al. 2010), has been proposed to mediate anthocyanin transport. Its normal transport activity was found to be competitively inhibited by quinoidal forms of different anthocyanins *in vitro*, suggesting that this transporter could be responsible for their quick transport into the portal and general circulations (Passamonti et al. 2002). The involvement of glucose transporter 1 (GLUT1) in the transport of anthocyanin glucosides has also been suggested (Oliveira et al. 2015). However, these proposed mechanisms of anthocyanin gastric absorption are based only on findings from *in vitro* studies and their relevance to the absorption and metabolism in humans is still uncertain.

The important site for anthocyanin absorption is the small intestine. There, similarly to other flavonoids, anthocyanins undergo deglycosylation (i.e. cleavage of the glycoside) that releases lipophilic aglycones that can enter the epithelial cells by passive diffusion (Del Rio et al. 2013). Deglycosylation can be mediated by β-glucosidase in the intestinal lumen and lactase-phloridzin hydrolase in the brush border of the intestinal epithelial cells (Day et al. 2000). Alternatively, absorption could involve the active transport of intact glycosides into the epithelial cells by the sodium-dependent glucose transporter 1 (SGLT1) (Hollman et al. 1999; Gee et al. 2000) or glucose transporter 2 (GLUT2) (Day et al. 2000; Manzano & Williamson 2010) and their subsequent deglycosylation by cytosolic β-glucosidase (Németh et al. 2003). However, due to some contradictory results (Walton et al. 2006; Kottra & Daniel 2007; Felgines et al. 2008), the involvement of SGLT1 in the anthocyanin absorption is still uncertain.

Anthocyanin aglycones that enter the intestinal epithelial cells may be metabolised there to some extent before reaching portal circulation. This involves the

biotransformation typical for many xenobiotics, which increases their hydrophilicity and facilitates elimination from the body through bile and urine. This metabolism includes the phase I metabolism (oxidation, reduction, hydrolysis reactions) and phase II metabolism (conjugation reaction). In the intestine, anthocyanins can undergo methylation, sulphation, and glucuronidation, mediated by phase II metabolising enzymes catechol-*O*-methyltransferase (COMT), sulfotransferase (SULT) and uridine-5'-diphospho-glucuronosyltransferase (UGT), respectively (Del Rio et al. 2013). These reactions can also take place in the liver (i.e. the most important site of xenobiotic metabolism) and kidneys (Talavéra et al. 2005). Consequently, following the intake of anthocyanin-rich foods, the methylated, sulphated and glucuronidated anthocyanins are detected in human plasma and urine (Kay et al. 2005; Mullen et al. 2008; Azzini et al. 2010; de Ferrars, Czank, et al. 2014).

Prior to conjugation, anthocyanin aglycones can alternatively undergo degradation to phenolic acids and aldehydes within the intestinal lumen or epithelial cells. Anthocyanin degradation can also be a result of the activity of colonic microbiota. Anthocyanins that reach the colon are there exposed to 300-500 different bacterial species, with *Bacteroides*, *Eubacterium, Bifidobacterium* and *Clostridium* presenting the most abundant genera (Salminen et al. 1998). Gut microbiota releases many deglycosylation enzymes that cleave the sugar moiety, giving rise to aglycones that further degrade to phenolic acids (e.g. PCA, ferulic, hippuric acids) or aldehydes (Faria et al. 2014; Hribar & Ulrih 2014). Consequently, the portion of ingested anthocyanin forms decreases along the GIT, whereas the portion of phenolic acids increases. The products of anthocyanin degradation may also be absorbed from the intestines and further metabolised in the liver or kidneys (Czank et al. 2013).

Taken together, the results from the available studies assessing anthocyanin absorption and metabolism show that the dietary anthocyanins may be absorbed from the different regions of GIT (stomach, small intestines and colon) and extensively metabolised before eliminated from the body. The involved metabolic reactions may include microbial degradation as well as phase I and phase II metabolism.

1.3.3.2. Anthocyanins in the circulation

The available data on anthocyanin ADME in humans shows that anthocyanins and their aglycone conjugates, formed by phase II biotransformation, appear rapidly in the circulation. They peak at around 100 nM within 1.5 hours after the doses ≤ 2400 mg of anthocyanins (Table 2), and disappear from the bloodstream by 6 hours post-consumption (Rechner et al. 2002; Stalmach et al. 2012). The maximal plasma concentrations (Cmax) of total anthocyanins reported in these studies were in the range of 1.4-591 nM (Table 2), while Cmax of individual anthocyanins in human plasma varied from 0.06 to 367 nM (Kay et al. 2005; Kuntz, Rudloff, et al. 2015).

Table 2. *Summary of anthocyanin concentrations in plasma from selected human bioavailability studies with anthocyanin rich-sources*

Anthocyanin source	Dose[a]	Duration[b] (h)	Cmax[c] (nM)	Tmax[d] (h)	Reference
Elderberry	720 mg	24	97.4	1.2	(Cao et al. 2001)
Red wine	68 mg	6	1.38	0.3	(Bub et al. 2001)
Blackcurrant juice	1000 mg	6	85.3	1	(Rechner et al. 2002)
Blackcurrant concentrate	2380 mg	8	147.4	1.5	(Matsumoto et al. 2001)
Blueberry powder	1200 mg	4	29	4	(Mazza et al. 2002)
Red grape juice	283.6 mg	7	165.4	0.5	(Frank et al. 2003)
Red wine	279.6 mg	7	100.2	1.5	
Chokeberry extract	1300 mg	2	591.7	2	(Kay et al. 2004)
Chokeberry extract	721 mg	24	96.1	2.8	(Kay et al. 2005)
Strawberries	222 µmol	24	274	1.1	(Mullen et al. 2008)
Red grape extract	183.8 mg	24	7.9	2	(Garcia-Alonso et al. 2009)
Chokeberry juice	0.8*	24	32.7	1.3	(Wiczkowski et al. 2010)
Cranberry juice	94.7 mg	4	13.61	1.5	(Milbury et al. 2010)
Concord grape juice	238 µmol	24	5.9	2.15	(Stalmach et al. 2012)
Bilberries	919 µmol	6	108	1.31	(Sakakibara et al. 2014)
Elderberry drink	500 mg	3	33	2.3	(de Ferrars, Cassidy, et al. 2014)
Grape/blueberry juice	277.4 mg	2	5.63	1	(Kuntz, Rudloff, et al. 2015)
Grape/blueberry smoothie	324.5 mg	2	5.36	1.2	
Strawberry drink	34.7 mg	10	44.2	1.8	(Sandhu et al. 2016)
Chokeberry extract	45.1 mg	24	439	2.1	(Xie et al. 2016)
Red cabbage	6 mg	24	86.39	2	(Wiczkowski et al. 2016)
Bilberry extract	2400 mg	8	91.2	2.6	(Mueller et al. 2017)

[a] Administrated anthocyanin dose. [b] Sampling duration. [c] Cmax - maximum concentration in plasma. [d] Tmax - time to reach Cmax. * mg/kg body weight.

It should be noted that the plasma anthocyanin levels in most of the available bioavailability studies were proportional to their levels in tested food (Milbury et al. 2010; Kuntz, Rudloff, et al. 2015). For example, in one study the maximum levels of cy-3-glc and peonidin-3-glucoside (pn-3-glc) measured in plasma of healthy subjects after the consumption of grape/blueberry juice or smoothie, providing 13.6±0.2 and 19.1±0.7 mg of cy-3-glc and 54.5±0.7 and 53.8±2.0 mg of pn-3-glc, were eight times higher for pn-3-glc (0.8 nM) than for cy-3-glc (0.1 nM) (Kuntz, Rudloff, et al. 2015). Therefore, the reasonable physiological levels of glycosides reached after their dietary intake in substantial doses could be much higher than reported.

In addition to anthocyanins and their phase II conjugates, several anthocyanin bioavailability studies have also reported the presence of other compounds in plasma (e.g. different phenolic acids) that may be a result of anthocyanin metabolism (Rechner et al. 2002; Azzini et al. 2010; Stalmach et al. 2012). However, since their origin was hard to trace, these compounds were ascribed to anthocyanin food source used in studies. In recent studies investigating ADME of isotopically labelled cy-3-glc administrated to male subjects in a 500 mg single oral dose, also detected different phenolic acids (e.g. PCA, vanillic, ferulic, hippuric acids) and their phase I and phase II metabolites in the circulation (Czank et al. 2013; de Ferrars, Czank, et al. 2014). The use of isotope-labelling allowed authors to define the origin of these phenolic compounds and report them as anthocyanin-derived metabolites. Interestingly, unlike their parent anthocyanin that reached Cmax of 141 nM by 1.8 hours and disappeared from the bloodstream by 6 hours, metabolites picked (0.2-2 μM) at around 10 hours and were detectable in the circulation up to 48 hours post-ingestion. Furthermore, metabolites displayed biphasic serum profiles, with the first peak between 0 and 5 hours and a second, more pronounced peak between 6 and 48 hours that corresponded to absorption of anthocyanin bacterial metabolites from the colon (Figure 9). Therefore, these studies provided evidence of the extensive anthocyanin metabolism in the human body. Furthermore, they demonstrated that metabolites, especially those derived from microbial metabolism, present the dominant anthocyanin form in the circulation and suggested that these compounds could, at least partly, contribute to the beneficial health effects associated with the consumption of anthocyanin-rich sources.

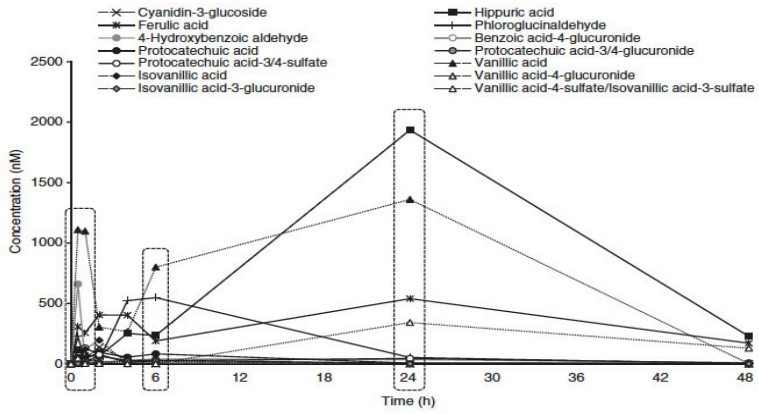

***Figure 9**. Biphasic serum profiles of anthocyanin forms in humans following the consumption of 500 mg of isotopically labelled cy-3-glc, from Warner et al. 2017.*

In summation, following the ingestion of dietary anthocyanins these compounds appear rapidly in the circulation where they are present for a short period of time at nanomolar concentrations, unlike their gut metabolites that appear later in the bloodstream and are present for significantly longer time and at higher, micromolar levels.

1.3.4. Cardiovascular health benefits of anthocyanins

Accumulating evidence suggests the protective effects of anthocyanin consumption against CVD. The overview of the data from epidemiological, clinical, preclinical and *in vitro* studies is provided in the following sections.

1.3.4.1. Evidence from epidemiological studies

Data from several epidemiological studies have reported an inverse correlation between anthocyanin intake and risk of CVD or CVD-related mortality. In a prospective study, following 34489 healthy postmenopausal women (55-69 years old) for 16 years, the anthocyanin intake (none versus any intake) was associated with a 12% and 9% lower risk of coronary heart disease (CHD) and CVD mortality, respectively (Mink et al. 2007). Similarly, a study of 38180 men and 60289 women (mean age of 70 and 69 years) with 7-year follow-up, observed a 21% reduction in risk of CHD mortality and 14% in CVD mortality in men and women when comparing higher (≥ 16.7 mg/day) with lower (< 5.5 mg/day) anthocyanin intakes (McCullough et al. 2012). Higher habitual anthocyanin intakes were also inversely associated with reduced risk of total MI in premenopausal

women (Cassidy et al. 2013) and non-fatal MI in men (Cassidy et al. 2016). The magnitude of this effect of anthocyanin consumption was higher in the study following 93600 premenopausal women (25-42 years old) for 18 years, with observed 32% decrease in MI risk when comparing extremes of anthocyanin intake (2.5 mg/day with 25.1 mg/day). Additionally, a food-based analysis in this study showed that combined intake of strawberries and blueberries tended to be associated with the reduced risk of MI. A 34% lower risk of MI was observed in women that consumed more than three portions per week compared with those that rarely consumed these anthocyanin-rich fruits (Cassidy et al. 2013).

Several cross-sectional and prospective studies have also shown the inverse association between anthocyanin intake and biomarkers of CVD risk, providing possible mechanistic support for the reported reduction in risk of CHD or CVD-related mortality. In a cross-sectional study investigating 1898 women aged between 18 and 75 years, higher anthocyanin intake was associated with significantly lower central blood pressure, mean arterial pressure and pulse wave velocity (PWV) that are direct measures of atherosclerosis and arterial stiffness (Jennings et al. 2012). In this study, a 44-mg increase in anthocyanin intake was associated with a reduction in PWV by 3.9% and a decrease of 3 mmHg in systolic blood pressure, suggesting that these effects could be easily achieved by incorporating around 1 to 2 portions of berries in an everyday diet. In several cross-sectional studies, higher anthocyanin intakes were also inversely correlated with different inflammatory biomarkers (e.g. IL-18 and C-reactive protein) and the overall inflammation score that combined several cytokines, markers of acute inflammation and oxidative stress (Chun et al. 2008; Jennings et al. 2014; Cassidy et al. 2015). Furthermore, a large prospective study following 156957 subjects for 14 years reported that the higher anthocyanin intake, mainly from strawberry and blueberry consumption, was associated with an 8% reduction in risk of hypertension (Cassidy et al. 2011). This reduction was the most pronounced in premenopausal women, which was in line with the most significant decrease in risk of MI also observed in this age group (Cassidy et al. 2013).

Taken together, results from the available epidemiological studies are promising regarding the role of anthocyanins against CVD, showing the inverse associations between anthocyanin consumption and CVD incidence, mortality or different biomarkers of CVD risks.

1.3.4.2. Evidence from clinical studies

The hypothesis created from epidemiological studies has initiated a number of clinical studies with the aim to provide cause-effect relationships that could explain the role of anthocyanins in the CVD prevention.

Several RCTs have investigated the effects of the consumption of different anthocyanin-rich sources on surrogate markers of CVD risk, such as hypertension, lipid profiles, endothelial dysfunction and platelet function. Results from short-term intervention studies have shown that the consumption of anthocyanin-rich berries and extracts can decrease both systolic and diastolic blood pressure and improve lipid profiles mainly in subjects at risk for CVD (Table 3). Few of these studies have also reported the improvements in arterial stiffness and endothelial function through a decrease in PWV and an increase in flow-mediated vasodilatation (FMD) of the brachial artery, respectively (Table 3). A double-blinded crossover RCT that investigated the acute effect of the consumption of a wild blueberry beverage containing 310 to 724 mg of anthocyanins on FMD in healthy men has reported the significant increase in FMD at 1, 2 and 6 hours post-consumption (Rodriguez-Mateos, Rendeiro, et al. 2013). Also, no significant difference in the effect between higher and lower anthocyanin doses was observed. Interestingly, the observed biphasic improvements in endothelial function correlated with the increased plasma levels of anthocyanins at around 2 hours and of their gut metabolites at 6 hours following the consumption of this blueberry drink. These results suggested that both anthocyanins and their gut metabolites could contribute to the reported beneficial effect of this anthocyanin-rich beverage. Several three- or six-month intervention trials that used purified anthocyanins have also reported the improvements in endothelial function, lipid profiles and inflammatory biomarkers in subjects with CVD risks (Table 3) therefore providing evidence that anthocyanins are at least partly responsible for the effects observed using anthocyanin-rich fruits and extracts.

To date, only a limited number of RCTs have investigated the effect of anthocyanins on platelet function. However, the available data do suggest that short-term dietary interventions with anthocyanin-rich foods and extracts can affect platelet function by decreasing platelet activation and platelet aggregation with other platelets and leukocytes and lowering the potential for clot formation and fibrinolysis (Sikora et al. 2012; Song et al. 2014; Santhakumar, Kundur, Fanning, et al. 2015; Santhakumar, Kundur, Sabapathy,

et al. 2015; Zhang et al. 2016; Thompson, Hosking, et al. 2017; Thompson, Pederick, et al. 2017).

In summation, evidence from clinical studies shows that anthocyanin-rich foods, extracts and purified anthocyanins can improve different markers of CVD risk. However, more well-designed long-term investigation trials that are focused on the effect of pure anthocyanins in both healthy and subjects with CVD risk are needed to strengthen the available evidence and establish the role of this compounds in the prevention of CVD.

Table 3. *Summary of the effect of anthocyanin-rich foods, extracts and purified anthocyanins reported in RCTs*

RCT design	Participants	Intervention (per day)	Dose* (mg/day)	Duration (weeks)	Significant findings	Reference
DB, PC, C	44 subjects, aged 62± 8y, with CHD	480 ml cranberry juice	94	4	↓carotid-femoral PWV (6%)	(Dohadwala et al. 2011)
DB, PC, P	54 subjects, ≥18 y, with hyperlipidemia	3x500 mg whortleberry extract	90	4	↓TG (30%) ↓TC (15.2%) ↓LDL (8.6%)	(Soltani et al. 2014)
DB, PC, C	21 healthy subjects, aged 21-45y	200 ml plum juice	202	4	↓platelet aggregation (2.7-5%) ↓platelet activation (17.2%), ↓plasma-fibrinogen (7.5%)	(Santhakumar, Kundur, Fanning, et al. 2015)
DB, PC, P	44 subjects, age 65.9±8.3y, post-MI	3×85 mg chokeberry extract	63.8	6	↓SBP (8.32%) ↓DBP (8.34%) ↓hsCRP (23%) ↓IL-6 (30%) ↓MCP-1 (29%) ↓sVCAM-1(28%) ↓sICAM-1 (15%) ↓ox-LDL (29%)	(Naruszewicz et al. 2007)
SB, PC, P	72 subjects, aged 57.5±6.3y, with CVD risk	bilberries, lingonberries black currants strawberry chokeberry, raspberries	515	8	↑HDL (5.2%) ↓SBP (1.2%) ↓platelet aggregation (11%)	(Erlund et al. 2008)
SB, PC, P	27 subjects, aged 47 ± 3y, with MtS	50g freeze-dried strawberries	154	8	↓TC (11%) ↓LDL (10%) ↓small LDL particles (16%) ↓VCAM-1 (18%)	(Basu, Fu, et al. 2010)
SB, PC, P	48 subjects, aged 50± 3y, with MtS	50 g freeze-dried blueberries	742	8	↓SBP (6%) ↓DBP (4%) ↓ox-LDL (28%)	(Basu, Du, et al. 2010)

Table 3. *(Continued)*

RCT design	Participants	Intervention (per day)	Dose* (mg/day)	Duration (weeks)	Significant findings	Reference
DB, PC, P	105 subjects, aged 20-60y, with primary hyperlipidemia	3x350 mg whortleberry extract	7.4	8	↓TG (19.2%) ↓TC (27.6%) ↓LDL (26.3) ↑HDL (37.5%)	(Kianbakht et al. 2014)
DB, PC, P	48 women, aged 45-60y, with pre- and stage 1 hypertension	22g freeze-dried blueberry powder	101.2	8	↓SBP (5.1%) ↓DBP (6.3%) ↓brachial-ankle PWV(6.5%)	(Johnson et al. 2015)
DB, PC, P	32 subjects, aged 65± 1y, with T2D	3x500 mg cranberry extract	NR	12	↓TC (8%) ↓LDL (12%) ↓TC:HDL (7.5 %)	(Lee et al. 2008)
PC, P	120 healthy subjects, aged 40–74y	Purified** anthocyanins	300	3	↓IL8 (45%), ↓CCL5(15%), ↓IFNα (40%)	(Karlsen et al. 2007)
DB, PC, C	16 subjects, mean age 38 y, sedentary, healthy	Purified** anthocyanins	320	4	↓platelet aggregation (29%) ↓platelet-leukocyte aggregation (39%), ↓platelet activation (10-14%)	(Thompson, Hosking, et al. 2017)
DB, PC, P	120 subjects, aged 40–65y, with dyslipidemia	Purified** anthocyanins	320	12	↓LDL (13.6%) ↑HDL (13.7%)	(Qin et al. 2009)
DB, PC, P	150 subjects, aged 40–65y, with hyper-cholesterolemia	Purified** anthocyanins	320	12	↑FMD (28.4%) ↑HDL (12%) ↓LDL (10%) ↑cGMP (12.6%) ↓sVCAM-1 (12%)	(Zhu et al. 2011)
DB, PC, P	150 subjects, aged 40–65y, with hyper-cholesterolemia	Purified** anthocyanins	320	24	↑HDL (14%) ↓LDL (10%) ↓hsCRP (21.6%) ↓sVCAM-1 (12%) ↓IL1β (12.8%)	(Zhu et al. 2013)
DB, PC, P	58 subjects, aged 56–67 y, with T2D	Purified** anthocyanins	320	24	↓LDL (7.9%) ↓HDL (19.4%) ↓TC (3.75%) ↓TG (23%) ↓apoB-48 (16.5%) ↓apoC-III (11.0%) ↓fasting plasma glucose (8.5%) ↓TNFα (8.6%) ↓IL6 (31.6%)	(Li et al. 2015)

*anthocyanin dose administrated in the study, ** purified from bilberry and black currant, DB-double-blinded, SB-single blinded, PC-placebo-controlled, P-parallel, C-crossover design, MtS-metabolic syndrome, T2D-type 2 diabetes, NR-not reported, SBP-systolic blood pressure, DBP-diastolic blood pressure, ox-LDL-oxidized LDL, TC-total cholesterol, HDL-high density lipoprotein, TG-triglycerides, hsCRP-high-sensitivity C reactive protein.

1.3.4.3. Evidence from animal studies

Findings from several animal studies also support the beneficial effects of anthocyanins on cardiovascular health. Several nutritional interventions performed with apolipoprotein E knockout ($ApoE^{-/-}$) mice that spontaneously develop atherosclerosis have reported that anthocyanin-rich extracts or pure compounds, administrated at nutritionally relevant doses, reduced the formation of atherosclerotic lesions in the aorta of these mice (Miyazaki et al. 2008; Mauray et al. 2009; Wang et al. 2010; Wu et al. 2010; Y. Wang et al. 2012). Furthermore, anthocyanin supplementation has been reported to increase survival following induced MI, decrease thrombus development and improve blood pressure, lipid profiles and endothelium-dependent vasorelaxation in several studies using different animal models of CVD (Ahmet et al. 2009; Suh et al. 2011; Yang et al. 2011; Rodriguez-Mateos, Ishisaka, et al. 2013; Zhang et al. 2013).

1.3.5. Molecular mechanisms of action of anthocyanins underlying their cardiovascular health properties

A number of *in vitro* and *in vivo* studies have been performed to identify mechanisms by which anthocyanins exert their cardioprotective effects. These health benefits were previously associated with their direct antioxidant properties, i.e. ability to transfer hydrogen (electron) to ROS and neutralise them. It was proposed that by exerting the direct antioxidant effect against ROS, which production is increased in the dysfunctional endothelium, anthocyanins could prevent LDL oxidation and associated inflammatory responses, and thus affect the development and progression of atherosclerosis (Tsuda et al. 1996; Yi et al. 2010). However, more recent studies have reviled the implication of more complex molecular mechanisms of action including modulation of gene expression, cell signalling and micro RNA expression that will be detailed in the following sections.

1.3.5.1. Effect on gene expression

Several *in vitro* studies have reported the ability of anthocyanins and their metabolites to reduce oxidative stress by modulating the expression of genes coding for antioxidant and detoxifying enzymes. Oxidative stress is an important promoter of inflammatory reactions and one of the hallmarks of endothelial dysfunction and atherosclerosis (Hajjar & Gotto 2013). Anthocyanin-mediated upregulation of the expression of genes encoding

enzymes involved in antioxidant defence, such as nicotinamide adenine dinucleotide phosphate (NADPH) quinone oxidoreductase 1, heme oxygenase-1 and superoxide dismutase (SOD), has been reported in different types of endothelial cells (Sorrenti et al. 2007; Cimino et al. 2013; Speciale et al. 2013; Fratantonio et al. 2015; Huang et al. 2016). Also, few studies have shown that anthocyanins can downregulate the expression of genes coding for different subunits of NADPH oxidase, which represents a major source of oxygen radical production (Lazzè et al. 2006; Chen et al. 2011; Speciale et al. 2013). These nutrigenomic effects were concomitant with reduced production of ROS and increased cell viability observed in these studies. Similar to *in vitro* evidence, the upregulation of the expression of genes encoding antioxidant enzymes like glutathione reductase, thioredoxin reductase 1 and SOD 1 and 2 has been observed in the aorta of $ApoE^{-/-}$ mice after 20-week long dietary supplementation with blueberries. These effects were accompanied by significant decreases in atherosclerotic lesion area in the aortic sinus and descending aorta of these mice (Wu et al. 2010). Results from these mechanistic studies suggest that the ability of anthocyanins to reduce oxidative stress by increasing the antioxidant defence and inhibiting lipid peroxidation can present one of the mechanisms underlying their observed anti-atherogenic effects.

In addition to the effect on oxidative stress, anthocyanins have been reported to modulate the expression of genes involved in the regulation of vascular tone. Anthocyanins at concentrations ranging from 0.1 to 100 μM have been shown to increase the expression of nitric oxide synthase 3 (*NOS3*) and decrease the expression of endothelin 1 (*EDN1*) in endothelial cells (Lazzè et al. 2006; Paixão et al. 2012; Edwards et al. 2015). Endothelin 1 is an endothelium-derived vasoactive peptide that contributes to the regulation of vascular tone and maintenance of cardiovascular homeostasis through the constriction of vascular smooth muscle. *NOS3* encodes an enzyme that produces the vasoactive nitric oxide (NO) from L-arginine, leading to a NO-dependent relaxation of vascular smooth muscle (Krga et al. 2016). Decreased bioavailability of endothelial-derived NO, the upregulation of *EDN1* and subsequently increased contractibility are important characteristics of endothelial dysfunction and pathogenesis of CVD (Böhm & Pernow 2007). Therefore, the increase in *NOS3* expression and NO synthesis, as well as downregulation of *EDN1* expression, could also represent a mechanism by which anthocyanins improve endothelial function and contribute to cardiovascular health.

Other available mechanistic studies have also shown the ability of anthocyanin extracts or pure compounds to affect the expression of genes involved in the regulation of inflammation, monocyte adhesion and transmigration (Chen et al. 2011; Chao, Lin, et al. 2013; Chao, Huang, et al. 2013; Huang, Liu, et al. 2014). As previously detailed, proinflammatory cytokines such as the interleukins and TNFα are produced in endothelial cells during the inflammatory insult, stimulating the expression of cell adhesion molecules on the surface of activated endothelium. The inflamed endothelium also promotes the production of chemotactic cytokines such as MCP-1 or IL-8 that guide leukocytes into the subendothelial space. Anthocyanins at concentrations ranging from 0.1 to 100 μM have been reported to modulate the expressions of genes coding for the adhesion molecules such as VCAM-1, ICAM-1 and E selectin and cytokines like IL-6, IL-8 and MCP-1 in different types of endothelial cells subjected to inflammatory mediators or oxidative stress (Speciale et al. 2010; Huang, Liu, et al. 2014; Huang, Wang, et al. 2014; Amin et al. 2015; Kuntz, Asseburg, et al. 2015). These effects were accompanied by a decrease in monocyte adhesion to activated endothelial cells observed in the cell adhesion experiments (Wang et al. 2010; Chen et al. 2011; Chao, Lin, et al. 2013; Chao, Huang, et al. 2013; Kuntz, Asseburg, et al. 2015). Similar to *in vitro* evidence, the inhibition of aortic expression of several proinflammatory factors and adhesion molecules involved in the recruitment of inflammatory cells (e.g. VCAM-1, ICAM-1, TNFα and inducible nitric oxide synthase) have also been reported in studies with ApoE$^{-/-}$ mice that consumed diet enriched in anthocyanin-based extracts or pure compounds (Xia et al. 2006; Wang et al. 2010; Xie et al. 2011). Furthermore, downregulation of aortic expression of scavenger receptors (scavenger receptor-A and CD36) responsible for the incorporation of modified LDL into macrophages, as well as decreased foam cell formation, were reported following a 20-week dietary supplementation with blueberries in ApoE$^{-/-}$ mice (Seymour et al. 2009). In addition to these studies that used targeted-based approach (focused on the impact on specific genes), there is one study that used a microarray-based holistic approach that allowed simultaneous investigation of the effect on several thousand genes. This microarray analysis of the gene expression in the aorta of ApoE$^{-/-}$ mice that consumed diet enriched in anthocyanin-rich bilberry extract during two weeks revealed changes in the expression of 1261 genes implicated in different cellular processes such as inflammation, cell

adhesion and transmigration (Mauray et al. 2012), proposing the multi-targeted mode of action of anthocyanins.

Taken together, mechanistic evidence suggests that anthocyanin-mediated modulations of the expression of different genes implicated in processes such as oxidative stress, inflammation, monocyte adhesion and transendothelial migration (Figure 10) could present the important mechanism in anthocyanin protection against the development of atherosclerosis and associated cardiovascular complications.

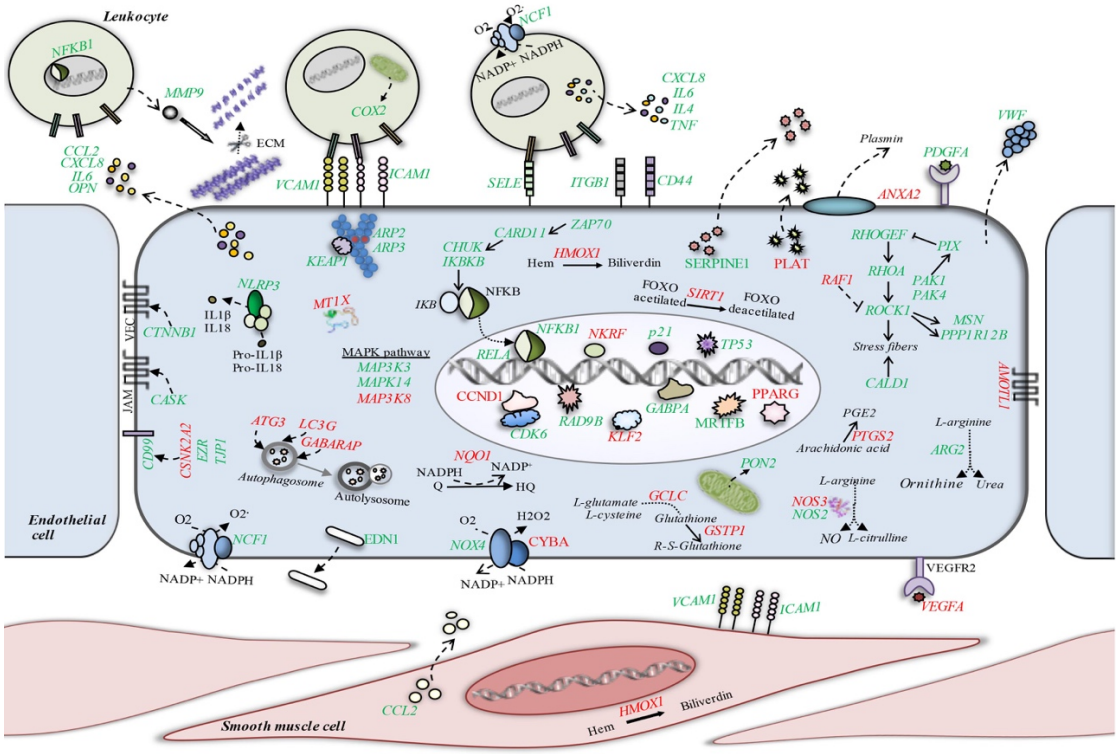

***Figure 10**. Summary of genes linked to vascular dysfunction, which expression has been identified as modulated by different polyphenols, from Krga et al. 2016.*

1.3.5.2. Regulation of cell signalling pathways

Cellular responses to changes in their environment require rapid and precise transmission of signals from the cell surface to the nucleus. These cell signalling pathways depend on protein phosphorylation and eventually lead to the activation of transcription factors, which induce the expression of target genes (Viatour et al. 2005). It has been suggested that the observed anthocyanin nutrigenomic effects are associated with their ability to affect cell signalling pathways such as the nuclear factor-κB (NF-κB) and mitogen-activated protein kinases (MAPK) pathways that play an essential role in

initiation and regulation of inflammatory processes. NF-κB presents the transcription factor that is closely associated with the development of atherosclerosis due to its important role in the regulation of multiple cellular processes such as inflammation, immune response, proliferation and apoptosis (Warboys 2011). This transcription factor functions as a dimer with the p50/p65 heterodimer as the most abundant form. Under normal physiological conditions, NF-κB heterodimer is bound to the inhibitor of kappa B (IκB) that keeps it in an inactive state in the cytoplasm. However, diverse extracellular stimuli, including oxidised LDL (ox-LDL) or cytokines such as TNFα can activate NF-κB signalling pathway in endothelial cells leading to stimulation of the IκB kinase (IKK) complex that triggers the phosphorylation of IκB, eventually causing its ubiquitination and proteasomal degradation (De Winther et al. 2005). Consequently, activated NF-κB dimer translocates freely to the nucleus where it regulates the expression of proinflammatory genes, such as the genes encoding adhesion molecules E-selectin, ICAM-1 and VCAM-1 or cytokines like TNFα, IL-1 and MCP-1, inducing the inflammatory response and promoting the leukocyte adhesion (Warboys 2011). In a few studies, anthocyanin-rich extracts or pure compounds have been shown to suppress ox-LDL or cytokine-stimulated NF-κB activation in endothelial cells through the inhibition of IκB phosphorylation and translocation of p65 subunit into the nucleus (Xia et al. 2007; Speciale et al. 2010; Yi et al. 2012; Chao, Lin, et al. 2013). This anthocyanin effect was associated with the observed decrease in the expression of genes encoding inflammatory mediators and adhesion molecules. Additionally, anthocyanins at concentrations ranging from 10 μM to 100 μM have also shown the ability to affect MAPK signalling pathways. This group of serine (Ser)/threonine (Thr) protein kinases includes the extracellular signal-regulated kinase (ERK), p38 and c-Jun N-terminal kinase (JNK) that play an important role in many cellular processes including inflammation, proliferation and apoptosis. Usually, activation of MAPK pathways is initiated by proinflammatory factors through the activation of cell surface receptors, activating a phosphorylation cascade that includes MAPK kinase kinases and MAPK kinases (Warboys 2011). Activated (phosphorylated) MAPK can then activate different transcription factors (e.g. NF-κB, activator protein 1 (AP-1), cyclic AMP-responsive element-binding protein 1 (CREB1)) that regulate transcription of proinflammatory genes. In a few studies, the anthocyanin-mediated decrease in the expression of proinflammatory genes in activated endothelial

cells has been associated with their ability to reduce JNK and p38 phosphorylation (Xia et al. 2009; Yi et al. 2012). Similarly, the effect of anthocyanins on MAPK and NF-κB pathways have also been shown in others cells involved in the pathogenies of atherosclerosis such as macrophages and smooth muscle cells (Hou et al. 2005; L. Li et al. 2014; Sogo et al. 2015).

These observations suggest that the ability of anthocyanins to affect cell signalling pathways and consequently modulate the expression of genes involved in inflammatory responses, thus maintaining endothelial cell function, could present one of the mechanisms underlying the cardioprotective effects of anthocyanins reported in clinical trials and animal studies.

1.3.5.3. Modulation of microRNA (miRNA) expression

Modulation of miRNA expression has recently emerged as a possible mechanism by which polyphenols, including anthocyanins, may exert their beneficial health effects. These endogenous, non-coding, single-stranded RNAs of around 22 nucleotides act as the post-transcriptional regulators of gene expression (Bartel 2004). They are initially transcribed by RNA polymerase II (primary miRNA) and treated with the RNase III enzymes Drosha and Dicer, to generate 18- to 24-nucleotides mature miRNAs, which can then regulate the gene expression depending on the degree of complementarity with its target (Milenkovic et al. 2013). These mature miRNAs that perfectly base-pair with their mRNA targets induce their cleavage, while imperfect binding blocks protein translation. Therefore, by changing mRNA availability and consequently protein synthesis, these single-stranded RNAs can control various processes in cells such as cell differentiation, growth, proliferation and apoptosis (Miska 2005). The changes in miRNA expression profiles have been associated with the development of cancer, neurodegeneration and CVD, thus presenting an interesting target for the prevention of these multifactorial diseases.

More than 100 miRNAs involved in the regulation of different cellular processes were identified as being modulated by different polyphenols (Milenkovic et al. 2012; Milenkovic et al. 2013). However, the effect of anthocyanins on miRNA expression is still largely unknown. One *in vivo* study has reviled that the supplementation of diet with anthocyanins or ferulic acid, at nutritionally relevant doses, modulated the expression of

45 and 28 miRNAs, respectively, in the liver of ApoE$^{-/-}$ mice compared to non-supplemented mice (Milenkovic et al. 2012). The ability of anthocyanin extracts or pure compounds to modulate miRNA expression in different cell types such as mesenchymal stem cell, macrophages and myoblast have been recently reported (Du et al. 2017; Murata et al. 2017; Su et al. 2017). However, the *in vitro* evidence is still limited. Therefore, more studies are necessary to fully understand weather anthocyanin-mediated modulation of miRNA expression present one of the mechanisms underlying their cardioprotective properties.

1.3.5.4. Limitations of studies investigating the mechanisms of anthocyanin action and recommendation for future research

Although the available mechanistic studies have shown the ability of anthocyanins to affect cell processes involved in the development of CVD by acting on cell signalling pathways, miRNA expression and gene expression, the majority of them present several limitations. Most of these studies are *in vitro* studies that did not consider the extensive metabolism of anthocyanins within the body. They predominantly used parent compounds or extracts rather than circulating metabolites, at high, supraphysiological concentrations (up to 200 μM) and long periods of cell exposure (up to 24 hours), thus, producing results with no physiological relevance. Furthermore, mechanistic studies mostly use targeted-based approach, focussing on the impact on a few specific targets, which is not suitable for the assessments of the proposed complex multi-target mode of action of polyphenols.

In contrast to the relatively large number of studies investigating the effect of anthocyanins on endothelial cell function, the number of studies examining their effects on platelet function is limited. These *in vitro* studies mostly focus on the ability of anthocyanin-rich extracts, pure anthocyanins or their metabolites to affect platelet activation, platelet granule secretion and platelet aggregation with endothelial cells and other platelets (Kim et al. 2012; Yang et al. 2012; Song et al. 2014; Olas 2016), not rarely lacking the physiological relevance. Also, the effect of anthocyanins and their metabolites on the agonist-induced platelet aggregation with leukocytes still needs to be established.

Taken together, results from mechanistic studies propose several mechanisms of action of anthocyanins that could underlie the reported beneficial effects of anthocyanin-

rich food consumption on cardiovascular health. These mechanisms include their ability to regulate the activity of cell signalling proteins and transcription factors and modulate gene expression thereby lowering inflammation and improving endothelial function. However, *in vitro* studies with physiologically relevant design that use omic approaches investigating the effect of anthocyanins and their metabolites on gene, protein and miRNA expressions are needed to fully understand the role of anthocyanins in CVD prevention. Aside from endothelial and immune cells, platelets also contribute to disturbed vascular homeostasis and present an interesting target for exploring the CVD prevention. Thus, future studies should focus on the assessments of anthocyanins and their metabolites on platelet activation and aggregation with immune cells.

2. THE AIM OF THE THESIS

Accumulating evidence suggests that anthocyanins, plant-food constitutes abundantly present in the human diet, could play an essential role in the cardioprotective effects associated with the consumption of anthocyanin-rich foods. These health benefits may be attributed to the ability of anthocyanins to affect endothelial or platelet function. Additionally, given the extensive metabolism of anthocyanins in the human body, it is also possible that their metabolites can at least partly contribute to observed cardioprotective effects of anthocyanin-rich foods. However, the underlying molecular mechanisms of action of anthocyanins and their metabolites are not fully understood. Therefore, this doctoral thesis aimed to examine the effect of anthocyanins and their metabolites, at physiologically relevant conditions, on endothelial cell and platelet function and to decipher, using the integrated omic approaches, the underlying molecular mechanisms of action.

Accordingly, the following research objectives included:

1. Investigations of the effect of anthocyanins and their metabolites on endothelial cell function and integrity by evaluating adhesion of monocytes to activated endothelial cells and their subsequent transendothelial migration.

2. Clarification of the molecular mechanism of action of anthocyanins and their metabolites in the endothelial cells by assessing their effects on gene expression, miRNA expression, and cell signalling pathways. The investigations of the cell signalling comprised *in silico* docking evaluation of the possible interactions between cell signalling proteins and anthocyanins and their metabolites as well as the western blot analysis of the impact on the phosphorylation of cell-signalling proteins and transcription factors.

3. Investigations of the effect of anthocyanins and their metabolites on the agonist-induced platelet activation and platelet-monocyte and platelet-neutrophil aggregation in human whole blood.

3. MATERIALS AND METHODS

3.1. Materials

All chemicals, antibodies, solutions, and kits that were used in the experimental work are listed in Table 4 to 10.

Table 4. *Anthocyanins and their metabolites tested in the experimental work*

	Compound	Chemical structure	Manufacturer
Anthocyanins	Cyanidin-3-O-arabinoside (cy-3-arab)	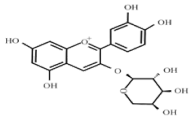	Extrasynthese (Genay, France)
	Cyanidin-3-O-galactoside (cy-3-gal)	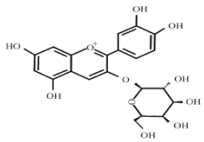	
	Cyanidin-3-O-glucoside (cy-3-glc)	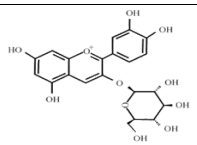	
	Delphinidin-3-O-glucoside (del-3-glc)	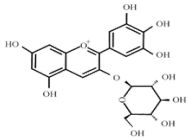	
	Peonidin-3-O-glucoside (pn-3-glc)	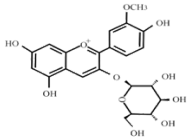	
Metabolites	4-hydroxybenzaldehyde (4-HBAL)	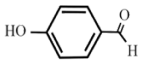	Sigma-Aldrich (St. Louis, USA)
	Protocatechuic acid (PCA)	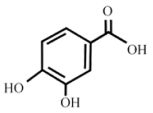	
	Vanillic acid	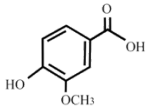	
	Ferulic acid	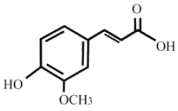	
	Hippuric acid	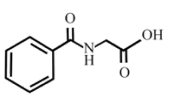	

Table 5. *Chemicals and commercially prepared solutions used in the experimental work*

Name	**Manufacturer**
Ethanol (≥99.8%, for molecular biology)	Sigma-Aldrich (St. Louis, USA)
Hydrochloric acid (HCl)	
Chloroform	VWR Prolabo Chemicals (Radnor, USA)
Bovine serum albumin (BSA)	Euromedex (Strasbourg, France)
Recombinant TNFα*	R&D Systems (Minneapolis, USA)
Human MCP-1*	Miltenyi Biotec (Bergisch Gladbach, Germany)
ADP	Sigma-Aldrich (St. Louis, USA)
Phosphate buffered saline (PBS 1X)	Dominique Dutscher (Brumath, France)
Trypsin/Ethylenediaminetetraacetic acid (EDTA) (0.05%/0.02%; w/o Ca, Mg, sterile, filtered)	Pan Biotech (Aidenbach, Germany)
Coulter ISOTON II electrolyte solution	Beckman Coulter (Fullerton, USA)
FCR-blocking reagent, human	Miltenyi Biotec (Bergisch Gladbach, Germany)
MS-SAFE protease and phosphatase inhibitor Cocktail	Sigma Aldrich (St. Louis, USA)
Radio-immunoprecipitation assay buffer (RIPA buffer)	
Sodium dodecyl sulphate (SDS)	
Ammonium persulfate (APS)	
Tetramethylethylenediamine (TEMED)	
40% Acrylamide/bisacrylamide solution (37.5/1)	Euromedex (Strasbourg, France)
Ponceau S solution	Sigma Aldrich (St. Louis, USA)
BD FACS Lysing Solution 10X	BD Biosciences (Franklin Lakes, USA)
CellFIX 10X	
BD FACS Flow Sheath Fluid	

* dissolved in PBS with 0.2% BSA

Table 6. *The cell culture media and supplements used in the cell-based assays*

Name	Manufacturer
Endothelial cell basal medium (w/o phenol red)	Lonza (Basel, Switzerland)
Endothelial cell growth medium SingleQuots™	
RPMI 1640 (L-glutamine, 2g/L NaHCO3, phenol red)	Pan Biotech (Aidenbach, Germany)
Penicillin/ streptomycin	
Fetal bovine serum (FBS) (inactive, Sterile, filtered)	Dominique Dutscher (Brumath, France)

Table 7. *List of commercially available kits and their components used in the experimental work*

Name	Components	Manufacturer
miRNeasy Micro Kit	QIAzol Lysis Reagent RNeasy MinElute Spin Columns Buffer RWT Buffer RPE RNase-Free Water	Qiagen (Hilden, Germany)
High Capacity cDNA RT kit	10X RT Buffer 10X RT Random Primers 25X dNTP Mix (100 mM) MultiScribe Reverse Transcriptase RNase Inhibitor	Applied Biosystems (Foster City, USA)
TaqMan Fast Advanced Master Mix	AmpliTaq® Fast DNA Polymerase Uracil-N-glycosylase (UNG) dNTPs (with dUTP) ROX™ dye (passive reference) optimised buffer	
Power SYBR Green PCR Master Mix	SYBR® Green 1 Dye AmpliTaq Gold DNA Polymerase LD dNTPs with dUTP/dTTP blend Passive Reference 1 optimised buffer	

Table 7 *(Continued)*

Name	Components	Manufacturer
miRNA Complete Labelling and Hyb Kit	10X Gene Expression Blocking Agent 2X Hi-RPM Hybridisation Buffer T4 RNA Ligase 10X T4 RNA Ligase Buffer Calf Intestinal Phosphatase 10X Calf Intestinal Phosphatase Buffer Dimethyl sulfoxide (DMSO) nuclease-free water Cyanine 3-pCp	Agilent Technologies (Santa Clara, USA)
MicroRNA Spike-In Kit	Labelling Spike-In Hyb Spike-In Dilution Buffer	
Gene Expression Wash Buffer Kit	Gene Expression Wash Buffer 1 Gene Expression Wash Buffer 2 Triton X-102 (10%)	
Bicinchoninic acid (BCA) Protein Quantitation Kit	BSA Standard stock solution (2 mg/ml) Reagent A Reagent B	Interchim (Montluçon, France)
LumiGLO reserve chemiluminescent substrate	Reagent A (luminol solution) Reagent B (reaction buffer) (1:2 v/v)	KPL (Gaithersburg, USA)

Table 8. *Solutions used in the experimental work*

Name	**Composition***
0.2% Gelatin solution	0.2% (w/v) Gelatin MiliQ water
Crystal violet solution	0.5% (w/v) Crystal violet 20% (v/v) Methanol
Solubilizing solution	0.1 M Sodium citrate (pH 7.4) 50% (v/v) Methanol
4% Paraformaldehyde (PFA) solution	4 % (w/v) PFA NaOH 5N 10X PBS MiliQ water
Flow cytometry analysis buffer	0.5% (w/v) BSA 2mM EDTA (pH 7.4) 1X PBS
1X Running buffer	0.25 M Tris-base 1.92 M Glycine 0.1% (w/v) SDS MiliQ water
4X Cracking buffer	0.166 M Tris-HCl, pH6.8 33.3 % (v/v) Glycerol 6.6 % (v/v) SDS 0.16% (v/v) β-mercaptoethanol 0.05% (w/v) Bromophenol blue
1X Transfer Buffer	0.25 M Tris-base 0.95 M Glycine 20% (v/v) Ethanol MiliQ water
1X Tris-Buffer-Tween20 (TBS-T)	0.032M Tris-base 0.168M Tris-HCl 1.5M NaCl 2% Tween20 MiliQ water pH 7.4
Blocking buffer	5% (w/v) Milk Powder 1X TBS-T
Modified HEPES-Tyrode's buffer (HTB)	10 mM HEPES 137 mM NaCl 2.8 mM KCl 1 mM $MgCl_2$ 12 mM $NaHCO_3$ 0.4 mM Na_2HPO_4 0.35% (w/v) BSA 5.5 mM glucose pH 7.4

* All chemicals used to prepare solutions were from Sigma-Aldrich (St. Louis, USA) unless differently stated

Table 9. *The antibodies used in flow cytometry analysis*

Name	Antigen	Isotype	Manufacturer
Fluorescein isothiocyanate-conjugated Anti-Human CD45 antibody (CD45-FITC)	CD45	Mouse IgG2a, κ	Miltenyi Biotec (Bergisch Gladbach, Germany)
Fluorescein isothiocyanate-conjugated Mouse Anti-Human CD61 antibody (CD61-FITC)	GPIIIa (part of GIIb/IIIa complex)	Mouse IgG1, κ	BD Biosciences (Franklin Lakes, USA)
Fluorescein isothiocyanate-conjugated Mouse Anti-Human PAC-1 antibody (PAC1-FITC)	GPIIb/IIIa (on activated platelets)	Mouse IgM, κ	
Phycoerythrin-conjugated Mouse Anti-Human antibody (CD62P-PE)	CD62P (syn. P-selectin)	Mouse IgG1, κ	
Phycoerythrin-conjugated Mouse Anti-Human CD11b antibody (CD11b-PE)	CD11b (syn. MAC1) (part of CD11b/CD18 heterodimer)	Mouse IgG2, κ	
Peridinin Chlorophyll Protein Complex-conjugated CD61 antibody (CD61-PerCP)	GPIIIa (part of GIIb/IIIa complex)	Mouse IgG1, κ	
Peridinin Chlorophyll Protein Complex-conjugated CD14 antibody (CD14-PerCP)	CD14	Mouse IgG2, κ	
Isotype controls			
Fluorescein isothiocyanate-conjugated Mouse IgG2a antibody (IgG2a -FITC)		Mouse IgG2a, κ	Miltenyi Biotec (Bergisch Gladbach, Germany)
Fluorescein isothiocyanate-conjugated Anti-Human IgG1 antibody (IgG1-FITC)		Mouse IgG1, κ	BD Biosciences (Franklin Lakes, USA)
Fluorescein isothiocyanate-conjugated Anti-Human IgM antibody (IgM-FITC)		Mouse IgM, κ	
Phycoerythrin-conjugated Anti-Human IgG1 antibody (IgG1-PE)		Mouse IgG1, κ	
Phycoerythrin-conjugated Anti-Human IgG2 antibody (IgG2-PE)		Mouse IgG2, κ	
Peridinin Chlorophyll Protein Complex-conjugated Anti-Human IgG1 antibody (IgG1-PerCP)		Mouse IgG1, κ	
Peridinin Chlorophyll Protein Complex-conjugated Anti-Human IgG2 antibody (IgG2-PerCP)		Mouse IgG1, κ	

Table 10. *Antibodies used in Western blot analysis*

Name	**Species type**	**Working dilution***	**Manufacturer**
p44/42 MAPK (ERK1/2)	Rabbit monoclonal	1/1000	Cell Signaling (Danvers, USA)
Phospho-p44/42 MAPK (ERK1/2) (Thr202/Tyr204)	Rabbit monoclonal	1/2000	
NF-κB p65	Rabbit polyclonal	1/1000	Genetex (Irvine, USA)
Phospho-NF-κB p65 (Ser536)	Rabbit monoclonal	1/1000	Cell Signaling (Danvers, USA)
Glyceraldehyde-3-phosphate dehydrogenase (GAPDH) (FL-335)	Rabbit polyclonal	1/1000	Santa Cruz Biotechnology (Santa Cruz, USA)
Horseradish peroxidase-conjugated Anti-Rabbit IgG antibody (IgG-HRP)	Goat Polyclonal	1/4000	Abbiotec (San Diego, USA)

3.2. Methods

To achieve the aim of this thesis, two *in vitro* studies were performed:

- a study of the impact of anthocyanins and their metabolites on endothelial cell function, conducted at the French National Institute for Agricultural Research in Saint-Genès-Champanelle, France
- a study of the effect of these compounds on platelet function, performed at the Centre of Research Excellence in Nutrition and Metabolism in Belgrade, Serbia.

3.2.1. Investigations of the effects of anthocyanins and their metabolites on endothelial cell function

The impact of anthocyanins and their metabolites on endothelial cell function was assessed by examining the adhesion of monocytes to activated endothelial cells as well as monocyte transendothelial migration. Further investigations of the effect of these bioactive compounds on gene expression, miRNA expression and cell signalling in endothelial cells were performed to identify the underlying molecular mechanisms of action.

3.2.1.1. Preparation of compounds

Each of the commercially available anthocyanins was dissolved in 70% ethanol with 1% HCl and metabolites in 70% ethanol, to obtain stock solutions of 10 mM and 20 mM, respectively. Aliquots of these solutions were stored at -80 °C until used.

3.2.1.2. Cell culturing

For the investigations of the effect of anthocyanins and their metabolites on endothelial cell function and endothelial-monocyte interactions, primary human umbilical vein endothelial cells (HUVECs) and THP1 monocytic cell line were used. Pooled donor HUVECs obtained from Lonza (Basel, Switzerland) were cultured in a phenol red-free endothelial growth medium supplemented with 2% FBS, 0.1% human epidermal growth factor, 0.1% vascular endothelial growth factor, 0.4 % human fibroblast growth factor, 0.1% insulin-like growth factor, 0.1% heparin, 0.1% ascorbic acid, 0.04% hydrocortisone and 0.1% gentamicin/amphotericin-B. THP1 cell line purchased from ATCC (Manassas, USA) was cultured in the basic growth medium RPMI 1640

supplemented with 10% fetal bovine serum and 1% penicillin/streptomycin. Cells were cultured at 37 °C in a humid air atmosphere with 5% carbon dioxide.

3.2.1.3. Cell viability assay

The available literature shows that anthocyanins and their metabolites do not exert a cytotoxic effect on endothelial cells when tested at up to 100 μM levels (Xie et al. 2012; Edwards et al. 2015). Therefore, only the effect of solvents (70% ethanol/1% HCl and 70% ethanol) on endothelial cell viability was tested. HUVECs at passage four were seeded in a 0.2% gelatin-coated 24-well plate (Becton Dickinson, Le Pont de Claix, France) at a density of 15000 cells/well. At 80% of confluence, cells were exposed for 3 and 24 hours to 70% ethanol/1% HCl or 70% ethanol, diluted in the cell culture medium to a final concentration of 0.1% (v/v). Cells treated only with the culture medium were used as a control. Following the treatment, cell viability was determined using the previously reported, adapted crystal violet staining assay (Cao et al. 2012). Briefly, cells were rinsed using 1X PBS and stained with 200 μl/well of crystal violet staining solution (Table 8) for 15 minutes at room temperature. Cells were then washed with water for four times and air-dried at room temperature overnight. Subsequently, 150 μl of solubilising solution (Table 8) was added per well to solubilise the colourant. Coloured solutions from each well were transferred to a 96-well plate (Becton Dickinson, Le Pont de Claix, France) and the optical density was measured at 550 nm using the Infinite 200 PRO NanoQuant microplate reader (TECAN, Zurich, Switzerland). Viability was presented as a percentage relative to the control.

3.2.1.4. Experimental conditions: compound concentrations and time of exposure

To test whether anthocyanins (cy-3-glc, cy-3-gal, cy-3-arab, cy-3-glc, del-3-glc, pn-3-glc) and their metabolites (4-HBAL, PCA, vanillic, ferulic or hippuric acids) can affect monocyte-endothelial cell interactions and if they exert a dose-response effect, all compounds were tested over a range of concentrations: 0.1 μM, 0.2 μM, 0.5 μM, 1 μM and 2 μM. The chosen concentration range was in accordance with the plasma levels of these compounds reported after the consumption of anthocyanin-rich sources (Table 11). The selected time of the exposure of cells with tested compounds was 3 hours for

anthocyanins and their degradation product 4-HBAL, and 18 hours for anthocyanin gut metabolites (PCA, vanillic, ferulic or hippuric acids). The chosen duration of the cell exposure was in agreement with the plasma residence time of tested compounds observed in anthocyanin bioavailability studies in humans (Figure 9) (Table 11).

***Table 11**. Summary of the maximum concentration in human plasma and the time to reach peak concentration of compounds used in this study*

Compound	Anthocyanin form in the circulation	Cmax (μM)*	Tmax (h)**	Reference
cy-3-arab	Intact	0.013	1.5	(Milbury et al. 2010)
cy-3-gal	Intact	0.098	2	(Kay et al. 2004)
cy-3-glc	Intact	0.14	1.8	(Czank et al. 2013)
del-3-glc	Intact	0.023	1.5	(Matsumoto et al. 2001)
pn-3-glc	Intact	0.059	0.5	(Frank et al. 2003)
4-HBAL	Upper GIT metabolite	0.67	5.6	(de Ferrars, Czank, et al. 2014)
PCA	Gut metabolite	0.15	3.3	(de Ferrars, Czank, et al. 2014)
Vanillic acid	Gut metabolite	1.85	12.5	(de Ferrars, Czank, et al. 2014)
Ferulic acid	Gut metabolite	0.94	11.3	(Czank et al. 2013)
Hippuric acid	Gut metabolite	1.96	15.7	(Czank et al. 2013)

*Cmax - maximum concentration in plasma. **Tmax - time to reach Cmax, GIT-gastrointestinal tract

For the investigations of the possible synergistic effect of anthocyanins and their metabolites at their circulating plasma concentrations, two mixtures of compounds were created. The first mixture, named mix A, was prepared with compounds that are present in the circulation from 1 to 5 hours after the consumption of anthocyanin-rich foods. This mixture contained cy-3-glc, cy-3-gal, cy-3-arab, del-3-glc, pn-3-glc and 4-HBAL. The final concentration of compounds in this mixture that was added to endothelial cells was 0.1 μM for anthocyanins and 0.5 μM for 4-HBAL. The second mixture, named mix B, contained metabolites that can be detected in the circulation for around 15 hours following the anthocyanin intake. This mixture consisted of PCA, vanillic acid, ferulic acid and hippuric acid, administrated to endothelial cells at the final concentration of 0.2 μM, 2 μM, 1 μM and 2 μM, respectively. The chosen concentrations of compounds of

these mixtures were closest to those previously reported in human plasma following the anthocyanin consumption (Table 11). Endothelial cells were exposed to the mix A for 3 hours and the mix B for 18 hours. In addition to this, an experimental condition named mix A+B, where the cells were first exposed to the mix A for 3 hours and then mix B for 18 hours, was designed to mimic as closely as possible the profiles of anthocyanin forms present in circulation after the intake of anthocyanin-rich sources (Figure 9).

3.2.1.5. Cell adhesion assay

HUVECs at passage four were seeded in 0.2% gelatin-coated 24-well plates at a density of 50000 cells/well. At 80% of confluence, cells were exposed to cy-3-gal, cy-3-arab, cy-3-glc, del-3-glc, pn-3-glc or 4-HBAL for 3 hours and to PCA, vanillic, ferulic or hippuric acids for 18 hours. Each compound was tested over a physiologically relevant range of concentrations from 0.1 µM to 2 µM. A series of dilutions of stock solutions of compounds were prepared using 70% ethanol/1% HCl or 70% ethanol and subsequently diluted in cell culture medium to reach working concentrations, right before application to cells. Cells exposed to 70% ethanol/1% HCl or 70% ethanol, diluted to a final concentration of 0.1% (v/v) in the culture medium were used as a control. Following the incubation, the medium containing treatments was discarded, and inflammation induced by stimulating cells with the fresh media containing 1 ng/ml TNFα for 4 hours. Cells treated only with the culture medium were used as the negative control ((-) TNFα condition). Subsequently, 400 µl of cell suspension containing 250000 THP1 cells was added to each well and cells were co-incubated for 15 minutes. Wells were then rinsed for three times with 1X PBS to remove non-adhering THP1 cells, and the remaining cells were detached by incubation with 100 µl/well of trypsin/EDTA solution for 3 min at 37°C. Afterwards, 200 µl of 1X PBS containing 10% FBS was added per well to neutralise trypsin. Samples of collected cells were then fixed with 200 µl/well of 4% PFA solution (1% final concentration) and stored at 4 °C until analysis by flow cytometry the following day. These cell adhesion assays were performed in triplicates for both treatments and controls. The schematic representation of this experimental design is given in Figure 11.

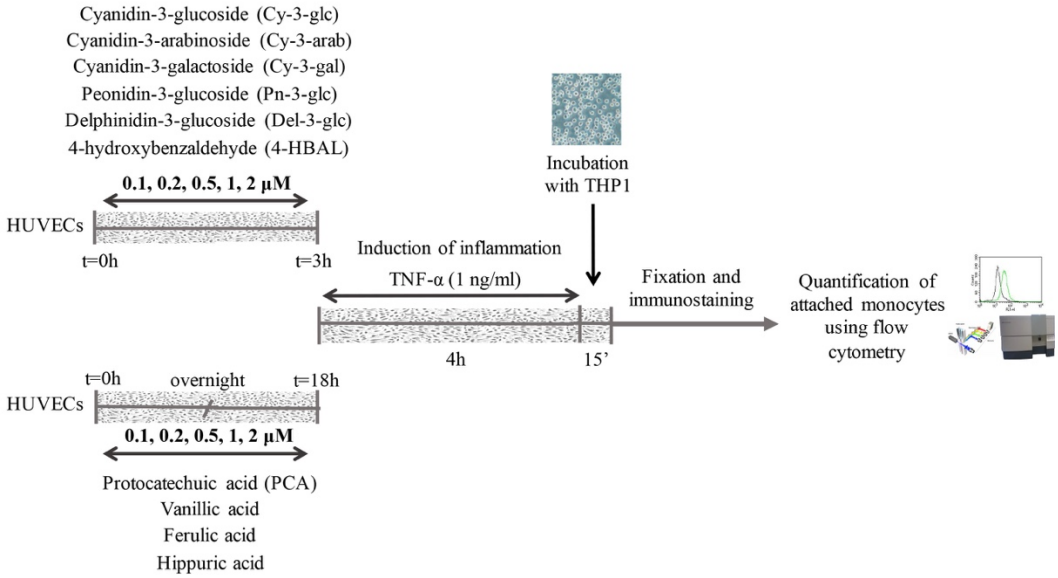

Figure 11. *Schematic representation of the* in vitro *investigations of the effect of individual anthocyanins and their metabolites on monocyte adhesion to HUVECs*

To further investigate the possible synergic effect of anthocyanins and their metabolites on monocyte adhesion, endothelial cells were exposed to mixtures of these compounds (section 3.2.1.4.). The adhesion assay was performed as described above except that the HUVECs were exposed to the mix A for 3 hours or mix B for 18 hours as well as to their corresponding controls (Figure 12). For the mix A+B, HUVECs were exposed to the mix A for 3 hours after which medium was replaced with the fresh one containing the mix B for 18 hours. Cells treated with the culture media containing 70% ethanol/1% HCl for 3 hours and 70% ethanol for further 18 hours, were used as a control for this experimental condition. These cell adhesion assays were performed in quintuplicates for both treatments and controls.

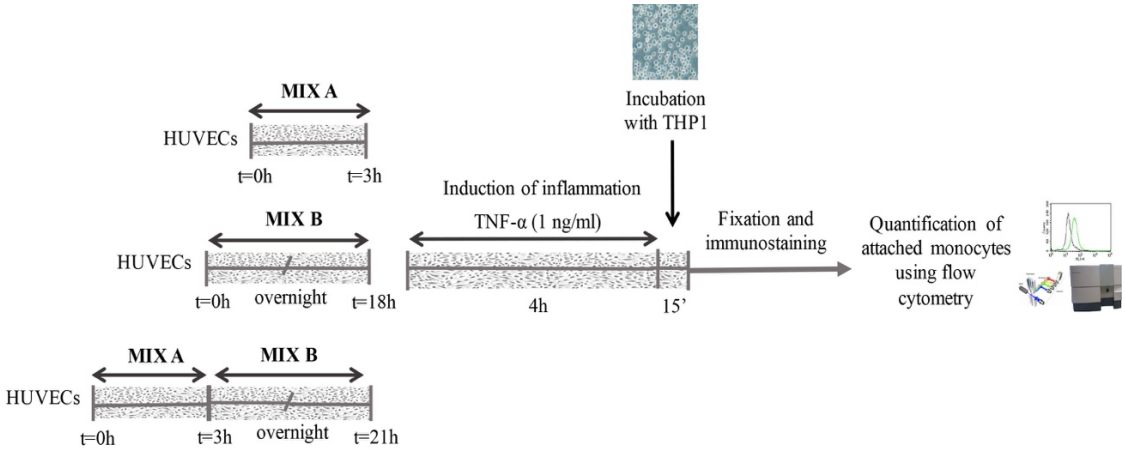

Figure 12. *Schematic representation of the* in vitro *investigations of the effect of mixtures on monocyte adhesion to HUVECs*

3.2.1.6. Quantification of monocyte adhesion to endothelial cells by flow cytometry methodology

The flow cytometry was used to measure the adhesion of THP1 monocytes to HUVECs. This technique allows distinction between different cell types in the same sample based on their morphological characteristics and presence of specific surface antigens. The morphological characterisation is based on light scattering that occurs when each cell is illuminated by the laser beam. The resulting forward scatter (FSC) is proportional to the size of the cell while the side scatter (SSC) gives information about cell granularity. Additionally, the use of antibodies conjugated to fluorescent dyes that bind to antigens expressed only on the surface of specific cell type allows to detect these cell markers and further distinguish between different cells (Brown & Wittwer 2000).

Differentiation between THP1 monocytes and HUVECs and their quantification in the samples collected from the adhesion assays was achieved with the use of the human CD45-FITC antibody that binds to CD45-antigen expressed on the surface of monocytes. In addition to samples obtained from cell adhesion assays, samples containing only THP1 cells or HUVECs were also prepared and fixed for the flow cytometry analyses to control the specific binding of antibodies. All cell samples were immunostained as recommended by the manufacturer. Briefly, samples were centrifuged for 10 minutes at 300 x g and incubated with FcR blocking reagent (dilution 1:8) for 10 minutes in the dark to inhibit nonspecific binding of antibodies. Subsequently, cell samples were incubated with the human CD45-FITC antibody (dilution 1:10) for 30 minutes in the dark. Mouse IgG2a-FITC antibody (dilution 1:10) was used as isotype control for determining nonspecific antibody binding. Both FcR blocking and antibody dilutions were prepared with the flow cytometry analysis buffer (Table 8). Following the immunostaining, 500 µl of this buffer was added to each sample. Samples were immediately measured and analysed on the FACSCalibur flow cytometer (BD Bioscience, San Jose, USA) using the integrated CellQuest Pro software, version 5.1.1. Following the acquisition set to 20000 events, the number of monocytes (i.e. CD45-positive cells) and HUVECs (i.e. unstained cells) in each sample were determined by the analysis of CD45-FITC/FSC diagrams. Monocyte adhesion was calculated as a ratio of quantified monocytes to HUVECs and expressed in comparison to positive control (TNFα-stimulated HUVECs) that was normalised to 100%.

3.2.1.7. Transmigration assay

The effects of mixtures on monocyte transendothelial migration were assessed using a transmigration model with Transwell® inserts (Corning, NY, USA) (Figure 13). These inserts of 6.5 mm in diameter contained 5 µm pores at a density of $4x10^5$ pores/cm^2 that allowed cell migration.

Fourth-passage HUVECs were seeded onto 0.2% gelatin-coated inserts at a density of 15000 cells/insert and cultured until reached confluence. Subsequently, the endothelial cell monolayer was exposed either to mix A for 3 hours, mix B for 18 hours or to mix A+B for 21 hours and their matching controls (as described in the section 3.2.1.5). Each of these treatments was added to both upper and lower chambers of the transwell system (100 µl and 500 µl, respectively). At the end of the exposure time, treatments were discarded, and 100 µl of THP1 cell suspension containing 0.5 x 10^6 cells/ml was added to the upper chambers. 500 µl of medium containing chemoattractant MCP-1 at a final concentration of 50 ng/ml was added to the lower chambers. The same volume of chemoattractant-free medium was used as a negative control. Cells were then co-incubated for 4 hours to allow the transmigration of monocytes. Following the incubation, samples of transmigrated THP1 cells were taken from the lower chambers and quantified with a Z1 Coulter particle counter system using the ISOTON II electrolyte solution as recommended by the manufacturer (Beckman Coulter, Fullerton, USA). This system uses the electrical sensing zone technology that allows accurate counting and sizing of cells based on quantifiable changes in electrical resistance produced by cells that are suspended in an electrolyte solution (Henriquez et al. 2004). Samples were measured for three times in a random order. Monocyte transmigration assays were performed in quadruplicates for both treatments and controls. The results were reported as a percentage of transmigrated monocytes relative to positive control (the (+) MCP-1 condition).

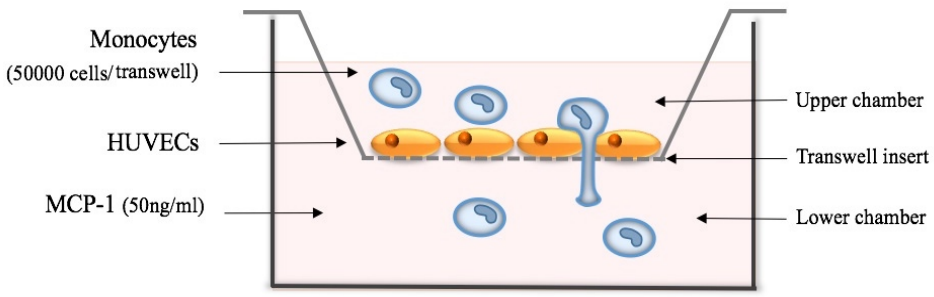

Figure 13. *The* in vitro *model of transendothelial migration using transwells*

3.2.1.8. Impact on gene expression

3.2.1.8.1. RNA extraction

For the investigations of the effect of anthocyanins and their metabolites on the gene expression, fourth-passage HUVECs were seeded in 0.2% gelatin-coated Petri dishes at a density of around 10^6 cells/ dish and cultured until reaching 80% confluence. Cells were then treated with the mix A, mix B, mix A+B and their matching controls as described in the section 3.2.1.5. Subsequently, inflammation was induced by incubation with 1 ng/µl TNFα for 4 hours, while the cell culture medium was used as negative control. The extraction of total RNA, including miRNA was performed using the Qiagen miRNeasy Micro Kit (Table 7). According to manufacturer's instructions, HUVECs were washed twice with 1X PBS before lysis with QIAzol lysis reagent for 5 minutes at room temperature. Collected lysates were separated into three phases by incubation with chloroform at room temperature for 2 minutes and subsequent centrifugation at 12000 x g at 4°C for 15 minutes. The RNA-containing aqueous phase was collected and mixed with 1.5 volume of 100% ethanol. These mixtures were transferred onto RNAeasy MinElute columns and centrifuged at 8000 x g for 30 seconds at room temperature to allow the binding of total RNA to the column's membrane. Membranes were then washed with RWT buffer, RPE buffer and 80% ethanol, respectively. Each wash was followed by quick centrifugation at 8000 x g to remove the impurities. Total RNA was eluted from each column using 30 µl of RNase-free water. Aliquots of total RNA samples were stored at -80°C.

RNA quality and quantity were determined by agarose gel electrophoresis and NanoDrop ND-1000 spectrophotometer using the ND-1000 software, version 3.8.1 (Thermo Fisher Scientific, Wilmington, USA). The electrophoresis on the 1% agarose gel stained with ethidium bromide allowed the RNA quality assessments by visualisation of bands corresponding to 28S and 18S ribosomal RNA. RNA was considered to be of high quality if the ratio of 28S:18S bands was around 2.0 or higher. The evaluation of RNA quality using NanoDrop spectrophotometer was based on the ratio of absorbance at 260 nm and 280 nm. Additionally, a ratio of absorbance at 260 nm and 230 nm was used as a secondary measure of quality. An RNA with the 260/280 ratio of around 2.0 and

260/230 values in the range of 2.0-2.2 was considered as pure. Only the RNA samples that passed these quality criteria were used for later experiments.

3.2.1.8.2. Reverse transcription of total RNA

Reverse transcription of total RNA samples was performed using the High Capacity cDNA RT kit. 10 µl of each total RNA sample (200 µg/µl) was mixed with the reaction solution containing 2 µl of 10X RT buffer, 0.8 µl of 25X dNTP Mix (100 mM), 2 µl of 10X RT random primers, 1 µl MultiScribe reverse transcriptase (50U/µl), 1 µl of RNase inhibitor and 3.2 µl of nuclease-free water. Reverse transcription was performed using a thermal cycler (Bibby Scientific, Stone, UK) under the following conditions: 10 minutes at 25 °C, 2 hours at 37 °C and 5 minutes at 85 °C. The obtained cDNAs were stored at -20 °C.

3.2.1.8.3. Quantitative real-time PCR analysis

The impact of mixtures of anthocyanins and their metabolites on the gene expression in HUVEC was investigated using the 384 Wells TaqMan Array Micro Fluidic Cards (TLDA cards) (Applied Biosystems, Foster City, USA) that allowed simultaneous assessments of gene expression levels of multiple genes. These TLDA cards consisted of eight loading ports, each connected to 48 wells preloaded with TaqMan probes and primers specific for target genes. TLDA cards were custom designed for investigation of expression of 91 different genes involved in regulation of endothelial function (Supplementary Table 1).

Before the investigations of gene expression with TLDA cards, a real-time PCR quantification of the expression of vascular cell adhesion molecule 1 (*VCAM1)* and selectin E (*SELE)* genes was performed with (-) TNFα and (+) TNFα cDNA samples to verify the efficiency of TNFα to induce inflammation and modulate the gene expression profiles in HUVECs. These gene show low levels of expression in basal conditions while their expression is markedly increased upon stimulation with the proinflammatory agents (Ley 1996). PCR reactions were prepared with 10 µl of Power SYBR Green PCR Master Mix, 0.4 µl of reverse and forward primers (both at 10 pm/µl concentration), and 2 µl of the cDNA in the final reaction volume of 20 µl. The primers that were used were: VCAM1-F: GGG AAG ATG GTC GTG ATC CTT, VCAM1-R: TCT GGG GTG GTC

TCG ATT TTA; SELE-F: AGA GTG GAG CCT GGT CTT ACA; SELE-R: CCT TTG CTG ACA ATA AGC ACT GG; GAPDH-F: CTG GGC TAC ACT GAG CAC C, GAPDH-R: AAG TGG TCG TTG AGG GCA ATG. Real-time quantitative PCR amplifications were performed in a MicroAmp Fast optical 96-well reaction plate (Applied Biosystems, Foster City, USA) using the 7900HT system (Applied Biosystems, Foster City, USA) with integrated Sequence Detection System software, version 2.4 under the following conditions: 2 minutes at 50 °C, 10 minutes at 95 °C, 40 cycles of 15 seconds at 95 °C and 1 minute at 60 °C.

Gene expression analyses with TLDA cards were performed with (+) TNFα, mix A, mix B and mix A+B cDNA samples. According to manufacturer's instructions, 1 000 ng of cDNA samples were diluted in nuclease-free water to a final volume of 105 µl and mixed with 105 µl of TaqMan Fast Advanced Master Mix. Each mixture was divided between the two loading ports of TLDA card. TLDA cards were centrifuged twice in Heraeus multifuge 3S centrifuge (Applied Biosystems, Foster City, USA) for one minute at 1200 rpm and subsequently sealed with a TLDA Sealer (Applied Biosystems, Foster City, USA) to prevent well-to-well contamination. Real-time quantitative PCR amplifications were performed by Applied Biosystems 7900HT system (Foster City, USA) under the same conditions as described above for the quantification of the *VCAM1* and *SELE* expression. The obtained raw data were analysed with the Relative Quantitation (RQ) web-based software from Thermo Fisher Scientific (https://www.thermofisher.com/fr/fr/home/cloud), which calculates relative gene expression using a comparative threshold cycle (Ct) method, also known as the $2^{-\Delta\Delta Ct}$ method (Schmittgen & Livak 2008). Briefly, Ct data (i.e. the number of cycles required for the amplified target to cross the fixed threshold) were used to calculate ΔCt values by subtracting Ct value of endogenous control from Ct value of each gene of interest. ΔΔCt values were then calculated by subtracting the calibrator ((+) TNFα condition) from the ΔCt value of each gene of interest. The relative gene expression was calculated as $2^{-\Delta\Delta Ct}$. Data were normalised to endogenous control (genes encoding GAPDH and alpha actin) and analysed using Student's t-tests with the (+) TNFα samples as a reference biological group.

3.2.1.9. Investigations of miRNA expression using miRNA microarrays

The investigations of the effect of mixtures of tested compounds on miRNA expression in HUVECs were performed using 8x15K miRNA microarrays (V3) from Agilent Technologies (Santa Clara, USA). This technology combines highly efficient direct labelling method and special probe design that allow accurate measurements of miRNA profiles (Wang et al. 2006; Mestdagh et al. 2014). The array format used in these experiments included eight microarrays printed on a single glass slide. Each of the microarrays contained around 15000 probes that corresponded to 866 human and 89 human viral miRNAs of the Sanger miRBase database, version 12.0. Labelling and hybridisation of total RNA samples were performed using miRNA complete labelling and hybridisation kits (Table 7) obtained from Agilent Technologies (Santa Clara, CA, USA). Agilent's miRNA Spike-in Kit was used to monitor the labelling and hybridisation efficiencies and therefore distinguish significant biological data from processing issues. This kit contained *in vitro* synthesised RNAs that were added to samples during the labelling and hybridisation steps as a control.

Following the manufacturer's instructions, 100 ng of each of the previously extracted total RNA samples (50 ng/µl) was dephosphorylated by incubation with calf intestinal phosphatase for 30 minutes at 37 °C. Samples were further denatured using 100% DMSO for 5 minutes at 100 °C and immediately transferred to ice-water bath to prevent reannealing. Subsequently, samples were labelled with cyanine 3-pCp fluorescent dye by incubation with T4 RNA ligase for 2 hours at 16 °C and vacuum dried for 1.5 hours at 55 °C to remove residual DMSO that could interfere with hybridisation process. Dried pellets were then suspended in nuclease-free water and incubated with the hybridisation mixture containing blocking reagent and hybridisation buffer for 5 minutes at 100 °C. Afterwards, samples were loaded onto microarray slides and hybridised to microarray probes using the SureHyb microarray hybridisation chamber (Agilent Technologies, Santa Clara, USA) set to 20 rpm and 55 °C for 20 hours. Following the hybridisation, microarrays were washed with the Gene expression washing buffer kit (Table 7) and scanned with the Agilent G2505 microarray scanner system (Santa Clara, USA). Feature Extraction software version 11.0. (Agilent Technologies, Santa Clara, USA) was used to extract the raw data from microarray images. Raw data were normalised to the 50th percentile and analysed with moderated t-tests corrected by Westfall-Young permutation

using the Gene Spring GX software version 14.5 (Agilent Technologies, Santa Clara, USA).

3.2.1.10. Bioinformatics analysis

Gene and miRNA expression data were examined using different bioinformatics tools:

- Kyoto Encyclopedia of Genes and Genomes (KEGG) database (http://www.genome.jp/kegg/tool/map_pathway2.html) was used for pathway analysis.
- MetaCore software (GeneGo, St Joseph, USA; https://portal.genego.com/) was used to identify the most significant transcription factors involved in the regulation of the genes identified as differentially expressed in the gene expression experiments. Identification of upstream cell signalling proteins involved in the regulation of these potential transcription factors was performed using KEGG database.
- Hierarchical clustering and heatmap visualisation of the miRNA expression profiles were carried out using PermutMatrix, version 1.9.3. (Caraux & Pinloche 2005).
- miRWalk 2.0 (Dweep & Gretz 2015), a comprehensive database that provides information on predicted and experimentally verified miRNA-mRNA interactions was used to identify possible gene targets of differentially expressed miRNA.
- BioVenn (http://www.cmbi.ru.nl/cdd/biovenn) and Venny 2.1.0. (http://bioinfogp.cnb.csic.es/tools/venny/) web applications were used to create Venn diagrams.

3.2.1.11. Investigations of the effect on cell signalling pathways

3.2.1.11.1. In silico *docking analyses*

The molecular docking was used to predict the possible binding interactions between anthocyanins/their metabolites (ligands) and transcription factors and signalling proteins (targets) that were identified using Metacore and KEGG bioinformatics tools as described in the previous section. These bindings could hypothetically affect the activity of cell

signalling proteins and transcription factors and explain the observed changes in gene expression and, ultimately, cellular response.

The *in silico* docking analyses were performed in collaboration with Dr Radu Tamaian from the National Institute for Research and Development for Cryogenic and Isotopic Technologies in Râmnicu Vâlcea, Romania. Before docking analyses, MarvinSketch chemical editor version 16.10.24.0 (ChemAxon, Budapest, Hungary, https://www.chemaxon.com) was used for drawing two-dimensional chemical structures of ligands, their three-dimensional (3D) optimisation and creation of input files for docking. Furthermore, MarvinSpace version 16.10.24.0 (ChemAxon, Budapest, Hungary, https://www.chemaxon.com/) was used to identify ligands' pharmacophore points, i.e. steric and electronic features necessary for molecular recognition of a ligand by a biological macromolecule (Wermuth et al. 1998). The Universal Protein Resource (UniProt) (http://www.uniprot.org/) and RCSB Protein Data Bank (RCSB-PDB) (http://www.rcsb.org/) online databases were used to obtain the high-resolution, complete 3D structure of targets needed for docking (i.e. a resolution higher than 2.0 Å and the coverage higher than 90%). High-resolution full-length 3D structures were available for only three targets, while for the rest of the targets the homologues models were constructed using the SWISS-MODEL (Supplementary Table 2), a fully automated protein structure homology-modelling server that is accessible through the ExPASy web server (https://swissmodel.expasy.org, Arnold et al. 2006).

All docking runs were performed by Python Prescription Virtual Screening Tool, version 0.9.4 using AutoDock Vina (Trott & Olson 2010) as a docking software. This software uses the X-score-inspired scoring function tuned with a PDBbind dataset (Wang et al. 2004; Wang et al. 2005) to predict noncovalent binding of a macromolecule with a ligand, and automatically calculates the grid maps (Trott & Olson 2010). Search space was set to cover the targets entirely to reveal all possible ligand-protein interactions and the accuracy of computations was improved by increasing the default exhaustiveness (the number of calculation repeats) by ten times. Following the docking, the most relevant results concerning binding affinity (BA) were thoroughly examined using the Molegro Molecular Viewer software, version 2.5 (CLC Bio, Aarhus, Denmark).

3.2.1.11.2. Western blot analysis

To associate results of molecular docking analyses with the *in vitro* effects on cell signalling, the phosphorylation of p65 (a subunit of NF-κB transcription factor) and ERK1/2 cell signalling protein were examined by Western blot.

For these investigations, the same cell treatments were used as described in the section 3.2.1.5. Cells were washed twice with 1X PBS and lysed with 700 µl of RIPA buffer with 1X MS-SAFE protease and phosphatase inhibitor cocktail (Table 5) by incubation on ice for five minutes. Plates were rapidly scraped and lysates were collected and frozen at -80 °C overnight. The following day, lysates were centrifuged at 8000 x g for 10 minutes at 4 °C, and supernatants containing the soluble proteins stored at -80 °C. Protein concentrations were determined by spectrophotometry using the BCA protein quantification kit (Table 7). Following the manufacturer's instructions, a series of BSA solutions prepared in RIPA buffer were used to obtain the standard curve. 25 µl of each sample and standard dilution were added into the 96-well multiple well plate (in technical triplicate), mixed with 200 µl of BCA working reagent containing reagents A and B in a 1:50 ratio, and then incubated for 30 minutes at room temperature in the dark. The absorbance was measured at 562 nm using the Infinite 200 PRO NanoQuant microplate reader (TECAN, Zurich, Switzerland). The protein concentrations in samples were calculated based on the BSA standard curve and the measured absorbance for each sample.

Proteins from the collected samples were first separated based on their molecular weight by sodium dodecyl sulphate polyacrylamide gel electrophoresis (SDS-PAGE) (Laemmli 1970). 20 µg of each protein sample were mixed with 4X cracking buffer (added in a 1:3 ratio) and denatured at 95 °C for 3 minutes. Samples were directly loaded onto polyacrylamide gels composed of a 4% stacking gel (containing 0.125 M Tris-HCl (pH 6.8), 4% acrylamide/bis, 0.1% SDS, 0.1% APS and 0.1% TEMED) and 10% or 12% resolving gel (containing 0.375 M Tris-base (pH 8.8), 10% or 12% Acrylamide/bis, 0.1% SDS, 0.1% APS solution and 0.1% TEMED). Electrophoresis was performed at 100 V for 90 minutes using the Mini-Protean Vertical Electrophoresis System (Biorad, Hercules, USA) and running buffer (Table 8).

Following the separation, protein transfer ("blotting") onto the Hybond-P polyvinylidene difluoride (PVDF) membrane (GE Healthcare Europe, Velizy-

Villacoublay, France) was carried out at 100 V for 80 min using the Mini Trans-Blot System (Biorad, Hercules, USA) filled with transfer buffer (Table 8). The efficiency of the transfer was checked by incubating membranes with the PonsoS solution for several seconds. Subsequently, membranes were blocked with the blocking buffer (Table 8) for one hour at room temperature and incubated with selected primary antibodies at 4 °C overnight. These antibodies included: p44/42 MAPK (ERK1/2), phospho-p44/42 MAPK (Thr202/Tyr204), NF-κB p65 and phospho-NF-κB p65 (Ser536) antibodies while GAPDH was used as a loading control. Following the incubation, membranes were washed for four times with 1X TBS-T solution (Table 8) and then incubated with a corresponding secondary antibody conjugated to horseradish peroxidase (HRP) for one hour at room temperature. The list of used antibodies and their dilutions is given in Table 10. Following the incubation with secondary antibody, membranes were again washed with 1X TBS-T solution and incubated for one minute with the LumiGLO reserve chemiluminescent substrate solution (Table 7) to detect the proteins. Chemiluminescent signals were captured using the Syngene G-Box (Ozyme, Saint Quentin Yvelines, France) with integrated Syngene GeneSys image acquisition software, version 1.2.5., and proteins were quantified by ImageJ software (National Institutes of Health, Rockville Pike, USA, http://rsb.info.nih.gov). The obtained protein levels were normalised to GAPDH.

3.2.2. Investigations of the effects of anthocyanins and their metabolites on platelet function

The investigations of the impact of anthocyanins and their metabolites on platelet function included the evaluation of their *in vitro* effect on platelet activation and platelet-leukocyte aggregation responses to ADP as platelet agonist. These investigations were performed using whole blood flow cytometry in accordance with the standardised protocols with slight modifications (Krueger et al. 2002; Barnard et al. 2003).

3.2.2.1. Volunteers and blood collection

The whole blood samples were taken from seven apparently healthy, non-smoking non-obese men, aged between 28 to 34 years. Their health status was estimated based on their medical history. Volunteers visited the research centre twice, with one visit corresponding to investigations of the effect of anthocyanins on platelet function and the other one to the evaluation of the impact of anthocyanin metabolites. There was at least a three-week wash out between these visits. Volunteers were asked to refrain from the consumption of alcohol, berry fruits, berry-derived products (e.g. juices and jams) and regularly consumed polyphenol-rich drinks such as tea and coffee for 72 hours before each blood collection to reduce the impact of bioactives from background diet on platelet function. Blood was drawn in the morning after an overnight fast of at least 12 hours and at least 20 minutes of seated rest. Blood collection was performed by venepuncture using the 21-gauge needle and no tourniquet, discarding the first 2 ml of drawn blood. This procedure was in accordance with previously published standardised protocols for blood sampling in platelet analyses (Krueger et al. 2002; Gerrits et al. 2016). The whole blood collected in Vacutainer tubes, with sodium citrate (3.2%) as an anticoagulant (BD Diagnostics, Franklin Lakes, USA), was used straightaway for the examinations of platelet function. Additional blood samples were taken for the assessments of haematological and biochemical parameters.

3.2.2.2. Whole blood treatments

Right after the blood collection, aliquots of whole blood were incubated with tested compounds for 10 min at 37 °C (Figure 14). This short incubation needed to fit into a narrow time frame between the blood collection and flow cytometry measurements,

determined as the maximum one hour (Krueger et al. 2002; Barnard et al. 2003). This short time frame was required to minimise the impact of extracorporeal platelet activation and influence of other factors affecting investigated parameters such as the effect of leukocytes activated by platelets.

Compounds were tested at following concentrations: anthocyanins at 0.1 µM, 4-HBAL at 0.5 µM, PCA at 0.2 µM, vanillic acid at 2 µM, ferulic acid at 1 µM and hippuric acid at 2 µM concentration. These chosen concentrations were closest to the plasma levels of these compounds reported after the consumption of anthocyanin-rich sources (de Ferrars, Cassidy, et al. 2014; de Ferrars, Czank, et al. 2014). Dilutions of anthocyanins and their metabolites were prepared from stock solutions (section 3.2.1.1.) using HTB and added to whole blood samples to reach the aforementioned working concentrations. The whole blood treated with 70% ethanol with 1% HCl or 70% ethanol in matched concentration was used as a blank for anthocyanins and metabolites, respectively. These blanks did not affect platelet activation and aggregation.

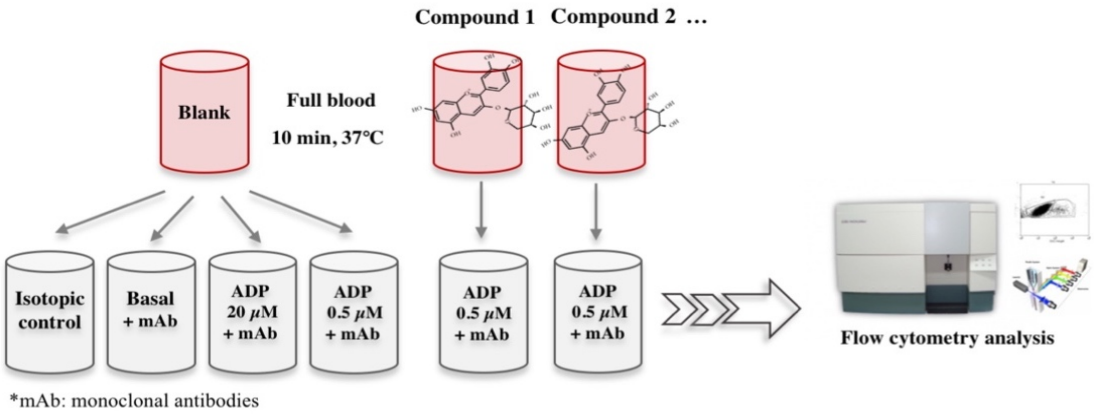

***Figure 14**. Schematic representation of the whole blood treatments used for the investigations of the* in vitro *effect of anthocyanins and their metabolites on platelet function.*

3.2.2.3. Assessments of platelet activation

Platelet activation was assessed based on the expression of P-selectin and GPIIb/IIIa on the surface of activated platelets.

Whole blood samples, treated with tested compounds or blank, were diluted with HTB (1:10) (Table 8). 20 µl of diluted whole blood samples were then activated with a suboptimal, 0.5 µM concentration of platelet agonists ADP and labelled with 5µl of antiCD61-PerCP (platelet identifier), antiCD62P-PE and PAC1-FITC antibody (Table 9) for 20 minutes at room temperature in the dark. Diluted blank blood, labelled with

monoclonal antibodies and treated with an optimal, 20 µM concentration of ADP was used to control the optimal response (Krueger et al. 2002; Barnard et al. 2003). Diluted and labelled blank blood without the addition of agonist and with the addition of an equal volume of HTB, was used to monitor platelet extracorporeal activation. At the end of the incubation time, samples were fixed with 400 µl of 1X CellFix solution for 15 minutes at room temperature in the dark and immediately analysed by FACSCalibur flow cytometer (BD Biosciences, Franklin Lakes, USA) and integrated CellQuest software, version 6.0. Schematic representation of a workflow is given in Figure 15.

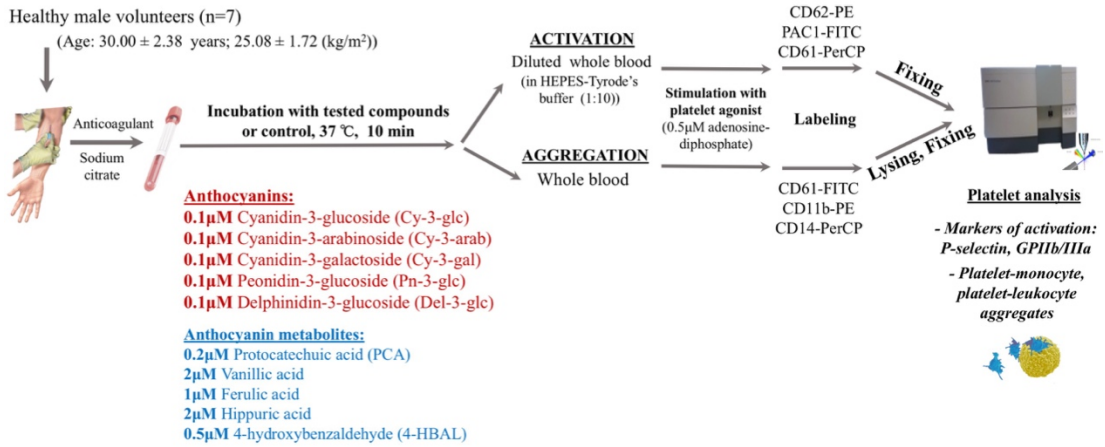

Figure 15. *Schematic representation of the platelet analyses workflow*

Anti-human IgG1-FITC, IgG2-PE and IgM-FITC antibodies (Table 9) were used as isotype controls for determining nonspecific antibody binding. Platelets were distinguished from leucocytes and red blood cells based on their specific forward and side light scatter and their CD61-PerCP fluorescence. The expression of the analysed markers of activation was expressed as a percentage or a mean fluorescence intensity (MFI) of P-selectin or GPIIb/IIIa positive platelets ($CD62P^+CD61^+$ or $PAC1^+CD61^+$) in a population of 20000 platelets ($CD61^+$ cells). The former represented the percentage of activated platelets in the total platelet population and later corresponded to a mean density of P-selectin or GPIIb/IIIa on activated platelets.

3.2.2.4. Assessments of platelet aggregation with monocytes and neutrophils

The whole blood samples treated with tested compounds or blank were used for the assessments of platelet-leucocyte aggregates. 25µl of whole blood samples were treated with a suboptimal, 0.5µM concentration of platelet agonists ADP and labelled with 5µl

of antiCD61-FITC (platelet identifier), antiCD14-PerCP (monocyte identifier) and antiCD11b-PE antibody (neutrophil identifier) (Table 9) by incubation for 15 minutes at room temperature in the dark. Labelled blank blood, treated with 20 μM ADP was used to control the optimal response. Labelled blank blood without the addition of agonist and with the addition of an equal volume of HTB, was used to monitor platelet extracorporeal activation. Following the incubation, samples were treated with 1.2 ml of 1X Lysing solution at room temperature in the dark for 12 minutes to lyse erythrocytes. Samples were then washed twice in HTB, fixed with 300 μl of 1X CellFix solution and immediately analysed on the flow cytometer (Figure 15). Anti-human IgG1-FITC, IgG2-PE, and IgG2-FITC antibodies (Table 9) were used as isotype controls for determining nonspecific antibody binding. Platelet aggregation with monocytes and neutrophils was expressed as a percentage of platelet-monocyte aggregates ($CD14^+CD61^+$ events) in the population of 1000 monocytes ($CD14^+$ cells) and platelet-neutrophil aggregates ($CD11b^+$ $CD61^+$ events) in the population of 10000 neutrophils ($CD11b^+$ cells).

3.2.2.5. Assessments of biochemical and haematological parameters

The biochemical and haematological analyses were performed to confirm volunteers' good health.

For the biochemical analysis, blood was collected in Vacutainer SSTTM II Advance tubes (BD Diagnostics, Franklin Lakes, USA), clotted at room temperature for l5-20 minutes and then centrifuged at 2000 rpm for 10 minutes to separate serum. 500 μl of serum was used for evaluation of defined biochemical parameters using the Cobas c111 clinical chemistry analyser (Roche Diagnostics, Basel, Switzerland) and appropriate Cobas reagent kits, as recommended by the manufacturer. The analysed parameters included: lipid status, glucose level, the activity of liver enzymes, levels of urea, uric acid, creatinine and iron.

For the haematological analysis, blood was collected in Vacutainer tubes containing K_2EDTA as an anticoagulant (BD Diagnostics, Franklin Lakes, USA). Haematological parameters were evaluated using the ABX micros 60 haematology analyser (Horiba, Kyoto, Japan).

3.2.2.6. Measurements of anthropometric parameters and blood pressure in healthy volunteers

Evaluated anthropometric parameters included body height, hip and waist circumferences as well as body weight measured using the TANITA UM-072 body composition analyser (Arlington Heights, USA).

The obtained values of body weight and height were used to calculate the body mass index (BMI) with the following equation: BMI = Weight (kg) / (Height (m))^2.

Systolic and diastolic blood pressure and heart rate were measured using the professional IntelliSense HEM-907XL blood pressure monitor (Omron, Bannockburn, USA) and expressed as an average value of three successive measurements.

3.2.3. Statistical analysis

Data from the cell adhesion and transmigration assays and Western blot experiments were analysed by one-way analysis of variance (ANOVA) followed by Dennett's post-hoc multiple comparison tests using Prism software, version 6.0.c for Mac OS X (GraphPad, La Jolla, CA, USA). For the assessments of the expression of platelet activation and aggregation markers, the obtained data was first examined by the Shapiro-Wilk normality test and then analysed by the paired samples t-test using the SPSS software, version 20.0. (SPSS, Chicago, USA), with the p-value<0.05 considered as significant. All of these data were graphically presented using the Prism software as mean with standard deviation (SD).

4. RESULTS

4.1. Investigations of the effect of anthocyanins and their metabolites on endothelial cell function

4.1.1. Cell viability assay

The results from the available literature show that anthocyanins and their metabolites do not significantly affect endothelial cell viability when tested at up to 100μM concentrations. Therefore, in this thesis, the cytotoxic effect of solvents that were used to dissolve anthocyanins and their metabolites was assessed prior to investigations of the impact of these compounds on endothelial cell function. Results from the cell viability assay using crystal violet revealed that both 3 and 24-hour exposure of HUVECs to either 70% ethanol or 70% ethanol with 1% HCl diluted to a final concentration of 0.1% (v/v) in the culture medium did not significantly affect the cell viability (Figure 16).

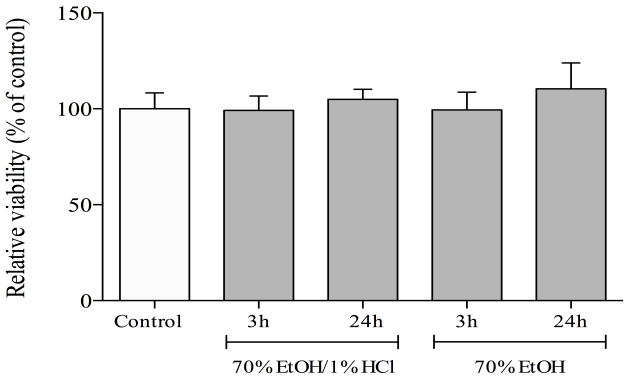

***Figure 16**. The effect of solvents (70% ethanol or 70% ethanol with 1% HCl, diluted to a final concentration of 0.1% (v/v)) on endothelial cell viability. Viability is represented in comparison to control (HUVECs treated with culture medium) that is normalised to 100%. Results are reported as mean ± SD of four replicates for both control and experimental treatments.*

4.1.2. The effect of anthocyanins and their upper GIT metabolite 4-HBAL on monocyte adhesion to TNFα-activated endothelial cells

To test whether anthocyanins and their upper GIT metabolite 4-HBAL alter monocyte adhesion to inflamed endothelial cells, cell adhesion assays were performed as described in the section 3.2.1.5. Following the co-incubation with unstimulated endothelial cells, monocyte exhibited low, basal levels of adhesion (Figure 17). This was significantly changed upon stimulation of HUVECs with TNFα when a 9.2-fold increase in monocytes adhesion was observed compared to unstimulated cells. Pretreatment of HUVECs for 3

hours with different anthocyanins displayed the ability of these compounds to reduce the TNFα-induced increase in monocyte adhesion (Figure 17). Cy-3-gal at 0.1μM, 0.2μM and 2μM concentrations significantly diminished monocyte adhesion by 21.0%, 15.4% and 22.8 %, respectively, while pre-exposure of endothelial cells with cy-3-arab at 0.1μM and 2μM levels decreased adhesion by 30.4% and 23.5%, respectively. Cy-3-glc significantly attenuated monocyte adhesion only at the highest tested concentrations, with a reduction of 26.3% and 29.9% observed at 1 μM and 2 μM concentrations, respectively. By contrast, pn-3-glc significantly decreased monocyte adhesion by 26 % at the lowest, 0.1 μM concentration, with no significant effect at other tested concentrations. Of all examined anthocyanins only del-3-glc displayed a significant effect on monocyte adhesion at all tested concentrations, with the highest decrease of 33.1 % observed at 0.1 μM concentration. Unlike anthocyanins, pretretement of HUVECs to the anthocyanin upper GIT metabolite 4-HBAL for 3 hours did not significantly affect monocyte adhesion to activated endothelial cells at any tested concentration (12.2 % reduction at 0.5 μM and 19.7% at 2 μM level) (Figure 17).

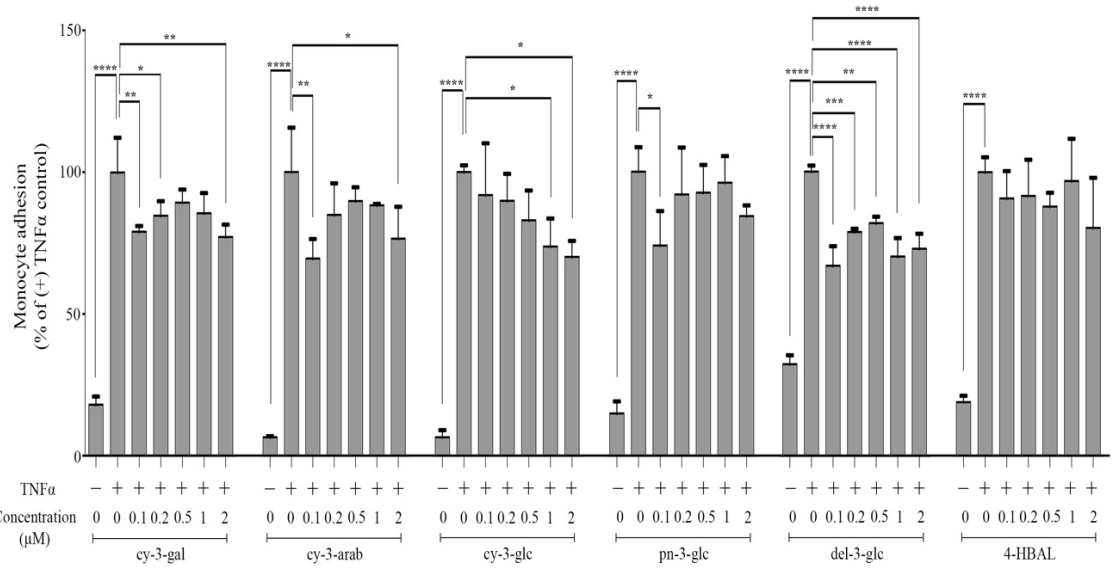

Figure 17*. The effect of pretreatment of endothelial cells with anthocyanins and their upper GIT metabolite 4-HBAL on monocyte adhesion to TNFα-stimulated HUVECs. Monocyte adhesion is represented in comparison to positive control (TNFα-stimulated HUVECs) that is normalised to 100%. Results are reported as mean ± SD of three replicates. *p<0.05, **p<0.01, ***p<0.001, ****p<0.0001.*

4.1.3. The impact of gut metabolites on monocyte adhesion to TNFα-stimulated endothelial cells

Similar to anthocyanins, all of the tested gut metabolites exhibited the ability to affect monocyte adhesion to activated endothelial cells (Figure 18). Pretreatment of HUVECs for 18 hours with vanillic acid at 0.2 μM and 2 μM concentrations significantly decreased monocyte adhesion by 25.8% and 19.0%, respectively. Both hippuric and ferulic acids significantly attenuated monocyte adhesion only at the highest tested concentrations, with a decrease of 18.1% observed with 2 μM hippuric acid and 21.3% and 31.5% with 1 μM and 2 μM ferulic acid, respectively. PCA showed the greatest ability to affect monocyte adhesion to TNFα-activated endothelial cells, causing the significant 31.9%, 28.7%, 38.4% and 47% reductions in monocyte adhesion at 0.2 μM, 0.5 μM, 1μM and 2 μM concentrations, respectively (Figure 18).

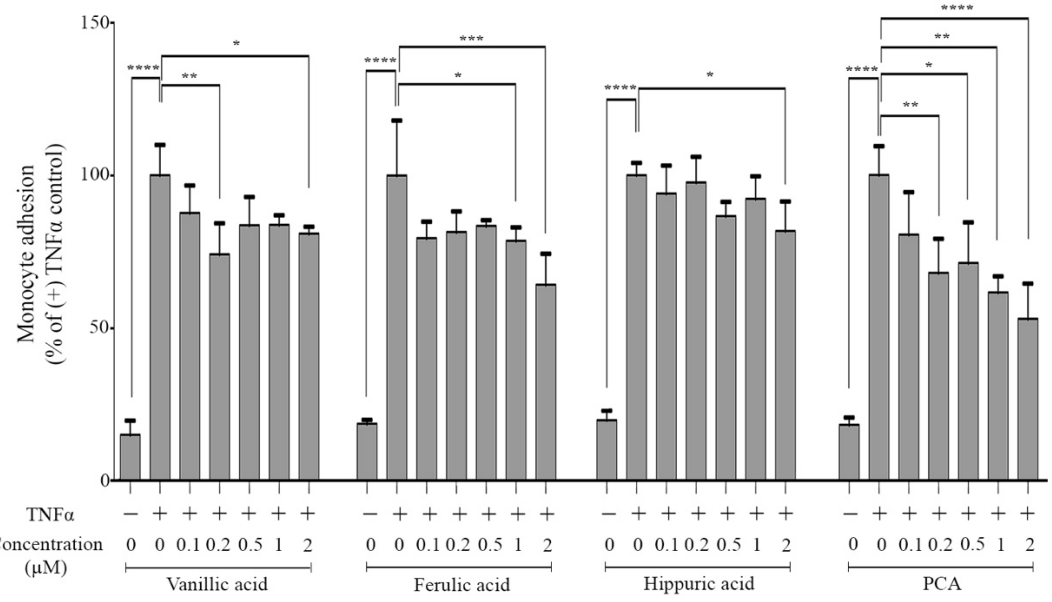

Figure 18. *The effect of pretreatment of endothelial cells with gut metabolites on monocyte adhesion to TNFα-stimulated HUVECs. Monocyte adhesion is represented in comparison to positive control (TNFα-stimulated HUVECs) that is normalised to 100%. Results are shown as mean ± SD of three replicates. *p<0.05, **p<0.01, ***p<0.001, ****p<0.0001.*

4.1.4. The impact of mixtures of anthocyanins and their metabolites on monocyte adhesion to TNFα-stimulated endothelial cells

With the aim to investigate the possible synergic effect of anthocyanins and their metabolites that are present in the circulation at the same time following the anthocyanin intake, HUVECs were pretreated with different mixtures of compounds, and monocyte adhesion to TNFα-activated endothelial cells was assessed. Pre-exposure of endothelial cells for 3 hours with the mixture of anthocyanins and their upper GIT metabolite 4-HBAL (mix A) significantly lowered monocyte adhesion by 26.4% (Figure 19A). The 18 hour-treatment with the mixture of anthocyanin gut metabolites (mix B) also significantly decreased monocyte adhesion by 18.7%, although to a lesser extent than mix A (Figure 19B). Pre-exposure of HUVECs with the mix A for 3 hours and then mix B for 18 hours, i.e. the experimental condition that mimicked the anthocyanin pharmacokinetic profiles in the circulation following the consumption of anthocyanin-rich foods (mix A+B), also significantly attenuated monocyte adhesion by 30.6% (Figure 19C).

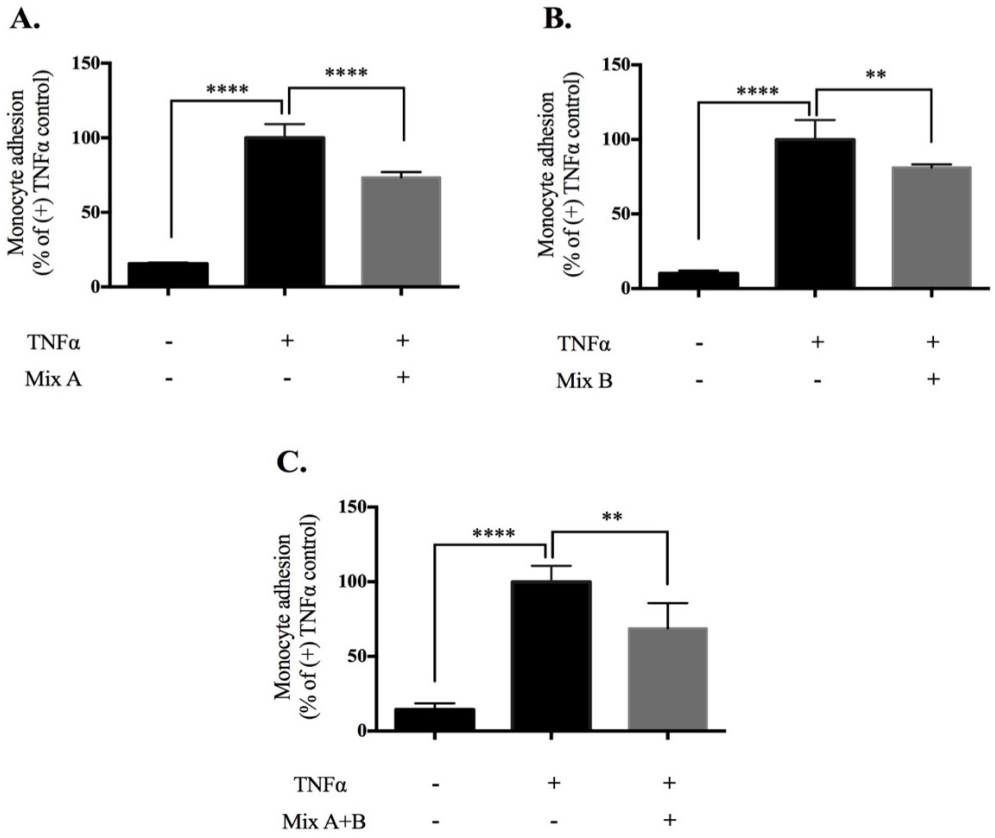

Figure 19. *The effect of pre-exposure of HUVECs with the mix A (A), mix B (B) and mix A+B (C) on monocyte adhesion to TNFα-stimulated HUVECs. Monocyte adhesion is represented in comparison to positive control (TNFα-stimulated HUVECs), normalised to 100%. Results are displayed as mean ± SD of three replicates. **p<0.01, ****p<0.0001.*

4.1.5. The effect of mixtures of anthocyanins and their metabolites on monocyte transendothelial migration

The effect of mixtures on monocyte transendothelial migration was examined using a transwell system as described in the section 3.2.1.7. As shown in Figure 20, the addition of chemoattractant cytokine MCP-1 to the lower compartments of transwell system resulted in a significant 3.2-fold increase in monocyte migration through HUVEC monolayer compared to condition with no added MCP-1. Pre-exposure of endothelial cells with different mixtures significantly attenuated the MCP-1 induced increase in monocyte transendothelial migration (Figure 20). Mix A displayed the ability to decrease the transmigration by 43.9%, mix B by 50.5% and mix A+B by 41.2%.

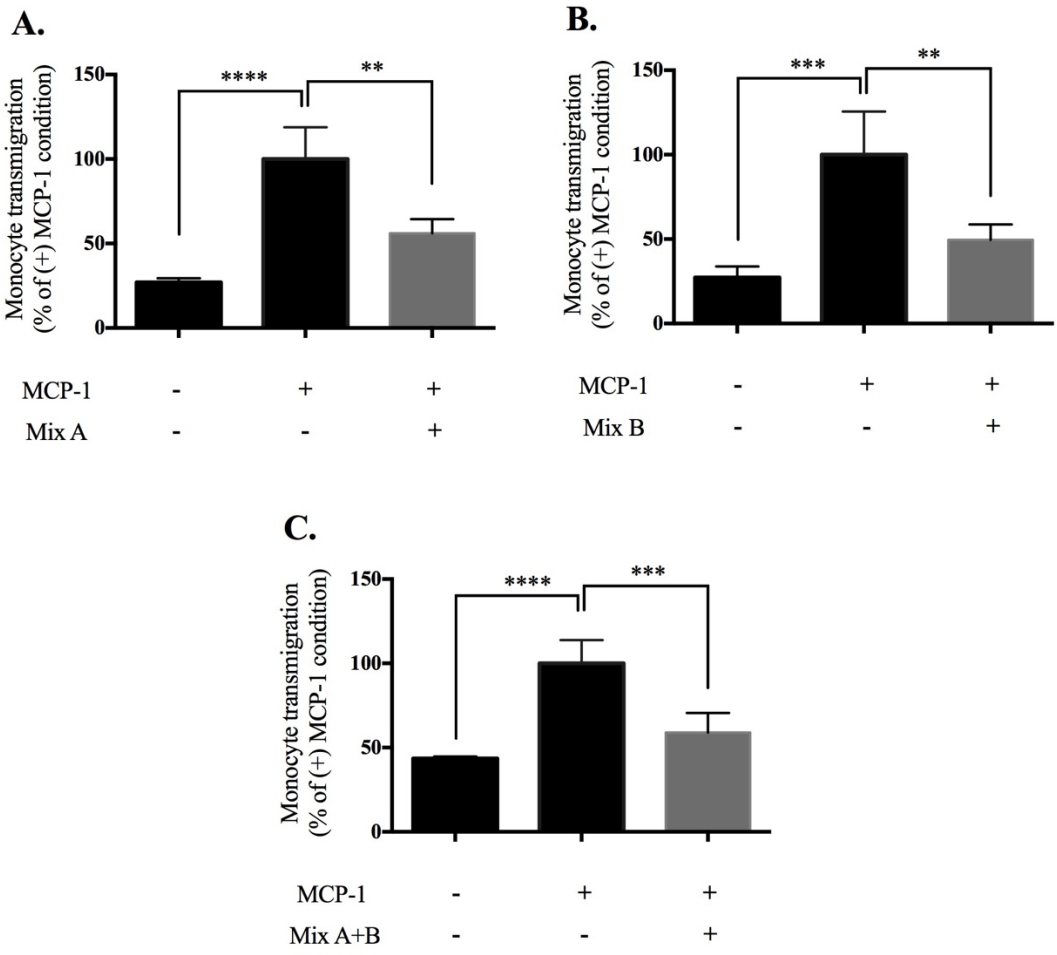

Figure 20. *The effect of pre-exposure of HUVECs with the mix A (A), mix B (B) and mix A+B (C) on MCP-1-induced monocyte transendothelial migration. The values are represented in comparison to positive control (MCP-1-stimulated HUVECs), normalised to 100%. Results are displayed as mean ± SD of four replicates. **p < 0.01, ***p < 0.001, ****p < 0.0001.*

4.1.6. The effect of mixtures of anthocyanins and their metabolites on gene expression in endothelial cells

The impact of anthocyanins and their metabolites on gene expression in endothelial cells was examined with an aim to identify the mechanisms by which these compounds could induce the observed effects on monocyte adhesion and transendothelial migration.

In the test experiments performed before the gene expression macroarray analysis using TLDA cards, the ability of TNFα to induce the inflammation and modulate the expression of inflammatory genes *VCAM1* and *SELE* in the endothelial cells was confirmed. This experiment showed that the low, basal expression of these genes in TNFα-non-activated endothelial cells was significantly increased upon the 4 hour-treatment with TNFα (Figure 21).

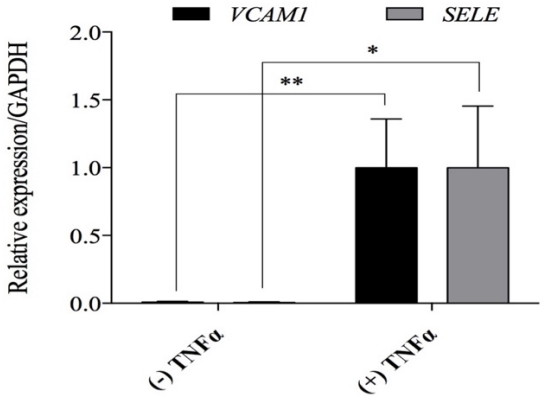

Figure 21. *The effect of TNFα on the relative expression of genes encoding cell adhesion molecules VCAM-1 and E-selectin in HUVECs. Relative gene expression was normalised to housekeeping gene GAPDH and shown as fold-change over TNFα-activated HUVECs. Results are displayed as mean ± SD of three replicates, *p<0.05, **p<0.01, student t-tests.*

The impact of mixtures of tested compounds on the expression of 91 genes involved in endothelial cell function was evaluated using macroarrays. These results revealed that the pre-exposure of endothelial cells to the mix A, mix B and mix A+B resulted in significant alterations in gene expression when compared to TNFα-stimulated cells nonexposed to mixtures (Table 12). Mix A significantly affected the expression of 7 genes such as *ICAM1*, *CXCL12* or *IKBKB* that encode proteins involved in the regulation of cell adhesion or NF-κB signalling pathway. Mix B significantly altered the expression of 10 genes, including genes like *CDH5, CLDN1, CAPN1* and *ITGA5*. These genes are involved in pathways that regulate leukocyte transendothelial migration cell adhesion, tight junction or focal adhesion. Pretreatment of endothelial cells with the mix A and then

mix B significantly modulated the expression of 7 genes, such as *GJA4, ITGA5, CXCL12* and *CAPN1* that are involved in the pathways regulating leukocyte transendothelial migration, actin cytoskeleton organisation or focal adhesion.

Table 12. *Genes identified as differentially expressed between endothelial cells pre-exposed to the mix A, mix B or mix A+B and stimulated with TNFα and those treated only with TNFα*

Gene symbol	Gene Name	FC
Mix A		
IKBKB	inhibitor of nuclear factor kappa B kinase subunit beta	0.44
CXCL12	C-X-C motif chemokine ligand 12	0.52
CLDN1	claudin 1	0.31
IGF1R	insulin-like growth factor 1 receptor	0.44
ICAM1	intercellular adhesion molecule 1	0.51
F11R	F11 receptor	0.49
FABP4	fatty acid binding protein 4	0.22
Mix B		
CDH5	cadherin 5	15.12
JAM3	junctional adhesion molecule 3	1.55
CALM1	calmodulin 1	3.01
CASK	calcium/calmodulin-dependent serine protein kinase	4.01
RHOC	ras homolog gene family member C	0.37
ITGA5	integrin subunit alpha 5	0.59
CAV1	caveolin 1	4.18
CLDN1	claudin 1	5.45
CALD1	caldesmon 1	9.14
CAPN1	calpain 1	0.45
Mix A+B		
GJA4	gap junction protein alpha 4	12.88
CDH5	cadherin 5	7.20
ITGA5	integrin subunit alpha 5	0.37
EZR	ezrin	2.06
CXCL12	C-X-C motif chemokine ligand 12	0.21
TLN1	talin 1	0.39
CAPN1	calpain 1	0.38

Results are expressed as fold change (FC) over TNFα-activated HUVECs, $p<0.05$.

4.1.7. The effect of anthocyanins and their metabolites on endothelial cell signalling

Gene expression is controlled at the transcriptional level by transcription factors which activity is regulated by signalling pathways. Therefore, differentially expressed genes from gene expression experiments were analysed to find possible transcription factors and signalling proteins that could mediate the observed nutrigenomic effect of tested compounds. The most significant transcription factors that were identified by Metacore included CREB1, SP1, c-Jun and NF-κB (Supplementary Table 3). Afterwards, the KEGG database was used to determine the upstream signalling proteins that are involved in regulation of the activity of these transcription factors. A network of 62 proteins (including transcription factors and their regulatory cell signalling proteins) was identified (Figure 22) and further analysed by molecular docking to investigate whether anthocyanins and their metabolites can bind to these proteins and possibly affect their activity, which could be associated with the observed modulations in gene expression.

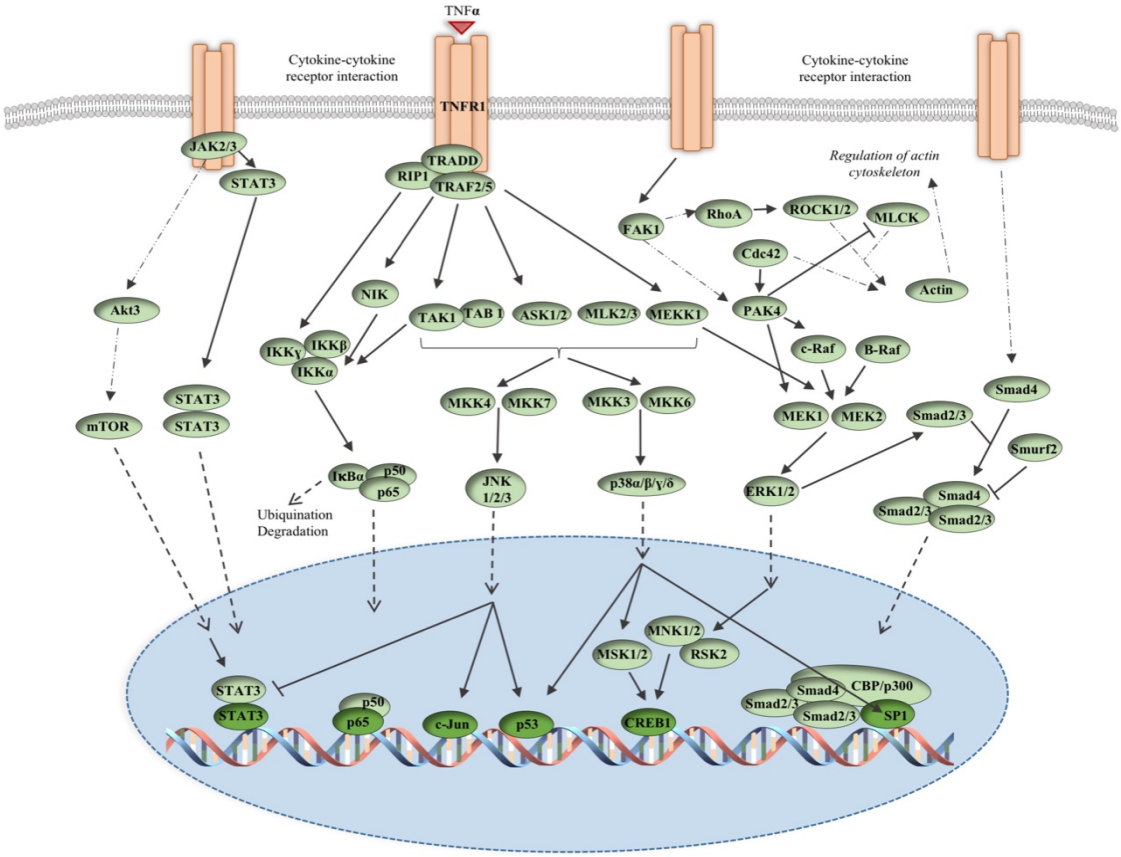

Figure 22. *Schematic representation of 62 proteins identified from gene expression data using Metacore and KEGG bioinformatics tools,*

Before docking, the chemical structures of anthocyanins and their metabolites were drawn (Figure 23) and their pharmacophore points examined.

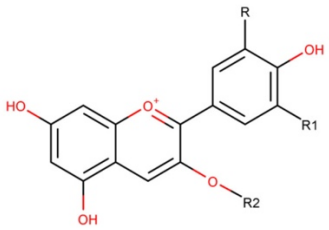

The framework structure of anthocyanidins (with substituents)

Anthocyanins	Substituents		
	R	R_1	R_2
Cyanidin-3-O-arabinoside	−OH	−H	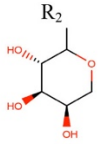
Cyanidin-3-O-galactoside	−OH	−H	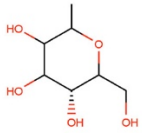
Cyanidin-3-O-glucoside	−OH	−H	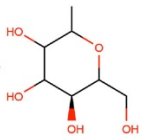
Delphinidin-3-O-glucoside	−OH	−OH	
Peonidin-3-O-glucoside	$-OCH_3$	−H	

Anthocyanin metabolites

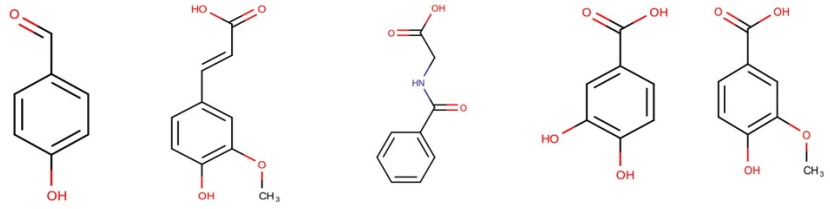

4-HBAL | Ferulic acid | Hippuric acid | PCA | Vanillic acid

Figure 23. *The chemical structures of anthocyanins and their metabolites*

The pharmacophore search (Figure 24) showed that the phenolic ring system of anthocyanins is planar and electron-rich. Their planar benzene ring is hydrophobic, but their phenolic hydroxyl group that is also present in their metabolites confers polarity and solubility in water as well as the capacity to form hydrogen (H) bonds with proteins. Additionally, hippuric acid has an electron donor (-NH-) and may form additional H-bonds with proteins. Only a few amino acid (AA) residues of investigated protein targets such as asparagine (Asn), glutamine (Gln), histidine (His), Ser, glutamic acid (Glu),

aspartic acid (Asp) or tyrosine (Tyr) can make H-bonds with the ligands. Extended hydrophobic regions of all ligands allow them to interact with the regions of targets that are rich in hydrophobic AA residues like alanine (Ala), leucine (Leu), isoleucine (Ile), valine (Val), methionine (Met), tryptophan (Trp) cysteine (Cys), phenylalanine (Phe) or proline (Pro).

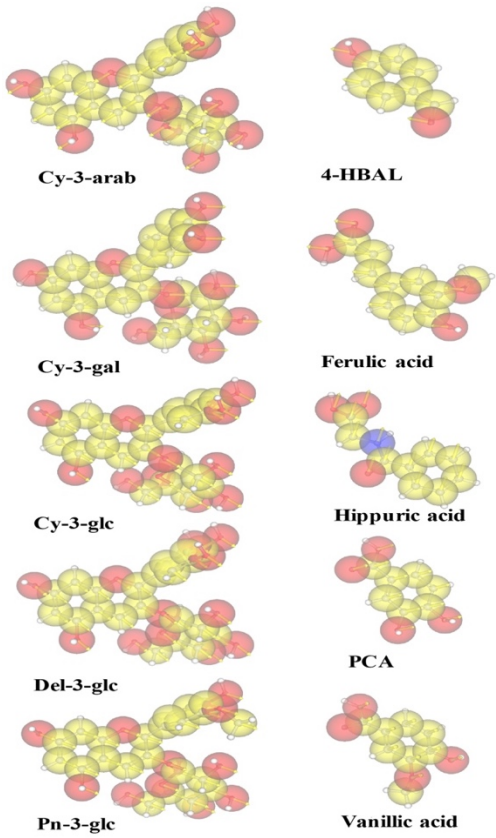

Figure 24. *Pharmacophore points of the examined ligands. Ligands are represented as stick and balls. Yellow spheres show the hydrophobic points, red spheres the electron acceptor points, blue spheres the electron donor point and yellow arrows the direction of the pharmacophore effects.*

The molecular docking analyses revealed that anthocyanins and their metabolites present capacity to bind to the identified cell signalling proteins (Supplementary Table 4). The BA of anthocyanins for the investigated targets ranged from -4.9 to -9.9 kcal/mol. Results show that anthocyanins can establish strong interactions (BA between -8.5 and -9.9 kcal/mol) with some of the investigated signalling proteins (Supplementary Table 4). Among these proteins were those belonging to STE Ser/Thr protein kinase family (dual specificity mitogen-activated protein kinase kinase 2 (MEK2)), CMGC Ser/Thr protein kinase family (mitogen-activated protein kinase 8 (JNK1)), Tyr protein kinase family

(focal adhesion kinase 1 (FAK1)), AGC Ser/Thr protein kinase family (Rho-associated protein kinase 2 (ROCK2)) and Ser/Thr protein kinase family (inhibitor of nuclear factor kappa-B kinase subunit alpha (IKKα)) of protein kinases (Supplemental table 5).

Results of molecular docking against MEK2 (Supplementary Table 5) revealed that tested anthocyanins interact only with the protein kinase domain of this target via adenosine triphosphate (ATP) binding site and Ser/Thr-protein kinase active site. Figure 25 shows different views of the best docking pose of del-3-glc that forms strong H-bonds and steric interactions with Ser/Thr-protein kinase active site (located between positions 190-202) and ATP binding site (located between positions 78-101) of MEK2, a binding pattern that may influence the protein kinase activity of this enzyme.

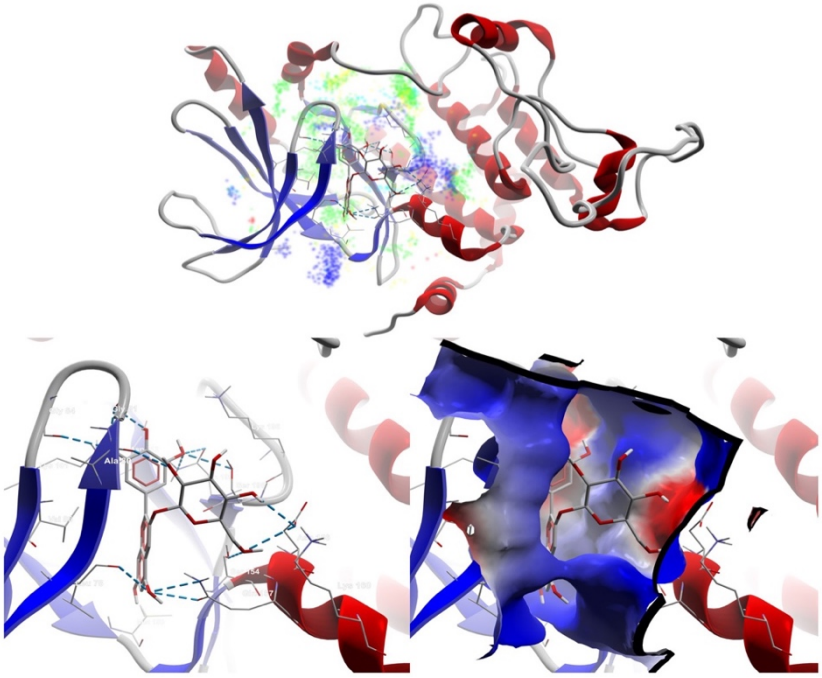

Figure 25*. Best docking pose of del-3-glc, the strongest binder of MEK2 (target presented as thin sticks with secondary structure drawn as cartoon backbone; ligand as sticks). The general view with H-bonds (light blue dashed lines) and energy grid (light blue-hydrogen acceptor favourable; green-steric favourable; yellow-hydrogen donor favourable; orange to red, dark blue-electrostatic interactions) (top image). Detailed view with H-bonds formed between ligand and target (bottom left). Target presented with molecular surface (cropped view) whit ligand deeply buried inside of the binding pocket (bottom right).*

Docking against JNK revealed that anthocyanins establish strong interactions with the protein kinase domain of this protein through H-bonds and steric interactions (Figure 26, Supplementary Table 5). All tested anthocyanins can bind to JNK1 in a large binding pocket described between Ile32 and Asp169, which includes the conserved signature

region of MAP kinases (located between positions 61-163) and the Ser/Thr-protein kinase active site (located between positions 145-159), which may affect the kinase functions of this cell signalling protein.

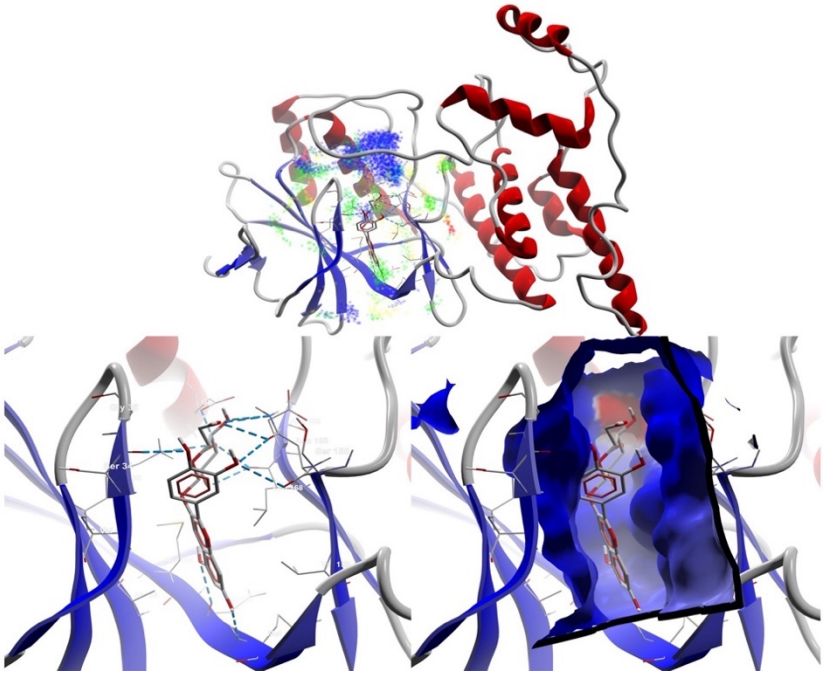

***Figure 26**. Best docking pose of cy-3-glc, the strongest binder of JNK1 (target presented as thin sticks with secondary structure drawn as cartoon backbone; ligand as sticks). The general view with H-bonds (light blue dashed lines) and energy grid (light blue-hydrogen acceptor favourable; green-steric favourable; yellow-hydrogen donor favourable; orange to red, dark blue-electrostatic interactions) (top image). Detailed view with H-bonds formed between ligand and target (bottom left). Target presented with molecular surface (cropped view) whit ligand deeply buried inside of the binding pocket (bottom right).*

Docking results against FAK1 showed that anthocyanins establish strong interactions with the protein kinase domain (cy-3-arb and cy-3-gal), FERM domain (pn-3-glc and cy-3-glc) or both protein kinase and FERM domain (del-3-glc, Figure 27) of FAK1 trough H-bonds and steric interactions (Supplementary Table 5). Interaction of ligands with the FERM domain could affect the localisation of this protein to the plasma membrane, while interactions of anthocyanins with the protein kinase ATP binding site (located between positions 428-454) and Tyr-protein kinase active site (located between positions 542-554) of FAK1 may affect its kinase function.

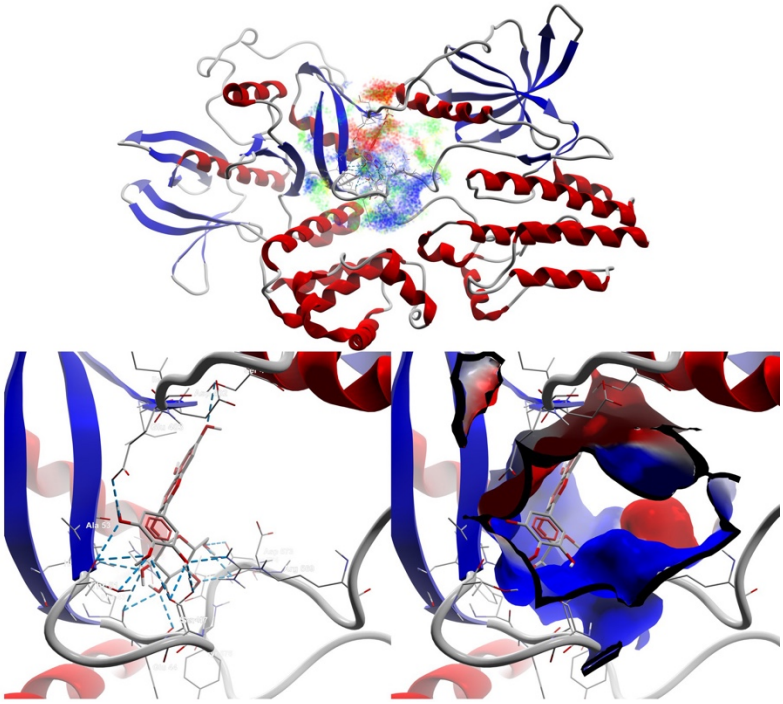

Figure 27*. Best docking pose of del-3-glc, the strongest binder of FAK1 (target presented as thin sticks with secondary structure drawn as cartoon backbone; ligand as sticks). The general view with H-bonds (light blue dashed lines) and energy grid (light blue-hydrogen acceptor favourable; green-steric favourable; yellow-hydrogen donor favourable; orange to red, dark blue-electrostatic interactions) (top image). Detailed view with H-bonds formed between ligand and target (bottom left). Target presented with molecular surface (cropped view) whit ligand deeply buried inside of the binding pocket (bottom right).*

Results of docking analyses against ROCK2 showed that investigated anthocyanins are deeply buried inside of the protein kinase domain (Ile98-Asp232), with ligands-protein interactions formed by H-bonds and electrostatic interaction (Supplementary Table 5, Figure 28). Additionally, weak steric interactions are established with AGC-kinase C-terminal domain (pn-3-glc, del-3-glc, cy-3-glc and cy-3-arab having steric interactions with Phe384, while cy-3-gal establishes steric interactions with Phe384 and Ile387). The binding pattern demonstrates that the bulky anthocyanins interplay concomitantly with Ser/Thr-protein kinase active site (located between positions 210-222) and protein kinase ATP binding site (located between positions 98-121).

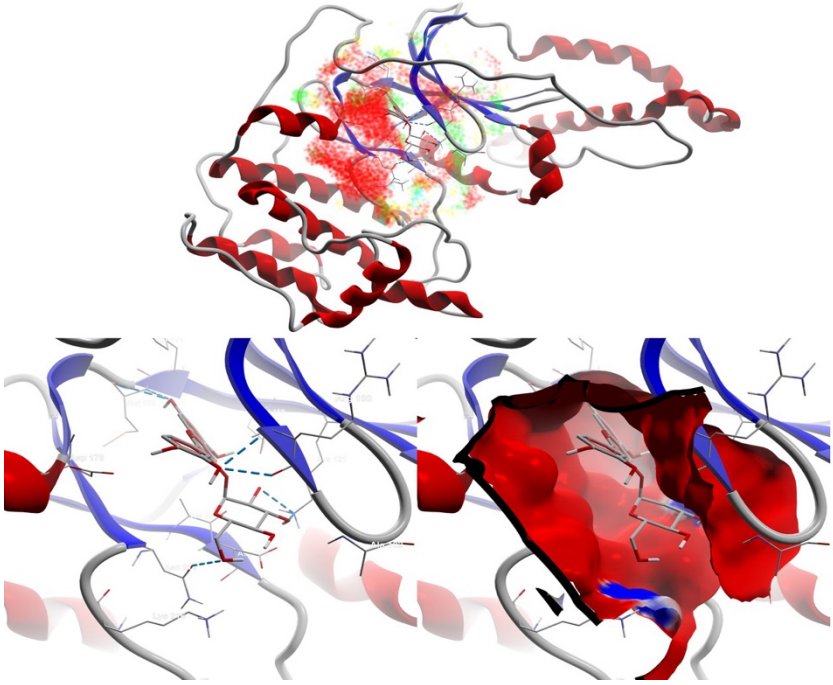

***Figure 28**. Best docking pose of cy-3-gal, the strongest binder of ROCK2 (target presented as thin sticks with secondary structure drawn as cartoon backbone; ligand as sticks). The general view with H-bonds (light blue dashed lines) and energy grid (light blue-hydrogen acceptor favourable; green-steric favourable; yellow-hydrogen donor favourable; orange to red, dark blue-electrostatic interactions) (top image). Detailed view with H-bonds formed between ligand and target (bottom left). Target presented with molecular surface (cropped view) whit ligand deeply buried inside of the binding pocket (bottom right).*

Docking results against IKKα showed that all investigated anthocyanins interact with the protein kinase domain (located between positions 15-302) and AAs of the α-helix that is located close to the Leucine-zipper (Figure 29, Supplementary Table 5). This indicates that tested anthocyanins do not interact with the protein kinase ATP binding site (located between positions 22-44) but establish strong interactions with Ser/Thr-protein kinase active site (located between positions 140-152) and surrounding area via H-bonds and steric interactions, which may affect Ser/Thr-protein kinase activity.

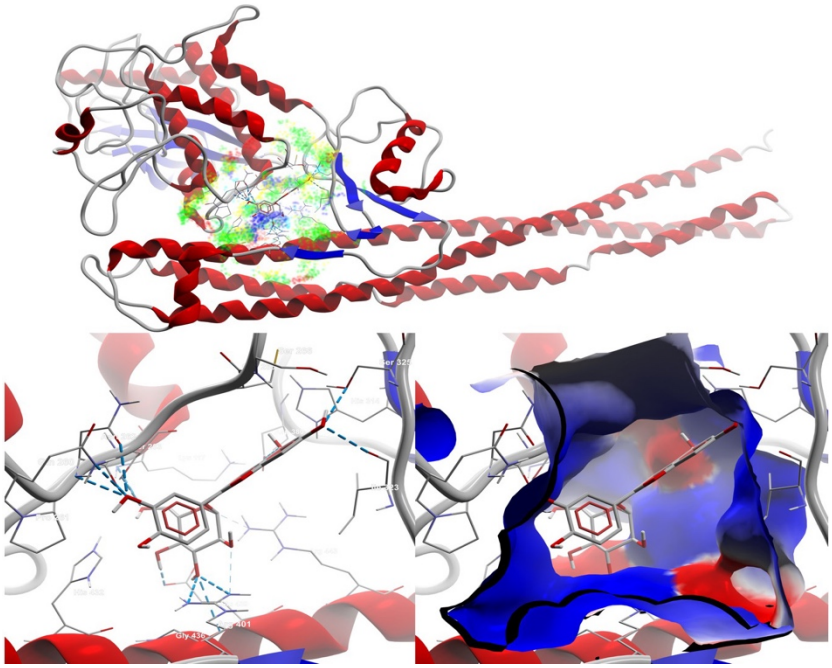

Figure 29. *Best docking pose of cy-3-gal, the strongest binder of IKKα (target presented as thin sticks with secondary structure drawn as cartoon backbone; ligand as sticks). The general view with H-bonds (light blue dashed lines) and energy grid (light blue-hydrogen acceptor favourable; green-steric favourable; yellow-hydrogen donor favourable; orange to red, dark blue-electrostatic interactions) (top picture). Detailed view with H-bonds formed between ligand and target (bottom left). Target presented with molecular surface (cropped view) whit ligand deeply buried inside of the binding pocket (bottom right).*

Regarding anthocyanin gut metabolites, docking results showed that these compounds can also bind cell signalling proteins with some ligand-target interactions BA reached or overpassed -7.0 kcal/mol: ferulic acid against protein Janus kinase 3 (JAK3), myosin light-chain kinase (MLCK), mitogen-activated protein kinase 11 (p38β) and b-Raf proto-oncogene (b-Raf), hippuric acid against p38β, b-Raf, Raf-1 proto-oncogene (c-Raf) and ERK1, PCA against and b-Raf and CREB binding protein (CREBBP). However, in general, these metabolites are weaker binders than anthocyanins (Supplementary Figure 1), with BA mainly between -3.3 and -6.9 kcal/mol (Supplementary Table 4). Results of docking analyses against JAK3, a Tyr-protein kinase with two described catalytic regions (between positions 521-777 and 822-1095), showed that ferulic acid interacts with this kinase in a small binding pocket deeply inside of its second catalytic domain (Figure 30, Supplementary Table 6). Ferulic acid interacts with the Tyr-protein kinase catalytic domain via two strong H-bonds (with Leu905 and Asp967 (Figure 30)) and weak steric interactions (Supplementary Table 6). Additional weak steric interactions

are made with the two functional regions of the catalytic domain: the ATP binding site and the Tyr kinase active site.

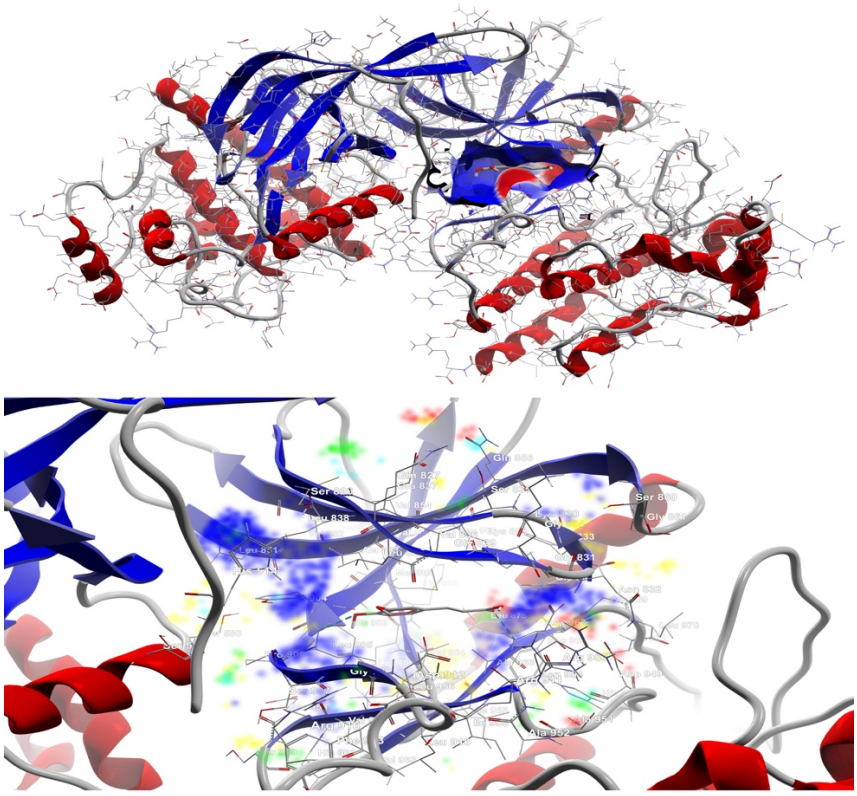

Figure 30. *General view (top image) and detail (bottom image) of the best docking pose of ferulic acid (figured as ball-and-stick, CPK coloured) against JAK3. Target is depicted as thin sticks with secondary structure drawn as cartoon backbone and semi-transparent electrostatic molecular surface (cropped to the docking site for a better view in the top image). The bottom image shows ferulic acid binding mode (the cropped view showing only the nearest AAs residue-until a 10.0 Å distance from ligand), emphasizing two H-bonds (shown as dashed blue lines) established with the AAs of the Tyr-protein kinase catalytic domain (Leu905 and Asp967). The energy grid components are depicted as fading dots: green-steric favourable; light blue-hydrogen acceptor favourable; yellow-hydrogen donor favourable; red and dark blue-electrostatic interactions.*

Docking against MLCK revealed that ferulic acid interacts with the protein kinase domain (located at MLCK between positions 106-361). Ferulic acid makes five H-bonds and weak steric interactions within the binding pocket (Figure 31, Supplementary Table 6). Weak H-bonds are established with glycine (Gly)114, Gly115 and lysine (Lys)135 of the ATP binding site and another two adjacent AAs (Glu181 and Val183). The binding pattern of this metabolite concomitantly blocks the access of substrate at the location of the active site of the Ser/Thr-protein kinase, by establishing weak steric interactions.

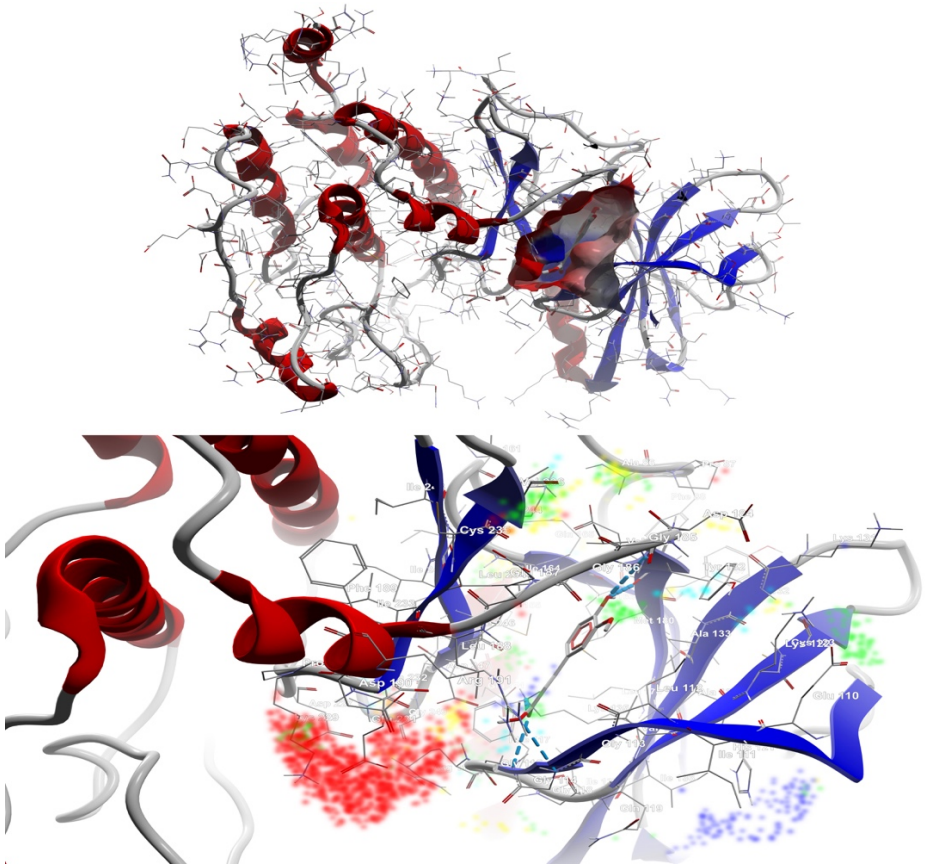

***Figure 31**. General view (top image) and detail (bottom image) of the best docking pose of ferulic acid (figured as ball-and-stick, CPK coloured) against MLCK. Target is depicted as thin sticks with secondary structure drawn as cartoon backbone and semi-transparent electrostatic molecular surface (cropped to the docking site for a better view in the top image). The bottom image shows ferulic acid binding mode (the cropped view showing only the nearest AAs residues-until a 10.0 Å distance from ligand), emphasizing five H-bonds (depicted as dashed blue lines) established with the AAs from ATP binding site (Gly114, Gly115 and Lys135) and protein kinase domain (Glu181 and Val183). The energy grid components are shown as fading dots: green-steric favourable; light blue-hydrogen acceptor favourable; yellow-hydrogen donor favourable; red and dark blue-electrostatic interactions.*

Docking results also showed that PCA interacts with a good BA (7.2 kcal/mol) with b-Raf (Supplementary Table 4). PCA forms five H-bonds and multiple steric interactions (both weaker and stronger) with the catalytic domain of this target (Ser-Thr/Tyr-protein kinase domain, located at b-Raf between positions 458-712) (Figure 32, Supplementary Table 6). All interactions are made with AAs from the active site and surrounding residues. PCA does not interact with the ATP binding site of b-Raf (located between positions 463-483).

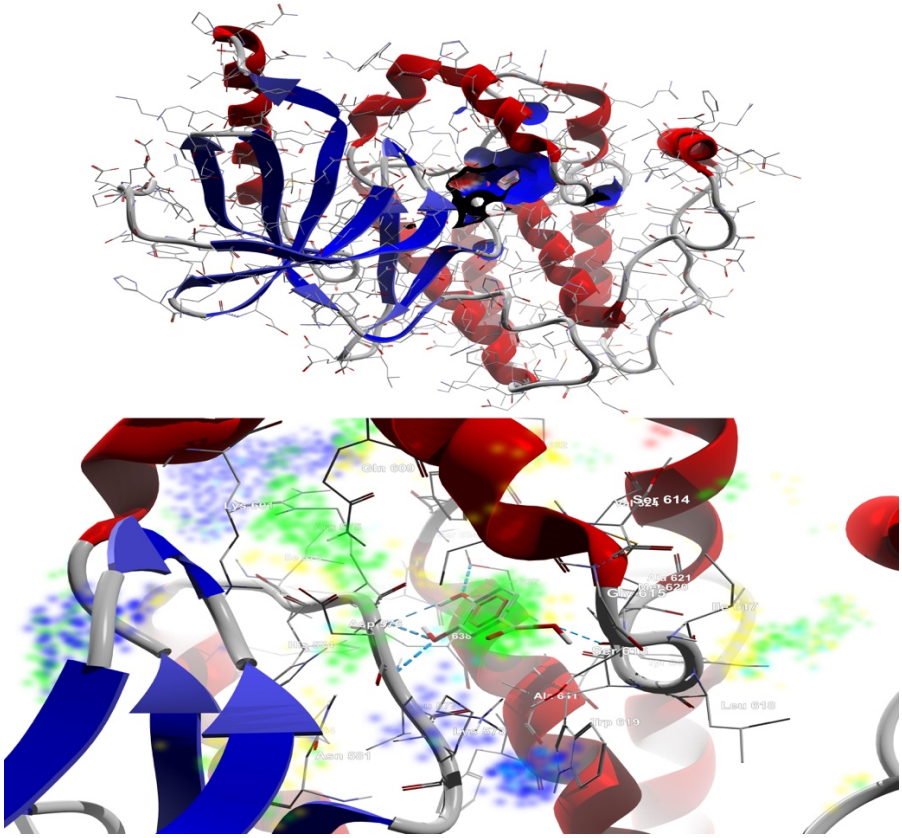

***Figure 32**. General view (top image) and detail (bottom image) of the best docking pose of PCA (figured as ball-and-stick, CPK coloured) against b-Raf. Target is depicted as thin sticks with secondary structure drawn as cartoon backbone and semi-transparent electrostatic molecular surface (cropped to the docking site for a better view in the top image). The bottom image shows PCA binding mode (the cropped view showing only the nearest AAs residues-until a 10.0 Å distance from PCA), emphasizing five H-bonds (depicted as dashed blue lines) established with the AAs of the active site located within the Ser-Thr/Tyr-protein kinase, catalytic domain (Leu577) and surrounding residues (Ser616, Ser637 and Asp638- two H-bonds). The energy grid components are shown as fading dots: green-steric favourable; light blue-hydrogen acceptor favourable; yellow-hydrogen donor favourable; red and dark blue-electrostatic interactions.*

Docking against P38β revealed that ferulic acid, hippuric acid and PCA bind into a small pocket described inside of protein kinase domain (located at P38β between positions 24-308) (Figure 33, Supplementary Table 6). All three metabolites have similar binding patterns, making H-bonds and steric interactions with the MAP kinase domain and the ATP binding site (Supplementary Table 6).

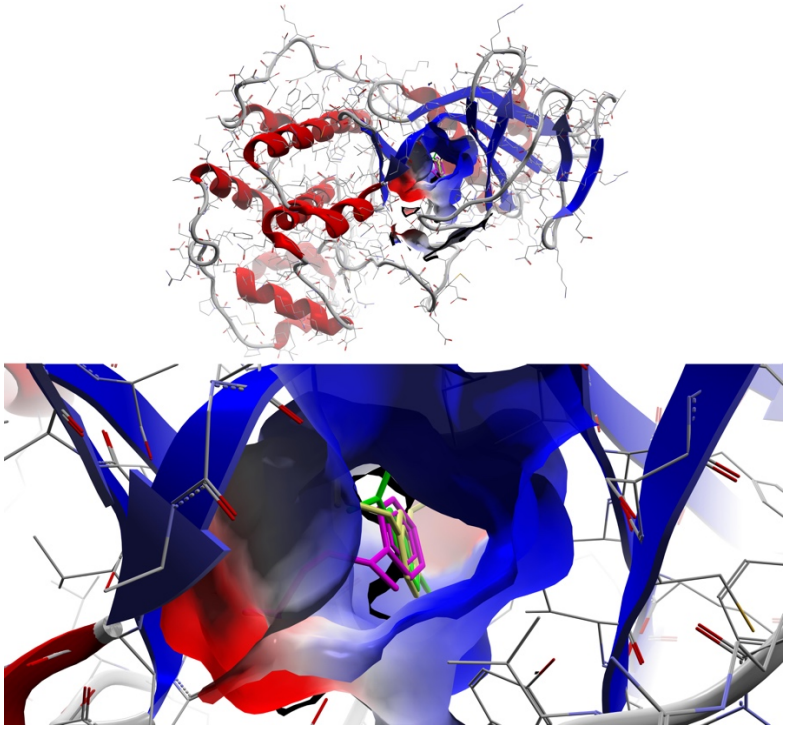

Figure 33. *General view (top image) and detail (bottom image) of the best docking pose of ferulic acid (yellow), hippuric acid (pink) and PCA (green) against P38β. Target is depicted as thin sticks with secondary structure drawn as cartoon backbone and semi-transparent electrostatic molecular surface (cropped to the docking site for a better view), metabolites are figured as ball-and-stick.*

These data suggest that anthocyanins and their metabolites can bind to cell signalling proteins and affect their function and phosphorylation of downstream cell signalling proteins that in consequence affect transcription factor activity and result in the observed nutrigenomic effect.

To associate results obtained by molecular docking with the possible *in vitro* effect on cell signalling pathways, the impact of anthocyanins and their metabolites on the activation of cell signalling proteins or transcription factors (assessed as a ratio of phosphorylated to total protein levels) was investigated in endothelial cells. Results revealed that pretreatment of HUVECs with the mix A significantly reduced the phosphorylation of ERK1/2 and the p65 subunit of NF-κB by 44.2% and 42.9%, respectively, compared to cells treated only with TNFα (Figure 34A, B). Mix B significantly reduced the phosphorylation of NF-κB-p65 by 26.8% (Figure 34C).

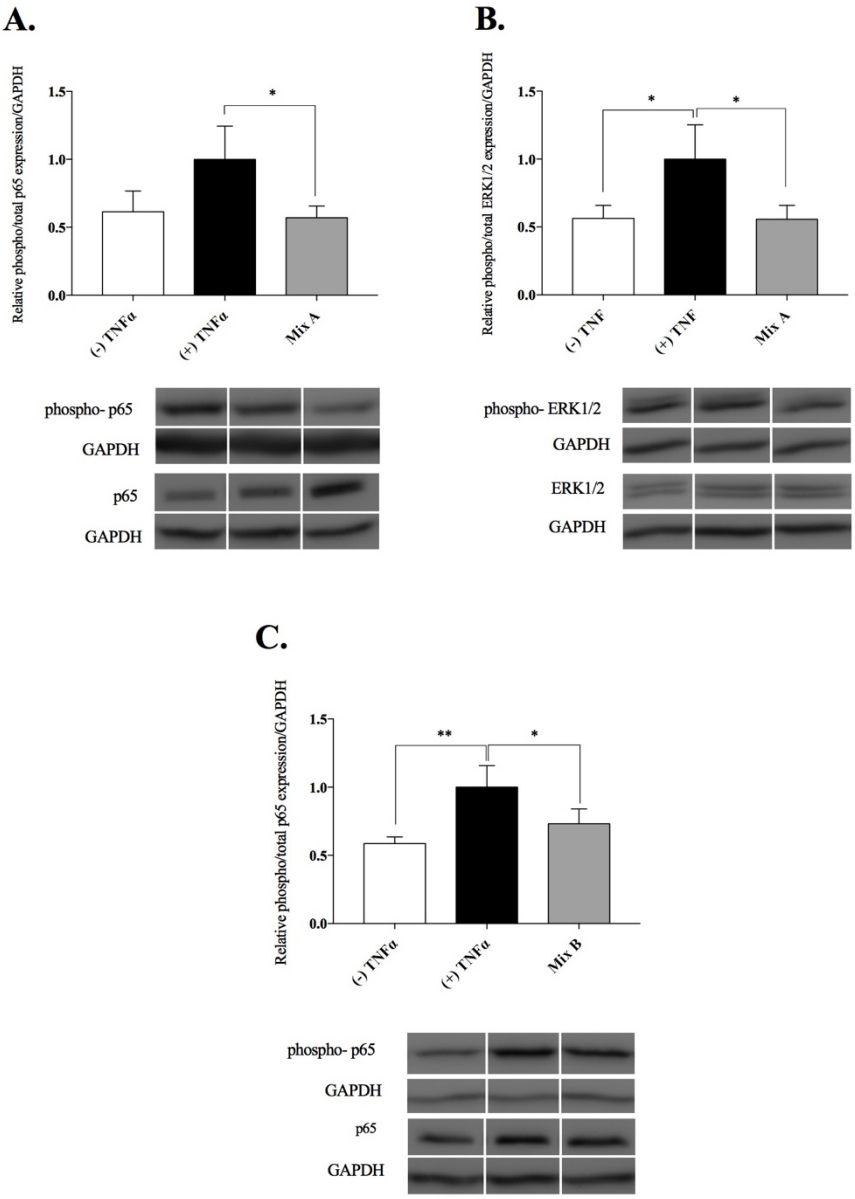

Figure 34. *The effect of mix A on the phosphorylation of p65 (A) and ERK1/2 (B) and the mix B on the phosphorylation of p65 (C) in HUVECs. Data are normalised to GAPDH and represented relative to positive control ((+) TNFα condition). Results are displayed as the mean ± SD from three replicates, *p < 0.05, **p < 0.01.*

4.1.8. The effect of mixtures of tested compounds on miRNA expression in endothelial cells

To further investigate how anthocyanins and their metabolites regulate the observed nutrigenomic effect, the impact of mixtures of these compounds on the expression of miRNAs, the post-transcriptional regulators of gene expression, was examined in endothelial cells.

miRNA microarray analysis revealed that the treatment of HUVECs with TNFα resulted in a significant modulation of the expression of 5 miRNAs when compared to nontreated cells. Among these differentially expressed miRNAs, four were found upregulated and one downregulated with the fold-change values ranging from -1.29 to 1.64 (Table 13). The exposure of endothelial cells to mix A, mix B or mix A+B before TNFα activation, significantly affected the expression of 14, 13 and 13 miRNAs, respectively, compared to TNFα-activated HUVECs nonexposed to mixtures. Of these differentially expressed miRNAs, all except one were identified as downregulated with fold-changes from -1.13 to -2.69 (Table 13).

Table 13. *miRNAs identified as differentially expressed in HUVECs*

(+) TNFα/ (-) TNFα		Mix A/(+) TNFα		Mix B/(+) TNFα		Mix A+B/(+) TNFα	
miRNA	***FC***	***miRNA***	***FC***	***miRNA***	***FC***	***miRNA***	***FC***
hsa-miR-146a	1.64	hsa-let-7f	-1.21	hsa-let-7a	-1.22	hsa-let-7c	-1.46
hsa-miR-155	1.56	hsa-miR-126*	-1.42	hsa-let-7f	-1.31	hsa-let-7f	-1.52
hsa-miR-320c	1.06	hsa-miR-1260	-1.42	hsa-miR-1246	-1.62	hsa-miR-1207-5p	-1.24
hsa-miR-455-3p	1.62	hsa-miR-1268	-1.21	hsa-miR-125b	-1.26	hsa-miR-1246	-1.81
hsa-miR-923	-1.29	hsa-miR-130a	-1.17	hsa-miR-126*	-1.41	hsa-miR-125a-5p	-1.44
		hsa-miR-181b	-1.71	hsa-miR-1260	-1.35	hsa-miR-125b	-1.60
		hsa-miR-1915	-1.13	hsa-miR-1275	1.33	hsa-miR-1305	-1.77
		hsa-miR-26a	-1.53	hsa-miR-196b	1.58	hsa-miR-181b	-2.34
		hsa-miR-30b	-1.46	hsa-miR-216a	2.09	hsa-miR-1915	-1.49
		hsa-miR-361-5p	-1.26	hsa-miR-23a	-1.26	hsa-miR-361-5p	-1.71
		hsa-miR-374a	-1.25	hsa-miR-374a	-1.26	hsa-miR-572	-1.21
		hsa-miR-376c	-1.51	hsa-miR-720	-1.15	hsa-miR-575	-2.69
		hsa-miR-455-3p	-1.44	hsa-miR-923	2.36	hsa-miR-638	-1.22
		hsa-miR-99b	-1.44				

FC-fold change, $p<0.05$

Hierarchical clustering of miRNAs that were identified as differentially expressed in at least one of the studied conditions revealed a cluster of miRNAs with an opposite expression profile in endothelial cells treated only with TNFα and those pretreated with the mixtures (Figure 35). In this cluster, miRNAs that were found upregulated by TNFα when compared to non-treated cells were downregulated when endothelial cells were pretreated with the mixtures. These results showed the ability of anthocyanins and their metabolites to modulate the miRNA expression in endothelial cells as well as to counteract the effect of TNFα.

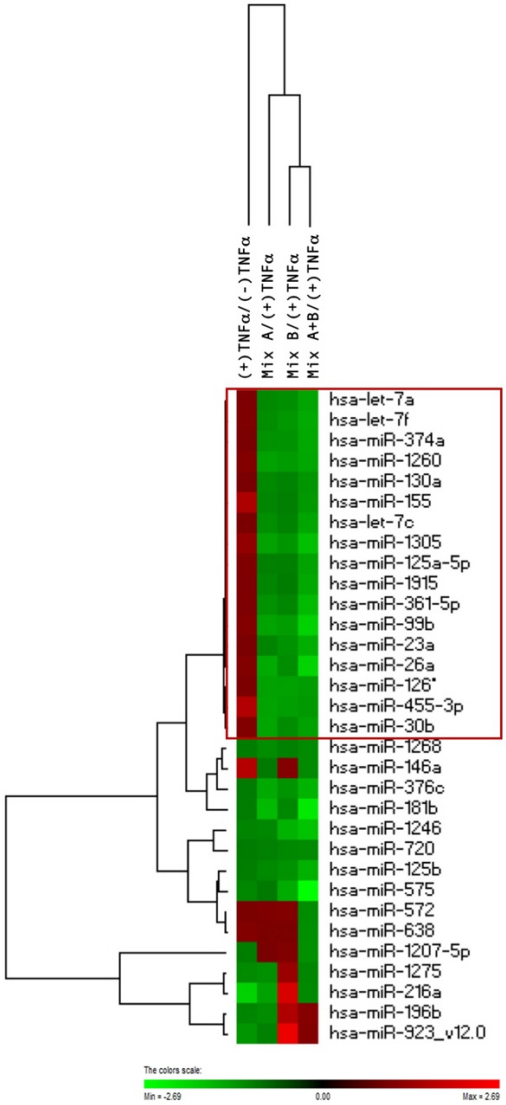

Figure 35. *Heat map of miRNA expression profiles. Each column presents different studied condition and each line a miRNA differently expressed in at least one of the conditions. Green represents downregulation and red upregulation.*

The next step of the analysis of miRNA data aimed to identify possible target genes of differentially expressed miRNAs by using the miRWalk database of experimentally confirmed miRNA-mRNA interactions. This analysis revealed 1635 target genes for the miRNAs which expression was significantly altered by TNFα, and 3158, 2114 and 2209 target genes for the miRNAs which expression was modulated by pretreatment of cells with the mix A, mix B and mix A+B, respectively. Comparison of the miRNA target genes identified for all of the studied conditions showed that 192 genes were in common, whereas 717 target genes were shared between the mixtures (Figure 36).

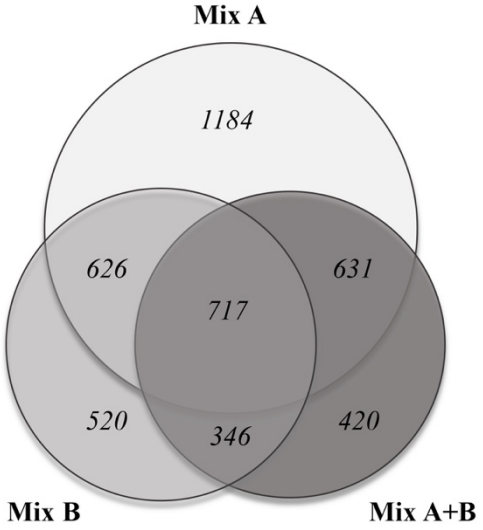

Figure 36. *Venn diagram of the verified target genes of miRNAs found modulated by pretreatment of HUVECs with the mixtures.*

Further bioinformatics analyses were carried out to identify cellular pathways in which these target genes of differently expressed miRNAs are involved and thereby determine probable cellular effects of the observed modulations of miRNA expression. These analyses, performed using KEGG database, showed that miRNA target genes could regulate various cellular pathways such as cell signalling pathways, metabolic pathways, cell-cell adhesion, cytoskeleton reorganisation and chemokine signalling pathways. Comparing the top 50 over-represented pathways in which miRNA target genes of all of the studied conditions are involved, revealed that 29 pathways are in common (Figure 37). These pathways included those regulating actin cytoskeleton and focal adhesion as well as Ras, Rap1, and chemokine signalling pathways, suggesting that the observed changes in the expression of miRNA can affect monocyte adhesion and transmigration processes and thus the integrity and function of endothelial cells.

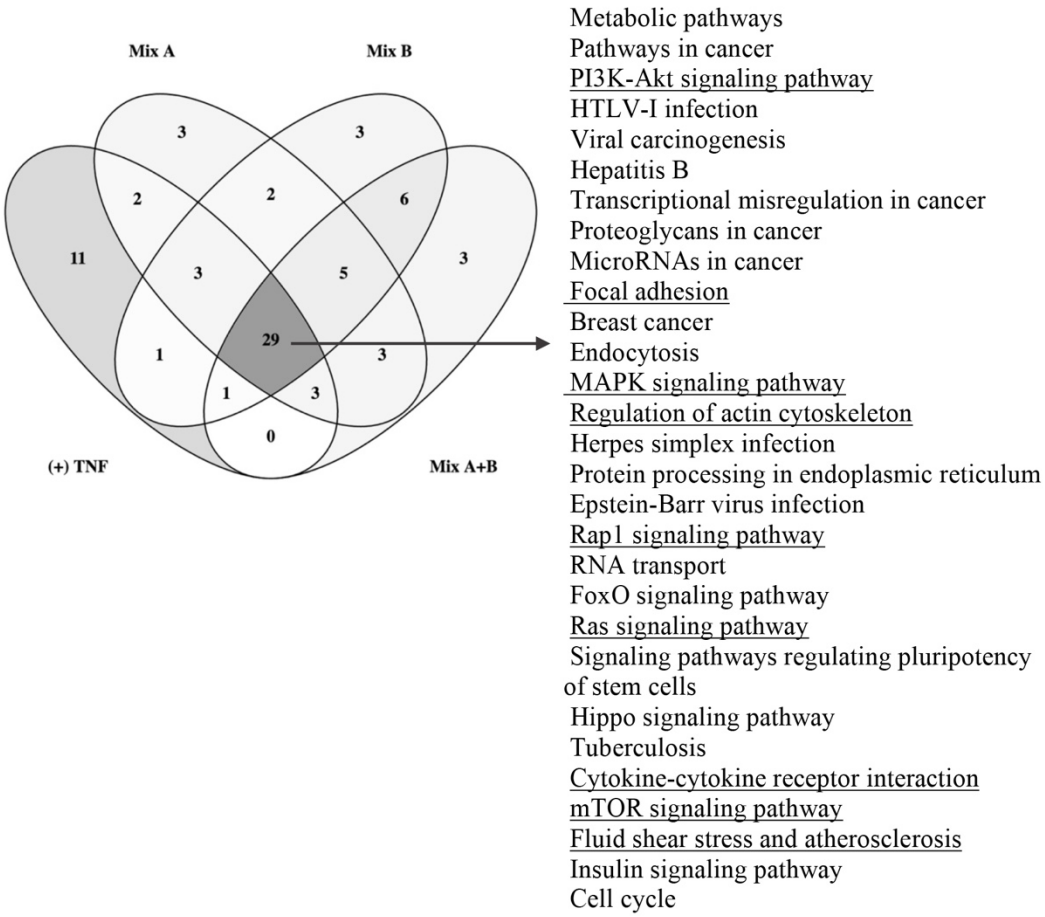

Figure 37. *Venn diagram of top 50 over-represented pathways in which the gene targets of differentially expressed miRNAs are involved.*

Finally, to establish the relationship between the differentially expressed genes and the target genes of differentially expressed miRNAs, the gene expression and miRNA expression data were compared. For the mix A, four out of seven significantly modulated genes were also the target genes of miRNAs which expressions were altered by the same mixture. Furthermore, for the mix B and mix A+B, 20% and 14.3% of significantly modulated genes were also miRNA target genes. These results suggest that the modulation of gene expression observed in response to mixtures of anthocyanins and their metabolites could be partly explained by the ability of these bioactives to affect the expression of miRNAs.

4.2. Investigations of the effect of anthocyanins and their metabolites on platelet function

4.2.1. Characteristics of volunteers-blood donors

Seven apparently healthy, non-smoking male volunteers, between 27 and 34 years old, were recruited for the investigations of the *in vitro* effect of anthocyanins and their metabolites on platelet function. Their characteristics are given in Table 14.

Table 14. *Characteristics of volunteers recruited for the* in vitro *examination of the impact of anthocyanins and their metabolites on platelet function*

Characteristics of volunteers	Values*	Reference value
Age (years)	30.00 ± 2.38	N/A
Height (cm)	185.14 ± 7.03	N/A
Body weight (kg)	86.04 ± 8.80	N/A
BMI (kg/m^2)	25.08 ± 1.72	<30[1]
Waist-hip ratio	0.83 ± 0.03	<0.9[1]
Systolic blood pressure (mmHg)	119.29 ± 8.48	<120; 120-129[2]
Diastolic blood pressure (mmHg)	68.07 ± 4.79	<80; 80-84[2]
HGB (g/l)	140.07 ± 9.99	110-165
HCT (l/l)	0.44 ± 0.04	0.35-0.50
RCB (x 10^{12}/l)	5.22 ± 0.42	3.8-5.8
WBC (x 10^9/l)	5.79 ± 0.72	3.5-10.0
PLT (x 10^9/l)	195.21 ± 11.81	150-390
PCT (x 10^{-2}l/l)	0.14 ± 0.01	0.1-0.5
MPV (fl)	7.46 ± 0.81	6.5-11.0
Total cholesterol (mmol/L)	5.02 ± 1.11	3.87- 5.20
LDL-cholesterol (mmol/L)	3.33 ± 1.09	< 3.4
HDL-cholesterol (mmol/L)	1.56 ± 0.25	>1.03
Triglycerides (mmol/L)	0.80 ± 0.31	0.46-1.70
Glucose (mmol/L)	5.04 ± 0.34	3.89-5.84
Iron (µmol/L)	20.90 ± 2.06	11.6-31.3
Urea (µmol/L)	5.31 ± 1.23	2.10-7.10
Uric acid (µmol/L)	350.29 ± 36.23	208-428
Creatinine (µmol/L)	103.59 ± 11.70	53-115
ALT (U/L)	21.67 ± 7.78	< 40
AST (U/L)	26.27 ± 5.07	< 40

*Results are expressed as mean ± SD, n=7. BMI-Body mass index, HGB-Hemoglobin, HCT- Hematocrit, RBC-Red blood cells, WBC-White blood cells, PLT-Platelet count, PCT- Plateletcrit, MPV-Mean platelet volume, LDL-Low-density lipoprotein, HDL-High-density lipoprotein, ALT-Alanine transaminase, AST-Aspartate transaminase. [1](WHO 1999), [2] (Mancia et al. 2007).

Volunteers were categorized as non-obese according to the World health organisation criteria, with BMI < 30 kg/m^2 and waist to hip ratio < 0.9 (WHO 1999). Systolic and diastolic blood pressure values were within the optimal (<120 and <80 mmHg) and normal (120-129 and/or 80-84 mmHg) categories of blood pressure established by the European Society of Cardiology and the European Society of Hypertension (Mancia et al. 2007). The examined haematological and biochemical parameters of volunteers were within normal ranges (Table 14).

4.2.2. Impact of anthocyanins on platelet activation markers

The impact of compounds on ADP-induced platelet activation response was evaluated based on their effect on P-selectin and GPIIb/IIIa activation markers assessed as the percentage of activated platelets in the total number of platelets and as P-selectin and GPIIb/IIIa receptor densities on activated platelets.

Pre-exposure of whole blood to cy-3-arab at 0.1 μM concentration lowered platelets' activation response to ADP. This effect of cy-3-arab was achieved through a reduction in the percentage of P-selectin positive platelets and P-selectin receptor density of 10.2% and 7.7%, respectively (Figure 38A, B), compared to agonist-treated control. By contrast, 0.1 μM cy-3-glc significantly reduced only GPIIb/IIIa density by 4.9% (Figure 38D), while cy-3-gal did not exert a significant effect on any of the examined markers of platelet activation (Figure 38). Preincubation of whole blood with del-3-glc significantly reduced the percentage of P-selectin positive cells by 10.8% and P-selectin density on activated platelets by 7.5% (Figure 38A, B), and did not affect GPIIb/IIIa. Similarly, a pre-exposure of whole blood to pn-3-glc significantly reduced the percentage of P-selectin positive platelets by 10.8% and lowered the density of this receptor by 5.9%, without attaining statistical significance (p=0.053) (Figure 38A, B).

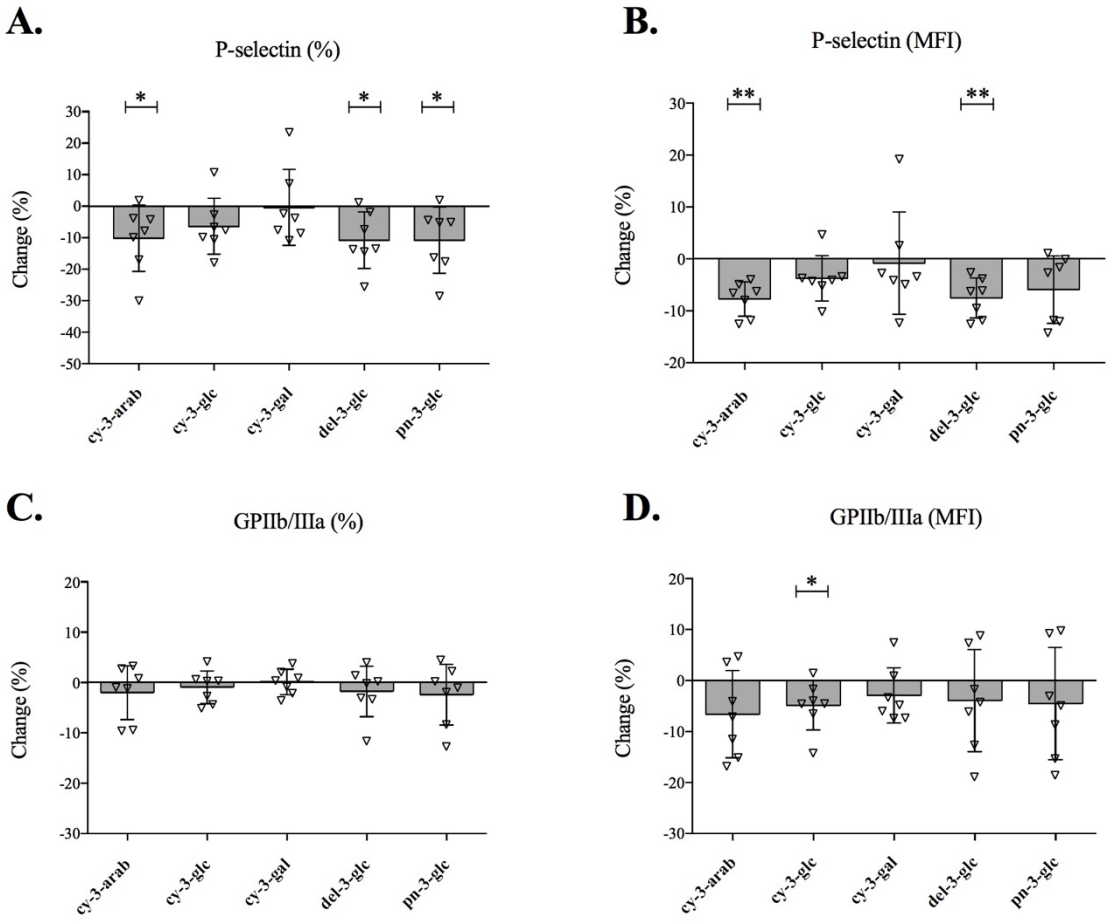

Figure 38. *The effect of anthocyanins on ADP-induced platelet activation assessed as the percentage of P-selectin positive platelets in a total number of platelets (A), the density of P-selectin on activated platelets (B), the percentage of GPIIb/IIIa positive platelet (C) and the density of GPIIb/IIIa on activated platelets (D). The results are presented as a change (%) of the value for each of the measured parameters in anthocyanin-treated, ADP-activated whole blood compared to control (vehicle-treated, ADP-activated samples). MFI-mean fluorescence intensity. Data are displayed as mean ± SD, n=7. *p < 0.05, **p < 0.01.*

4.2.3. Effect of anthocyanin metabolites on platelet activation markers

Preincubation of whole blood with 0.5 μM 4-HBAL affected ADP-induced platelet activation, significantly reducing the percentage of P-selectin positive platelets by 6.9% (Figure 39A). By contrast, PCA at 0.2 μM concentration attenuated both examined platelet activation markers. It significantly reduced the percentage of P-selectin and GPIIb/IIIa positive platelets as well as the GPIIb/IIIa density by 5.9%, 3.3% and 5.9% respectively (Figure 39A, C, D). A pretreatment of whole blood with hippuric acid, at 2 μM level, significantly decreased the percentage of P-selectin positive platelets by 4.3%

(Figure 39A), while neither ferulic nor vanillic acids significantly affected any of the assessed platelet activation markers (Figure 39).

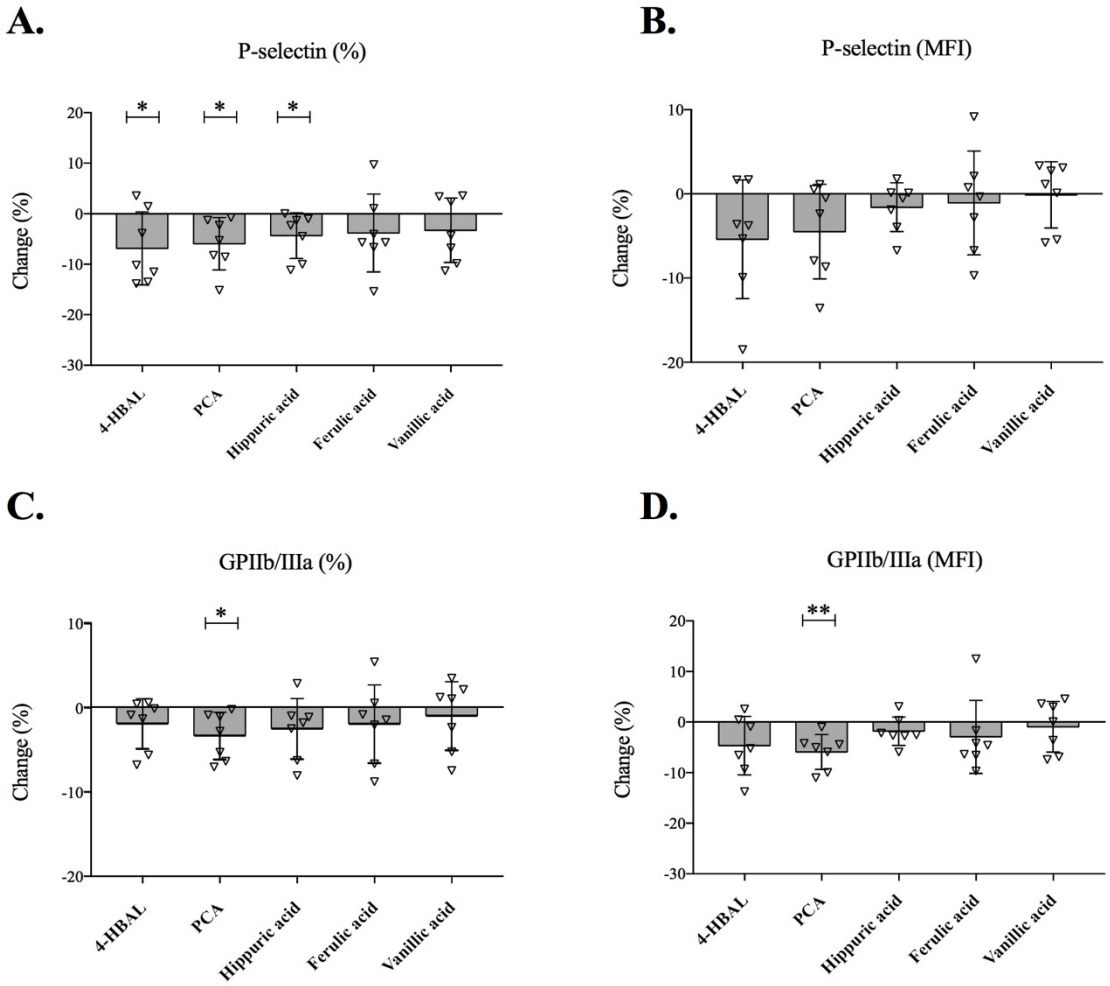

Figure 39. *The effect of anthocyanin metabolites on ADP-induced platelet activation assessed as the percentage of P-selectin positive platelets (A), density of P-selectin on activated platelets (B), percentage of GPIIb/IIIa positive platelet (C) and density of GPIIb/IIIa on activated platelets (D). The results are presented as a change (%) of the value for each of the measured parameters in anthocyanin-treated, ADP-activated whole blood compared to vehicle-treated, ADP-activated control. Data are displayed as mean ± SD, n=7. *p < 0.05, **p < 0.01.*

4.2.4. Effect of anthocyanins on platelet-leukocyte aggregation

The impact of compounds on agonist-induced platelet aggregation with leukocytes was examined based on their effect on the percentage of platelet-monocyte (PMA) and platelet-neutrophil aggregates (PNA).

Pre-exposure of whole blood to 0.1 μM cy-3-arab significantly reduced the ADP-induced formation of PNA by 15.2% and had no effect on platelet aggregation with

monocytes (Figure 40). Cy-3-gal significantly attenuated platelet aggregation with neutrophils by 19.6%, while cy-3-glc, del-3-glc and pn-3-glc showed no significant effect on both platelet-neutrophil and platelet-monocyte aggregation.

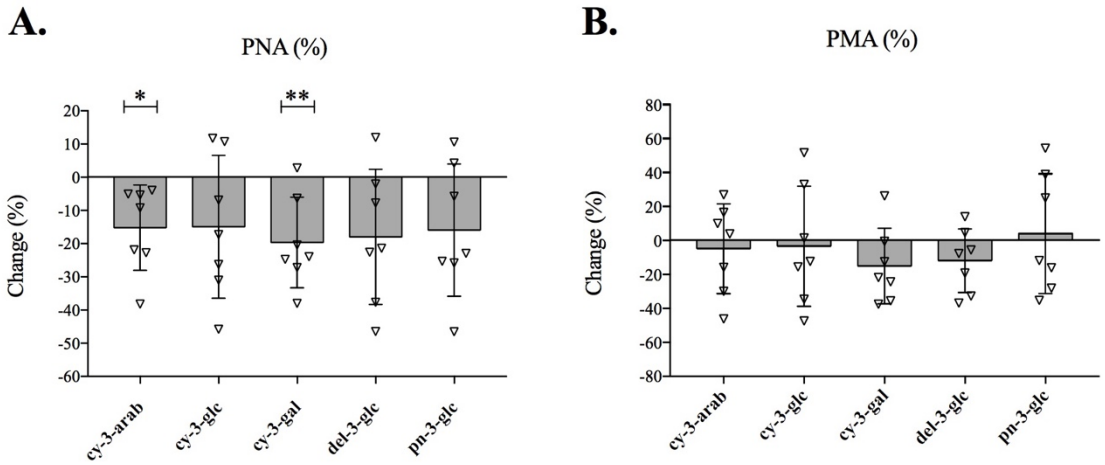

Figure 40. *Impact of anthocyanins on ADP-induced platelet-leukocyte aggregation assessed as the percentage of platelet-neutrophil aggregates (A) and platelet-monocyte aggregates (B). The results are presented as change (%) compared to vehicle-treated, ADP-activated control. Data are reported as mean ± SD, n=7. *p < 0.05, **p<0.01.*

4.2.5. Impact of anthocyanin metabolites on platelet-leukocyte aggregation

4-HBAL, tested at 0.5 μM concentration, significantly affected platelet aggregation with both neutrophils and monocytes, reducing the formation of PNA by 14.8% and PMA by 10%, compared to agonist-treated control (Figure 41). By contrast, 0.2μM PCA, 2 μM hippuric acid 2 μM vanillic acid did not significantly affect neither platelet-neutrophil nor platelet-monocyte aggregation. Pre-exposure of whole blood to 1 μM ferulic acid significantly reduced the percentage of PMA by 11.4% and showed no effect on platelet aggregation with neutrophils (Figure 41).

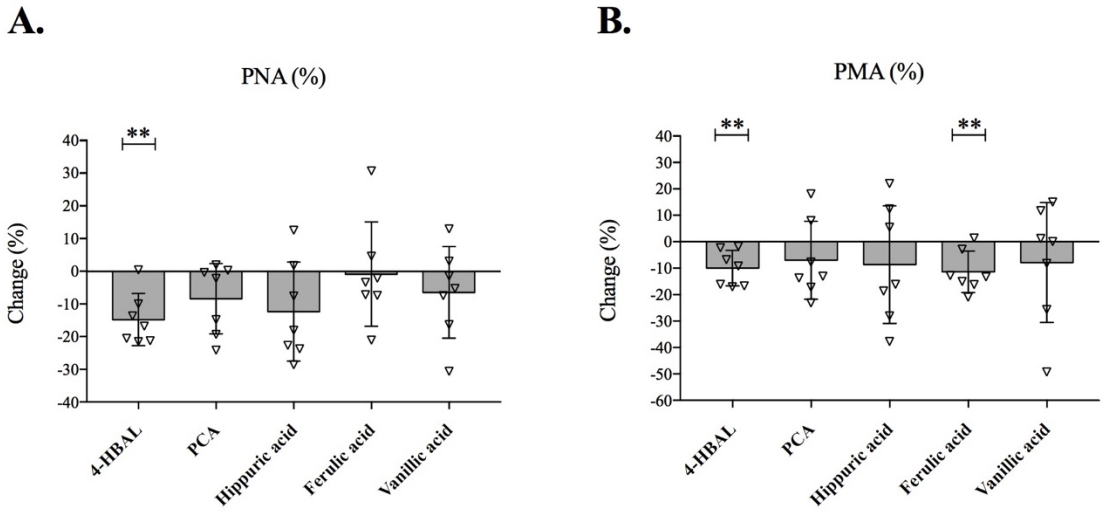

Figure 41. *Impact of anthocyanin metabolites on ADP-induced platelet-leukocyte aggregation assessed as the percentage of platelet-neutrophil aggregates (A) and platelet-monocyte aggregates (B). The results are presented as change (%) compared to vehicle-treated, ADP-activated control. Data are reported as mean ± SD, n=7. **p<0.01.*

5. DISCUSSION

CVD represent the leading global cause of morbidity and mortality, with atherosclerosis as the major underlying pathologic process responsible for their development (Galkina & Ley 2009; Mendis et al. 2011). Atherosclerosis, a chronic inflammatory disorder of large and medium-sized arteries, is initiated by alterations in endothelial function that promote the recruitment and adhesion of circulating leukocytes and their subsequent transendothelial migration into the blood vessel wall. In the subendothelial space, leukocytes differentiate into activated macrophages, take up oxidised lipoproteins and form foam cells, which accumulation eventually leads to the formation of atherosclerotic lesions that restrict blood flow (Galkina & Ley 2009; Libby et al. 2011). Platelets also contribute to the development of this disorder through their interactions with leukocytes and endothelial cells that occur upon platelet activation. These interactions promote leukocyte adhesion and transendothelial migration, further increasing the inflammatory responses and the progression of atherosclerosis (van Gils et al. 2009; Konic-Ristic et al. 2015). Therefore, the interplay between endothelial cells, leukocytes and platelets represent an attractive target for the prevention of CVD.

A growing body of evidence coming from epidemiological, clinical and preclinical studies suggest the important role of dietary anthocyanins, the plant-food phytochemicals, in the prevention and treatment of CVD (Mauray et al. 2009; Qin et al. 2009; Cassidy et al. 2011; Cassidy et al. 2013; Rodriguez-Mateos, Rendeiro, et al. 2013; Li et al. 2015). Cardiovascular benefits of anthocyanin consumption may be attributed to their effect on endothelial but also platelet function. However, the molecular mechanisms through which they exert these effects are still not fully understood. Furthermore, given the extensive metabolism of dietary anthocyanins within the human body, the reported health benefits could be at least partly attributed to their metabolites as well (de Ferrars, Czank, et al. 2014). Therefore, the aim of this doctoral dissertation was to investigate the impact of anthocyanins and their metabolites on endothelial and platelet function and identify the underlying mechanisms of their action, using physiologically relevant study design and integrated omics approaches.

Anthocyanins that were tested in this work are present in substantial amounts in various fruits, particularly berry fruits, some vegetables, cereals and different fruit-derived products (e.g. juices and wines), presenting the significant components of the

human diet. Also, they are all found in blueberries that are the most commonly eaten anthocyanin source (Andersen & Jordheim 2013). Anthocyanin metabolites that were examined in this thesis were previously reported in the bloodstream following the consumption of various anthocyanin-rich foods (Rechner et al. 2002; de Ferrars, Cassidy, et al. 2014; Xie et al. 2016). Moreover, they were confirmed as products of anthocyanin degradation created in the small intestine and colon in a relatively recent human feeding study with the isotopically-labelled cy-3-glc (de Ferrars, Czank, et al. 2014).

For the investigations of the effect of anthocyanins and their metabolites on endothelial function, compounds were first examined over a range of concentration, from 0.1 μM to 2 μM, which corresponded to their previously reported circulating plasma levels after the intake of anthocyanin-rich foods. Findings from anthocyanin bioavailability studies show that anthocyanins are present in the bloodstream for a short time, unlike their gut metabolites that are detectable up to 48 hours post-consumption (Stalmach et al. 2012; Czank et al. 2013; de Ferrars, Czank, et al. 2014). Also, in a two recent studies that used anthocyanin-rich elderberries or isotopically-labelled cy-3-glc, a significant amount of 4-HBAL was observed early in plasma (de Ferrars, Czank, et al. 2014; de Ferrars, Cassidy, et al. 2014), suggesting that this compound is probably a product of anthocyanin degradation produced in the upper GIT. Therefore, different lengths of treatment of endothelial cells with anthocyanins and their metabolites were used, i.e. a 3-hour long treatment for anthocyanins and 4-HBAL and 18 hour-long for gut metabolites.

The impact of tested compounds on endothelial function was evaluated by measuring monocyte-endothelial cells interactions, i.e. the adhesion of monocytes to activated endothelial cells and their transendothelial migration, which are the initial key steps in the development of atherosclerosis. These investigations were performed using primary endothelial cells, HUVECs, a commonly employed *in vitro* model system for exploring vascular inflammation in atherosclerosis (Onat et al. 2011). To create a proatherogenic environment, these cells were stimulated with TNFα. This cytokine is a key regulator of inflammation that causes endothelial dysfunction and is observed at elevated levels in the circulation of people at increased CVD risk (Zhang et al. 2009). This activation of endothelial cells induced monocyte adhesion to an endothelial monolayer, which was in line with findings from previous studies (Speciale et al. 2010; Chao, Lin, et al. 2013; Claude et al. 2014). Results from monocyte adhesion assays showed that, with the

exception of 4-HBAL, treatment of HUVECs with tested anthocyanins and their metabolites, before TNFα activation, resulted in a significant reduction in monocyte adhesion to endothelial cells. Interestingly, this effect was observed especially at concentrations of compounds that are closest to their previously reported circulating plasma levels. The dose-response effect of tested compounds on monocyte-endothelial cell interactions mainly appeared non-linear, which was in line with a lack of a dose-response effect reported for other polyphenols (e.g. flavanones, flavanols, flavonols) in endothelial or other types of cells (de Pascual-Teresa et al. 2004; Chanet et al. 2013; Claude et al. 2014). Among the examined anthocyanins, del-3-glc displayed the greatest capacity to attenuate monocyte adhesion. These results may be explained by the presence of an additional hydroxyl group on the B-ring of del-3-glc compared to other tested anthocyanins that may influence its activity. Anthocyanin metabolite 4-HBAL was the only compound that showed no effect on monocyte adhesion at any of the examined concentrations. The impact of this compound on the endothelial function has not been studied before. Results from monocyte adhesion assays also revealed the potency of gut metabolites to decrease the adhesion of monocytes to activated endothelial cells, with the strongest effect observed for PCA. The impact of these compounds was similar to that of anthocyanins, suggesting that gut microbial transformation produces metabolites that can have similar beneficial effects on endothelial function as their parent compounds. These results imply that in addition to anthocyanins, their metabolites that are detectable in the circulation for significantly longer time than their parent forms, can exert biological activity in endothelial cells and probably contribute to cardioprotective effects associated with the habitual intake of anthocyanin-rich foods.

The impact of anthocyanins on the adhesion of monocytes to activated endothelial cells has been previously reported. For example, treatment of human aortic endothelial cells with 100 μg/mL of anthocyanin-based extract from purple sweet potato or 10 μM cyanidin, prior to TNFα stimulation, resulted in a significant decrease in the adhesion of monocytic U937 cells (Chao, Lin, et al. 2013). A similar reduction in monocyte adhesion was observed with TNFα-activated HUVECs pretreated with cy-3-glc (20-40 μM levels) (Speciale et al. 2010) or activated endothelial cells (EAhy92) pre-exposed to delphinidin (50-100 μM) (Chen et al. 2011). However, these effects were observed using anthocyanin-based extracts and aglycones as well as supraphysiological concentrations

of glycosides, with long periods of cell exposure. Thus, the findings from this thesis present the first physiologically relevant evidence of the impact of tested anthocyanins on monocyte-endothelial cell adhesion. The effects of some of the anthocyanin metabolites have been previously assessed in a few studies. Wang et al. (2010) showed that the exposure of mouse aortic endothelial cells (MAEC) to 0.05-40 μM PCA, prior to TNFα activation, significantly reduced monocyte adhesion only at 20 μM and 40 μM levels. The difference between these results and those of this thesis could be explained by the use of a rather high level of TNFα (10μg/l in comparison to 1 μg/l) to induce MAEC activation, which allowed the effect of this metabolite to be observed only at the highest tested concentrations. Similar to results presented in this thesis, Kuntz, Asseburg, et al. (2015) showed the capacity of PCA, at 1μM concentration, to significantly decrease the adhesion of leukocytes to TNFα-stimulated HUVECs, while no effect was observed at the 0.1μM level of this compound. The impact of ferulic acid on monocyte adhesion was previously investigated using endothelial cells exposed to radiation (Ma et al. 2010). However, concentrations that were used were higher than those examined in this thesis. The effects of hippuric and vanillic acids on monocyte adhesion to activated endothelial cells have not been reported before.

To further investigate a potential synergistic effect of compounds that are simultaneously present in the bloodstream after the intake of anthocyanin-rich foods, two mixtures of compounds present in the circulation for a short (mix A) or for a long time (mix B) were prepared. The concentrations of compounds in these mixtures were closest to those previously identified in human plasma in the anthocyanin bioavailability studies (Czank et al. 2013; de Ferrars, Czank, et al. 2014). Additionally, the condition mix A+B was created to imitate as closely as possible anthocyanin pharmacokinetics following the ingestion of anthocyanin-rich sources by treating endothelial cells with the mixture of compounds that appear rapidly in the bloodstream and then with the mixture of gut metabolites that appear later and are present in the circulation for a longer time. Results from these adhesion assays revealed the ability of mixtures to significantly decrease the adhesion of monocytes to TNFα-activated HUVECs. However, no additive effect of the individual compounds of the mixtures was observed, as well as of the successive treatment with the mixtures in the mix A+B condition. The absence of an additive effect has been previously observed with different polyphenol mixtures (Boath et al. 2012;

Khandelwal et al. 2012; Horcajada et al. 2015) and may be explained by possible competition between the compounds of the mixture for the same target of action.

The mixtures of anthocyanins and their metabolites were then used to investigate the impact of these compounds on monocyte transendothelial migration, the step that follows the adhesion. Results from these experiments showed a significant reduction in MCP-1-induced migration of monocytes through the endothelial monolayer pretreated with the mixtures. There are only two studies that previously evaluated the impact of anthocyanin on leukocyte transendothelial migration. However, they only showed the effect of aglycones (e.g. pelargonidin, delphinidin) over a range of supraphysiological concentrations, 10 μM to 200 μM (Chen et al. 2011; Jeong et al. 2017). Thus, this thesis reports for the first time the ability of anthocyanins and their gut metabolites to reduce monocyte transendothelial migration at physiologically relevant conditions. These results suggest that both anthocyanins and their gut metabolites can affect the initial steps in the development of atherosclerosis by lowering the permeability of endothelial cells to leukocytes, thus implying their potential anti-atherogenic effect. This hypothesis could be supported by findings from several animal studies that reported the reduced formation of atherosclerotic lesions in $ApoE^{-/-}$ mice that consumed a diet supplemented with anthocyanin-rich extracts or pure compounds (Miyazaki et al. 2008; Mauray et al. 2009; Y. Wang et al. 2012).

To identify the molecular mechanisms underlying the observed effects of the mixtures of anthocyanins and their metabolites on monocyte adhesion and transendothelial migration, the impact of these compounds on the expression of 91 genes involved in the regulation of endothelial cell permeability was then evaluated. The ability of anthocyanins and their metabolites to modulate the gene expression in endothelial cells has been described in several *in vitro* studies (Huang, Liu, et al. 2014; Amin et al. 2015; Edwards et al. 2015; Kuntz, Asseburg, et al. 2015; Warner et al. 2017). Of these, only a few recent studies reported the effect on gene expression using physiologically relevant forms and concentrations of compounds (Edwards et al. 2015; Kuntz, Asseburg, et al. 2015; Warner et al. 2017). Still, these studies have largely been focused on the investigations of the impact on a few specific genes of interest, such as genes encoding different inflammatory mediators, cell adhesion molecules or enzymes involved in antioxidant defence. This targeted approach does not allow the evaluation of the multi-

target mode of action of these compounds previously reported *in vivo* (Mauray et al. 2012). In this thesis, macroarray analysis revealed that the pretreatment of HUVECs with physiologically relevant mixtures of anthocyanins and their gut metabolites significantly modulated the gene expression in these cells. Genes that were identified as differentially expressed are involved in the regulation of tight junction, cell-cell adhesion, reorganisation of actin cytoskeleton, focal adhesion or chemokine signalling that all regulate endothelial cell permeability to immune cells, i.e. their adhesion and transendothelial migration (van Buul & Hordijk 2004). Leukocyte adhesion and transendothelial migration are finely controlled multistep processes governed by chemoattractants, cell adhesion molecules and their receptors. Gene expression analysis revealed that mix A significantly reduced the expression of *CXCL12*, a gene encoding chemokine CXCL12. Chemokines are a large group of cytokines that can act as chemotactic factors and direct the movement of leukocytes to specific sites within tissues during different inflammatory situations (Speyer & Ward 2011). CXCL12 plays an essential role in critical functions such as leukocyte traffic, haematopoiesis, and vascularisation (van der Toorn et al. 2015), and its increased expression has been associated with the development of atherosclerotic lesions and coronary artery disease (Abi-Younes et al. 2000; Schutt et al. 2012). Furthermore, mix A significantly downregulated the expression of a gene coding for ICAM-1. This cell adhesion molecule regulates the initial capture, tethering and rolling of leukocytes along the endothelium as well as their transendothelial migration (Čejková et al. 2016). It has been shown that ICAM-1 increases vascular permeability and loosens endothelial barrier while its inactivation reduces leukocyte adhesion and vascular permeability in both mouse intracranial and cremaster vessels (Gaber et al. 2004; Sumagin et al. 2008; Sarelius & Glading 2015). Gene expression experiments also showed the ability of mix A to significantly decrease the expression of a gene coding for IκB kinase β (IKBKB). As detailed in the introduction section of this thesis, this kinase is a part of a protein complex that phosphorylates IκB, an inhibitor of a transcription factor NF-κB, leading to its dissociation and degradation and consequent NF-κB activation. The released NF-κB then rapidly translocates to the nucleus and induces the transcription of different inflammatory genes such as ICAM-1 (Anwar et al. 2004). It has been reported that IKBKB is necessary for the cytokine-induced inflammatory phenotype of vascular endothelium and the

endothelial recruitment of monocytes (Meiler et al. 2002). Taken together, these observations propose that the downregulation of these inflammatory genes by mix A results in reduced migration of monocytes toward endothelial cells and their subsequent interactions, which can be associated with decreased adhesion and transendothelial migration observed in the cell assays.

Pretreatment of endothelial cells with the mixture of gut metabolites for 18 hours also significantly modulated the expression of several genes. For example, mix B decreased the expression of a gene encoding integrin alpha-5 (ITGA5), a member of integrin cell adhesion molecules. Integrins play a significant role in the firm adhesion of monocytes to endothelial cells (Čejková et al. 2016), and the overexpression of *ITGA5* has been reported to increase cell adhesion and migration (Qin et al. 2011). Furthermore, mix B upregulated the expression of a gene encoding CDH5. This adhesion molecule is exclusively expressed in endothelial cells and plays a critical role in the assembly and maintenance of adherens junction (Ley 2013). Loss and reduction of CDH5 at cell junctions have been reported to reduce endothelial integrity and increase endothelial permeability, allowing transendothelial migration of immune cells (Del Maschio et al. 1996; Sawant et al. 2011; Herwig et al. 2013). Gut metabolites also reduced the expression of *CAPN1*, a gene coding for calpain 1. Calpains are ubiquitously expressed, Ca^{2+} activated, neutral cysteine proteases present in the vascular wall where they control important endothelial functions (Scalia et al. 2011). Activation of vascular calpains has been reported to cause endothelial dysfunction and increases leukocyte-endothelial interactions in the microcirculation. The increase in calpain activity has been shown to induce calpain-dependent degradation of IκBα, together with the upregulation of NF-κB-regulated cell adhesion molecules (Scalia et al. 2011). Thus, downregulation of *CAPN1* by gut metabolites may result in decreased calpain activity and IκBα degradation and consequently reduced NF-κB-induced expression of cell adhesion molecules and decreased monocyte adhesion as reported in the cell assays of this thesis.

Pretreatment of endothelial cells with mix A and then mix B induced significant alterations in the expression of several genes including *ITGA5, CAPN1, CDH5*, and *GJA4. GJA4*, a gene that encodes gap junction alpha-4 protein also known as connexin 37, was found upregulated by mix A+B. Connexins represent transmembrane proteins that form gap junctions and allow direct cell-cell communication. The expression of *GJA4*

was found to be modulated in advanced atherosclerotic plaques, with a loss of GJA4 in endothelial cells covering plaques (Kwak et al. 2002; Pfenniger et al. 2015). It has also been reported that ApoE$^{-/-}$ GJA4$^{-/-}$ mice present an increase in the size of atherosclerotic plaques compared to ApoE$^{-/-}$ mice, with an increase in the number of macrophages in the plaques (Wong et al. 2006; Pfenniger et al. 2015), suggesting lower transendothelial migration of leukocytes. Thus, modulations in endothelial cell gene expression by mix A+B can be associated with a decrease in monocyte adhesion and transendothelial migration, presenting molecular targets underlying the observed effect on endothelial cells.

The results form gene expression experiments were further analysed with different bioinformatics tools to identify possible transcription factors and signalling proteins that could mediate the observed nutrigenomic effect of tested compounds. Molecular docking was employed to predict whether anthocyanins and their metabolites can bind these cell signalling proteins and transcription factors and theoretically affect their biological activity. This computational technique is more and more used as a tool for the identification of molecular targets of natural bioactive compounds. Several studies have previously described possible binding interactions between anthocyanins or their metabolites and a few targets including membrane transporters (Oliveira et al. 2015; Muthusamy et al. 2016), digestive enzymes (Olivas-Aguirre et al. 2016; Zengin et al. 2017), protein kinases (Hou & Kumamoto 2010; Doss et al. 2016; Bhattacharjee et al. 2017), estrogen receptors (Nanashima et al. 2015) or antioxidant defence enzymes (Laksmiani et al. 2016). In this thesis, molecular docking was performed with 62 identified signalling proteins and transcription factors that are involved in the regulation of different cellular processes such as inflammation, cell proliferation, migration and survival. Results from these analyses suggest that anthocyanins and their metabolites present the capacity to bind cell signalling proteins. Anthocyanins appear to be stronger binders then their metabolites. The similar BAs for the same targets were observed when comparing compounds within the anthocyanin and metabolite groups, contributing to the hypothesis that the lack of cumulative effect of compounds within the mixtures is the result of their competition for the same target of action. Docking results revealed that anthocyanins could bind to the protein kinase domain of cell signalling proteins such as FAK1, ROCK2 and MEK2 and possibly affect the kinase activity of these targets.

Binding of mitoxantrone to the kinase domain of FAK has been shown to inhibit FAK kinase activity (Golubovskaya et al. 2013). This non-receptor kinase has an essential role in the regulation of cell adhesion, migration and actin cytoskeleton rearrangement, and its reduced activity has been associated with lower monocyte adhesion to endothelial cells (Hu et al. 2018). Previous studies have also shown that binding of fasudil and Y-27632 to kinase domains of ROCK1/2, the signalling proteins involved in cell migration by regulation of actin cytoskeletal assembly and cell contractility (Noma et al. 2012), inhibits their activity (Liao et al. 2007). These ROCK1/2 inhibitors led to improvements in endothelial cell integrity and decreased transmigration of immune cells (Breslin & Yuan 2004; Rao et al. 2017), results that could be correlated with the ones observed in this thesis. Furthermore, several inhibitors of MEK1/2, kinases involved in ERK signalling pathway, have been previously described (Krepinsky et al. 2002). The reduced activity of MEK1/2 has been associated with a decrease in the ERK activation and reduced transmigration of leukocytes across a monolayer of activated endothelial cells (Stein et al. 2003; Hu et al. 2018). In this thesis, following the treatment of endothelial cells with the mix A, a significant decrease in ERK1/2 phosphorylation, as well as lower monocyte-endothelial cell interactions were observed. These results suggest that the binding to MEK2 may present one of the mechanisms by which anthocyanins may induce the observed changes in endothelial function. Results from docking analyses also showed that anthocyanins could bind IKKα within its active site, suggesting an inhibitory effect. Inhibition of this cell signalling protein results in reduced NF-κB activation and has been associated with reduced neutrophil infiltration in LPS-induced TNFα production rat model (Llona-Minguez et al. 2013). In this thesis, mix A induced significant decrease in NF-κB-p65 phosphorylation and attenuated monocyte adhesion and transendothelial migration, proposing that binding of anthocyanins to IKKα may represent one of the anthocyanin targets that underlies their observed impact on the expression of proinflammatory genes and ultimately endothelial cell function. It is noteworthy, that the effects of anthocyanins on the phosphorylation of NF-κB-p65 and ERK1/2 have been previously reported in different endothelial cells but only using anthocyanin-based extracts, aglycones or high concentrations of glycosides (Martin et al. 2003; Speciale et al. 2010; Favot et al. 2015; Medda et al. 2015; Sivasinprasasn et al. 2016).

As for anthocyanins, their metabolites have also displayed a potential for binding several cell signalling proteins. For example, docking results revealed that ferulic acid could bind to the protein kinase domain of JAK3 and MLCK. Binding of molecule NSC163088 to the JAK3-kinase domain has been reported to inhibit its catalytic function (Kim et al. 2011). This signalling protein is involved in the regulation of inflammatory cascade and its suppressed activity has been associated with alleviated inflammatory responses and lower endothelial permeability (Kim et al. 2011; Lee et al. 2012). Furthermore, several inhibitors of MLCK, a kinase involved in the regulation of cell contractility, have been previously described (Krepinsky et al. 2002). The treatment of endothelial cells with the inhibitors such as ML-9 and ML-7 has been reported to result in reduced myosin filament formation, F-actin formation, and lower neutrophil transmigration (Saito et al. 1998; Stroka & Aranda-Espinoza 2011). Docking analyses also revealed that PCA could interact with b-Raf within its active site, suggesting an inhibitory effect. The activation of this protein of ERK signalling pathway, has been shown to result in the phosphorylation of the cytoskeletal protein caldesmon, stress fibre formation and increased endothelial permeability (Liu et al. 2001). Recently, suppression of b-Raf activity by an inhibitor, dabrafenib, has been associated with reduced barrier disruption and decreased leukocyte adhesion and transmigration through LPS-activated HUVECs (Lee et al. 2017). Regarding these published data, it can be suggested that binding of anthocyanin metabolites to these signaling proteins will decrease endothelial cell permeability, a hypothesis that can be correlated with the observed reduced monocyte adhesion and transendothelial migration. Docking results also showed that hippuric, ferulic acid and PCA could bind to the kinase domain of p38β, a signalling protein of p38 MAPK pathway involved in the regulation of inflammation and cellular stress responses (Adams et al. 2016). Inhibition of p38 has been associated with a reduced NF-κB activation (Schulze-Osthoff et al. 1997; Rahman et al. 2004; Olson et al. 2007). Furthermore, treatment of endothelial cells with specific p38 inhibitors have been shown to decrease not only leukocyte adhesion but also leukocyte transmigration (Scaldaferri et al. 2009). In agreement with these observations, pretreatment of endothelial cells with the mix B resulted in a significant decrease in the phosphorylation of NF-κB-p65 as well as in reduced monocyte-endothelial cell interactions. This observed effect on NF-κB-p65 activation is in line with a recently reported ability of physiologically relevant doses of

vanillic acid and PCA to decrease phosphorylation of NF-κB-p65 in IL-6-activated HUVECs (Amin 2015).

Taken together, anthocyanins and their metabolites by binding to different cell signalling proteins may affect their activity and consequently that of transcription factors and result in decrease endothelial permeability, presenting new mechanisms of action underlying their health properties.

Aside from regulation by cell signalling proteins and transcription factors, gene expression can also be regulated at the posttranscriptional level by miRNAs. These non-coding RNAs control various cellular processes, and changes in their expression profiles have been described in different diseases including CVD (Miska 2005). The capacity of anthocyanins or their metabolites to modulate miRNA expression has been reported in few *in vivo* studies (Milenkovic et al. 2012; D. Wang et al. 2012), however the *in vitro* evidence is still limited (Du et al. 2017; Murata et al. 2017; Su et al. 2017). In this thesis, the effect of anthocyanins and their metabolites on miRNA expression was examined using the microarray-based holistic approach. Findings from these experiments revealed the capacity of inflammatory cytokine TNFα to induce the changes in miRNA expression compared to non-activated endothelial cells. A significant increase in the expression of miRNAs like miR-155, miR-455 or miR-146a was observed, which was in line with the previously described upregulation of these miRNAs in endothelial cells exposed to inflammatory stress (Ruan et al. 2012; Lee et al. 2015; Pfeiffer et al. 2017; Yee et al. 2017). Results from microarray analysis have shown for the first time the capacity of anthocyanins and their metabolites, at physiologically relevant conditions, to modulate the expression of miRNA in TNFα-stimulated endothelial cells. Interestingly, pretreatment of endothelial cells with mixtures predominantly resulted in decreased miRNA expression, an expression profile that is opposite to the one observed in endothelial cells following their stimulation with TNFα (Figure 35). This observation suggests that anthocyanins and their metabolites can possibly prevent the harmful effects of TNFα by counteracting miRNA expression induced by this inflammatory cytokine. The miRNAs identified as downregulated by mix A included let-7f, miR-181b and miR-125a. The let-7 family of miRNAs is associated with the development of atherosclerosis and coronary artery disease, and the increased expression of let-7f has been reported in the sclerotic intima of peripheral artery disease patients (Li et al. 2010). Furthermore,

miR-181b and miR-125a have been found overexpressed in human atherosclerotic lesions (Bidzhekov et al. 2012; Di Gregoli et al. 2017), while the administration of miR-181b inhibitor (anti-miR-181b) has been shown to delay both the development and progression of plaques in $ApoE^{-/-}$ mice (Di Gregoli et al. 2017). Mix A also reduced the expression of miR-130a. An increase in the expression of this miRNA has been recently observed in the brain endothelial cells and associated with an increase in endothelial monolayer permeability following ischemia (Wang et al. 2018). This effect was reduced when an agonist of miR-130a was used. Additionally, mix A significantly decreased the expression of other miRNAs involved in endothelial dysfunction such as miR-361-5p (H.-W. Wang et al. 2014), miR-26a (Silambarasan et al. 2016) or miR-455-3p (Pearson-Leary et al. 2017). As for the mix A, treatment of endothelial cells with the mix B also induced changes in miRNA expression, revealing for the first time the ability of gut metabolites to modulate the expression of these post-transcriptional mRNA regulators in endothelial cells. Similar to mix A, mix B modulated the expression of let-7f, miR-126*, miR-374a and miR-1260 but also of other miRNAs like miR-23a that was shown to increase endothelial permeability by targeting tight junction proteins (Hsu et al. 2017). It is noteworthy, that mix B also upregulated the expression of miR-923, the only miRNA which expression was significantly reduced by TNFα treatment. This miRNA is involved in cancer development and have also been proposed to affect leukocyte diapedesis (Altmäe et al. 2013). Treatment of endothelial cells with the mix A and then mix B also affected miRNA expression. As for the two other mixtures, a significant reduction in the expression of let-7f was observed, presenting a shared molecular target between these three experimental conditions. Additionally, miR-125b and miR-1246 were identified in common with the mix B and miR-181b, miR-361-5p and miR-1915 with the mix A. The changes in the expression profiles of these miRNAs have been previously described in endothelial cell dysfunction (Lee et al. 2015; Silambarasan et al. 2016; Fang et al. 2017).

These results suggest that the treatment of endothelial cells with anthocyanins and their gut metabolites, at physiologically relevant levels and times of cell exposure, results in changes in the expression of miRNAs that are involved in the regulation of endothelial function, presenting a novel mechanism underlying their observed cellular effects.

In addition to investigations of the effect of anthocyanins and their metabolites on endothelial cell function as one of the important targets in CVD prevention, this thesis

also aimed to evaluate the impact of these compounds on platelet function. These investigations included the assessments of the *in vitro* effect of anthocyanins and their metabolites on platelet activation and platelet-leukocyte aggregation in response to exogenously added ADP. This molecule is a platelet agonist that is stored in their dense granule and released following their activation (Brass et al. 2013). Platelet activation/aggregation response to low levels of ADP has been reported as a parameter with a predictive value for cardiovascular events (Elwood et al. 1991) and therefore presents a rational target for the evaluation of beneficial effects of these compounds on cardiovascular health. Anthocyanins and their metabolites were examined at concentrations that were closest to their previously reported circulating plasma levels (Czank et al. 2013; de Ferrars, Czank, et al. 2014). Their impact on platelet function was evaluated by measuring the surface expression of activation markers P-selectin and GPIIb/IIIa as well as platelet-monocyte and platelet-neutrophil aggregates, using the whole blood flow cytometry. P-selectin, a cell adhesion molecule, is stored in the α granules of platelets and translocated to platelet surface only upon their activation. It mediates the initial contact with neutrophils and monocytes by binding to its ligand PSGL-1 expressed on the leukocyte surface (Evangelista & Smyth 2013). Platelet activation is also associated with a conformational activation of GPIIb/IIIa, a receptor for fibrinogen that mediates platelet aggregation with other platelets but also contributes to platelet-leukocyte aggregation (Jennings 2009; Aukrust et al. 2010). The use of whole blood flow cytometry allowed not only to sensitively measure these markers that are highly relevant in the prevention of CVD but also to diminish platelet extracorporeal activation and produce reliable results that can be exclusively attributed to a direct effect of tested compounds on platelet function.

Results from these experiments showed that except vanillic acid, both anthocyanins and their metabolites significantly affected at least one of the investigated parameters, *i.e.* platelet activation or platelet-leukocyte aggregation. These findings imply that the beneficial, anti-platelet effects associated with the anthocyanin-rich food consumption could also be a consequence of the combined action of anthocyanins and their metabolites on platelet function. The tested compounds had a variable effect on platelet function. Among tested anthocyanins, cy-3-arab displayed the greatest capacity to modulate platelet function, as it reduced the percentage of P-selectin positive platelets as well as

the density of this surface receptor that was reflected in a significantly reduced formation of platelet-neutrophil aggregates. By contrast, pn-3-glc, del-3-glc or cy-3-glc affected platelet activation by attenuating P-selectin or GPIIb/IIIa surface expression, while cy-3-gal only showed the effect on platelet aggregation with neutrophils. These variable effects could possibly be explained by differences in the type of sugar moiety attached to the C-ring of investigated anthocyanins, suggesting that the presence of arabinose is responsible for the higher effect on platelet function. 4-HBAL was the most effective among anthocyanin metabolites, as it induced a significant reduction in platelet activation as well as in their aggregation with both neutrophils and monocytes. Interestingly, 4-HBAL was the only tested compound that did not show a significant effect on the adhesion of monocytes to activated endothelial cells as observed in cell adhesion experiments. These results suggest that by acting on platelets and not on endothelial cells, this metabolite could potentially still lower the leukocyte-endothelial cell interactions and exert a protective effect against atherosclerosis development.

The effects of anthocyanins and their metabolites on platelet activation have been studied before. A few studies failed to observe the effect of lower concentrations of cy-3-glc (0.5μM and 1μM) on P-selectin surface expression (Rechner & Kroner 2005; Song et al. 2014; Yao et al. 2017), which was in agreement with the lack of impact of 0.1μM cy-3-glc reported in this thesis. Studies of Yang et al. (2012) and Song et al. (2014) showed that a pre-exposure of human platelet-rich plasma or gel-filtered platelets to del-3-glc, significantly reduced the agonist-induced P-selectin and GPIIb/IIIa surface expressions at 5 μM and 50 μM levels, and not at 0.5 μM concentration. By contrast, the results from this thesis revealed the capacity of 0.1 μM del-3-glc to reduce platelet activation by modulating P-selectin expression. These observed discrepancies could be explained by differences in the methodology used to assess the effect on platelet activation. Unlike whole blood flow cytometry, the use of platelet-rich plasma or gel-filtered platelets requires the additional manipulation of blood samples and therefore increases the probability of platelet artefactual activation that can mask subtle changes in platelet activation induced by low physiological concentrations of tested anthocyanin. Furthermore, the use of platelet agonists at relatively high levels (e.g. 200 μM ADP) may also explain why these studies only reported the effect at supraphysiological levels of this anthocyanin. The capacity of hippuric acid and PCA to modulate platelet function has

been previously described (Rechner & Kroner 2005; Kim et al. 2012; Santhakumar, Stanley, et al. 2015). However, these compounds were examined at levels that were higher than those achieved in the bloodstream after the ingestion of anthocyanin-rich sources (Vitaglione et al. 2007; de Ferrars, Czank, et al. 2014). Finally, recent work of Baeza et al. showed that pretreatment of whole blood with ferulic acid, at 0.01μM to 100μM levels, significantly reduced ADP-induced P-selectin expression only at higher tested concentrations (Baeza et al. 2017). Similar to findings from this thesis, the effect was not observed at 1μM level. The impact of anthocyanins pn-3-glc, cy-3-gal and cy-3-arab, as well as metabolites 4-HBAL and vanillic acid on platelet activation, has not been evaluated before. Also, this thesis reports, for the first time, the capacity of anthocyanins and their metabolites to affect platelet aggregation with leukocytes, a marker that has been shown to be an even more sensitive indicator of CVD risk than platelet activation (Michelson et al. 2001).

6. CONCLUSION

In accordance with the aim of this thesis, based on the obtained results the following conclusions can be made:

- Pretreatment of endothelial cells with anthocyanin and their metabolites, at physiologically relevant concentrations and time of cell exposure, can reduce the adhesion of monocytes to TNFα-activated endothelial cells. Of tested compounds, 4-HBAL is the only compound that does not seem to impact monocyte adhesion, while the most prominent effects are caused by anthocyanin del-3-glc and the gut metabolite PCA. Mixtures of anthocyanins and their metabolites that are simultaneously present in the circulation following the consumption of anthocyanin-rich sources also significantly reduce monocyte adhesion to activated endothelial cells. Lack of the additive effect of individual compounds suggests the competition for the same target of action between compounds of the mixtures.
- Pre-exposure of endothelial cells to mixtures of anthocyanins and their gut metabolites also attenuates the migration of monocytes through the endothelial monolayer.
- Mixtures of tested compounds also show the capacity to modulate the expression of genes in endothelial cells, especially those involved in the regulation of cell-cell adhesion, actin cytoskeleton reorganisation and focal adhesion.
- The observed nutrigenomic effects can be explained by the affinity of anthocyanins and their metabolites to bind different signalling proteins (as predicted by molecular docking) and affect their activity and the activity of transcription factors that they regulate (as shown by Western blot analysis), consequently modulating the expression of target genes.
- Mixtures of anthocyanins and their metabolites also exert their nutrigenomic effect by significantly altering the miRNA expression in endothelial cells, especially those miRNAs associated with endothelial cell permeability, dysfunction and atherosclerosis development.

- In platelets, anthocyanins and their metabolites display the capacity to modulate at least one of the investigated parameters of platelet function, i.e. agonist-induced platelet activation and their aggregation with neutrophils and monocytes. Of these compounds, vanillic acid does not seem to affect platelet function, while anthocyanin cy-3-arab and metabolite 4-HBAL are the most efficient in attenuating both platelet activation and aggregation.

Taken together, results from this thesis show that both anthocyanins and their metabolites, at physiologically relevant conditions, can reduce monocyte adhesion and transendothelial migration, the initial steps in the development of atherosclerosis, by maintaining the endothelial integrity and function during the inflammatory stress. These effects seem to be mediated by complex molecular mechanisms of action of these compounds. These mechanisms include the ability of anthocyanins and their metabolites to interact with cell signalling proteins and modulate their activity and consequently the activity of transcription factors, leading to changes in gene expression as well as their capacity to modulate miRNA expression (Figure 42). Furthermore, results from this thesis also showed the potency of physiologically relevant levels of circulating anthocyanins and their metabolites to attenuate platelet activation and aggregation with leukocytes, the processes that are key contributors to the development of CVD. Thus, these findings provide potential proof of a cause-and-effect relationship for the beneficial effect of the habitual consumption of anthocyanin-rich foods on endothelial and platelet function and mechanisms underlying their cardioprotective effects.

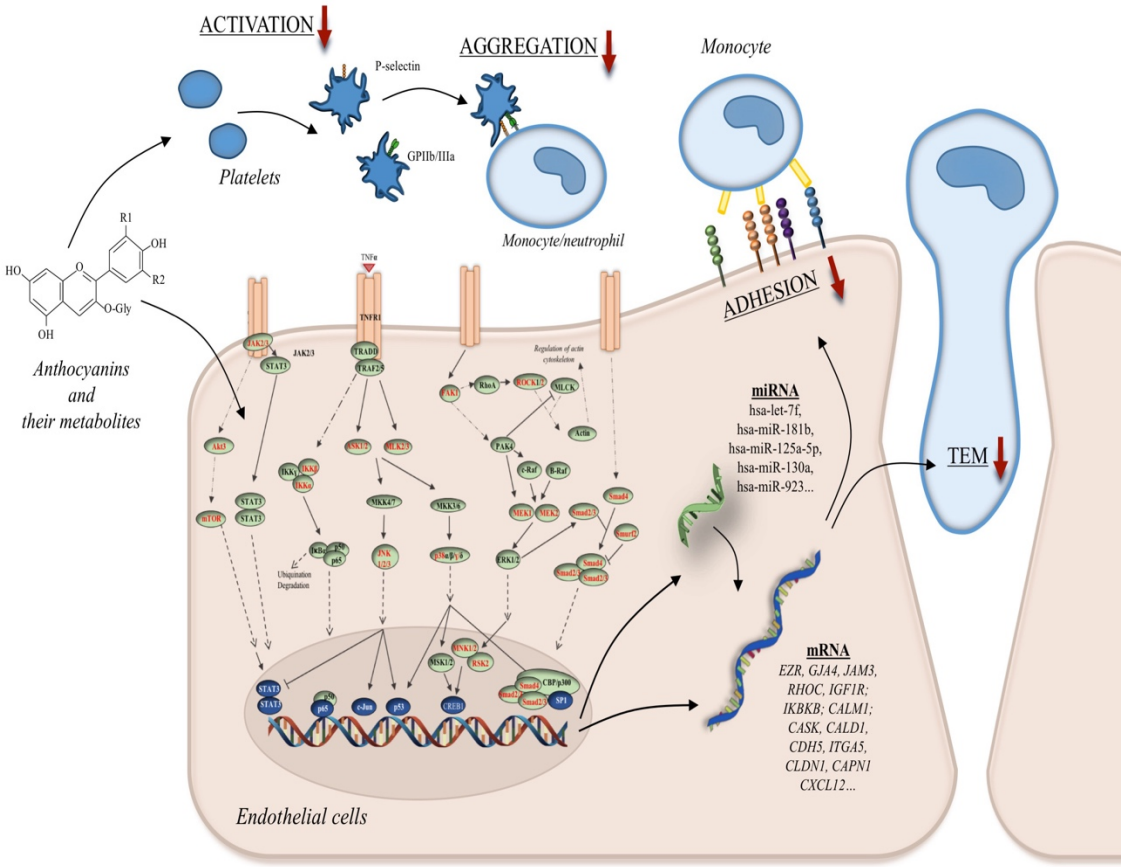

Figure 42. *Summary of the effects of anthocyanins and their metabolites.*
(In red-cell signaling proteins for which binding affinity of tested compounds was identified as lower than -8.5 kcal/mol).

7. REFERENCES

Abi-Younes S, Sauty A, Mach F, Sukhova GK, Libby P, Luster AD. 2000. The stromal cell-derived factor-1 chemokine is a potent platelet agonist highly expressed in atherosclerotic plaques. Circ Res. 86:131–138.

Adams M, Kobayashi T, Lawson JD, Saitoh M, Shimokawa K, Bigi S V., Hixon MS, Smith CR, Tatamiya T, Goto M, et al. 2016. Fragment-based drug discovery of potent and selective MKK3/6 inhibitors. Bioorganic Med Chem Lett. 26:1086–1089.

Ahmet I, Spangler E, Shukitt-Hale B, Joseph JA, Ingram DK, Talan M. 2009. Survival and cardioprotective benefits of long-term blueberry enriched diet in dilated cardiomyopathy following myocardial infarction in rats. PLoS One. 4:e7975.

Altmäe S, Martinez-Conejero JA, Esteban FJ, Ruiz-Alonso M, Stavreus-Evers A, Horcajadas JA, Salumets A. 2013. MicroRNAs miR-30b, miR-30d, and miR-494 regulate human endometrial receptivity. Reprod Sci. 20:308–317.

Amin HP. 2015. The vascular and anti-inflammatory activity of cyanidin-3-glucoside and its metabolites in human vascular endothelial cells. [place unknown]: University of East Anglia.

Amin HP, Czank C, Raheem S, Zhang Q, Botting NP, Cassidy A, Kay CD. 2015. Anthocyanins and their physiologically relevant metabolites alter the expression of IL-6 and VCAM-1 in CD40L and oxidized LDL challenged vascular endothelial cells. Mol Nutr Food Res. 59:1095–1106.

Andersen ØM, Jordheim M. 2010. Anthocyanins. In: Encycl Life Sci. Chichester: John Wiley & Sons; p. 1–12.

Andersen ØM, Jordheim M. 2013. Basic Anthocyanin Chemistry and Dietary Sources. In: Wallace T, Giusti M, editors. Anthocyanins Heal Dis. New York: CRC Press; p. 13–90.

Anwar KN, Fazal F, Malik AB, Rahman A. 2004. RhoA/Rho-associated kinase pathway selectively regulates thrombin-induced intercellular adhesion molecule-1 expression in endothelial cells via activation of I kappa B kinase beta and phosphorylation of RelA/p65. J Immunol. 173:6965–6972.

Arfan M, Khan R, Rybarczyk A, Amarowicz R. 2012. Antioxidant activity of mulberry fruit extracts. Int J Mol Sci. 13:2472–2480.

Arnold K, Bordoli L, Kopp J, Schwede T. 2006. The SWISS-MODEL workspace: A web-based environment for protein structure homology modelling. Bioinformatics. 22:195–201.

Aukrust P, Halvorsen B, Ueland T. 2010. Activated platelets and atherosclerosis. Expert Rev Cardiovasc Ther. 8:1297–1307.

Azzini E, Vitaglione P, Intorre F, Napolitano A, Durazzo A, Foddai MS, Fumagalli A, Catasta G, Rossi L, Venneria E, et al. 2010. Bioavailability of strawberry antioxidants in human subjects. Br J Nutr. 104:1165–73.

Baeza G, Bachmair E-M, Wood S, Mateos R, Bravo L, de Roos B. 2017. The colonic metabolites dihydrocaffeic acid and dihydroferulic acid are more effective inhibitors of in vitro platelet activation than their phenolic precursors. Food Funct. 8:1333–

1342.

Barnard MR, Krueger LA, Frelinger A, Furman MI, Michelson AD. 2003. Whole Blood Analysis of Leukocyte-Platelet Aggregates. Curr Protoc Cytom. 24:6.15.1–6.15.8.

Bartel DP. 2004. MicroRNAs: Genomics, Biogenesis, Mechanism, and Function. Cell. 116:281–297.

Basu A, Du M, Leyva MJ, Sanchez K, Betts NM, Wu M, Aston CE, Lyons TJ. 2010. Blueberries Decrease Cardiovascular Risk Factors in Obese Men and Women with Metabolic Syndrome. J Nutr. 140:1582–1587.

Basu A, Fu DX, Wilkinson M, Simmons B, Wu M, Betts NM, Du M, Lyons TJ. 2010. Strawberries decrease atherosclerotic markers in subjects with metabolic syndrome. Nutr Res. 30:462–469.

Basu A, Rhone M, Lyons TJ. 2010. Berries: Emerging impact on cardiovascular health. Nutr Rev. 68:168–177.

Bazzoni G. 2004. Endothelial Cell-to-Cell Junctions: Molecular Organization and Role in Vascular Homeostasis. Physiol Rev. 84:869–901.

Bhattacharjee N, Dua TK, Khanra R, Joardar S, Nandy A, Saha A, De Feo V, Dewanjee S. 2017. Protocatechuic acid, a phenolic from sansevieria roxburghiana leaves, suppresses diabetic cardiomyopathy via stimulating glucose metabolism, ameliorating oxidative stress, and inhibiting inflammation. Front Pharmacol. 8:251.

Bidzhekov K, Gan L, Denecke B, Rostalsky A, Hristov M, Koeppel TA, Zernecke A, Weber C. 2012. microRNA expression signatures and parallels between monocyte subsets and atherosclerotic plaque in humans. Thromb Haemost. 107:619–625.

Biesiada A, Tomczak A. 2012. Biotic and Abiotic Factors Affecting the Content of the Chosen Antioxidant Compounds in Vegetables. Veg Crop Res Bull. 76:55–78.

Boath AS, Stewart D, McDougall GJ. 2012. Berry components inhibit α-glucosidase in vitro: Synergies between acarbose and polyphenols from black currant and rowanberry. Food Chem. 135:929–936.

Böhm F, Pernow J. 2007. The importance of endothelin-1 for vascular dysfunction in cardiovascular disease. Cardiovasc Res. 76:8–18.

Bonetti PO, Lerman LO, Lerman A. 2003. Endothelial dysfunction: A marker of atherosclerotic risk. Arterioscler Thromb Vasc Biol. 23:168–175.

Brass LF, Newman DK, Wannermacher KM, Zhu L, Stalker TJ. 2013. Signal Transduction During Platelet Plug Formation. In: Michelson AD, editor. Platelets. 3rd Editio. London: Elsevier; p. 367–398.

Breslin JW, Yuan SY. 2004. Involvement of RhoA and Rho kinase in neutrophil-stimulated endothelial hyperpermeability. Am J Physiol Heart Circ Physiol. 286:H1057–H1062.

Brevetti G, Schiano V, Chiariello M. 2008. Endothelial dysfunction: A key to the pathophysiology and natural history of peripheral arterial disease? Atherosclerosis. 197:1–11.

Brown M, Wittwer C. 2000. Flow cytometry: Principles and clinical applications in

hematology. Clin Chem. 46:1221–1229.

Bub A, Watzl B, Heeb D, Rechkemmer G, Briviba K. 2001. Malvidin-3-glucoside bioavailability in humans after ingestion of red wine, dealcoholized red wine and red grape juice. Eur J Nutr. 40:113–120.

Burton-Freeman B. 2010. Postprandial metabolic events and fruit-derived phenolics: a review of the science. Br J Nutr. 104 Suppl:S1-14.

van Buul J, Hordijk P. 2004. Signaling in leukocyte transendothelial migration. Arter Thromb Vasc Biol. 24:824–833.

Cao G, Muccitelli HU, Sánchez-Moreno C, Prior RL. 2001. Anthocyanins are absorbed in glycated forms in elderly women: A pharmacokinetic study. Am J Clin Nutr. 73:920–926.

Cao Y, Marks JD, Huang Q, Rudnick SI, Xiong C, Hittelman WN, Wen X, Marks JW, Cheung LH, Boland K, et al. 2012. Single-Chain Antibody-Based Immunotoxins Targeting Her2/neu: Design Optimization and Impact of Affinity on Antitumor Efficacy and Off-Target Toxicity. Mol Cancer Ther. 11:143–153.

Caraux G, Pinloche S. 2005. PermutMatrix: A graphical environment to arrange gene expression profiles in optimal linear order. Bioinformatics. 21:1280–1281.

Cassidy A, Bertoia M, Chiuve S, Flint A, Forman J, Rimm EB. 2016. Habitual intake of anthocyanins and flavanones and risk of cardiovascular disease in men. Am J Clin Nutr. 104:587–594.

Cassidy A, O'Reilly ÉJ, Kay C, Sampson L, Franz M, Forman J, Curhan G, Rimm EB. 2011. Habitual intake of flavonoid subclasses and incident hypertension in adults. Am J Clin Nutr. 93:338–347.

Cassidy A, O'Reilly ÉJ, Liu L, Franz M, Eliassen a. H, Rimm EB. 2013. High Anthocyanin Intake Is Associated With a Reduced Risk of Myocardial Infarction in Young and Middle-Aged Women. Circulation. 127:188–196.

Cassidy A, Rogers G, Peterson JJ, Dwyer JT, Lin H, Jacques PF. 2015. Higher dietary anthocyanin and flavonol intakes are associated with anti-inflammatory effects in a population of US adults. Am J Clin Nutr. 102:172–181.

Castañeda-Ovando A, Pacheco-Hernández M de L, Páez-Hernández ME, Rodríguez JA, Galán-Vidall CA. 2009. Chemical studies of anthocyanins: A review. Food Chem. 113:859–871.

Čejková S, Králová-Lesná I, Poledne R. 2016. Monocyte adhesion to the endothelium is an initial stage of atherosclerosis development. Cor Vasa. 58:e419–e425.

Chalker-Scott L. 1999. Environmental significance of anthocyanins in plant stress responses. Photochem Photobiol. 70:1–9.

Chanet A, Milenkovic D, Claude S, Maier JAM, Kamran Khan M, Rakotomanomana N, Shinkaruk S, Bérard AM, Bennetau-Pelissero C, Mazur A, Morand C. 2013. Flavanone metabolites decrease monocyte adhesion to TNFα-activated endothelial cells by modulating expression of atherosclerosis-related genes. Br J Nutr. 110:587–598.

Chanet A, Milenkovic D, Manach C, Mazur A, Morand C. 2012. Citrus flavanones: What

is their role in cardiovascular protection? J Agric Food Chem. 60:8809–8822.

Chao PY, Huang YP, Hsieh W Bin. 2013. Inhibitive effect of purple sweet potato leaf extract and its components on cell adhesion and inflammatory response in human aortic endothelial cells. Cell Adhes Migr. 7:237–245.

Chao PY, Lin K-H, Chiu C-C, Yang Y-Y, Huang M-Y, Yang C-M. 2013. Inhibitive effects of mulberry leaf-related extracts on cell adhesion and inflammatory response in human aortic endothelial cells. Evidence-based Complement Altern Med. 2013:14.

Chen CY, Yi L, Jin X, Zhang T, Fu YJ, Zhu JD, Mi MT, Zhang QY, Ling WH, Yu B. 2011. Inhibitory Effect of Delphinidin on Monocyte-Endothelial Cell Adhesion Induced by Oxidized Low-Density Lipoprotein via ROS/p38MAPK/NF-κB Pathway. Cell Biochem Biophys. 61:337–348.

Chun OK, Chung S-J, Claycombe KJ, Song WO. 2008. Serum C-reactive protein concentrations are inversely associated with dietary flavonoid intake in U.S. adults. J Nutr. 138:753–60.

Cimino F, Speciale A, Anwar S, Canali R, Ricciardi E, Virgili F, Trombetta D, Saija A. 2013. Anthocyanins protect human endothelial cells from mild hyperoxia damage through modulation of Nrf2 pathway. Genes Nutr. 8:391–399.

Claude S, Boby C, Rodriguez-Mateos A, Spencer JPE, Gérard N, Morand C, Milenkovic D. 2014. Flavanol metabolites reduce monocyte adhesion to endothelial cells through modulation of expression of genes via p38-MAPK and p65-Nf-kB pathways. Mol Nutr Food Res. 58:1016–1027.

Clifford M, Brown JE. 2006. Dietary Flavonoids and Health-Broadening the Perspective. In: Øyvind M. Andersen and Kenneth R. Markham, editor. Flavonoids Chem Biochem Appl. Boca Raton: CRC Press/Taylor & Francis; p. 319–370.

Czank C, Cassidy A, Zhang Q, Morrison DJ, Preston T, Kroon P a., Botting NP, Kay CD. 2013. Human metabolism and elimination of the anthocyanin, cyanidin-3-glucoside: A 13C-tracer study. Am J Clin Nutr. 97:995–1003.

Dauchet L, Amouyel P, Hercberg S, Dallongeville J. 2006. Fruit and Vegetable Consumption and Risk of Coronary Heart Disease: A Meta-Analysis of Cohort Studies 1. J Nutr. 136:2588–2593.

Day AJ, Cañada FJ, Díaz JC, Kroon PA, McLauchlan R, Faulds CB, Plumb GW, Morgan MRA, Williamson G. 2000. Dietary flavonoid and isoflavone glycosides are hydrolysed by the lactase site of lactase phlorizin hydrolase. FEBS Lett. 468:166–170.

Dohadwala MM, Holbrook M, Hamburg NM, Shenouda SM, Chung WB, Titas M, Kluge MA, Wang N, Palmisano J, Milbury PE, et al. 2011. Effects of cranberry juice consumption on vascular function in patients with coronary artery disease. Am J Clin Nutr. 93:934–940.

Dohadwala MM, Vita JA. 2009. Grapes and cardiovascular disease. J Nutr. 139:1788S–1793S.

Doss HM, Dey C, Sudandiradoss C, Rasool MK. 2016. Targeting inflammatory mediators with ferulic acid, a dietary polyphenol, for the suppression of monosodium urate crystal-induced inflammation in rats. Life Sci. 148:201–210.

Du K, Li Z, Fang X, Cao T, Xu Y. 2017. Ferulic acid promotes osteogenesis of bone marrow-derived mesenchymal stem cells by inhibiting microRNA-340 to induce β-catenin expression through hypoxia. Eur J Cell Biol. 96:496–503.

Dweep H, Gretz N. 2015. miRWalk2.0: a comprehensive atlas of microRNA-target interactions. Nat Methods. 12:697–697.

Eckel RH, Jakicic JM, Ard JD, De Jesus JM, Houston Miller N, Hubbard VS, Lee IM, Lichtenstein AH, Loria CM, Millen BE, et al. 2014. 2013 AHA/ACC guideline on lifestyle management to reduce cardiovascular risk: A report of the American college of cardiology/American heart association task force on practice guidelines. J Am Coll Cardiol. 63:2960–2984.

Edwards M, Czank C, Woodward GM, Cassidy A, Kay CD. 2015. Phenolic metabolites of anthocyanins modulate mechanisms of endothelial function. J Agric Food Chem. 63:2423–2431.

El-Seedi HR, El-Said AMA, Khalifa SAM, Göransson U, Bohlin L, Borg-Karlson AK, Verpoorte R. 2012. Biosynthesis, natural sources, dietary intake, pharmacokinetic properties, and biological activities of hydroxycinnamic acids. J Agric Food Chem. 60:10877–10895.

Elalamy I, Chakroun T, Gerotziafas GT, Petropoulou A, Robert F, Karroum A, Elgrably F, Samama MM, Hatmi M. 2008. Circulating platelet-leukocyte aggregates: A marker of microvascular injury in diabetic patients. Thromb Res. 121:843–848.

Elwood PC, Renaud S, Sharp DS, Beswick AD, O'Brien JR, Yarnell JW. 1991. Ischemic heart disease and platelet aggregation. The Caerphilly Collaborative Heart Disease Study. Circulation. 83:38–44.

Erlund I, Koli R, Alfthan G, Marniemi J, Puukka P, Mustonen P, Mattila P, Jula A. 2008. Favorable effects of berry consumption on platelet function, blood pressure, and HDL cholesterol. Am J Clin Nutr. 87:323–331.

Evangelista V, Smyth SS. 2013. Interactions Between Platelets, Leukocytes and the Endothelium. 3rd Editio. Michelson AD, editor. London: Elsevier Inc.

Fang J. 2014. Bioavailability of anthocyanins. Drug Metab Rev. 46:508–20.

Fang Y, Gao F, Hao J, Liu Z. 2017. MicroRNA-1246 mediates lipopolysaccharide-induced pulmonary endothelial cell apoptosis and acute lung injury by targeting angiotensin-converting enzyme 2. Am J Transl Res. 9:1287–1296.

FAO/WHO. 2004. Fruit and Vegetables for Health. Kobe.

Faria A, Fernandes I, Norberto S, Mateus N, Calhau C. 2014. Interplay between anthocyanins and gut microbiota. J Agric Food Chem. 62:6898–902.

Favot L, Abusnina AA, Anton A. 2015. Delphinidin Inhibits Tumor Growth by Acting on VEGF Signalling in Endothelial Cells. PLoS One. 10:e0145291.

Felgines C, Texier O, Besson C, Vitaglione P, Lamaison JL, Fogliano V, Scalbert A, Vanella L, Galvano F. 2008. Influence of glucose on cyanidin 3-glucoside absorption in rats. Mol Nutr Food Res. 52:959–964.

de Ferrars R, Cassidy A, Curtis P, Kay C. 2014. Phenolic metabolites of anthocyanins following a dietary intervention study in post-menopausal women. Mol Nutr Food

Res. 58:490–502.

de Ferrars R, Czank C, Zhang Q, Botting N, Kroon P, Cassidy A, Kay C. 2014. The pharmacokinetics of anthocyanins and their metabolites in humans. Br J Pharmacol. 171:3268–3282.

Fossen T, Cabrita L, Andersen OM. 1998. Colour and stability of pure anthocyanins influenced by pH including the alkaline region. Food Chem. 63:435–440.

Fraga CG, Galleano M, Verstraeten S V., Oteiza PI. 2010. Basic biochemical mechanisms behind the health benefits of polyphenols. Mol Aspects Med. 31:435–445.

Francis FJ, Markakis PC. 1989. Food colorants: Anthocyanins. Crit Rev Food Sci Nutr. 28:273–314.

Frank T, Netzel M, Strass G, Bitsch R, Bitsch I. 2003. Bioavailability of anthocyanidin-3-glucosides following consumption of red wine and red grape juice. Can J Physiol Pharmacol. 81:423–435.

Fratantonio D, Speciale A, Ferrari D, Cristani M, Saija A, Cimino F. 2015. Palmitate-induced endothelial dysfunction is attenuated by cyanidin-3-O-glucoside through modulation of Nrf2/Bach1 and NF-κB pathways. Toxicol Lett. 239:152–160.

Furman MI, Barnard MR, Krueger LA, Fox ML, Shilale EA, Lessard DM, Marchese P, Frelinger AL, Goldberg RJ, Michelson AD. 2001. Circulating monocyte-platelet aggregates are an early marker of acute myocardial infarction. J Am Coll Cardiol. 38:1002–1006.

Gaber MW, Yuan H, Killmar JT, Naimark MD, Kiani MF, Merchant TE. 2004. An intravital microscopy study of radiation-induced changes in permeability and leukocyte-endothelial cell interactions in the microvessels of the rat pia mater and cremaster muscle. Brain Res Protoc. 13:1–10.

Galkina E, Ley K. 2009. Immune and Inflammatory Mechanisms of Atherosclerosis. Annu Rev Immunol. 27:165–197.

Galleano M, Oteiza PI, Fraga CG. 2009. Cocoa, chocolate, and cardiovascular disease. J Cardiovasc Pharmacol. 54:483–90.

Gan Y, Tong X, Li L, Cao S, Yin X, Gao C, Herath C, Li W, Jin Z, Chen Y, Lu Z. 2015. Consumption of fruit and vegetable and risk of coronary heart disease: A meta-analysis of prospective cohort studies. Int J Cardiol. 183:129–137.

Garcia-Alonso M, Minihane AM, Rimbach G, Rivas-Gonzalo JC, de Pascual-Teresa S. 2009. Red wine anthocyanins are rapidly absorbed in humans and affect monocyte chemoattractant protein 1 levels and antioxidant capacity of plasma. J Nutr Biochem. 20:521–529.

Gawaz M, Brand K, Dickfeld T, Pogatsa-Murray G, Page S, Bogner C, Koch W, Schömig A, Neumann FJ. 2000. Platelets induce alterations of chemotactic and adhesive properties of endothelial cells mediated through an interleukin-1-dependent mechanism. Implications for atherogenesis. Atherosclerosis. 148:75–85.

Gawaz M, Langer H, May AE. 2005. Platelets in inflammation and atherogenesis. J Clin Invest. 115:3378–3384.

Gee JM, DuPont MS, Day a J, Plumb GW, Williamson G, Johnson IT. 2000. Intestinal

transport of quercetin glycosides in rats involves both deglycosylation and interaction with the hexose transport pathway. J Nutr. 130:2765–2771.

Gerhardt T, Ley K. 2015. Monocyte trafficking across the vessel wall. Cardiovasc Res. 107:321–330.

Gerrits AJ, Frelinger AL, Michelson AD. 2016. Whole Blood Analysis of Leukocyte-Platelet Aggregates. Curr Protoc Cytom. 24:6.15.1-6.15.10.

Gerszten RE, Garcia-Zepeda EA, Lim Y-C, Yoshida M, Ding HA, Jr MAG, Luster AD, Rosenzweig FWLA. 1999. MCP-1 and IL-8 trigger firm adhesion of monocytes to vascular endothelium under flow conditions. Nature. 398:718–723.

van Gils J, Zwaginga JJ, Hordijk PL. 2009. Molecular and functional interactions among monocytes, platelets, and endothelial cells and their relevance for cardiovascular diseases. J Leukoc Biol. 85:195–204.

van Gils JM, Da Costa Martins PA, Mol A, Hordijk PL, Zwaginga JJ. 2008. Transendothelial migration drives dissociation of platelet-monocyte complexes. Thromb Haemost. 100:271–279.

Golubovskaya V, Ho B, Zheng M, Magis A, Ostrov D, G. Cance W. 2013. Mitoxantrone Targets the ATP-binding Site of FAK, Binds the FAK Kinase Domain and Decreases FAK, Pyk-2, c-Src, and IGF-1R In Vitro Kinase Activities. Anticancer Agents Med Chem. 13:546–554.

Di Gregoli K, Mohamad Anuar NN, Bianco R, White SJ, Newby AC, George SJ, Johnson JL. 2017. MicroRNA-181b Controls Atherosclerosis and Aneurysms Through Regulation of TIMP-3 and Elastin. Circ Res. 120:49–65.

Grosso G, Marventano S, Yang J, Micek A, Pajak A, Scalfi L, Galvano F, Kales SN. 2017. A Comprehensive Meta-analysis on Evidence of Mediterranean Diet and Cardiovascular Disease: Are Individual Components Equal? Crit Rev Food Sci Nutr. 57:3218–3232.

Hajjar DP, Gotto AM. 2013. Biological relevance of inflammation and oxidative stress in the pathogenesis of arterial diseases. Am J Pathol. 182:1474–1481.

He J, Magnuson BA, Giusti MM. 2005. Analysis of anthocyanins in rat intestinal contents - Impact of anthocyanin chemical structure on fecal excretion. J Agric Food Chem. 53:2859–2866.

Heinonen M. 2001. Anthocyanins as dietary antioxidants. In: Voutilainen S, Salonen J, editors. Third Int Conf Nat antioxidants Anticarcinog food, Heal Dis. Helsinki, Finland: Kuopion Yliopisto; p. 25.

Henriquez R, Ito T, Sun L, Crooks R. 2004. The resurgence of Coulter counting for analyzing nanoscale objects. Analyst. 129:478.

Herwig MC, Tsokos M, Hermanns MI, Kirkpatrick CJ, Müller AM. 2013. Vascular endothelial cadherin expression in lung specimens of patients with sepsis-induced acute respiratory distress syndrome and endothelial cell cultures. Pathobiology. 80:245–251.

Hollman PC, Bijsman MN, van Gameren Y, Cnossen EP, de Vries JH, Katan MB. 1999. The sugar moiety is a major determinant of the absorption of dietary flavonoid

glycosides in man. Free Radic Res. 31:569–573.

Horcajada M-N, Sanchez C, Membrez Scalfo F, Drion P, Comblain F, Taralla S, Donneau A-F, Offord EA, Henrotin Y. 2015. Oleuropein or rutin consumption decreases the spontaneous development of osteoarthritis in the Hartley guinea pig. Osteoarthritis Cartilage. 23:94–102.

Hordijk P. 2006. Endothelial signalling events during leukocyte transmigration. FEBS J. 273:4408–4415.

Hordijk P, van Buul J. 2009. Endothelial adapter proteins in leukocyte transmigration. Thromb Haemost. 101:649–655.

Hou D-X, Kumamoto T. 2010. Flavonoids as protein kinase inhibitors for cancer chemoprevention: direct binding and molecular modeling. Antioxid Redox Signal. 13:691–719.

Hou DX, Yanagita T, Uto T, Masuzaki S, Fujii M. 2005. Anthocyanidins inhibit cyclooxygenase-2 expression in LPS-evoked macrophages: Structure-activity relationship and molecular mechanisms involved. Biochem Pharmacol. 70:417–425.

Hou L, Li F, Wang Y, Ou Z, Xu D, Tan W, Dai M. 2015. Association between dietary patterns and coronary heart disease: a meta-analysis of prospective cohort studies. Int J Clin Exp Med. 8:781–790.

Hribar U, Ulrih NP. 2014. The metabolism of anthocyanins. Curr Drug Metab. 15:3–13.

Hsu YL, Hung JY, Chang WA, Lin YS, Pan YC, Tsai PH, Wu CY, Kuo PL. 2017. Hypoxic lung cancer-secreted exosomal MIR-23a increased angiogenesis and vascular permeability by targeting prolyl hydroxylase and tight junction protein ZO-1. Oncogene. 36:4929–4942.

Hu D, Huang J, Wang Y, Zhang D, Qu Y. 2014. Fruits and Vegetables Consumption and Risk of Stroke: A Meta-Analysis of Prospective Cohort Studies. Stroke. 45:1613–1619.

Hu S, Liu Y, You T, Heath J, Xu L, Zheng X, Wang A, Wang Y, Li F, Yang F, et al. 2018. Vascular Semaphorin 7A Upregulation by Disturbed Flow Promotes Atherosclerosis Through Endothelial β1 Integrin. Arterioscler Thromb Vasc Biol. 38:335–343.

Huang W, Zhu Y, Li C, Sui Z, Min W. 2016. Effect of blueberry anthocyanins malvidin and glycosides on the antioxidant properties in endothelial cells. Oxid Med Cell Longev.:10.

Huang WY, Liu YM, Wang J, Wang XN, Li CY. 2014. Anti-inflammatory effect of the blueberry anthocyanins malvidin-3-glucoside and malvidin-3-galactoside in endothelial cells. Molecules. 19:12827–12841.

Huang WY, Wang J, Liu YM, Zheng QS, Li CY. 2014. Inhibitory effect of Malvidin on TNF-α-induced inflammatory response in endothelial cells. Eur J Pharmacol. 723:67–72.

von Hundelshausen P, Weber KSC, Huo Y, Proudfoot AEI, Nelson PJ, Ley K, Weber C. 2001. RANTES Deposition by Platelets Triggers Monocyte Arrest on Inflamed and Atherosclerotic Endothelium. Circulation. 103:1772–1777.

Jennings A, Welch AA, Fairweather-Tait SJ, Kay C, Minihane AM, Chowienczyk P, Jiang B, Cecelja M, Spector T, Macgregor A, Cassidy A. 2012. Higher anthocyanin intake is associated with lower arterial stiffness and central blood pressure in women. Am J Clin Nutr. 96:781–788.

Jennings A, Welch AA, Spector T, Macgregor A, Cassidy A. 2014. Intakes of Anthocyanins and Flavones Are Associated with Biomarkers of Insulin Resistance and Inflammation in Women 1,2. J Nutr. 144:202–208.

Jennings L. 2009. Role of Platelets in Atherothrombosis. Am J Cardiol. 103:4A–10A.

Jeong S, Ku S, Bae J. 2017. Anti-inflammatory effects of pelargonidin on TGFBIp-induced responses. Can J Physiol Pharmacol. 95:372–381.

Jing P, Bomser JA, Schwartz SJ, He J, Magnuson BA, Giusti MM. 2008. Structure-function relationships of anthocyanins from various anthocyanin-rich extracts on the inhibition of colon cancer cell growth. J Agric Food Chem. 56:9391–9398.

Johnson SA, Figueroa A, Navaei N, Wong A, Kalfon R, Ormsbee LT, Feresin RG, Elam ML, Hooshmand S, Payton ME, Arjmandi BH. 2015. Daily blueberry consumption improves blood pressure and arterial stiffness in postmenopausal women with pre- and stage 1-hypertension: A randomized, double-blind, placebo-controlled clinical trial. J Acad Nutr Diet. 115:369–377.

Karlsen A, Retterstol L, Laake P, Paur I, Bøhn SK, Sandvik L, Blomhoff R. 2007. Anthocyanins inhibit nuclear factor-kappaB activation in monocytes and reduce plasma concentrations of pro-inflammatory mediators in healthy adults. J Nutr. 137:1951–4.

Kay CD, Mazza G, Holub BJ, Wang J. 2004. Anthocyanin metabolites in human urine and serum. Br J Nutr. 91:933–942.

Kay CD, Mazza GJ, Holub BJ. 2005. Anthocyanins exist in the circulation primarily as metabolites in adult men. J Nutr. 135:2582–2588.

Khandelwal AR, Hebert VY, Kleinedler JJ, Rogers LK, Ullevig SL, Asmis R, Shi R, Dugas TR. 2012. Resveratrol and quercetin interact to inhibit neointimal hyperplasia in mice with a carotid injury. J Nutr. 142:1487–1494.

Kianbakht S, Abasi B, Hashem Dabaghian F. 2014. Improved lipid profile in hyperlipidemic patients taking vaccinium arctostaphylos fruit hydroalcoholic extract: A randomized double-blind placebo-controlled clinical trial. Phyther Res. 28:432–436.

Kim BH, Kim M, Yin CH, Jee JG, Sandoval C, Lee H, Bach EA, Hahm DH, Baeg GH. 2011. Inhibition of the signalling kinase JAK3 alleviates inflammation in monoarthritic rats. Br J Pharmacol. 164:106–118.

Kim K, Bae ON, Lim KM, Noh JY, Kang S, Chung KY, Chung JH. 2012. Novel antiplatelet activity of protocatechuic acid through the inhibition of high shear stress-induced platelet aggregation. J Pharmacol Exp Ther. 343:704–711.

Kong JM, Chia LS, Goh NK, Chia TF, Brouillard R. 2003. Analysis and biological activities of anthocyanins. Phytochemistry. 64:923–933.

Konic-Ristic A, Kroon PA, Glibetic M. 2015. Modulation of platelet function with dietary

polyphenols. A promising strategy in the prevention of cardiovascular disease. Agro FOOD Indusrty Hi Tech. 26:15–19.

Kottra G, Daniel H. 2007. Flavonoid Glycosides Are Not Transported by the Human Na+/Glucose Transporter When Expressed in Xenopus laevis Oocytes, but Effectively Inhibit Electrogenic Glucose Uptake. J Pharmacol Exp Ther. 322:829–835.

Krepinsky J, Wu D, Ingram A, Scholey J. 2002. Developments in mitogen- induced extracellular kinase 1 inhibitors and their use in the treatment of disease. Expert Opin Ther Pat. 12:795–1811.

Krga I, Milenkovic D, Morand C, Monfoulet L-E. 2016. An update on the role of nutrigenomic modulations in mediating the cardiovascular protective effect of fruit polyphenols. Food Funct. 7:3656–3676.

Krueger LA, Barnard MR, Frelinger AL, Furman MI, Michelson AD. 2002. Immunophenotypic Analysis of Platelets. In: Curr Protoc Cytom. Vol. 19. Hoboken, NJ, USA: John Wiley & Sons, Inc.; p. 6.10.1–6.10.17.

Kuijper PH, Gallardo Torres HI, Houben LA, Lammers JW, Zwaginga JJ, Koenderman L, Torres HIG, Houben LA. 1998. P-selectin and MAC-1 mediate monocyte rolling and adhesion to ECM-bound platelets under flow conditions. J Leokocyte Biol. 64:467–473.

Kuntz S, Asseburg H, Dold S, Römpp A, Fröhling B, Kunz C, Rudloff S. 2015. Inhibition of low-grade inflammation by anthocyanins from grape extract in an in vitro epithelial-endothelial co-culture model. Food Funct. 6:1136–49.

Kuntz S, Rudloff S, Asseburg H, Borsch C, Fröhling B, Unger F, Dold S, Spengler B, Römpp A, Kunz C. 2015. Uptake and bioavailability of anthocyanins and phenolic acids from grape/blueberry juice and smoothie in vitro and in vivo. Br J Nutr. 113:1044–1055.

Kwak BR, Mulhaupt F, Veillard N, Gros DB, Mach F. 2002. Altered pattern of vascular connexin expression in atherosclerotic plaques. Arterioscler Thromb Vasc Biol. 22:225–230.

Laemmli UK. 1970. Cleavage of structural proteins during the assembly of the head of bacteriophage T4. Nature. 227:680–5.

Laksmiani NPL, Vidya Paramita NLP, Wirasuta IMAG. 2016. In vitro and in silico antioxidant activity of purified fractions from purple sweet potato ethanolic extract. Int J Pharm Pharm Sci. 8:177–181.

Lazzè MC, Pizzala R, Perucca P, Cazzalini O, Savio M, Forti L, Vannini V, Bianchi L. 2006. Anthocyanidins decrease endothelin-1 production and increase endothelial nitric oxide synthase in human endothelial cells. Mol Nutr Food Res. 50:44–51.

Lee I-C, Kim J, Bae J-S. 2017. Anti-inflammatory effects of dabrafenib in vitro and in vivo. Can J Physiol Pharmacol [Internet]. 95:697–707. Available from: http://www.nrcresearchpress.com/doi/10.1139/cjpp-2016-0519%0Ahttp://www.ncbi.nlm.nih.gov/pubmed/28177661

Lee IT, Chan YC, Lin CW, Lee WJ, Sheu WHH. 2008. Effect of cranberry extracts on lipid profiles in subjects with type 2 diabetes. Diabet Med. 25:1473–1477.

Lee JE, Lee AS, Kim DH, Jung YJ, Lee S, Park BH, Lee SH, Park SK, Kim W, Kang KP. 2012. JANEX-1, a JAK3 inhibitor, ameliorates tumor necrosis factor-α- induced expression of cell adhesion molecules and improves myocardial vascular permeability in endotoxemic mice. Int J Mol Med. 29:864–870.

Lee SE, Yang H, Son GW, Park HR, Cho JJ, Ahn HJ, Park CS, Park YS. 2015. Identification and characterization of MicroRNAs in acrolein-stimulated endothelial cells: Implications for vascular disease. Biochip J. 9:144–155.

Ley K. 1996. Molecular mechanisms of leukocyte recruitment in the inflammatory process. Cardiovasc Res. 32:733–742.

Ley K. 2013. Leukocytes talking to VE-cadherin. Blood. 122:2300–2301.

Ley K, Laudanna C, Cybulsky MI, Nourshargh S. 2007. Getting to the site of inflammation: The leukocyte adhesion cascade updated. Nat Rev Immunol. 7:678–689.

Li AN, Li S, Zhang YJ, Xu XR, Chen YM, Li H Bin. 2014. Resources and biological activities of natural polyphenols. Nutrients. 6:6020–6047.

Li D, Zhang Y, Liu Y, Sun R, Xia M. 2015. Purified anthocyanin supplementation reduces dyslipidemia, enhances antioxidant capacity, and prevents insulin resistance in diabetic patients. J Nutr. 145:742–748.

Li L, Wang L, Wu Z, Yao L, Wu Y, Huang L, Liu K, Zhou X, Gou D. 2014. Anthocyanin-rich fractions from red raspberries attenuate inflammation in both RAW264.7 macrophages and a mouse model of colitis. Sci Rep. 4:6234.

Li T, Cao H, Zhuang J, Wan J, Guan M, Yu B, Li X, Zhang W. 2010. Identification of miR-130a, miR-27b and miR-210 as serum biomarkers for atherosclerosis obliterans. Clin Chim Acta. 412:66–70.

Liao JK, Seto M, Noma K. 2007. Rho kinase (ROCK) inhibitors. J Cardiovasc Pharmacol. 50:17–24.

Libby P, Ridker PM, Hansson GK. 2011. Progress and challenges in translating the biology of atherosclerosis. Nature. 473:317–325.

Libby P, Ridker PM, Maseri A. 2002. Inflammation and atherosclerosis. Circulation. 105:1135–1143.

Lievens D, von Hundelshausen P. 2011. Platelets in atherosclerosis. Thromb Haemost. 106:827–838.

Lila MA, Burton-Freeman B, Grace M, Kalt W. 2016. Unraveling Anthocyanin Bioavailability for Human Health. Annu Rev Food Sci Technol. 7:375–394.

Liu F, Verin AD, Borbiev T, Garcia JG. 2001. Role of cAMP-dependent protein kinase A activity in endothelial cell cytoskeleton rearrangement. AmJPhysiol Lung Cell MolPhysiol. 280:L1309–L1317.

Llona-Minguez S, Baiget J, Mackay SP. 2013. Small-molecule inhibitors of IκB kinase (IKK) and IKK-related kinases. Pharm Pat Anal. 2:481–498.

Lusis AJ. 2000. Atherosclerosis. Nature. 407:233–241.

Ma Z-C, Hong Q, Wang Y-G, Tan H-L, Xiao C-R, Liang Q-D, Cai S-H, Gao Y. 2010.

Ferulic acid attenuates adhesion molecule expression in gamma-radiated human umbilical vascular endothelial cells. Biol Pharm Bull. 33:752–758.

Maestro A, Terdoslavich M, Vanzo A, Kuku A, Tramer F, Nicolin V, Micali F, Decorti G, Passamonti S. 2010. Expression of bilitranslocase in the vascular endothelium and its function as a flavonoid transporter. Cardiovasc Res. 85:175–183.

Mancia G, De Backer G, Dominiczak A, Cifkova R, Fagard R, Germano G, Grassi G, Heagerty AM, Kjeldsen SE, Laurent S, et al. 2007. 2007 Guidelines for the Management of Arterial Hypertension. J Hypertens. 25:1105–1187.

Manzano S, Williamson G. 2010. Polyphenols and phenolic acids from strawberry and apple decrease glucose uptake and transport by human intestinal Caco-2 cells. Mol Nutr Food Res. 54:1773–1780.

Martin S, Favot L, Matz R, Lugnier C, Andriantsitohaina R. 2003. Delphinidin inhibits endothelial cell proliferation and cell cycle progression through a transient activation of ERK-1 /-2. Biochem Pharmacol. 65:669–675.

Martins PA d. C. 2005. Platelet binding to monocytes increases the adhesive properties of monocytes by up-regulating the expression and functionality of beta 1 and 2 integrins. J Leukoc Biol. 79:499–507.

Del Maschio A, Zanetti A, Corada M, Rival Y, Ruco L, Lampugnani MG, Dejana E. 1996. Polymorphonuclear leukocyte adhesion triggers the disorganization of endothelial cell-to-cell adherens junctions. J Cell Biol. 135:497–510.

Matsumoto H, Inaba H, Kishi M, Tominaga S, Hirayama M, Tsuda T. 2001. Orally administered delphinidin 3-rutinoside and cyanidin 3-rutinoside are directly absorbed in rats and humans and appear in the blood as the intact forms. J Agric Food Chem. 49:1546–1551.

Mauray A, Felgines C, Morand C, Mazur A, Scalbert A, Milenkovic D. 2012. Bilberry anthocyanin-rich extract alters expression of genes related to atherosclerosis development in aorta of apo E-deficient mice. Nutr Metab Cardiovasc Dis. 22:72–80.

Mauray A, Milenkovic D, Besson C, Caccia N, Morand C, Michel F, Mazur A, Scalbert A, Felgines C. 2009. Atheroprotective effects of bilberry extracts in apo E-deficient mice. J Agric Food Chem. 57:11106–11111.

Mazza G, Brouillard R. 1987. Recent developments in the stabilization of anthocyanins in food products. Food Chem. 25:207–225.

Mazza G, Kay CD, Cottrell T, Holub BJ. 2002. Absorption of anthocyanins from blueberries and serum antioxidant status in human subjects. J Agric Food Chem. 50:7731–7737.

McCabe DJH, Harrison P, Mackie IJ, Sidhu PS, Purdy G, Lawrie AS, Watt H, Brown MM, Machin SJ. 2004. Platelet degranulation and monocyte-platelet complex formation are increased in the acute and convalescent phases after ischaemic stroke or transient ischaemic attack. Br J Haematol. 125:777–787.

McCullough ML, Peterson JJ, Patel R, Jacques PF, Shah R, Dwyer JT. 2012. Flavonoid intake and cardiovascular disease mortality in a prospective cohort of US adults. Am J Clin Nutr. 95:454–464.

Medda R, Lyros O, Schmidt JL, Jovanovic N, Nie L, Link BJ, Otterson MF, Stoner GD, Shaker R, Rafiee P. 2015. Anti inflammatory and anti angiogenic effect of black raspberry extract on human esophageal and intestinal microvascular endothelial cells. Microvasc Res.:167–180.

Medina-Remón A, Casas R, Tressserra-Rimbau A, Ros E, Martínez-González MA, Fitó M, Corella D, Salas-Salvadó J, Lamuela-Raventos RM, Estruch R. 2017. Polyphenol intake from a Mediterranean diet decreases inflammatory biomarkers related to atherosclerosis: a substudy of the PREDIMED trial. Br J Clin Pharmacol. 83:114–128.

Meiler SE, Hung RR, Gerszten RE, Gianetti J, Li L, Matsui T, Gimbrone MA, Rosenzweig A. 2002. Endothelial IKK beta signaling is required for monocyte adhesion under laminar flow conditions. J Mol Cell Cardiol. 34:349–359.

De Mello VDF, Schwab U, Kolehmainen M, Koenig W, Siloaho M, Poutanen K, Mykkanen H. 2011. A diet high in whole grain, fatty fish, and bilberry improves markers of endothelial function and inflammation in individuals with impaired glucose metabolism. Diabetologia. 54:2755–2767.

Mendis S, Puska P, Norrving B. 2011. Global atlas on cardiovascular disease prevention and control. Geneva.

Mestdagh P, Hartmann N, Baeriswyl L, Andreasen D, Bernard N, Chen C, Cheo D, D'Andrade P, DeMayo M, Dennis L, et al. 2014. Evaluation of quantitative miRNA expression platforms in the microRNA quality control (miRQC) study. Nat Methods. 11:809–815.

Milbury PE, Vita JA, Blumberg JB. 2010. Anthocyanins are bioavailable in humans following an acute dose of cranberry juice. J Nutr. 140:1099–1104.

Milenkovic D, Deval C, Gouranton E, Landrier JF, Scalbert A, Morand C, Mazur A. 2012. Modulation of miRNA expression by dietary polyphenols in apoE deficient mice: A new mechanism of the action of polyphenols. PLoS One. 7:e29837.

Milenkovic D, Jude B, Morand C. 2013. miRNA as molecular target of polyphenols underlying their biological effects. Free Radic Biol Med. 64:40–51.

Mink PJ, Scrafford CG, Barraj LM, Harnack L, Hong CP, Nettleton JA, Jacobs DR. 2007. Flavonoid intake and cardiovascular disease mortality: A prospective study in postmenopausal women. Am J Clin Nutr. 85:895–909.

Miska EA. 2005. How microRNAs control cell division, differentiation and death. Curr Opin Genet Dev. 15:563–568.

Miyazaki K, Makino K, Iwadate E, Deguchi Y, Ishikawa F. 2008. Anthocyanins from purple sweet potato Ipomoea batatas cultivar Ayamurasaki suppress the development of atherosclerotic lesions and both enhancements of oxidative stress and soluble vascular cell adhesion molecule-1 in apolipoprotein E-deficient mice. J Agric Food Chem. 56:11485–92.

Morand C, Dubray C, Milenkovic D, Lioger D, Franc J, Scalbert A. 2011. Hesperidin contributes to the vascular protective effects of orange juice : a randomized crossover study in healthy volunteers. Am J Clin Nutr. 93:73–80.

Mueller D, Jung K, Winter M, Rogoll D, Melcher R, Richling E. 2017. Human

intervention study to investigate the intestinal accessibility and bioavailability of anthocyanins from bilberries. Food Chem. 231:275–286.

Mullen W, Edwards CA, Serafini M, Crozier A. 2008. Bioavailability of pelargonidin-3-O-glucoside and its metabolites in humans following the ingestion of strawberries with and without cream. J Agric Food Chem. 56:713–719.

Muller W. 2011. Mechanisms of Leukocyte Transendothelial Migration. Annu Rev Pathol Mech Dis. 6:323–344.

Muller W. 2013. Getting Leukocytes to the Site of Inflammation. Vet Pathol. 50:7–22.

Mullie P, Clarys P, Deriemaeker P, Hebbelinck M. 2007. Estimation of daily human intake of food flavonoids. Plant Foods Hum Nutr. 62:93–98.

Murata M, Nonaka H, Komatsu S, Goto M, Morozumi M, Yamada S, Lin IC, Yamashita S, Tachibana H. 2017. Delphinidin prevents muscle atrophy and upregulates MIR-23a expression. J Agric Food Chem. 65:45–50.

Muthusamy G, Balupillai A, Ramasamy K, Shanmugam M, Gunaseelan S, Mary B, Prasad NR. 2016. Ferulic acid reverses ABCB1-mediated paclitaxel resistance in MDR cell lines. Eur J Pharmacol. 786:194–203.

Nanashima N, Horie K, Tomisawa T, Chiba M, Nakano M, Fujita T, Maeda H, Kitajima M, Takamagi S, Uchiyama D, et al. 2015. Phytoestrogenic activity of blackcurrant (Ribes nigrum) anthocyanins is mediated through estrogen receptor alpha. Mol Nutr Food Res. 59:2419–2431.

Naruszewicz M, Laniewska I, Millo B, Duzniewski M. 2007. Combination therapy of statin with flavonoids rich extract from chokeberry fruits enhanced reduction in cardiovascular risk markers in patients after myocardial infraction (MI). Atherosclerosis. 194:e179–e184.

Németh K, Plumb GW, Berrin JG, Juge N, Jacob R, Naim HY, Williamson G, Swallow DM, Kroon PA. 2003. Deglycosylation by small intestinal epithelial cell β-glucosidases is a critical step in the absorption and metabolism of dietary flavonoid glycosides in humans. Eur J Nutr. 42:29–42.

Noma K, Kihara Y, Higashi Y. 2012. Striking crosstalk of ROCK signaling with endothelial function. J Cardiol. 60:1–6.

Nomura S, Kanazawa S, Fukuhara S. 2002. Effects of efonidipine on platelet and monocyte activation markers in hypertensive patients with and without type 2 diabetes mellitus. J Hum Hypertens. 16:539–547.

Nurden AT. 2011. Platelets, inflammation and tissue regeneration. Thromb Haemost. 105:S13–S33.

Olas B. 2016. The multifunctionality of berries toward blood platelets and the role of berry phenolics in cardiovascular disorders. Platelets.:1–10.

Olivas-Aguirre FJ, Rodrigo-García J, Martínez-Ruiz NDR, Cárdenas-Robles AI, Mendoza-Díaz SO, Álvarez-Parrilla E, González-Aguilar GA, De La Rosa LA, Ramos-Jiménez A, Wall-Medrano A. 2016. Cyanidin-3-O-glucoside: Physical-chemistry, foodomics and health effects. Molecules. 21:e1264.

Oliveira H, Fernandes I, Brás NF, Faria A, De Freitas V, Calhau C, Mateus N. 2015.

Experimental and Theoretical Data on the Mechanism by Which Red Wine Anthocyanins Are Transported through a Human MKN-28 Gastric Cell Model. J Agric Food Chem. 63:7685–7692.

Olson CM, Hedrick MN, Izadi H, Bates TC, Olivera ER, Anguita J. 2007. p38 mitogen-activated protein kinase controls NF-κB transcriptional activation and tumor necrosis factor alpha production through RelA phosphorylation mediated by mitogen- and stress-activated protein kinase 1 in response to Borrelia burgdorferi antigens. Infect Immun. 75:270–277.

Onat D, Brillon D, Colombo PC, Schmidt AM. 2011. Human vascular endothelial cells: A model system for studying vascular inflammation in diabetes and atherosclerosis. Curr Diab Rep. 11:193–202.

Osterud B, Bjorklid E. 2003. Role of Monocytes in Atherogenesis. Physiol Rev. 83:1069–1112.

Paixão J, Dinis TCP, Almeida LM. 2012. Malvidin-3-glucoside protects endothelial cells up-regulating endothelial NO synthase and inhibiting peroxynitrite-induced NF-kB activation. Chem Biol Interact. 199:192–200.

Pan M-H, Lai C-S, Ho C-T. 2010. Anti-inflammatory activity of natural dietary flavonoids. Food Funct. 1:15.

Pandey KB, Rizvi SI. 2009. Plant Polyphenols as Dietary Antioxidants in Human Health and Disease. Oxid Med Cell Longev. 2:270–278.

de Pascual-Teresa S, Johnston KL, Dupont MS, O'Leary KA, Needs PW, Morgan LM, Clifford MN, Bao YP, Williamson G. 2004. Quercetin metabolites downregulate cyclooxygenase-2 transcription in human lymphocytes ex vivo but not in vivo. J Nutr. 134:552–557.

de Pascual-Teresa S, Sanchez-Ballesta MT. 2008. Anthocyanins: from plant to health. Phytochem Rev. 7:281–299.

Passamonti S, Vanzo A, Vrhovsek U, Terdoslavich M, Cocolo A, Decorti G, Mattivi F. 2005. Hepatic uptake of grape anthocyanins and the role of bilitranslocase. Food Res Int. 38:953–960.

Passamonti S, Vrhovsek U, Mattivi F. 2002. The interaction of anthocyanins with bilitranslocase. Biochem Biophys Res Commun. 296:631–636.

Pearson-Leary J, Eacret D, Chen R, Takano H, Nicholas B, Bhatnagar S. 2017. Inflammation and vascular remodeling in the ventral hippocampus contributes to vulnerability to stress. Transl Psychiatry. 7:e1160.

Pérez-Jiménez J, Fezeu L, Touvier M, Arnault N, Manach C, Hercberg S, Galan P, Scalbert A. 2011. Dietary intake of 337 polyphenols in French adults. Am J Clin Nutr. 93:1220–1228.

Perk J, De Backer G, Gohlke H, Graham I, Reiner Z, Verschuren M, Albus C, Benlian P, Boysen G, Cifkova R, et al. 2012. European Guidelines on cardiovascular disease prevention in clinical practice (version 2012). Eur Heart J. 33:1635–1701.

Pfeiffer D, Roûmanith E, Lang I, Falkenhagen D. 2017. MIR-146a, MIR-146b, and MIR-155 increase expression of IL-6 and IL-8 and support HSP10 in an in vitro sepsis

model. PLoS One. 12:e0179850.

Pfenniger A, Meens MJ, Pedrigi RM, Foglia B, Sutter E, Pelli G, Rochemont V, Petrova T V., Krams R, Kwak BR. 2015. Shear stress-induced atherosclerotic plaque composition in ApoE-/-mice is modulated by connexin37. Atherosclerosis. 243:1–10.

Porrini M, Riso P. 2008. Factors influencing the bioavailability of antioxidants in foods: A critical appraisal. Nutr Metab Cardiovasc Dis. 18:647–650.

Qin L, Chen X, Wu Y, Feng Z, He T, Wang L, Liao L, Xu J. 2011. Steroid receptor coactivator-1 upregulates integrin α5 expression to promote breast cancer cell adhesion and migration. Cancer Res. 71:1742–1751.

Qin Y, Xia M, Ma J, Hao Y, Liu J. 2009. Anthocyanin supplementation improves serum LDL-and HDL-cholesterol concentrations associated with the inhibition of cholesteryl ester transfer protein in dyslipidemic subjects. Am J Clin Nutr. 90:485–492.

Rahman A, Anwar KN, Minhajuddin M, Bijli KM, Javaid K, True AL, Malik AB. 2004. cAMP targeting of p38 MAP kinase inhibits thrombin-induced NF-kappaB activation and ICAM-1 expression in endothelial cells. Am J Physiol Lung Cell Mol Physiol. 287:L1017-24.

Rao J, Ye Z, Tang H, Wang C, Peng H, Lai W, Li Y, Huang W, Lou T. 2017. The RhoA/ROCK Pathway Ameliorates Adhesion and Inflammatory Infiltration Induced by AGEs in Glomerular Endothelial Cells. Sci Rep. 7:39727.

Rechner AR, Kroner C. 2005. Anthocyanins and colonic metabolites of dietary polyphenols inhibit platelet function. Thromb Res. 116:327—334.

Rechner AR, Kuhnle G, Hu H, Roedig-Penman A, van den Braak MH, Moore KP, Rice-Evans CA. 2002. The metabolism of dietary polyphenols and the relevance to circulating levels of conjugated metabolites. Free Radic Res. 36:1229–41.

Del Rio D, Rodriguez-Mateos A, Spencer JPE, Tognolini M, Borges G, Crozier A. 2013. Dietary (Poly)phenolics in Human Health: Structures, Bioavailability, and Evidence of Protective Effects Against Chronic Diseases. Antioxid Redox Signal. 18:1818–1892.

Rodriguez-Mateos A, Heiss C, Borges G, Crozier A. 2014. Berry (poly)phenols and cardiovascular health. J Agric Food Chem. 62:3842–3851.

Rodriguez-Mateos A, Ishisaka A, Mawatari K, Vidal-Diez A, Spencer JPE, Terao J. 2013. Blueberry intervention improves vascular reactivity and lowers blood pressure in high-fat-, high-cholesterol-fed rats. Br J Nutr. 109:1746–1754.

Rodriguez-Mateos A, Rendeiro C, Bergillos-Meca T, Tabatabaee S, George TW, Heiss C, Spencer JPE. 2013. Intake and time dependence of blueberry flavonoid-induced improvements in vascular function: A randomized, controlled, double-blind, crossover intervention study with mechanistic insights into biological activity. Am J Clin Nutr. 98:1179–1191.

Ruan W, Xu JM, Li SB, Yuan LQ, Dai RP. 2012. Effects of down-regulation of microRNA-23a on TNF-α-induced endothelial cell apoptosis through caspase-dependent pathways. Cardiovasc Res. 93:623–632.

Saito H, Minamiya Y, Kitamura M, Saito S, Enomoto K, Terada K, Ogawa J. 1998. Endothelial myosin light chain kinase regulates neutrophil migration across human umbilical vein endothelial cell monolayer. J Immunol. 161:1533–1540.

Sakakibara H, Ichikawa Y, Tajima S, Makino Y, Wakasugi Y, Shimoi K, Kobayashi S, Kumazawa S, Goda T. 2014. Practical application of flavonoid-poor menu meals to the study of the bioavailability of bilberry anthocyanins in human subjects. Biosci Biotechnol Biochem. 78:1748–1752.

Sala-Vila A, Estruch R, Ros E. 2015. New Insights into the Role of Nutrition in CVD Prevention. Curr Cardiol Rep. 17:26.

Salminen S, Bouley C, Boutron-Ruault MC, Cummings JH, Franck A, Gibson GR, Isolauri E, Moreau MC, Roberfroid M, Rowland I. 1998. Functional food science and gastrointestinal physiology and function. Br J Nutr. 80:S147–S171.

Sandhu AK, Huang Y, Xiao D, Park E, Edirisinghe I, Burton-Freeman B. 2016. Pharmacokinetic Characterization and Bioavailability of Strawberry Anthocyanins Relative to Meal Intake. J Agric Food Chem. 64:4891–4899.

Santhakumar AB, Kundur AR, Fanning K, Netzel M, Stanley R, Singh I. 2015. Consumption of anthocyanin-rich Queen Garnet plum juice reduces platelet activation related thrombogenesis in healthy volunteers. J Funct Foods. 12:11–22.

Santhakumar AB, Kundur AR, Sabapathy S, Stanley R, Singh I. 2015. The potential of anthocyanin-rich Queen Garnet plum juice supplementation in alleviating thrombotic risk under induced oxidative stress conditions. J Funct Foods. 14:747–757.

Santhakumar AB, Stanley R, Singh I. 2015. The ex vivo antiplatelet activation potential of fruit phenolic metabolite hippuric acid. Food Funct. 6:2679–2683.

Sarelius IH, Glading AJ. 2015. Control of vascular permeability by adhesion molecules. Tissue Barriers. 3.

Sawant DA, Tharakan B, Adekanbi A, Hunter FA, Smythe WR, Childs EW. 2011. Inhibition of VE-Cadherin Proteasomal Degradation Attenuates Microvascular Hyperpermeability. Microcirculation. 18:46–55.

Scalbert A, Williamson G. 2000. Chocolate: Modern Science Investigates an Ancient Medicine. J Med Food. 3:121–125.

Scaldaferri F, Correale C, Gasbarrini A, Danese S. 2009. Molecular signaling blockade as a new approach to inhibit leukocyte-endothelial interactions for inflammatory bowel disease treatment. Cell Adhes Migr. 3:296–299.

Scalia R, Gong Y, Berzins B, Freund B, Feather D, Landesberg G, Mishra G. 2011. A novel role for calpain in the endothelial dysfunction induced by activation of angiotensin II type 1 receptor signaling. Circ Res. 108:1102–1111.

Schmittgen TD, Livak KJ. 2008. Analyzing real-time PCR data by the comparative CT method. Nat Protoc. 3:1101–1108.

Schnoor M. 2015. Endothelial Actin-Binding Proteins and Actin Dynamics in Leukocyte Transendothelial Migration. J Immunol. 194:3535–3541.

Schulze-Osthoff K, Ferrari D, Riehemann K, Wesselborg S. 1997. Regulation of NF-κB Activation by MAP Kinase Cascades. Immunobiology. 198:35–49.

Schutt RC, Burdick MD, Strieter RM, Mehrad B, Keeley EC. 2012. Plasma CXCL12 levels as a predictor of future stroke. Stroke. 43:3382–3386.

Schwingshackl L, Hoffmann G. 2014. Mediterranean dietary pattern, inflammation and endothelial function: A systematic review and meta-analysis of intervention trials. Nutr Metab Cardiovasc Dis. 24:929–939.

Seymour EM, Lewis SK, Urcuyo-Llanes DE, Tanone II, Kirakosyan A, Kaufman PB, Bolling SF. 2009. Regular tart cherry intake alters abdominal adiposity, adipose gene transcription, and inflammation in obesity-prone rats fed a high fat diet. J Med Food. 12:935–942.

Sikora J, Broncel M, Markowicz M, Chałubiński M, Wojdan K, Mikiciuk-Olasik E. 2012. Short-term supplementation with Aronia melanocarpa extract improves platelet aggregation, clotting, and fibrinolysis in patients with metabolic syndrome. Eur J Nutr. 51:549–556.

Silambarasan M, Tan J, Karolina D, Armugam A, Kaur C, Jeyaseelan K. 2016. MicroRNAs in Hyperglycemia Induced Endothelial Cell Dysfunction. Int J Mol Sci. 17:518.

Sivasinprasasn S, Pantan R, Thummayot S, Tocharus J. 2016. Cyanidin-3-glucoside attenuates angiotensin II-induced oxidative stress and inflammation in vascular endothelial cells. Chem Biol Interact. 260:67–74.

Sogo T, Terahara N, Hisanaga A, Kumamoto T, Yamashiro T, Wu S, Sakao K, Hou DX. 2015. Anti-inflammatory activity and molecular mechanism of delphinidin 3-sambubioside, a Hibiscus anthocyanin. BioFactors. 41:58–65.

Soltani R, Hakimi M, Asgary S, Ghanadian S., Keshvari M. 2014. Evaluation of the effects of Vaccinium arctostaphylos L. Fruit extract on serum lipids and hs-CRP levels and oxidative stress in adult patients with hyperlipidemia: A randomized, double-blind, placebo-controlled clinical trial. Evidence-based Complement Altern Med. 2014:6.

Song F, Zhu Y, Shi Z, Tian J, Deng X, Ren J, Andrews MC, Ni H, Ling W, Yang Y. 2014. Plant food anthocyanins inhibit platelet granule secretion in hypercholesterolaemia: Involving the signalling pathway of PI3K-Akt. Thromb Haemost. 112:981–991.

Sorrenti V, Mazza F, Campisi A, Di Giacomo C, Acquaviva R, Vanella L, Galvano F. 2007. Heme oxygenase induction by cyanidin-3-O-beta-glucoside in cultured human endothelial cells. Mol Nutr Food Res. 51:580–586.

Speciale A, Anwar S, Canali R, Chirafisi J, Saija A, Virgili F, Cimino F. 2013. Cyanidin-3-O-glucoside counters the response to TNF-alpha of endothelial cells by activating Nrf2 pathway. Mol Nutr Food Res. 57:1979–1987.

Speciale A, Canali R, Chirafisi J, Saija A, Virgili F, Cimino F. 2010. Cyanidin-3-O-glucoside protection against TNF-α-induced endothelial dysfunction: Involvement of nuclear factor-κB signaling. J Agric Food Chem. 58:12048–12054.

Speyer CL, Ward PA. 2011. Role of endothelial chemokines and their receptors during inflammation. J Investig Surg. 24:18–27.

Stalmach A, Edwards CA, Wightman JD, Crozier A. 2012. Gastrointestinal stability and

bioavailability of (poly)phenolic compounds following ingestion of Concord grape juice by humans. Mol Nutr Food Res. 56:497–509.

Stein BN, Gamble JR, Pitson SM, Vadas MA, Khew-Goodall Y. 2003. Activation of Endothelial Extracellular Signal-Regulated Kinase Is Essential for Neutrophil Transmigration: Potential Involvement of a Soluble Neutrophil Factor in Endothelial Activation. J Immunol. 171:6097–6104.

Stroka KM, Aranda-Espinoza H. 2011. Endothelial cell substrate stiffness influences neutrophil transmigration via myosin light chain kinase-dependent cell contraction. Blood. 118:1632–1640.

Su X, Zhang J, Wang H, Xu J, He J, Liu L, Zhang T, Chen R, Kang J. 2017. Phenolic Acid Profiling, Antioxidant, and Anti-Inflammatory Activities, and miRNA Regulation in the Polyphenols of 16 Blueberry Samples from China. Molecules. 22:312.

Subash S, Essa MM, Al-Adawi S, Memon MA, Manivasagam T, Akbar M. 2014. Neuroprotective effects of berry fruits on neurodegenerative diseases. Neural Regen Res. 9:1557–1566.

Suh J-H, Romain C, González-Barrio R, Cristol J-P, Teissèdre P-L, Crozier A, Rouanet J-M. 2011. Raspberry juice consumption, oxidative stress and reduction of atherosclerosis risk factors in hypercholesterolemic golden Syrian hamsters. Food Funct. 2:400–5.

Sumagin R, Lomakina E, Sarelius IH. 2008. Leukocyte-endothelial cell interactions are linked to vascular permeability via ICAM-1-mediated signaling. Am J Physiol Circ Physiol. 295:H969–H977.

Talavéra S, Felgines C, Texier O, Besson C, Gil-Izquierdo A, Lamaison JL, Rémésy C. 2005. Anthocyanin metabolism in rats and their distribution to digestive area, kidney, and brain. J Agric Food Chem. 53:3902–3908.

Talavéra S, Felgines C, Texier O, Besson C, Manach C, Lamaison J-L, Rémésy C. 2004. Anthocyanins are efficiently absorbed from the small intestine in rats. J Nutr. 134:2275–2279.

Thompson K, Hosking H, Pederick W, Singh I, Santhakumar AB. 2017. The effect of anthocyanin supplementation in modulating platelet function in sedentary population: a randomised, double-blind, placebo-controlled, cross-over trial. Br J Nutr. 118:368–374.

Thompson K, Pederick W, Singh I, Santhakumar AB. 2017. Anthocyanin supplementation in alleviating thrombogenesis in overweight and obese population: A randomized, double-blind, placebo-controlled study. J Funct Foods. 32:131–138.

van der Toorn M, Frentzel S, Goedertier D, Peitsch M, Hoeng J, De Leon H. 2015. A prototypic modified risk tobacco product exhibits reduced effects on chemotaxis and transendothelial migration of monocytes compared with a reference cigarette. Food Chem Toxicol. 80:277–286.

Trott O, Olson A. 2010. AutoDock Vina: improving the speed and accuracy of docking with a new scoring function, efficient optimization and multithreading. J Comput Chem. 31:455–461.

Tsao R. 2010. Chemistry and biochemistry of dietary polyphenols. Nutrients. 2:1231–1246.

Tsuda T, Shiga K, Ohshima K, Kawakishi S, Osawa T. 1996. Inhibition of lipid peroxidation and the active oxygen radical scavenging effect of anthocyanin pigments isolated from Phaseolus vulgaris L. Biochem Pharmacol. 52:1033–1039.

Vanzo A, Terdoslavich M, Brandoni A, Torres AM, Vrhovsek U, Passamonti S. 2008. Uptake of grape anthocyanins into the rat kidney and the involvement of bilitranslocase. Mol Nutr Food Res. 52:1106–1116.

Viatour P, Merville MP, Bours V, Chariot A. 2005. Phosphorylation of NF-kB and IkB proteins: Implications in cancer and inflammation. Trends Biochem Sci. 30:43–52.

Vitaglione P, Donnarumma G, Napolitano A, Galvano F, Gallo A, Scalfi L, Fogliano V. 2007. Protocatechuic acid is the major human metabolite of cyanidin-glucosides. J Nutr. 137:2043–2048.

Wallace TC. 2011. Anthocyanins in Cardiovascular Disease. Adv Nutr. 2:1–7.

Walton MC, McGhie TK, Reynolds GW, Hendriks WH. 2006. The flavonol quercetin-3-glucoside inhibits cyanidin-3-glucoside absorption in vitro. J Agric Food Chem. 54:4913–4920.

Wang D, Wei X, Yan X, Jin T, Ling W. 2010. Protocatechuic acid, a metabolite of anthocyanins, inhibits monocyte adhesion and reduces atherosclerosis in apolipoprotein E-deficient mice. J Agric Food Chem. 58:12722–12728.

Wang D, Xia M, Yan X, Li D, Wang L, Xu Y, Jin T, Ling W. 2012. Gut microbiota metabolism of anthocyanin promotes reverse cholesterol transport in mice via repressing miRNA-10b. Circ Res. 111:967–981.

Wang H-W, Lo H-H, Chiu Y-L, Chang S-J, Huang P-H, Liao K-H, Tasi C-F, Wu C-H, Tsai T-N, Cheng C-C, Cheng S-M. 2014. Dysregulated miR-361-5p/VEGF Axis in the Plasma and Endothelial Progenitor Cells of Patients with Coronary Artery Disease. PLoS One. 9:e98070.

Wang H, Ach RA, Curry B. 2006. Direct and sensitive miRNA profiling from low-input total RNA. RNA. 13:151–159.

Wang R, Fang X, Lu Y, Wang S. 2004. The PDBbind database: Collection of binding affinities for protein-ligand complexes with known three-dimensional structures. J Med Chem. 47:2977–2980.

Wang R, Fang X, Lu Y, Yang CY, Wang S. 2005. The PDBbind database: Methodologies and updates. J Med Chem. 48:4111–4119.

Wang X, Ouyang Y, Liu J, Zhu M, Zhao G, Bao W, Hu FB. 2014. Fruit and vegetable consumption and mortality from all causes, cardiovascular disease, and cancer: systematic review and dose-response meta-analysis of prospective cohort studies. BMJ. 349:g4490–g4490.

Wang Y, Wang M-D, Xia Y-P, Gao Y, Zhu Y-Y, Chen S-C, Mao L, He Q-W, Yue Z-Y, Hu B. 2018. MicroRNA-130a regulates cerebral ischemia–induced blood–brain barrier permeability by targeting Homeobox A5. FASEB J. 32:935–944.

Wang Y, Zhang Y, Wang X, Liu Y, Xia M. 2012. Supplementation with cyanidin-3-O-

beta-glucoside protects against hypercholesterolemia-mediated endothelial dysfunction and attenuates atherosclerosis in apolipoprotein E-deficient mice. J Nutr. 142:1033–1037.

Warboys C. 2011. The role of blood flow in determining the sites of atherosclerotic plaques. F1000 Med Rep. 3:1–8.

Warner EF, Smith MJ, Zhang Q, Raheem KS, O'Hagan D, O'Connell MA, Kay CD. 2017. Signatures of anthocyanin metabolites identified in humans inhibit biomarkers of vascular inflammation in human endothelial cells. Mol Nutr Food Res.:1700053.

Watzl B., Briviba K., Rechkemmer G. 2002. Anthocyanne. Ernährungsumschau.:148–150.

Wermuth CG, Granellin CR, Lindberg P, Mitscher LA. 1998. Glossary of terms used in medicinal chemistry. Pure Appl Chem. 70:1129–1143.

WHO. 1999. Definition, diagnosis and classification of diabetes mellitus and its complications : report of a WHO consultation. Part 1, Diagnosis and classification of diabetes mellitus. Geneva : World Health Organization.

Wiczkowski W, Romaszko E, Piskula MK. 2010. Bioavailability of cyanidin glycosides from natural chokeberry (Aronia melanocarpa) juice with dietary-relevant dose of anthocyanins in humans. J Agric Food Chem. 58:12130–12136.

Wiczkowski W, Szawara-Nowak D, Romaszko J. 2016. The impact of red cabbage fermentation on bioavailability of anthocyanins and antioxidant capacity of human plasma. Food Chem. 190:730–740.

Widlansky ME, Gokce N, Keaney JF, Vita JA. 2003. The clinical implications of endothelial dysfunction. J Am Coll Cardiol. 42:1149–1160.

Wilkins E, Wilson L, Wickramasinghe K, Bhatnagar P, Leal J, Luengo-Fernandez R, Burns R, Rayner M, Townsend N. 2017. European Cardiovascular Disease Statistics 2017 edition. Brussels.

Willoughby S, Holmes A, Loscalzo J. 2002. Platelets and cardiovascular disease. Eur J Cardiovasc Nurs. 1:273–288.

De Winther MPJ, Kanters E, Kraal G, Hofker MH. 2005. Nuclear factor κB signaling in atherogenesis. Arterioscler Thromb Vasc Biol. 25:904–914.

Wong CW, Christen T, Roth I, Chadjichristos CE, Derouette JP, Foglia BF, Chanson M, Goodenough DA, Kwak BR. 2006. Connexin 37 protects against atherosclerosis by regulating monocyte adhesion. Nat Med. 12:950–954.

Wu X, Beecher GR, Holden JM, Haytowitz DB, Gebhardt SE, Prior RL. 2006. Concentrations of anthocyanins in common foods in the United States and estimation of normal consumption. J Agric Food Chem. 54:4069–4075.

Wu X, Kang J, Xie C, Burris R, Ferguson ME, Badger TM, Nagarajan S. 2010. Dietary blueberries attenuate atherosclerosis in apolipoprotein E-deficient mice by upregulating antioxidant enzyme expression. J Nutr. 140:1628–32.

Xia M, Ling W, Zhu H, Ma J, Wang Q, Hou M, Tang Z, Guo H, Liu C, Ye Q. 2009. Anthocyanin attenuates CD40-mediated endothelial cell activation and apoptosis by inhibiting CD40-induced MAPK activation. Atherosclerosis. 202:41–47.

Xia M, Ling W, Zhu H, Wang Q, Ma J, Hou M, Tang Z, Li L, Ye Q. 2007. Anthocyanin prevents CD40-activated proinflammatory signaling in endothelial cells by regulating cholesterol distribution. Arterioscler Thromb Vasc Biol. 27:519–524.

Xia XD, Ling WH, Ma J, Xia M, Hou MJ, Wang Q, Zhu HL, Tang ZH. 2006. An anthocyanin-rich extract from black rice enhances atherosclerotic plaque stabilization in apolipoprotein e-deficient mice. J Nutr. 136:2220–2225.

Xie C, Kang J, Chen JR, Lazarenko OP, Ferguson ME, Badger TM, Nagarajan S, Wu X. 2011. Lowbush blueberries inhibit scavenger receptors CD36 and SR-A expression and attenuate foam cell formation in ApoE-deficient mice. Food Funct. 2:588–594.

Xie L, Lee SG, Vance TM, Wang Y, Kim B, Lee JY, Chun OK, Bolling BW. 2016. Bioavailability of anthocyanins and colonic polyphenol metabolites following consumption of aronia berry extract. Food Chem. 211:860–868.

Xie X, Zhao R, Shen GX. 2012. Influence of delphinidin-3-glucoside on oxidized low-density lipoprotein-induced oxidative stress and apoptosis in cultured endothelial cells. J Agric Food Chem. 60:1850–1856.

Yang Y, Andrews MC, Hu Y, Wang D, Qin Y, Zhu Y, Ni H, Ling W. 2011. Anthocyanin extract from black rice significantly ameliorates platelet hyperactivity and hypertriglyceridemia in dyslipidemic rats induced by high fat diets. J Agric Food Chem. 59:6759–6764.

Yang Y, Shi Z, Reheman A, Jin JW, Li C, Wang Y, Andrews MC, Chen P, Zhu G, Ling W, Ni H. 2012. Plant food delphinidin-3-glucoside significantly inhibits platelet activation and thrombosis: Novel protective roles against cardiovascular diseases. PLoS One. 7:e37323.

Yao Y, Chen Y, Adili R, McKeown T, Chen P, Zhu G, Li D, Ling W, Ni H, Yang Y. 2017. Plant-based Food Cyanidin-3-Glucoside Modulates Human Platelet Glycoprotein VI Signaling and Inhibits Platelet Activation and Thrombus Formation. J Nutr. 147:1917–1925.

Yee D, Shah KM, Coles MC, Sharp T V., Lagos D. 2017. MicroRNA-155 induction via TNF-α and IFN-γ suppresses expression of programmed death ligand-1 (PD-L1) in human primary cells. J Biol Chem. 292:20683–20693.

Yi L, Chen C ye, Jin X, Mi M tian, Yu B, Chang H, Ling W hua, Zhang T. 2010. Structural requirements of anthocyanins in relation to inhibition of endothelial injury induced by oxidized low-density lipoprotein and correlation with radical scavenging activity. FEBS Lett. 584:583–590.

Yi L, Chen CY, Jin X, Zhang T, Zhou Y, Zhang QY, Zhu JD, Mi MT. 2012. Differential suppression of intracellular reactive oxygen species-mediated signaling pathway in vascular endothelial cells by several subclasses of flavonoids. Biochimie. 94:2035–2044.

Yu G, Rux AH, Ma P, Bdeir K, Sachais BS. 2005. Endothelial expression of E-selectin is induced by the platelet-specific chemokine platelet factor 4 through LRP in an NF-kB-dependent manner. Blood. 105:3545–3551.

Yusuf PS, Hawken S, Ôunpuu S, Dans T, Avezum A, Lanas F, McQueen M, Budaj A, Pais P, Varigos J, Lisheng L. 2004. Effect of potentially modifiable risk factors

associated with myocardial infarction in 52 countries (the INTERHEART study): Case-control study. Lancet. 364:937–952.

Zamora-Ros R, Knaze V, Rothwell JA, Hemon B, Moskal A, Overvad K, Tjønneland A, Kyrø C, Fagherazzi G, Boutron-Ruault MC, et al. 2016. Dietary polyphenol intake in europe: The european prospective investigation into cancer and nutrition (EPIC) study. Eur J Nutr. 55:1359–1375.

Zengin G, Ceylan R, Katanić J, Mollica A, Aktumsek A, Boroja T, Matić S, Mihailović V, Stanić S, Aumeeruddy-Elalfi Z, et al. 2017. Combining in vitro, in vivo and in silico approaches to evaluate nutraceutical potentials and chemical fingerprints of Moltkia aurea and Moltkia coerulea. Food Chem Toxicol. 107:540–553.

Zhang H, Park Y, Wu J, Chen X, Lee S, Yang J, Dellsperger KC, Zhang C. 2009. Role of TNF-alpha in vascular dysfunction. Clin Sci. 116:219–230.

Zhang X-Y, Shu L, Si C-J, Yu X-L, Liao D, Gao W, Zhang L, Zheng P-F. 2015. Dietary Patterns, Alcohol Consumption and Risk of Coronary Heart Disease in Adults: A Meta-Analysis. Nutrients. 7:6582–6605.

Zhang X, Zhu Y, Song F, Yao Y, Ya F, Li D, Ling W, Yang Y. 2016. Effects of purified anthocyanin supplementation on platelet chemokines in hypocholesterolemic individuals: a randomized controlled trial. Nutr Metab (Lond). 13:86.

Zhang Y, Wang X, Wang Y, Liu Y, Xia M. 2013. Supplementation of cyanidin-3-O-beta-glucoside promotes endothelial repair and prevents enhanced atherogenesis in diabetic apolipoprotein E-deficient mice. J Nutr. 143:1248–1253.

Zhao CL, Chen ZJ, Bai XS, Ding C, Long TJ, Wei FG, Miao KR. 2014. Structure-activity relationships of anthocyanidin glycosylation. Mol Divers. 18:687–700.

Zheng J, Zhou Y, Li S, Zhang P, Zhou T, Xu DP, Li H Bin. 2017. Effects and mechanisms of fruit and vegetable juices on cardiovascular diseases. Int J Mol Sci. 18:555.

Zhu Y, Ling W, Guo H, Song F, Ye Q, Zou T, Li D, Zhang Y, Li G, Xiao Y, et al. 2013. Anti-inflammatory effect of purified dietary anthocyanin in adults with hypercholesterolemia: A randomized controlled trial. Nutr Metab Cardiovasc Dis. 23:843–849.

Zhu Y, Xia M, Yang Y, Liu F, Li Z, Hao Y, Mi M, Jin T, Ling W. 2011. Purified anthocyanin supplementation improves endothelial function via NO-cGMP activation in hypercholesterolemic individuals. Clin Chem. 57:1524–1533.

8. SUPPLEMENTARY FILES

Supplementary Table 1. *List of genes examined by TaqMan-low density arrays and their function in the cell*

Gene symbol	Gene name	Biological process
ADAM10	ADAM metallopeptidase domain 10	proteolysis
SOD1	superoxide dismutase 1, soluble	response to odative stress
VWF	von Willebrand factor	cell adhesion
F11R	F11 receptor	cell adhesion
CXCL12	chemokine (C-X-C motif) ligand 12	cell chemotaxis
RHO	rhodopsin	actin cytoskeleton organization
CXCR5	chemokine (C-X-C motif) receptor 5	cell chemotaxis
CCR2	chemokine (C-C motif) receptor 2	cell chemotaxis
CCR1	chemokine (C-C motif) receptor 1	cell chemotaxis
CDH5	cadherin 5, type 2 (vascular endothelium)	cell adhesion
IKBKG	inhibitor of kappa light polypeptide gene enhancer in B-cells, kinase gamma	inflammatory response
PDPK1	3-phosphoinositide dependent protein kinase-1	regulation of protein phosphorylation
CDC42BPA	CDC42 binding protein kinase alpha (DMPK-like)	cytoskeletal reorganization
CASK	calcium/calmodulin-dependent serine protein kinase (MAGUK family)	cell adhesion
PAK4	p21 protein (Cdc42/Rac)-activated kinase 4	protein amino acid phosphorylation
MYLK	myosin light chain kinase	actin-myosin interactions
MYD88	myeloid differentiation primary response gene (88)	signal transduction
PDGFRB	platelet-derived growth factor receptor, beta polypeptide	cell chemotaxis
RASGRF1	Ras protein-specific guanine nucleotide-releasing factor 1	signal transduction
PDGFRA	platelet-derived growth factor receptor, alpha polypeptide	cell cell signaling
CAV1	caveolin 1, caveolae protein, 22kDa	cholesterol homeostasis
ADAM12	ADAM metallopeptidase domain 12	cell adhesion
ARPC1B	actin related protein 2/3 complex, subunit 1B, 41kDa	regulation of actin filament polymerization

Supplementary Table 1 *(Continued)*

Gene symbol	Gene name	Biological process
VAV3	vav 3 guanine nucleotide exchange factor	angiogenesis
TLN1	talin 1	cell-cell junction assembly
CDC42EP2	CDC42 effector protein (Rho GTPase binding) 2	cytoskeletal reorganization
JAM2	junctional adhesion molecule 2	cell adhesion
JAM3	junctional adhesion molecule 3	cell adhesion
NFKB1	nuclear factor of kappa light polypeptide gene enhancer in B-cells 1	inflammatory response
IKBKB	inhibitor of kappa light polypeptide gene enhancer in B-cells, kinase beta	inflammatory response
ITGA5	integrin, alpha 5 (fibronectin receptor, alpha polypeptide)	cell adhesion
PLCG1	phospholipase C, gamma 1	lipid metabolic process
RAF1	v-raf-1 murine leukemia viral oncogene homolog 1	regulation of protein phosphorylation
CCL2	chemokine (C-C motif) ligand 2	cell chemotaxis
ITGB1	integrin, beta 1 (fibronectin receptor, beta polypeptide, antigen CD29 includes MDF2, MSK12)	cell adhesion
CALM1	calmodulin 1 (phosphorylase kinase, delta)	cell adhesion
ACTN1	actin, alpha 1	actin cytoskeleton organization
VCL	vinculin	cell adhesion
AGTR1	angiotensin II receptor, type 1	regulation of vasoconstriction
MYLK2	myosin light chain kinase 2	actin-myosin interactions
CALD1	caldesmon 1	cell adhesion
TJP1	tight junction protein 1 (zona occludens 1)	cell-cell junction assembly
FABP3	fatty acid binding protein 3, muscle and heart (mammary-derived growth inhibitor)	lipid metabolic process
ARPC5	actin related protein 2/3 complex, subunit 5, 16kDa	regulation of actin filament polymerization
RRAS2	related RAS viral (r-ras) oncogene homolog 2	signal transduction
TJP3	tight junction protein 3 (zona occludens 3)	cell-cell junction assembly
S100A8	S100 calcium binding protein A8	inflammatory response

Supplementary Table 1 *(Continued)*

Gene symbol	Gene name	Biological process
RACGAP1	Rac GTPase activating protein 1	mitotic cytokinesis
CDC42EP3	CDC42 effector protein (Rho GTPase binding) 3	cytoskeletal reorganization
MYL9	myosin, light chain 9, regulatory	actin-myosin interactions
ARHGEF7	Rho guanine nucleotide exchange factor (GEF) 7	signal transduction
CAPN1	calpain 1, (mu/I) large subunit	cytoskeletal reorganization
FABP4	fatty acid binding protein 4, adipocyte	lipid metabolic process
S100A9	S100 calcium binding protein A9	inflammatory response
GJA4	gap junction protein, alpha 4, 37kDa	cell-cell junction assembly
RHOC	ras homolog gene family, member C	actin cytoskeleton organization
MSN	moesin	actin cytoskeleton organization
CDC42	cell division cycle 42 (GTP binding protein, 25kDa)	actin cytoskeleton organization
ARPC4	actin related protein 2/3 complex, subunit 4, 20kDa	regulation of actin filament polymerization
TJP2	tight junction protein 2 (zona occludens 2)	cell-cell junction assembly
CLDN11	claudin 11	cell adhesion
AKT1	v-akt murine thymoma viral oncogene homolog 1	protein amino acid phosphorylation
EZR	ezrin	actin filament bundle assembly
PAK1	p21 protein (Cdc42/Rac)-activated kinase 1	protein amino acid phosphorylation
SELE	selectin E	cell adhesion
MMP9	matrix metallopeptidase 9 (gelatinase B, 92kDa gelatinase, 92kDa type IV collagenase)	proteolysis of the extracellular matrix
VIM	vimentin	movement of cell or subcellular component
GJA5	gap junction protein, alpha 5, 40kDa	cell-cell junction assembly
RDX	radixin	actin filament capping
VCAM1	vascular cell adhesion molecule 1	cell adhesion
RND3	Rho family GTPase 3	actin cytoskeleton organization

Supplementary Table 1 *(Continued)*

Gene symbol	Gene name	Biological process
CDH1	cadherin 1, type 1, E-cadherin (epithelial)	cell adhesion
RAC1	ras-related C3 botulinum toxin substrate 1 (rho family, small GTP binding protein Rac1)	cell adhesion
ARPC2	actin related protein 2/3 complex, subunit 2, 34kDa	regulation of actin filament polymerization
RAC2	ras-related C3 botulinum toxin substrate 2 (rho family, small GTP binding protein Rac2)	actin filament organization
OCLN	occludin	cell adhesion
RHOA	ras homolog gene family, member A	actin cytoskeleton organization
PTK2	PTK2 protein tyrosine kinase 2	angiogenesis
PECAM1	platelet/endothelial cell adhesion molecule	cell adhesion
NOS2	nitric oxide synthase 2, inducible	nitrite oxyde biosynthetic process
CLDN1	claudin 1	cell adhesion
JUN	jun proto-oncogene	angiogenesis
PXN	paxillin	cell adhesion
ROCK1	Rho-associated, coiled-coil containing protein kinase 1	actin cytoskeleton organization
18S	Eukaryotic 18S rRNA	
MMP2	matrix metallopeptidase 2 (gelatinase A, 72kDa gelatinase, 72kDa type IV collagenase)	proteolysis of the extracellular matrix
CLDN5	claudin 5	cell adhesion
NOS3	nitric oxide synthase 3 (endothelial cell)	nitrite oxyde biosynthetic process
AGT	angiotensinogen (serpin peptidase inhibitor, clade A, member 8)	regulation of vasoconstriction
IGF1R	insulin-like growth factor 1 receptor	signal transduction
IL7	interleukin 7	inflammatory response
CCL5	chemokine (C-C motif) ligand 5	cell chemotaxis
ICAM1	intercellular adhesion molecule 1	cell adhesion
GAPDH	glyceraldehyde-3-phosphate dehydrogenase	glycolysis

***Supplementary Table 2**. List of cell signalling proteins used in molecular docking analyses*

Protein ID	***Alias***	***UniProt ID***	***3D structure***	***Gene***	***Full name***	***Classification***
Akt	AKT3	Q9Y243	HM based on 4ENJ	*AKT3*	RAC-gamma serine/threonine-protein kinase	Protein kinase superfamily. AGC Ser/Thr protein kinase family. RAC subfamily
ASK1	M3K5	Q99683	HM based on 4BIB	*MAP3K5*	Mitogen-activated protein kinase kinase kinase 5	Protein kinase superfamily. STE Ser/Thr protein kinase family. MAP kinase kinase kinase subfamily
ASK2	M3K6	O95382	HM based on 2CLQ	*MAP3K6*	Mitogen-activated protein kinase kinase kinase 6	Protein kinase superfamily. STE Ser/Thr protein kinase family. MAP kinase kinase kinase subfamily
b-Raf	BRAF	P15056	HM based on 4RZV	*BRAF*	B-Raf proto-oncogene, serine/threonine-protein kinase	Protein kinase superfamily. TKL Ser/Thr protein kinase family. RAF subfamily
c-JUN	JUN	P05412	HM based on 1T2K	*JUN*	Transcription factor AP-1	bZIP family. Jun subfamily
c-Raf	RAF1	P04049	HM based 3OMV	*RAF1*	Raf-1 proto-oncogene, serine/threonine-protein kinase	Protein kinase superfamily. TKL Ser/Thr protein kinase family. RAF subfamily
Cdc42	CDC42	P60953	HM based on 5C2J	*CDC42*	Cell division control protein 42 homolog	Small GTPase superfamily. Rho family. CDC42 subfamily
CREB1	CREB1	P16220	HM based on 1DH3	*CREB1*	Cyclic AMP-responsive element-binding protein 1	bZIP family
CREBBP	CBP	Q92793	HM based on 5LKZ	*CREBBP*	CREB binding protein	Transcription coregulator. Coactivator (Bromodomain, Repeat, Zinc-finger)
EP300	EP300	Q09472	HM based on 5LKZ	*EP300*	Histone acetyltransferase p300	Transcription coregulator. Coactivator (Bromodomain, Repeat, Zinc-finger)
ERK1	MK03	P27361	4QTB	*MAPK3*	Mitogen-activated protein kinase 3	Protein kinase superfamily. CMGC Ser/Thr protein kinase family. MAP kinase subfamily
ERK2	MK01	P28482	4QTA	*MAPK1*	Mitogen-activated protein kinase 1	Protein kinase superfamily. CMGC Ser/Thr protein kinase family. MAP kinase subfamily
FAK	FAK1	Q05397	HM based on 2J0K	*PTK2*	Focal Adhesion Kinase 1	Protein kinase superfamily. Tyr protein kinase family. FAK subfamily
IKKɣ	NEMO	Q9Y6K9	HM based on 4UXV	*IKBKG*	Inhibitor of nuclear factor kappa-B kinase subunit gamma/NEMO	Protein (family membership not predicted)
IKKα	IKKA	O15111	HM based on 5EBZ	*CHUK*	Inhibitor of nuclear factor kappa-B kinase subunit alpha	Protein kinase superfamily. Ser/Thr protein kinase family. I-kappa-B kinase subfamily

Supplementary Table 2 *(Continued)*

Protein ID	***Alias***	***UniProt ID***	***3D structure***	***Gene***	***Full name***	***Classification***
IKKβ	IKKB	O14920	HM based on 4E3C	IKBKB	Inhibitor of nuclear factor kappa-B kinase subunit alpha	Protein kinase superfamily. Ser/Thr protein kinase family. I-kappa-B kinase subfamily
IKBα	IKBA	P25963	HM based on 1NFI	NFKBIA	NF-kappa-B inhibitor alpha	NF-kappa-B inhibitor family
Jak2	JAK2	O60674	HM based on 4OLI	JAK2	Janus kinase 2	Protein kinase superfamily. Tyr protein kinase family. JAK subfamily
Jak3	JAK3	P52333	HM based on 4OLI	JAK3	Janus kinase 3	Protein kinase superfamily. Tyr protein kinase family. JAK subfamily
JNK1	MK08	P45983	HM based on 4QTD	MAPK8	Mitogen-activated protein kinase 8	Protein kinase superfamily. CMGC Ser/Thr protein kinase family. MAP kinase subfamily
JNK2	MK09	P45984	HM based on 1JNK	MAPK9	Mitogen-activated protein kinase 9	Protein kinase superfamily. CMGC Ser/Thr protein kinase family. MAP kinase subfamily
JNK3	MK10	P53779	HM based on 1JNK	MAPK10	Mitogen-activated protein kinase 10	Protein kinase superfamily. CMGC Ser/Thr protein kinase family. MAP kinase subfamily
MEK1	MP2K1	Q02750	HM based on 5KKR	MAP2K1	Dual Specificity Mitogen-Activated Protein Kinase Kinase 1	Protein kinase superfamily. STE Ser/Thr protein kinase family. MAP kinase kinase subfamily
MEK2	MP2K2	P36507	HM based on 1S9I	MAP2K2	Dual Specificity Mitogen-Activated Protein Kinase Kinase 2	Protein kinase superfamily. STE Ser/Thr protein kinase family. MAP kinase kinase subfamily
MEK4	MP2K4	P45985	HM based on 3ALO	MAP2K4	Dual specificity mitogen-activated protein kinase kinase 4	Protein kinase superfamily. STE Ser/Thr protein kinase family. MAP kinase kinase subfamily
MEK7	MP2K7	O14733	HM based on 5B2L	MAP2K7	Dual specificity mitogen-activated protein kinase kinase 7	Protein kinase superfamily. STE Ser/Thr protein kinase family. MAP kinase kinase subfamily
MEKK1	M3K1	Q13233	HM based on 4YSM	MAP3K1	Mitogen-activated protein kinase kinase kinase 1	Protein kinase superfamily. STE Ser/Thr protein kinase family. MAP kinase kinase kinase subfamily
MKK3	MP2K3	P46734	HM based on 3VN9	MAP2K3	Dual specificity mitogen-activated protein kinase kinase 3	Protein kinase superfamily. STE Ser/Thr protein kinase family. MAP kinase kinase subfamily
MKK6	MP2K6	P52564	HM based on 3VN9	MAP2K6	Dual Specificity Mitogen-Activated Protein Kinase Kinase 6	Protein kinase superfamily. STE Ser/Thr protein kinase family. MAP kinase kinase subfamily
MLCK	MYLK4	Q86YV6	HM based on 2X4F	MYLK4	Myosin light chain kinase family member 4	Protein kinase superfamily. CAMK Ser/Thr protein kinase family

Supplementary Table 2 *(Continued)*

Protein ID	***Alias***	***UniProt ID***	***3D structure***	***Gene***	***Full name***	***Classification***
MLK2	M3K10	Q02779	HM based on 4UY9	MAP3K10	Mitogen-activated protein kinase kinase kinase 10	Protein kinase superfamily. STE Ser/Thr protein kinase family. MAP kinase kinase kinase subfamily
MLK3	M3K11	Q16584	HM based on 4UY9	MAP3K11	Mitogen-activated protein kinase kinase kinase 11	Protein kinase superfamily. STE Ser/Thr protein kinase family. MAP kinase kinase kinase subfamily
MNK1	MKNK1	Q9BUB5	HM based on 2AC3	MKNK1	MAP kinase-interacting serine/threonine-protein kinase 1	Protein kinase superfamily. CAMK Ser/Thr protein kinase family
MNK2	MKNK2	Q9HBH9	HM based on 2AC3	MKNK2	MAP kinase-interacting serine/threonine-protein kinase 2	Protein kinase superfamily. CAMK Ser/Thr protein kinase family
MSK1[RP]	KS6A5	O75582	HM based on 1VZO	RPS6KA5	Ribosomal protein S6 kinase alpha-5	Protein kinase superfamily. AGC Ser/Thr protein kinase family. S6 kinase subfamily
MSK2[RP]	KS6A4	O75676	HM based on 4OLI	RPS6KA4	Ribosomal protein S6 kinase alpha-4	Protein kinase superfamily. AGC Ser/Thr protein kinase family. S6 kinase subfamily
mTOR	MTOR	P42345	HM based on 5H64	MTOR	Serine/threonine-protein kinase mTOR	PI3/PI4-kinase family
NIK	M3K14	Q99558	HM based on 5T8Q	MAP3K14	Mitogen-activated protein kinase kinase kinase 14	Protein kinase superfamily. STE Ser/Thr protein kinase family. MAP kinase kinase kinase subfamily
p38ɣ	MAK12	P53778	HM based on 1CM8	MAPK12	Mitogen-activated protein kinase 12	Protein kinase superfamily. CMGC Ser/Thr protein kinase family. MAP kinase subfamily.
p38α	MAK14	Q16539	3FMK	MAPK14	Mitogen-activated protein kinase 14	Protein kinase superfamily. CMGC Ser/Thr protein kinase family. MAP kinase subfamily.
p38β	MAK11	Q15759	HM based on 3GP0	MAPK11	Mitogen-activated protein kinase 11	Protein kinase superfamily. CMGC Ser/Thr protein kinase family. MAP kinase subfamily.
p38δ	MAK13	O15264	HM based on 3COI	MAPK13	Mitogen-activated protein kinase 13	Protein kinase superfamily. CMGC Ser/Thr protein kinase family. MAP kinase subfamily.
p53	P53	P04637	HM based on 4MZR	TP53	Cellular tumor antigen p53	P53 family
p65	TF65	Q04206	HM based on 1NFI	RELA	Transcription factor p65	Transcription factor
PAK	PAK4	O96013	HM based on 4FIE	PAK4	Serine/threonine-protein kinase PAK 4	Protein kinase superfamily. STE Ser/Thr protein kinase family. STE20 subfamily
RhoA	RHOA	P61586	HM based on 5C2K	RHOA	Transforming protein RhoA	Small GTPase superfamily. Rho family

Supplementary Table 2 *(Continued)*

Protein ID	***Alias***	***UniProt ID***	***3D structure***	***Gene***	***Full name***	***Classification***
RIP1	RIPK1	Q13546	HM based on 4ITJ	RIPK1	Receptor-interacting serine/threonine-protein kinase 1	Protein kinase superfamily. TKL Ser/Thr protein kinase family
ROCK1	ROCK1	Q13464	HM based on 3NCZ	ROCK1	Rho-associated protein kinase 1	Protein kinase superfamily. AGC Ser/Thr protein kinase family
ROCK2	ROCK2	O75116	HM based on 4WOT	ROCK2	Rho-associated protein kinase 2	Protein kinase superfamily. AGC Ser/Thr protein kinase family
RSK2[RP]	KS6A3	P51812	HM based on 4NIF	RPS6KA3	Ribosomal protein S6 kinase alpha-3	Protein kinase superfamily. AGC Ser/Thr protein kinase family. S6 kinase subfamily
Smad2	SMAD2	Q15796	HM based on 1KHX	SMAD2	Mothers against decapentaplegic homolog 2	Dwarfin/SMAD family
Smad3	SMAD3	P84022	HM based on 1KHX	SMAD3	Mothers against decapentaplegic homolog 3	Dwarfin/SMAD family
Smad4	SMAD4	Q13485	HM based on 1DD1	SMAD4	Mothers against decapentaplegic homolog 4	Dwarfin/SMAD family
Smuf2	SMUF2	Q9HAU4	HM based on 1ZVD	SMUF2	E3 ubiquitin-protein ligase SMURF2	Ligase
Sp1	SP1	P08047	HM based on 5KE6	SP1	Transcription factor Sp1	Sp1 C2H2-type zinc-finger protein family
Stat3	STAT3	P40763	HM based on 1YVL	STAT3	Signal transducer and activator of transcription 3	Transcription factor
TAB1	TAB1	Q15750	HM based on 2J4O	TAB1	TGF-beta-activated kinase 1 and MAP3K7-binding protein 1	Binding (regulation) protein
TAK1	M3K7	O43318	HM based on 5GJF	MAP3K7	Mitogen-activated protein kinase kinase kinase 7	Protein kinase superfamily. STE Ser/Thr protein kinase family. MAP kinase kinase kinase subfamily
TNFR1	TNR1A	P19438	HM based on 1EXT	TNFRSF1A	Tumor necrosis factor receptor superfamily member 1A	Receptor protein
TRADD	TRADD	Q15628	HM based on 1F2H	TRADD	Tumor necrosis factor receptor type 1-associated DEATH domain protein	Binding protein
TRAF2	TRAF2	Q12933	HM based on 1CA9	TRAF2	TNF receptor-associated factor 2	TNF receptor-associated factor family. A subfamily
TRAF5	TRAF5	O00463	HM based on 1FLL	TRAF5	TNF receptor-associated factor 5	TNF receptor-associated factor family. A subfamily

[HM] - Homologue model, [RP] - Ribosomal protein

Supplementary Table 3. *The most significant transcription factors identified from significantly modulated genes using Metacore*

Anthocyanins			Metabolites		
#	**Transcription factor**	**p-Value**	**#**	**Transcription factor**	**p-Value**
1	SP1	1.220E-36	1	SP1	1.100E-32
2	CREB1	1.830E-32	2	CREB1	1.620E-28
3	HIF1A	1.830E-32	3	GCR	2.170E-24
4	c-Jun	2.490E-28	4	Androgen receptor	2.170E-24
5	p53	3.110E-24	5	p53	2.170E-24
6	RelA (p65 NF-kB subunit)	3.110E-24	6	ESR1 (nuclear)	2.940E-16
7	STAT3	3.540E-20	7	SP3	2.940E-16
8	C/EBPbeta	3.680E-16	8	RelA (p65 NF-kB subunit)	2.940E-16
9	C/EBPalpha	3.680E-16	9	EPAS1	2.940E-16
10	ESR1 (nuclear)	3.680E-16	10	HIF1A	2.940E-16
11	RelB (NF-kB subunit)	3.680E-16	11	STAT3	2.940E-16
12	EPAS1	3.680E-16	12	TWIST1	2.940E-16
13	Androgen receptor	3.680E-16	13	KLF4	2.930E-12
14	Lef-1	3.680E-16	14	C/EBPalpha	2.930E-12
15	TWIST1	3.680E-16	15	SLUG	2.930E-12
16	p63	3.680E-16	16	ETS1	2.930E-12
17	Beta-catenin	3.680E-16	17	c-Jun	2.930E-12
18	NF-kB1 (p105)	3.680E-16	18	SRF	2.930E-12
19	SP3	3.680E-16	19	FKHR	2.930E-12
20	c-Fos	3.680E-16	20	Lef-1	2.930E-12
21	NF-kB1 (p50)	3.680E-16	21	NF-kB1 (p50)	2.930E-12
22	c-Myc	3.450E-12	22	NANOG	2.930E-12
23	GCR	3.450E-12	23	EGR1	2.580E-08
24	FOXO3A	3.450E-12	24	C/EBPbeta	2.580E-08
25	E2F1	3.450E-12	25	STAT6	2.580E-08
26	SLUG	3.450E-12	26	KLF2	2.580E-08
27	ETS1	3.450E-12	27	E2F1	2.580E-08
28	STAT1	3.450E-12	28	FOXM1	2.580E-08
29	MKL1	3.450E-12	29	RelB (NF-kB subunit)	2.580E-08
30	EGR1	3.450E-12	30	c-Myc	2.580E-08

Supplementary Table 4. *Values of binding affinities (BA) for all targets and ligand (in kcal/mol).*

Protein ID	***Cy-3-arab***	***Cy-3-gal***	***Cy-3-glc***	***Del-3-glc***	***Pn-3-glc***	***4-HBAL***	***Ferulic acid***	***Hippuric acid***	***PCA***	***Vanillic acid***
AKT3	-9.0	-8.8	-9.2	-8.8	-8.9	-5.3	-6.7	-6.4	-6.2	-6.0
ASK1	-9.6	-8.9	-9.0	-8.7	-9.2	-5	-6.4	-6.2	-5.6	-5.6
ASK2	-8.6	-8.5	-8.8	-8.9	-8.8	-5	-6.0	-5.8	-5.3	-5.4
b-Raf	-8.0	-7.2	-7.5	-8.1	-7.6	-6.4	-7.5	-7.9	-7.1	-6.8
JUN	-5.2	-5.0	-4.9	-5.1	-4.9	-3.4	-4.3	-4.3	-3.7	-3.7
c-Raf	-8.5	-7.5	-8.9	-7.9	-7.9	-6.5	-6.9	-7.2	-7.1	-6.7
CDC42	-8.1	-7.0	-7.6	-7.7	-7.3	-5.2	-6.5	-6.7	-6.0	-6.0
CREB1	-5.9	-5.2	-5.6	-5.5	-5.2	-3.7	-4.7	-4.6	-3.7	-3.9
CREBBP	-7.6	-8.2	-8.0	-7.9	-8.1	-5.1	-6.7	-6.7	-7.2	-5.8
EP300	-8.5	-8.1	-8.2	-8.0	-8.0	-5.2	-6.7	-6.6	-5.9	-5.8
ERK1	-8.7	-8.7	-8.5	-8.5	-8.6	-5.1	-6.4	-7.1	-6.2	-5.9
ERK2	-7.7	-7.6	-7.7	-7.6	-7.7	-4.8	-6.1	-5.9	-5.8	-5.7
FAK	-9.0	-8.8	-8.5	-9.1	-8.7	-5.2	-6.9	-6.4	-6.1	-6.1
IKKɣ	-7.6	-7.3	-7.1	-7.4	-7.1	-4.8	-6.3	-5.7	-5.6	-5.1
IKKα	-8.2	-8.6	-8.0	-8.2	-8.1	-5.4	-6.7	-6.4	-5.9	-6.0
IKKβ	-8.8	-9.6	-8.9	-9.0	-8.9	-5.1	-6.4	-5.9	-6.2	-5.8
IKBα	-7.9	-6.6	-7.0	-6.8	-6.8	-4.1	-5.4	-5.4	-4.7	-4.7
JAK2	-8.7	-9.1	-9.2	-8.8	-9.1	-5.5	-6.9	-6.8	-5.9	-6.1
JAK3	-8.4	-7.9	-8.7	-8.8	-8.7	-5.7	-7.2	-6.8	-6.1	-6.1
JNK1	-9.8	-8.7	-9.9	-9.8	-9.4	-5.3	-6.5	-6.1	-5.6	-5.8
JNK2	-8.5	-8.6	-8.6	-8.8	-8.5	-5.1	-6.3	-6.1	-5.5	-5.7
JNK3	-8.7	-8.2	-8.9	-8.6	-8.1	-5.2	-6.3	-6.1	-5.9	-5.7
MEK1	-8.9	-8.4	-8.8	-8.5	-8.4	-0.5	-5.9	-6.1	-5.6	-5.6
MEK2	-8.5	-8.7	-8.6	-8.9	-8.1	-5.2	-6.6	-6.6	-6.0	-5.9
MEK4	-9.3	-9.2	-9.3	-8.9	-8.6	-5.2	-6.7	-6.3	-6.0	-5.8
MEK7	-7.8	-7.6	-8.1	-8.1	-7.9	-4.6	-5.6	-5.5	-5.2	-5.3
MEKK1	-7.0	-7.0	-6.7	-6.8	-6.9	-4.9	-5.4	-5.4	-5.1	-5.0
MKK3	-8.9	-8.5	-8.7	-8.4	-7.9	-5.2	-6.5	-6.4	-5.9	-5.8
MKK6	-8.6	-8.8	-8.6	-8.3	-7.7	-5.1	-6.6	-6.4	-5.9	-5.8
MLCK	-8.3	-7.9	-8.1	-8.2	-7.9	-5.6	-7.0	-6.5	-6.4	-6.3
MLK2	-9.3	-8.8	-9.1	-8.8	-8.2	-5	-5.9	-5.8	-5.6	-5.5
MLK3	-9.4	-8.5	-9.1	-8.7	-8.2	-4.9	-5.9	-5.9	-5.6	-5.5
MNK1	-7.9	-8.0	-7.9	-7.6	-7.8	-5.4	-6.4	-6.6	-6.2	-6.4
MNK2	-7.8	-8.3	-8.0	-8.3	-8.3	-4.9	-6.2	-6.2	-5.7	-5.7
$MSK1^{RP}$	-8.8	-8.4	-8.9	-8.9	-8.0	-5.5	-5.9	-6.9	-6.5	-5.8

Supplementary Table 4 *(Continued)*

Protein ID	***Cy-3-arab***	***Cy-3-gal***	***Cy-3-glc***	***Del-3-glc***	***Pn-3-glc***	***4-HBAL***	***Ferulic acid***	***Hippuric acid***	***PCA***	***Vanillic acid***
MSK2[RP]	-8.7	-7.7	-7.7	-8.4	-7.7	-5.4	-6.5	-6.9	-6.0	-6.1
mTOR	-8.4	-8.5	-8.6	-8.5	-8.5	-5.5	-6.7	-6.5	-6.7	-6.5
NIK	-7.9	-7.6	-7.9	-7.3	-7.3	-5.8	-6.3	-6.4	-6.9	-5.9
p38ɣ	-8.9	-8.7	-8.8	-8.6	-8.5	-5.8	-6.7	-6.4	-6.4	-6.0
p38α	-7.8	-7.6	-7.9	-7.2	-7.8	-4.8	-5.9	-5.6	-5.6	-5.3
p38β	-8.2	-9.1	-8.2	-8.1	-8.3	-5.9	-7.4	-7.1	-6.3	-6.4
p38δ	-7.9	-7.7	-8.0	-7.7	-7.6	-4.9	-6.1	-5.9	-5.9	-5.6
p53	-7.3	-7.4	-7.3	-7.4	-7.2	-4.7	-5.8	-6.0	-5.5	-5.4
p65	-7.8	-7.0	-7.3	-7.5	-7.4	-4.9	-5.9	-5.6	-5.8	-5.4
PAK	-8.4	-8.2	-7.9	-8.1	-8.0	-5.1	-6.1	-5.9	-5.8	-5.8
RHOA	-8.3	-8.9	-8.1	-8.1	-8.2	-5.8	-6.7	-6.7	-6.1	-6.1
RIP1	-8.0	-7.7	-8.1	-8.3	-7.8	-5.4	-6.6	-6.8	-6.0	-6.0
ROCK1	-8.3	-8.4	-8.4	-8.4	-8.1	-5.2	-6.2	-6.1	-6.1	-6.0
ROCK2	-8.9	-9.3	-8.9	-9.1	-8.8	-5.6	-6.5	-6.7	-6.7	-6.3
RSK2[RP]	-9.4	-8.7	-9.1	-8.8	-9.0	-4.7	-6.1	-6.1	-5.4	-5.1
SMAD2	-9.3	-9.7	-9.7	-9.8	-9.5	-5.5	-6.6	-6.6	-6.1	-6.4
SMAD3	-9.3	-9.7	-9.7	-9.9	-9.6	-5.5	-6.6	-6.5	-6.3	-5.5
SMAD4	-9.2	-8.9	-9.4	-9.4	-9.2	-5.5	-6.3	-6.3	-6.0	-5.9
SMURF2	-9.3	-8.7	-8.7	-8.5	-8.3	-5.5	-6.7	-6.6	-6.6	-6.2
SP1	-6.2	-6.6	-6.7	-6.7	-6.1	-4.4	-5.1	-4.7	-5.3	-5.1
STAT3	-8.1	-7.9	-8.2	-8.3	-8.0	-5.5	-6.8	-6.3	-6.5	-6.1
TAB1	-7.7	-7.5	-7.6	-7.8	-7.6	-5.1	-6.0	-5.7	-6.1	-6.1
TAK1	-8.1	-8.1	-8.0	-8.0	-8.0	-4.9	-5.9	-6.0	-5.9	-5.9
TNFR1	-6.8	-6.3	-6.9	-7.4	-7.3	-4	-5.0	-5.1	-4.8	-4.6
TRADD	-7.2	-6.9	-6.8	-6.9	-6.9	-4.6	-5.6	-6.0	-5.1	-5.1
TRAF2	-7.3	-7.6	-7.3	-7.2	-6.9	-4.9	-5.2	-5.2	-5.3	-5.3
TRAF5	-7.1	-7.0	-6.9	-7.0	-7.1	-4.7	-5.6	-5.4	-5.0	-5.1

[RP] - Ribosomal protein

Supplementary Table 5. *Results of the molecular docking analyses for the most relevant targets*

Target	Ligand	Hydrogen bonding					Steric interactions			BA (kcal/mol)	Ligand map with depiction of H-bonds interactions
		Energy donor	Bonding energy (KJ/mol)	H-bond length (Å)	Ligand contribution with atom type (no.)	Target contribution	AA residue	Localisation	EPair (KJ/mol)*		
MEK2	*Cy-3-arab*	target	-0.958805	3.12045	O (34)	Ser154	Leu78	Protein kinase domain	-8.70731	-8.5	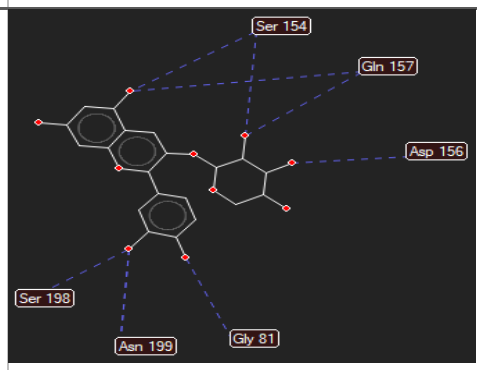
		ligand	-2.5	2.84628	O (34)	Gln157	Gly79	Protein kinase domain	-4.14582		
		either	-2.5	2.78607	O (22)	Ser154	Ala80	Protein kinase domain	-7.31413		
		target	-2.5	3.00686	O (22)	Gln157	Gly81	Protein kinase domain	-6.81849		
		ligand	-0.0846128	3.58308	O (20)	Asp156	Asn82	Protein kinase domain	-2.25093		
		ligand	-1.83742	2.88328	O (32)	Gly81	Gly84	Protein kinase domain	-0.540116		
		either	-2.44647	3.11071	O (30)	Ser198	Val86	Protein kinase domain	-8.56736		
		ligand	-2.5	2.88042	O (30)	Asn199	Ala99	Protein kinase domain	-0.938854		
		target	-1.11876	3.2355	O (30)	Asn199	Lys101	Protein kinase domain	-2.96826		
							Met147	Protein kinase domain	-2.08473		
							Met150	Protein kinase domain	-1.69911		
							Gly153	Protein kinase domain	-1.56612		
							Ser154	Protein kinase domain	-13.4514		
							Asp156	Protein kinase domain	-4.79669		
							Gln157	Protein kinase domain	-15.8214		
							Lys160	Protein kinase domain	-1.10912		
							Lys196	Protein kinase domain	-1.86355		
							Ser198	Protein kinase domain	-20.1535		
							Asn199	Protein kinase domain	-9.58221		
							Leu201	Protein kinase domain	-9.43612		
							Cys211	Protein kinase domain	-0.860976		
							Asp212	Protein kinase domain	-3.16923		
	Cy-3-gal	target	-1.09368	3.11535	O (37)	Ser154	Leu78	Protein kinase domain	-7.13973	-8.7	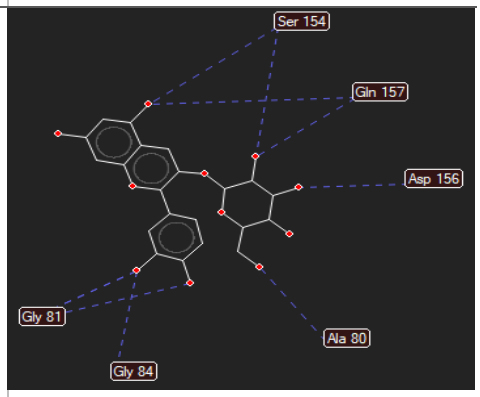
		ligand	-2.5	2.70228	O (37)	Gln157	Gly79	Protein kinase domain	-2.13809		
		either	-2.5	3.03054	O (25)	Ser154	Ala80	Protein kinase domain	-10.0251		
		target	-2.5	2.79768	O (25)	Gln157	Gly81	Protein kinase domain	-13.3508		
		ligand	-1.83681	2.92798	O (23)	Asp156	Asn82	Protein kinase domain	-2.91642		
		ligand	-2.5	2.95098	O (19)	Ala80	Gly84	Protein kinase domain	-4.18052		
		ligand	-2.5	2.71842	O (35)	Gly81	Val86	Protein kinase domain	-9.36782		
		target	-0.0293223	3.27686	O (33)	Gly81	Ala99	Protein kinase domain	-0.988764		
		ligand	-2.5	2.69506	O (33)	Gly81	Lys101	Protein kinase domain	-5.08145		
		ligand	-2.13172	3.17366	O (33)	Gly84	Met147	Protein kinase domain	-1.85852		
							His149	Protein kinase domain	-0.309629		
							Met150	Protein kinase domain	-2.92664		
							Gly153	Protein kinase domain	-2.02888		
							Ser154	Protein kinase domain	-13.6046		
							Asp156	Protein kinase domain	-7.473		
							Gln157	Protein kinase domain	-12.7897		
							Lys160	Protein kinase domain	-0.549381		
							Lys196	Protein kinase domain	-1.15392		
							Ser198	Protein kinase domain	-20.4991		
							Asn199	Protein kinase domain	-5.50698		
							Leu201	Protein kinase domain	-9.88294		
							Cys211	Protein kinase domain	-0.958946		
							Asp212	Protein kinase domain	-4.39603		
	Cy-3-glc	ligand	-2.5	2.96463	O (37)	Leu78	Leu78	Protein kinase domain	-16.8185	-8.6	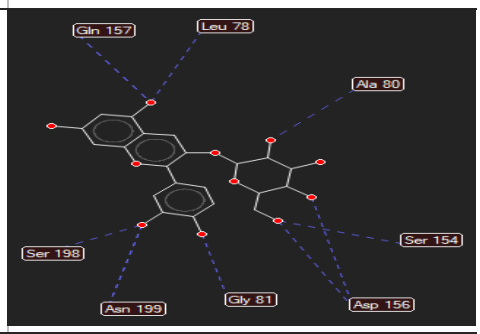
		ligand	-2.5	2.97878	O (37)	Gln157	Gly79	Protein kinase domain	-8.14971		
		target	-2.12729	3.17454	O (37)	Gln157	Ala80	Protein kinase domain	-12.6958		
		ligand	-2.5	3.08275	O (25)	Ala80	Gly81	Protein kinase domain	-8.81552		
		ligand	-1.86472	3.05115	O (21)	Asp156	Asn82	Protein kinase domain	-2.24504		
		either	-2.39222	3.12156	O (19)	Ser154	Gly84	Protein kinase domain	-1.17276		
		ligand	-1.37883	3.21548	O (19)	Asp156	Val86	Protein kinase domain	-9.13943		
		ligand	-2.5	3.02429	O (35)	Gly81	Lys101	Protein kinase domain	-3.62662		
		either	-2.5	2.94544	O (33)	Ser198	Met150	Protein kinase domain	-2.41926		
		ligand	-2.07085	2.9783	O (33)	Asn199	Gly153	Protein kinase domain	-3.971		
		target	-2.08553	3.13239	O (33)	Asn199	Ser154	Protein kinase domain	-10.1626		
							Asp156	Protein kinase domain	-10.2972		
							Gln157	Protein kinase domain	-16.1986		
							Lys160	Protein kinase domain	-2.71117		
							Lys196	Protein kinase domain	-2.16182		
							Ser198	Protein kinase domain	-16.812		
							Asn199	Protein kinase domain	-9.62154		
							Leu201	Protein kinase domain	-5.6016		
							Asp212	Protein kinase domain	-3.55274		
	Del-3-glc	ligand	-2.39188	3.12162	O (39)	Leu78	Leu78	Protein kinase domain	-17.1584	-8.9	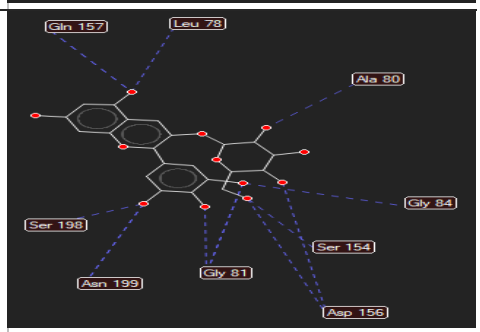
		ligand	-2.5	2.86091	O (39)	Gln157	Gly79	Protein kinase domain	-8.84265		
		target	-2.17702	3.1646	O (39)	Gln157	Ala80	Protein kinase domain	-13.4655		
		ligand	-2.5	3.02218	O (25)	Ala80	Gly81	Protein kinase domain	-12.3195		
		ligand	-1.38228	3.16124	O (21)	Asp156	Asn82	Protein kinase domain	-1.97977		
		either	-2.5	3.05366	O (19)	Ser154	Gly84	Protein kinase domain	-4.71225		
		ligand	-1.09869	3.23626	O (19)	Asp156	Val86	Protein kinase domain	-9.61557		
		target	-0.0837623	3.28578	O (37)	Gly81	Lys101	Protein kinase domain	-4.67926		
		ligand	-2.5	2.62064	O (37)	Gly81	Met150	Protein kinase domain	-3.05856		
		ligand	-2.48855	3.10229	O (37)	Gly84	Gly153	Protein kinase domain	-4.8706		
		ligand	-2.5	2.93276	O (35)	Gly81	Ser154	Protein kinase domain	-10.706		
		either	-2.5	3.05341	O (33)	Ser198	Asp156	Protein kinase domain	-9.20782		
		ligand	-1.07312	3.13439	O (33)	Asn199	Gln157	Protein kinase domain	-16.2255		
		target	-2.44505	3.11099	O (33)	Asn199	Lys160	Protein kinase domain	-2.55438		
							Lys196	Protein kinase domain	-0.981435		
							Ser198	Protein kinase domain	-16.0853		
							Asn199	Protein kinase domain	-8.73065		
							Leu201	Protein kinase domain	-5.93964		
							Asp212	Protein kinase domain	-3.62141		
	Pn-3-glc	target	-0.195522	3.5609	O (1)	Gln157	Leu78	Protein kinase domain	-11.4296	-8.1	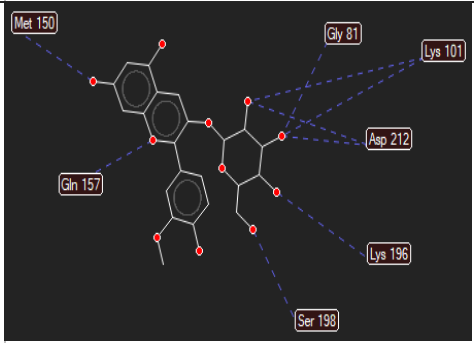
		ligand	-2.5	2.97423	O (39)	Met150	Gly79	Protein kinase domain	-8.23925		
		target	-2.5	2.80572	O (25)	Lys101	Ala80	Protein kinase domain	-7.79422		
		ligand	-2.38147	3.12371	O (25)	Asp212	Gly81	Protein kinase domain	-9.66031		
		ligand	-1.81225	3.23755	O (23)	Gly81	Asn82	Protein kinase domain	-3.06648		
		target	-2.5	2.96384	O (23)	Lys101	Val86	Protein kinase domain	-9.29691		
		ligand	-1.57326	3.28535	O (23)	Asp212	Ala99	Protein kinase domain	-0.625892		
		target	-1.61234	3.27753	O (21)	Lys196	Lys101	Protein kinase domain	-8.4458		
		either	-2.5	3.02394	O (19)	Ser198	Met147	Protein kinase domain	-1.26104		
							Met150	Protein kinase domain	-6.81132		
							Gly153	Protein kinase domain	-4.39568		
							Ser154	Protein kinase domain	-9.29673		
							Asp156	Protein kinase domain	-2.91008		
							Gln157	Protein kinase domain	-10.6831		
							Lys160	Protein kinase domain	-0.705827		
							Lys196	Protein kinase domain	-4.67905		
							Ser198	Protein kinase domain	-16.4962		
							Asn199	Protein kinase domain	-3.58847		
							Leu201	Protein kinase domain	-9.55088		
							Cys211	Protein kinase domain	-0.879063		
							Asp212	Protein kinase domain	-7.22799		

Supplementary Table 5. *(Continued)*

Target	Ligand	Hydrogen bonding					Steric interactions			BA (kcal/mol)	Ligand map with depiction of H-bonds interactions
		Energy donor	Bonding energy (KJ/mol)	H-bond length (Å)	Ligand contribution with atom type (no.)	Target contribution	AA residue	Localisation	EPair (KJ/mol)*		
JNK1	*Cy-3-arab*	ligand	-1.51653	3.29669	O (34)	Glu109	Ile32	Protein kinase domain	-4.3533	-9.8	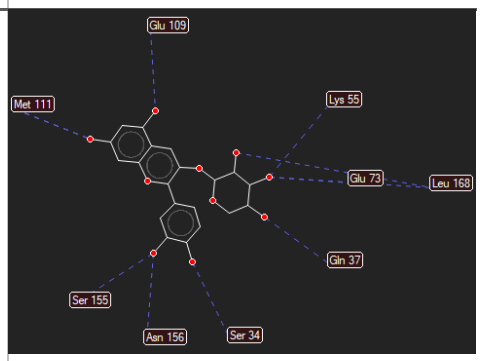
		target	-2.05041	3.09281	O (36)	Met111	Gly33	Protein kinase domain	-5.33913		
		ligand	-0.754338	3.15141	O (36)	Met111	Ser34	Protein kinase domain	-8.17859		
		ligand	-1.59148	3.2817	O (22)	Leu168	Gly35	Protein kinase domain	-2.48219		
		target	-1.2662	3.31309	O (20)	Lys55	Gln37	Protein kinase domain	-6.64229		
		ligand	-2.5	3.07369	O (20)	Glu73	Gly38	Protein kinase domain	-0.643803		
		ligand	-2.5	2.9044	O (20)	Leu168	Val40	Protein kinase domain	-12.515		
		ligand	-2.5	2.68272	O (18)	Gln37	Ala53	Protein kinase domain	-3.33504		
		ligand	-2.5	2.73071	O (32)	Ser34	Lys55	Protein kinase domain	-8.90095		
		ligand	-2.5	2.70895	O (30)	Ser155	Glu73	Protein kinase domain	-4.65616		
		ligand	-2.5	2.99876	O (30)	Asn156	Ile86	Protein kinase domain	-3.17396		
							Met108	Protein kinase domain	-7.55751		
							Glu109	Protein kinase domain	-3.90021		
							Leu110	Protein kinase domain	-6.24495		
							Met111	Protein kinase domain	-9.40684		
							Asn114	Protein kinase domain	-1.08501		
							Ser155	Protein kinase domain	-6.74051		
							Asn156	Protein kinase domain	-12.2007		
							Val158	Protein kinase domain	-7.24434		
							Leu168	Protein kinase domain	-31.2161		
							Asp169	Protein kinase domain	-4.95215		
	Cy-3-gal	target	-2.25318	3.03615	O (39)	Met111	Ile32	Protein kinase domain	-6.65509	-8.7	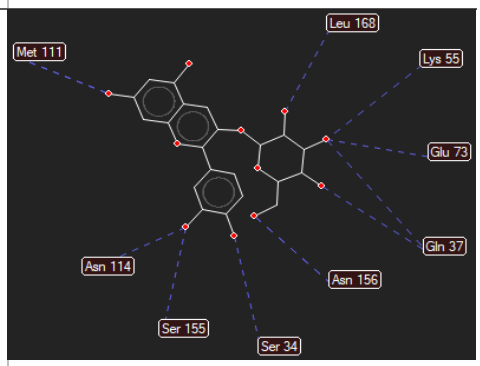
		ligand	-2.24511	3.15098	O (39)	Met111	Gly33	Protein kinase domain	-6.89674		
		ligand	-0.585833	3.48283	O (25)	Leu168	Ser34	Protein kinase domain	-8.16323		
		ligand	-2.5	2.70191	O (23)	Gln37	Gly35	Protein kinase domain	-2.72442		
		target	-2.5	2.7964	O (23)	Lys55	Gln37	Protein kinase domain	-9.9494		
		ligand	-0.356212	3.52876	O (23)	Glu73	Gly38	Protein kinase domain	-0.320576		
		ligand	-2.5	3.03613	O (21)	Gln37	Val40	Protein kinase domain	-11.9136		
		ligand	-2.5	2.96479	O (19)	Asn156	Ala53	Protein kinase domain	-3.73958		
		target	-1.73317	3.25337	O (19)	Asn156	Lys55	Protein kinase domain	-8.27181		
		ligand	-2.5	2.88379	O (35)	Ser34	Glu73	Protein kinase domain	-1.19596		
		target	-2.5	3.06097	O (33)	Asn114	Ile86	Protein kinase domain	-2.37069		
		ligand	-2.5	2.92095	O (33)	Ser155	Met108	Protein kinase domain	-5.17397		
							Glu109	Protein kinase domain	-2.34468		
							Leu110	Protein kinase domain	-5.1026		
							Met111	Protein kinase domain	-11.0628		
							Asn114	Protein kinase domain	-5.56896		
							Ser155	Protein kinase domain	-8.61214		
							Asn156	Protein kinase domain	-14.5702		
							Val158	Protein kinase domain	-6.86399		
							Leu168	Protein kinase domain	-19.2392		
							Asp169	Protein kinase domain	-1.72792		
	Cy-3-glc	ligand	-1.20949	3.3581	O (37)	Glu109	Ile32	Protein kinase domain	-3.93138	-9.9	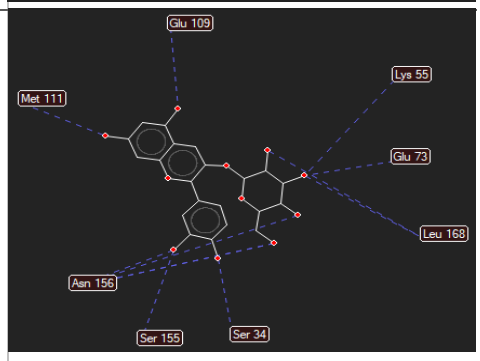
		target	-1.86692	3.13895	O (39)	Met111	Gly33	Protein kinase domain	-5.04226		
		ligand	-1.67198	3.2656	O (25)	Leu168	Ser34	Protein kinase domain	-8.10112		
		target	-0.753198	3.32609	O (23)	Lys55	Gly35	Protein kinase domain	-3.2235		
		ligand	-2.30956	3.13809	O (23)	Glu73	Gln37	Protein kinase domain	-4.76853		
		ligand	-2.5	2.84924	O (23)	Leu168	Gly38	Protein kinase domain	-0.697418		
		target	-2.5	2.97507	O (21)	Asn156	Val40	Protein kinase domain	-12.1267		
		ligand	-2.5	2.79241	O (19)	Asn156	Ala53	Protein kinase domain	-3.13272		
		target	-1.91447	3.21711	O (19)	Asn156	Lys55	Protein kinase domain	-8.54192		
		ligand	-2.5	2.74124	O (35)	Ser34	Glu73	Protein kinase domain	-4.56026		
		ligand	-2.5	2.83449	O (33)	Ser155	Ile86	Protein kinase domain	-3.24935		
		ligand	-2.5	2.77183	O (33)	Asn156	Met108	Protein kinase domain	-7.62319		
							Glu109	Protein kinase domain	-3.55203		
							Leu110	Protein kinase domain	-5.59937		
							Met111	Protein kinase domain	-8.04897		
							Asn114	Protein kinase domain	-1.02123		
							Ser155	Protein kinase domain	-6.75459		
							Asn156	Protein kinase domain	-21.2905		
							Val158	Protein kinase domain	-7.37457		
							Leu168	Protein kinase domain	-31.5828		
							Asp169	Protein kinase domain	-4.95338		
	Del-3-glc	ligand	-1.99865	3.20027	O (39)	Glu109	Ile32	Protein kinase domain	-3.85583	-9.8	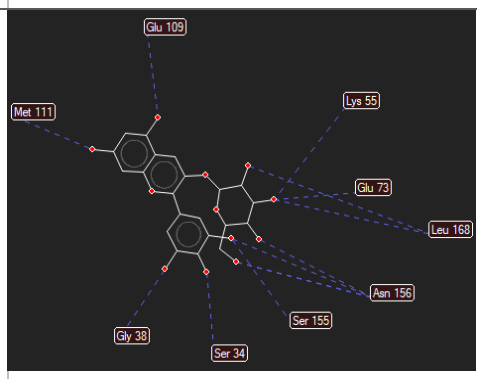
		target	-1.91152	3.12435	O (41)	Met111	Gly33	Protein kinase domain	-5.48384		
		ligand	-2.29899	3.1402	O (25)	Leu168	Ser34	Protein kinase domain	-3.12251		
		target	-0.582712	3.28866	O (23)	Lys55	Gly35	Protein kinase domain	-3.75022		
		ligand	-2.5	3.0155	O (23)	Glu73	Gln37	Protein kinase domain	-4.92628		
		ligand	-2.5	2.8362	O (23)	Leu168	Gly38	Protein kinase domain	-3.20607		
		target	-2.5	3.07001	O (21)	Asn156	Ile39	Protein kinase domain	-0.327181		
		ligand	-1.67589	2.96591	O (19)	Asn156	Val40	Protein kinase domain	-12.376		
		target	-2.5	2.97641	O (19)	Asn156	Ala53	Protein kinase domain	-3.26889		
		ligand	-2.5	2.78154	O (37)	Ser155	Lys55	Protein kinase domain	-8.30276		
		ligand	-2.5	3.00855	O (37)	Asn156	Glu73	Protein kinase domain	-4.94823		
		ligand	-2.5	2.8611	O (35)	Ser34	Ile86	Protein kinase domain	-3.63057		
		ligand	-1.93757	3.21249	O (33)	Gly38	Met108	Protein kinase domain	-8.09609		
							Glu109	Protein kinase domain	-4.37629		
							Leu110	Protein kinase domain	-5.98106		
							Met111	Protein kinase domain	-8.34731		
							Asn114	Protein kinase domain	-0.952609		
							Ser155	Protein kinase domain	-6.4215		
							Asn156	Protein kinase domain	-20.4376		
							Val158	Protein kinase domain	-7.52768		
							Leu168	Protein kinase domain	-32.3861		
							Asp169	Protein kinase domain	-4.92197		
	Pn-3-glc	ligand	-1.8165	3.2367	O (37)	Glu109	Ile32	Protein kinase domain	-4.21036	-9.4	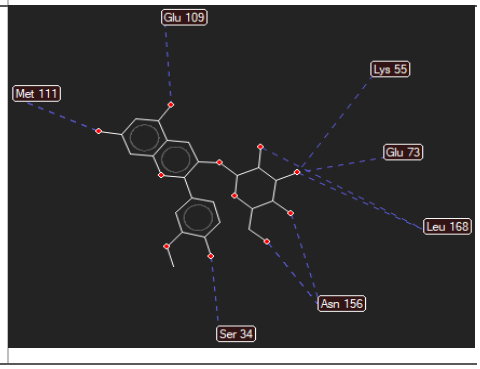
		target	-1.71821	3.17388	O (39)	Met111	Gly33	Protein kinase domain	-5.73266		
		ligand	-0.234642	3.22837	O (39)	Met111	Ser34	Protein kinase domain	-7.91157		
		ligand	-2.04814	3.19037	O (25)	Leu168	Gly35	Protein kinase domain	-3.07994		
		target	-0.646789	3.33148	O (23)	Lys55	Gln37	Protein kinase domain	-4.6766		
		ligand	-2.5	3.08532	O (23)	Glu73	Gly38	Protein kinase domain	-0.841993		
		ligand	-2.5	2.86609	O (23)	Leu168	Val40	Protein kinase domain	-11.5144		
		target	-2.5	2.94328	O (21)	Asn156	Ala53	Protein kinase domain	-3.3479		
		ligand	-1.45261	3.0306	O (19)	Asn156	Lys55	Protein kinase domain	-8.40906		
		target	-2.5	2.98135	O (19)	Asn156	Glu73	Protein kinase domain	-4.75666		
		ligand	-2.30009	2.57601	O (35)	Ser34	Ile86	Protein kinase domain	-3.38861		
							Met108	Protein kinase domain	-7.87837		
							Glu109	Protein kinase domain	-4.17578		
							Leu110	Protein kinase domain	-5.97472		
							Met111	Protein kinase domain	-8.54614		
							Asn114	Protein kinase domain	-1.8454		
							Ser155	Protein kinase domain	-2.99974		
							Asn156	Protein kinase domain	-17.8322		
							Val158	Protein kinase domain	-7.37627		
							Leu168	Protein kinase domain	-31.8014		
							Asp169	Protein kinase domain	-5.12863		

Supplementary Table 5. *(Continued)*

Target	Ligand	Hydrogen bonding					Steric interactions			BA (kcal/mol)	Ligand map with depiction of H-bonds interactions
		Energy donor	Bonding energy (KJ/mol)	H-bond length (Å)	Ligand contribution with atom type (no.)	Target contribution	AA residue	Localisation	EPair (KJ/mol)*		
FAK1	*Cy-3-arab*	ligand	-2.5	2.78631	O (34)	Ile428	Ile428	Protein kinase domain	-19.3835	-9.0	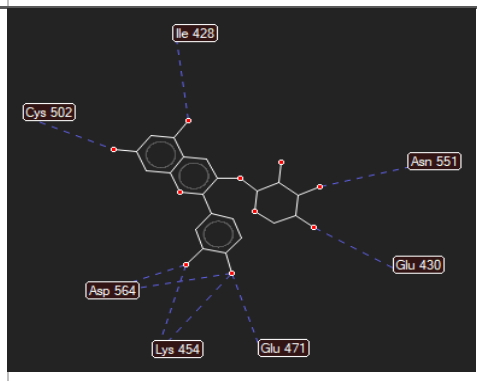
		target	-0.590916	3.30325	O (36)	Cys502	Gly429	Protein kinase domain	-8.05173		
		ligand	-2.5	2.64044	O (36)	Cys502	Glu430	Protein kinase domain	-9.97306		
		target	-0.277513	3.33865	O (13)	Glu430	Gly431	Protein kinase domain	-0.637014		
		ligand	-2.5	3.01172	O (20)	Asn551	Phe433	Protein kinase domain	-1.19162		
		ligand	-2.5	2.92756	O (18)	Glu430	Val436	Protein kinase domain	-13.5346		
		target	-2.5	2.80825	O (32)	Lys454	Ala452	Protein kinase domain	-1.15332		
		ligand	-2.5	2.75113	O (32)	Glu471	Lys454	Protein kinase domain	-11.8114		
		ligand	-2.5	2.81952	O (32)	Asp564	Glu471	Protein kinase domain	-4.67251		
		target	-2.5	2.88436	O (30)	Lys454	Val484	Protein kinase domain	-0.436098		
		ligand	-2.5	2.98725	O (30)	Asp564	Met499	Protein kinase domain	-2.74567		
							Leu501	Protein kinase domain	-3.01758		
							Cys502	Protein kinase domain	-8.11531		
							Thr503	Protein kinase domain	-0.312845		
							Gly505	Protein kinase domain	-1.69448		
							Glu506	Protein kinase domain	-1.22462		
							Arg550	Protein kinase domain	-2.35843		
							Asn551	Protein kinase domain	-5.22722		
							Leu553	Protein kinase domain	-11.5558		
							Gly563	Protein kinase domain	-2.96267		
							Asp564	Protein kinase domain	-17.387		
							Gly566	Protein kinase domain	-0.48297		
	Cy-3-gal	ligand	-1.21619	3.35676	O (37)	Ile428	Ile428	Protein kinase domain	-14.6138	-8.8	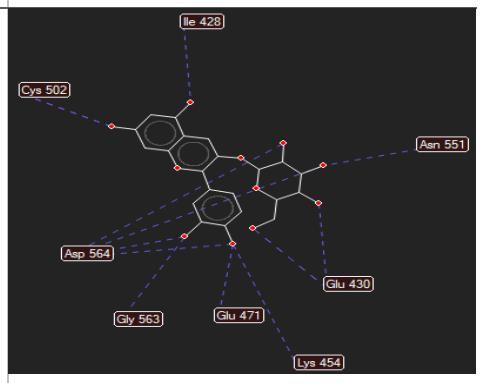
		target	-0.834313	3.19175	O (39)	Cys502	Gly429	Protein kinase domain	-4.94723		
		ligand	-2.5	2.77932	O (39)	Cys502	Glu430	Protein kinase domain	-14.0403		
		ligand	-2.5	2.9667	O (25)	Asp564	Gly431	Protein kinase domain	-0.690979		
		ligand	-1.93555	3.21289	O (23)	Asn551	Val436	Protein kinase domain	-9.92503		
		ligand	-2.2915	3.1417	O (23)	Asp564	Ala452	Protein kinase domain	-1.21647		
		ligand	-2.5	2.9589	O (21)	Glu430	Lys454	Protein kinase domain	-8.00962		
		target	-1.87829	3.13366	O (19)	Glu430	Glu471	Protein kinase domain	-4.56558		
		ligand	-2.5	2.70415	O (19)	Glu430	Met475	Protein kinase domain	-0.541482		
		target	-2.5	2.81247	O (35)	Lys454	Val484	Protein kinase domain	-1.2592		
		ligand	-2.5	2.73769	O (35)	Glu471	Met499	Protein kinase domain	-3.57753		
		ligand	-2.5	2.82183	O (35)	Asp564	Leu501	Protein kinase domain	-1.67315		
		ligand	-2.5	2.70012	O (33)	Gly563	Cys502	Protein kinase domain	-8.88988		
		ligand	-1.74096	3.25181	O (33)	Asp564	Thr503	Protein kinase domain	-0.309132		
							Gly505	Protein kinase domain	-2.41967		
							Glu506	Protein kinase domain	-1.51257		
							Arg550	Protein kinase domain	-1.73123		
							Asn551	Protein kinase domain	-6.15944		
							Leu553	Protein kinase domain	-13.6558		
							Gly563	Protein kinase domain	-7.16757		
							Asp564	Protein kinase domain	-26.2551		
							Gly566	Protein kinase domain	-0.394005		
	Cy-3-glc	target	-2.5	2.95864	O (37)	Trp97	Arg86	FERM domain	-4.6009	-8.5	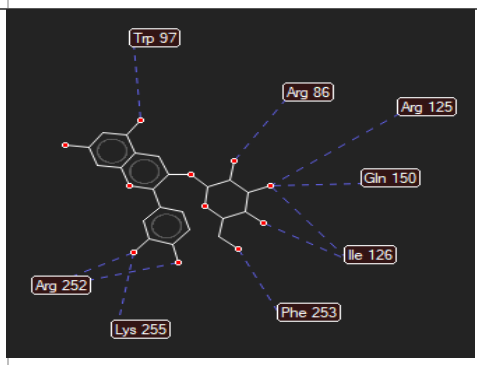
		target	-1.30221	3.33956	O (25)	Arg86	Val95	FERM domain	-0.473331		
		target	-0.0777386	3.07119	O (25)	Arg125	Trp97	FERM domain	-10.1382		
		target	-2.23705	3.02449	O (23)	Arg125	Arg125	FERM domain	-10.9962		
		ligand	-2.5	2.88181	O (23)	Ile126	Ile126	FERM domain	-8.40551		
		target	-2.5	3.02576	O (23)	Gln150	Arg127	FERM domain	-10.9881		
		ligand	-2.5	2.76454	O (21)	Ile126	Leu129	FERM domain	-1.45842		
		ligand	-2.39631	3.12074	O (19)	Phe253	Phe147	FERM domain	-0.670751		
		either	-0.370844	3.35308	O (35)	Tyr251	Gln150	FERM domain	-6.28643		
		ligand	-2.5	2.72453	O (35)	Arg252	Asp154	FERM domain	-1.43335		
		ligand	-2.5	2.75963	O (33)	Arg252	Glu158	FERM domain	-3.48663		
		ligand	-2.25931	3.14814	O (33)	Lys255	Tyr251	FERM domain	-7.05939		
							Arg252	FERM domain	-14.2623		
							Phe253	FERM domain	-7.25417		
							Asp254	FERM domain	-1.02438		
							Lys255	FERM domain	-7.45798		
							Glu256	FERM domain	-28.6701		
							Cys257	FERM domain	-1.18251		
							Phe258	FERM domain	-7.06819		
							Ile336	FERM domain	-0.917517		
							Asn339	FERM domain	-4.38361		
	Del-3-glc	either	-2.5	2.96793	O (41)	Ser463	His41	FERM domain	-7.49264	-9.1	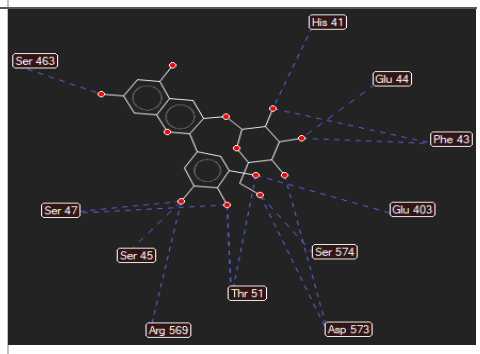
		target	-2.5	3.00589	O (25)	His41	Phe43	FERM domain	-7.23045		
		ligand	-1.7136	3.25728	O (25)	Phe43	Glu44	FERM domain	-6.34625		
		ligand	-0.976273	2.8489	O (23)	Phe43	Ser45	FERM domain	-12.4378		
		ligand	-2.5	2.72539	O (23)	Glu44	Ser47	FERM domain	-8.54256		
		ligand	-2.5	2.69844	O (21)	Asp573	Thr51	FERM domain	-11.1571		
		ligand	-2.5	2.92741	O (19)	Asp573	Trp52	FERM domain	-5.71532		
		ligand	-2.5	3.02604	O (19)	Ser574	Ala53	FERM domain	-9.06047		
		ligand	-2.5	2.75684	O (37)	Thr51	Ser54	FERM domain	-6.16734		
		ligand	-2.5	2.706	O (37)	Glu403	Ile55	FERM domain	-3.96006		
		either	-2.5	2.9683	O (35)	Ser47	His75	FERM domain	-8.56406		
		ligand	-2.5	3.07879	O (35)	Thr51	Ile400	Protein kinase domain	-11.9829		
		either	-0.762197	3.44756	O (35)	Thr51	Ile401	Protein kinase domain	-8.4377		
		either	-2.5	2.92853	O (33)	Ser45	Asp402	Protein kinase domain	-5.98489		
		either	-2.5	2.73763	O (33)	Ser47	Glu403	Protein kinase domain	-6.88544		
		target	-2.5	2.90931	O (33)	Arg569	Ser463	Protein kinase domain	-3.40974		
							Arg569	Protein kinase domain	-8.38305		
							Asp573	Protein kinase domain	-15.1464		
							Ser574	Protein kinase domain	-5.45127		
							Thr575	Protein kinase domain	-5.09553		
							Tyr576	Protein kinase domain	-1.79229		
	Pn-3-glc	target	-1.21021	3.27794	O (37)	Trp97	Arg86	FERM domain	-2.12782	-8.7	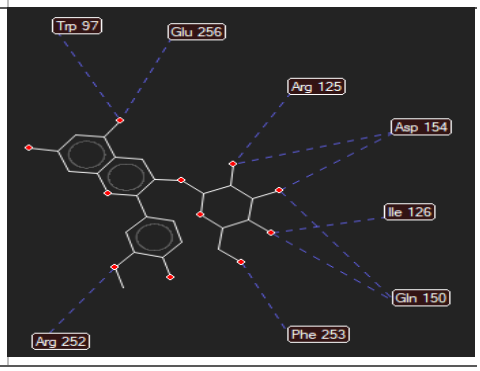
		ligand	-1.74881	3.21167	O (37)	Glu256	Val95	FERM domain	-5.18153		
		target	-0.601477	3.27478	O (25)	Arg125	Trp97	FERM domain	-5.33383		
		ligand	-2.5	2.81516	O (25)	Asp154	Arg125	FERM domain	-3.70614		
		target	-2.5	2.89396	O (23)	Gln150	Ile126	FERM domain	-4.3775		
		ligand	-2.5	2.98748	O (23)	Asp154	Arg127	FERM domain	-5.71102		
		ligand	-2.5	2.93071	O (21)	Ile126	Leu129	FERM domain	-1.91991		
		target	-2.5	2.90434	O (21)	Gln150	Phe147	FERM domain	-2.24795		
		ligand	-2.5	2.86628	O (19)	Phe253	Gln150	FERM domain	-8.93921		
		target	-0.0696032	3.58608	O (33)	Arg252	Val151	FERM domain	-1.15858		
							Asp154	FERM domain	-8.59771		
							Glu158	FERM domain	-3.69262		
							Tyr251	FERM domain	-5.59171		
							Arg252	FERM domain	-13.7078		
							Phe253	FERM domain	-7.31449		
							Asp254	FERM domain	-1.27291		
							Lys255	FERM domain	-4.92663		
							Glu256	FERM domain	-24.893		
							Cys257	FERM domain	-3.63614		
							Phe258	FERM domain	-0.713526		
							Asn339	FERM domain	-1.05442		

Supplementary Table 5. (*Continued*)

Target	Ligand	Hydrogen bonding					Steric interactions			BA (kcal/mol)	Ligand map with depiction of H-bonds interactions
		Energy donor	Bonding energy (KJ/mol)	H-bond length (Å)	Ligand contribution with atom type (no.)	Target contribution	AA residue	Localisation	EPair (KJ/mol)*		
ROCK2	*Cy-3-arab*	target	-0.989466	3.24158	O (13)	Arg100	Ile98	Protein kinase domain	-1.08868	-8.9	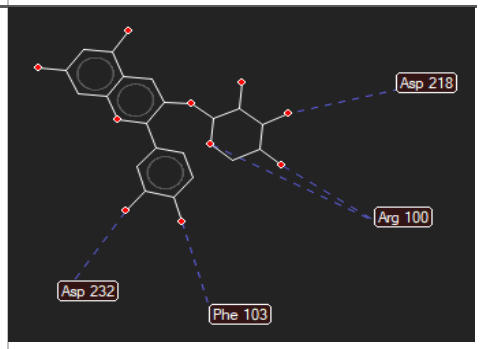
		ligand	-2.5	2.95696	O (20)	Asp218	Gly99	Protein kinase domain	-5.27951		
		ligand	-2.11124	3.17775	O (18)	Arg100	Arg100	Protein kinase domain	-12.4983		
		target	-2.31788	3.13642	O (32)	Phe103	Gly101	Protein kinase domain	-10.1176		
		ligand	-2.5	3.06889	O (30)	Asp232	Ala102	Protein kinase domain	-4.43168		
							Phe103	Protein kinase domain	-6.91318		
							Gly104	Protein kinase domain	-4.13237		
							Glu105	Protein kinase domain	-3.2347		
							Val106	Protein kinase domain	-11.6344		
							Ala119	Protein kinase domain	-0.318821		
							Lys121	Protein kinase domain	-15.3976		
							Leu122	Protein kinase domain	-0.567196		
							Leu123	Protein kinase domain	-2.52246		
							Val153	Protein kinase domain	-1.78325		
							Met169	Protein kinase domain	-4.43228		
							Met172	Protein kinase domain	-0.42389		
							Asp176	Protein kinase domain	-1.1908		
							Asp218	Protein kinase domain	-10.3982		
							Leu221	Protein kinase domain	-6.3043		
							Ala231	Protein kinase domain	-8.36264		
							Asp232	Protein kinase domain	-12.2317		
							Phe384	AGC-kinase C-terminal domain	-1.05269		
	Cy-3-gal	target	-2.35198	2.79738	O (39)	Met172	Ile98	Protein kinase domain	-10.6908	-9.3	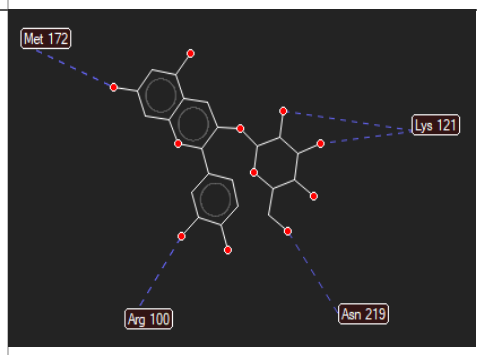
		ligand	-1.71928	3.25614	O (39)	Met172	Gly99	Protein kinase domain	-8.88427		
		target	-1.53488	3.29302	O (25)	Lys121	Arg100	Protein kinase domain	-10.7359		
		target	-1.56451	3.2871	O (23)	Lys121	Gly101	Protein kinase domain	-2.96415		
		ligand	-2.5	2.94632	O (19)	Asn219	Val106	Protein kinase domain	-11.4048		
		target	-0.727846	3.38138	O (33)	Arg100	Ala119	Protein kinase domain	-2.42063		
		ligand	-2.5	2.65726	O (33)	Arg100	Lys121	Protein kinase domain	-7.99534		
							Val153	Protein kinase domain	-1.78213		
							Met169	Protein kinase domain	-3.56375		
							Glu170	Protein kinase domain	-1.35306		
							Tyr171	Protein kinase domain	-4.31707		
							Met172	Protein kinase domain	-10.9348		
							Asp176	Protein kinase domain	-4.15871		
							Lys216	Protein kinase domain	-1.40979		
							Asp218	Protein kinase domain	-8.33534		
							Asn219	Protein kinase domain	-7.99573		
							Leu221	Protein kinase domain	-12.8657		
							Ala231	Protein kinase domain	-5.64848		
							Asp232	Protein kinase domain	-12.8251		
							Phe384	AGC-kinase C-terminal domain	-10.0599		
							Ile387	AGC-kinase C-terminal domain	-0.614797		
	Cy-3-glc	ligand	-2.22477	3.15505	O (23)	Asp218	Ile98	Protein kinase domain	-0.624485	-8.9	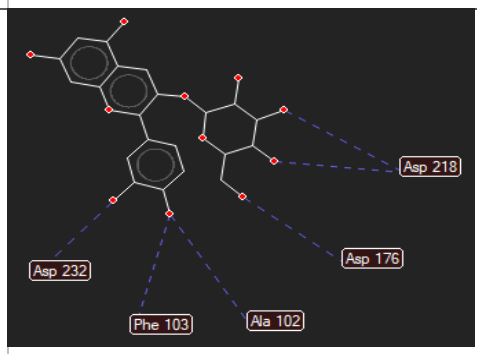
		ligand	-2.5	2.97464	O (21)	Asp218	Gly99	Protein kinase domain	-4.02096		
		ligand	-2.5	2.97614	O (19)	Asp176	Arg100	Protein kinase domain	-9.73222		
		target	-0.0018934	3.34878	O (35)	Ala102	Gly101	Protein kinase domain	-10.7862		
		target	-2.5	3.03995	O (35)	Phe103	Ala102	Protein kinase domain	-4.76164		
		ligand	-2.5	3.06525	O (33)	Asp232	Phe103	Protein kinase domain	-7.11543		
							Gly104	Protein kinase domain	-4.17929		
							Glu105	Protein kinase domain	-3.16826		
							Val106	Protein kinase domain	-11.5444		
							Ala119	Protein kinase domain	-0.319893		
							Lys121	Protein kinase domain	-14.9476		
							Leu122	Protein kinase domain	-0.500899		
							Leu123	Protein kinase domain	-2.26875		
							Val153	Protein kinase domain	-1.77138		
							Met169	Protein kinase domain	-4.38797		
							Met172	Protein kinase domain	-0.389118		
							Asp176	Protein kinase domain	-5.48688		
							Val178	Protein kinase domain	-1.12772		
							Lys216	Protein kinase domain	-0.478855		
							Asp218	Protein kinase domain	-16.1899		
							Asn219	Protein kinase domain	-0.602131		
							Leu221	Protein kinase domain	-6.23002		
							Ala231	Protein kinase domain	-8.31887		
							Asp232	Protein kinase domain	-12.586		
							Phe384	AGC-kinase C-terminal domain	-1.36677		
	Del-3-glc	ligand	-2.36362	3.12728	O (23)	Asp218	Ile98	Protein kinase domain	-0.936166	-9.1	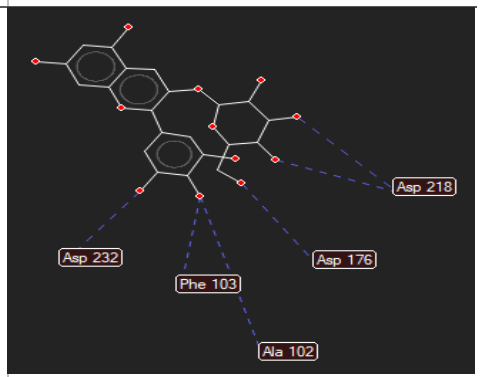
		ligand	-2.5	2.98229	O (21)	Asp218	Gly99	Protein kinase domain	-3.57837		
		ligand	-2.5	2.94509	O (19)	Asp176	Arg100	Protein kinase domain	-9.94353		
		target	-0.103789	3.25017	O (35)	Ala102	Gly101	Protein kinase domain	-11.3397		
		target	-2.5	3.09736	O (35)	Phe103	Ala102	Protein kinase domain	-5.16204		
		ligand	-2.5	2.99472	O (33)	Asp232	Phe103	Protein kinase domain	-7.94873		
							Gly104	Protein kinase domain	-2.7129		
							Glu105	Protein kinase domain	-3.54646		
							Val106	Protein kinase domain	-11.6461		
							Ala119	Protein kinase domain	-0.359882		
							Lys121	Protein kinase domain	-15.5628		
							Leu122	Protein kinase domain	-0.725341		
							Leu123	Protein kinase domain	-2.61811		
							Val153	Protein kinase domain	-1.74347		
							Met169	Protein kinase domain	-4.38147		
							Met172	Protein kinase domain	-0.430175		
							Asp176	Protein kinase domain	-5.55861		
							Val178	Protein kinase domain	-1.14393		
							Lys216	Protein kinase domain	-0.488526		
							Asp218	Protein kinase domain	-16.63		
							Asn219	Protein kinase domain	-0.652372		
							Leu221	Protein kinase domain	-6.45535		
							Ala231	Protein kinase domain	-8.20139		
							Asp232	Protein kinase domain	-12.8494		
							Phe384	AGC-kinase C-terminal domain	-1.53531		

Supplementary Table 5. *(Continued)*

Target	Ligand	Hydrogen bonding					Steric interactions			BA (kcal/mol)	Ligand map with depiction of H-bonds interactions
		Energy donor	Bonding energy (KJ/mol)	H-bond length (Å)	Ligand contribution with atom type (no.)	Target contribution	AA residue	Localisation	EPair (KJ/mol)*		
ROCK2	*Pn-3-glc*	ligand	-2.31279	3.13744	O (23)	Asp218	Ile98	Protein kinase domain	-0.587221	-8.8	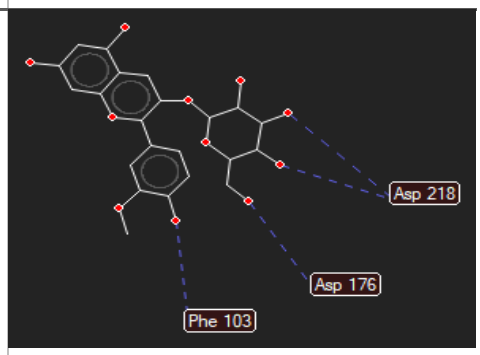
		ligand	-2.5	2.94494	O (21)	Asp218	Gly99	Protein kinase domain	-3.95869		
		ligand	-2.5	2.9887	O (19)	Asp176	Arg100	Protein kinase domain	-9.65929		
		target	-2.5	2.95484	O (35)	Phe103	Gly101	Protein kinase domain	-12.16		
							Ala102	Protein kinase domain	-6.33161		
							Phe103	Protein kinase domain	-7.50571		
							Gly104	Protein kinase domain	-4.46784		
							Glu105	Protein kinase domain	-3.43505		
							Val106	Protein kinase domain	-11.3496		
							Lys121	Protein kinase domain	-15.09		
							Leu122	Protein kinase domain	-0.589805		
							Leu123	Protein kinase domain	-2.3976		
							Val153	Protein kinase domain	-1.74482		
							Met169	Protein kinase domain	-4.21298		
							Met172	Protein kinase domain	-0.336137		
							Asp176	Protein kinase domain	-5.45748		
							Val178	Protein kinase domain	-1.14287		
							Lys216	Protein kinase domain	-0.497045		
							Asp218	Protein kinase domain	-16.3781		
							Asn219	Protein kinase domain	-0.576024		
							Leu221	Protein kinase domain	-5.99112		
							Ala231	Protein kinase domain	-8.36595		
							Asp232	Protein kinase domain	-11.0729		
							Phe384	AGC-kinase C-terminal domain	-0.95591		
IKKα	*Cy-3-arab*	target	-1.95278	3.20944	O (34)	Gln260	Gly115	Protein kinase domain	-1.24993	-8.2	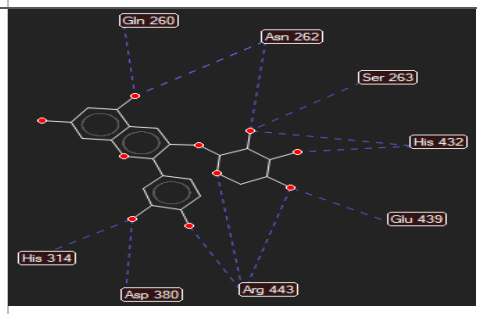
		target	-1.85608	3.13613	O (34)	Asn262	Lys117	Protein kinase domain	-0.33155		
		ligand	-1.43597	3.31281	O (34)	Asn262	Gln260	Protein kinase domain	-5.06319		
		ligand	-2.5	2.78835	O (34)	Asn262	Pro261	Protein kinase domain	-2.41996		
		target	-0.34228	3.43202	O (13)	Arg443	Asn262	Protein kinase domain	-20.3728		
		ligand	-2.5	2.69103	O (22)	Asn262	Ser263	Protein kinase domain	-13.3991		
		either	-2.5	2.98657	O (22)	Ser263	Leu264	Protein kinase domain	-2.31861		
		target	-0.371335	3.41092	O (22)	His432	Cys265	Protein kinase domain	-0.439987		
		target	-0.980082	3.15097	O (20)	His432	His314	NA	-3.81379		
		ligand	-2.5	2.699	O (18)	Glu439	Ile323	NA	-10.7088		
		target	-0.329882	3.0746	O (18)	Arg443	Asp380	NA	-5.95592		
		target	-1.17486	3.36503	O (32)	Arg443	Met383	NA	-1.49096		
		target	-0.316863	3.06003	O (30)	His314	Arg401	NA	-4.68817		
		ligand	-2.5	2.93576	O (30)	Asp380	His432	NA	-6.91256		
							Gly436	NA	-1.2159		
							Glu439	NA	-8.25046		
							Asp440	NA	-1.87208		
							Arg443	NA	-15.0648		
	Cy-3-gal	ligand	-2.5	2.70358	O (37)	Asp380	Gly115	Protein kinase domain	-0.812102	-8.6	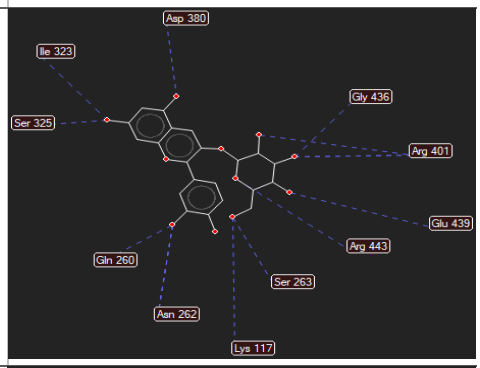
		ligand	-2.5	2.71507	O (39)	Ile323	Leu116	Protein kinase domain	-0.876259		
		either	-2.5	2.99318	O (39)	Ser325	Lys117	Protein kinase domain	-6.66495		
		target	-0.0743586	3.2243	O (13)	Arg443	Gln260	Protein kinase domain	-3.9837		
		target	-0.0824638	2.7973	O (25)	Arg401	Pro261	Protein kinase domain	-4.87845		
		target	-1.65509	3.26898	O (23)	Arg401	Asn262	Protein kinase domain	-16.0839		
		target	-2.5	2.87245	O (23)	Arg401	Ser263	Protein kinase domain	-14.6044		
		ligand	-0.421153	3.5154	O (23)	Gly436	Leu264	Protein kinase domain	-5.22754		
		ligand	-2.23228	3.15354	O (21)	Glu439	Cys265	Protein kinase domain	-11.0853		
		target	-1.21085	3.23898	O (19)	Lys117	Ser266	Protein kinase domain	-2.46205		
		either	-2.5	2.84283	O (19)	Ser263	His314	NA	-5.38707		
		target	-2.5	3.09926	O (33)	Gln260	Ile323	NA	-14.2498		
		target	-1.90618	2.85941	O (33)	Asn262	Ile324	NA	-0.976057		
		ligand	-1.95904	3.20819	O (33)	Asn262	Ser325	NA	-5.36831		
		ligand	-2.5	2.75452	O (33)	Asn262	Asp380	NA	-6.54345		
							Arg401	NA	-14.0768		
							His432	NA	-3.84939		
							Gly436	NA	-2.58155		
							Glu439	NA	-10.5082		
							Asp440	NA	-1.12969		
							Arg443	NA	-7.26105		
	Cy-3-glc	target	-2.31294	3.13741	O (39)	Gln260	Lys117	Protein kinase domain	-3.50616	-8.0	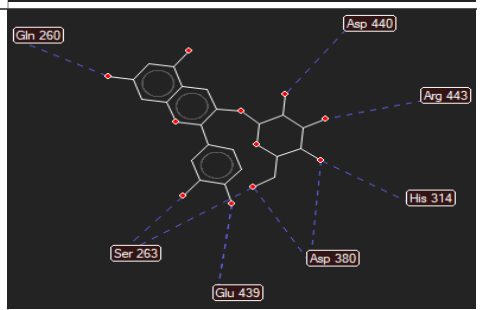
		ligand	-2.5	3.02847	O (25)	Asp440	Glu118	Protein kinase domain	-1.50064		
		target	-1.92062	3.21588	O (23)	Arg443	Gln260	Protein kinase domain	-5.46867		
		target	-0.0576321	3.26945	O (21)	His314	Pro261	Protein kinase domain	-5.88759		
		ligand	-1.53457	3.29309	O (21)	Asp380	Asn262	Protein kinase domain	-8.14388		
		ligand	-2.5	3.09447	O (19)	Ser263	Ser263	Protein kinase domain	-14.9934		
		ligand	-2.5	3.01884	O (19)	Asp380	Leu264	Protein kinase domain	-2.87839		
		ligand	-1.98611	2.88482	O (35)	Glu439	Cys265	Protein kinase domain	-3.12405		
		ligand	-0.283207	3.03285	O (35)	Glu439	His314	NA	-3.98179		
		either	-2.45732	2.99843	O (33)	Ser263	Ile323	NA	-9.05072		
							Asp380	NA	-8.51323		
							Met383	NA	-0.883239		
							Arg401	NA	-15.6476		
							His432	NA	-10.229		
							Gly436	NA	-2.27427		
							Glu439	NA	-7.86641		
							Asp440	NA	-4.99381		
							Arg443	NA	-12.5079		
	Del-3-glc	target	-2.5	2.97173	O (41)	Gln260	Lys117	Protein kinase domain	-2.97891	-8.2	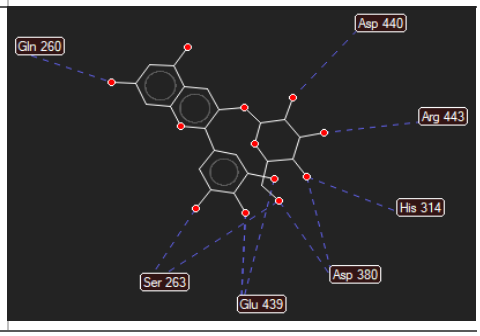
		ligand	-2.5	3.00702	O (25)	Asp440	Glu118	Protein kinase domain	-1.49373		
		target	-2.38209	3.12358	O (23)	Arg443	Gln260	Protein kinase domain	-5.91544		
		target	-0.104725	3.22389	O (21)	His314	Pro261	Protein kinase domain	-5.88643		
		ligand	-1.82715	3.23457	O (21)	Asp380	Asn262	Protein kinase domain	-8.49888		
		ligand	-2.07353	3.18529	O (19)	Ser263	Ser263	Protein kinase domain	-14.045		
		ligand	-2.5	3.01443	O (19)	Asp380	Leu264	Protein kinase domain	-2.84971		
		ligand	-2.5	2.70541	O (37)	Glu439	Cys265	Protein kinase domain	-3.14341		
		ligand	-1.30599	3.04224	O (35)	Glu439	His314	NA	-4.08838		
		ligand	-1.23231	3.05214	O (35)	Glu439	Ile323	NA	-9.183		
		either	-1.8175	3.09881	O (33)	Ser263	Asp380	NA	-8.72677		
							Met383	NA	-0.954067		
							Arg401	NA	-14.9397		
							His432	NA	-11.3597		
							Ser435	NA	-0.491019		
							Gly436	NA	-2.76156		
							Glu439	NA	-11.4591		
							Asp440	NA	-4.96654		
							Arg443	NA	-12.8573		

Supplementary Table 5. *(Continued)*

Target	Ligand	Hydrogen bonding					Steric interactions			BA (kcal/mol)	Ligand map with depiction of H-bonds interactions
		Energy donor	Bonding energy (KJ/mol)	H-bond length (Å)	Ligand contribution with atom type (no.)	Target contribution	AA residue	Localisation	EPair (KJ/mol)*		
IKKα	***Pn-3-glc***	target	-2.5	3.04661	O (39)	Gln260	Lys117	Protein kinase domain	-5.92493	-8.1	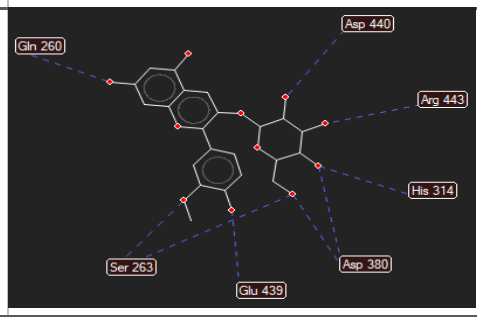
		ligand	-2.5	2.98759	O (25)	Asp440	Glu118	Protein kinase domain	-2.45351		
		target	-2.36162	3.12768	O (23)	Arg443	Gln260	Protein kinase domain	-5.79015		
		target	-0.106498	3.24617	O (21)	His314	Pro261	Protein kinase domain	-5.91525		
		ligand	-1.82107	3.23579	O (21)	Asp380	Asn262	Protein kinase domain	-8.544		
		ligand	-2.32512	3.13498	O (19)	Ser263	Ser263	Protein kinase domain	-17.3831		
		ligand	-2.5	3.00509	O (19)	Asp380	Leu264	Protein kinase domain	-2.84707		
		ligand	-2.30936	2.88309	O (35)	Glu439	Cys265	Protein kinase domain	-3.01275		
		target	-2.5	3.04841	O (33)	Ser263	His314	NA	-3.98636		
							Ile323	NA	-9.20259		
							Asp380	NA	-10.1967		
							Met383	NA	-0.953811		
							Arg401	NA	-15.4146		
							His432	NA	-9.77698		
							Gly436	NA	-2.21965		
							Glu439	NA	-8.20338		
							Asp440	NA	-5.03907		
							Arg443	NA	-13.7896		

*The H-bonding mode and steric interactions evaluated as EPair (the pairwise steric and hydrogen bonding energy between a ligand atom and a receptor atom)

Supplementary Table 6. *Results of the molecular docking analyses for the most relevant targets of metabolites*

Target	Ligand	Hydrogen bonding					Steric interactions			BA (kcal/mol)	Ligand map H-bonds: blue dashed lines Strong steric interactions: red dashed lines (if present) Weak steric interactions: not figured (only the corresponding AAs are presented)
		Energy donor	Bonding energy (KJ/mol)	H-bond length (Å)	Ligand contribution with atom type (no.)	Target contribution	AA residue	Localisation	EPair (KJ/mol)*		
JAK3	***Ferulic acid***	target	-2.5	2.83082	O (6)	Leu905	Leu828	Tyr-protein kinase (catalytic domain): ATP binding site (PROSITE pattern)	-10.2467	-7.2	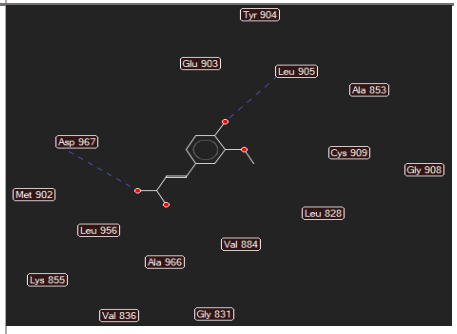
		target	-1.51054	3.08687	O (13)	Asp967	Gly831	Tyr-protein kinase (catalytic domain): ATP binding site (PROSITE pattern)	-0.841605		
							Val836	Tyr-protein kinase (catalytic domain): ATP binding site (PROSITE pattern)	-9.29768		
							Ala853	Tyr-protein kinase (catalytic domain): ATP binding site (PROSITE pattern)	-2.96766		
							Lys855	Tyr-protein kinase (catalytic domain): ATP binding site (PROSITE pattern)	-3.31742		
							Val884	Tyr-protein kinase (catalytic domain)	-1.50362		
							Met902	Tyr-protein kinase (catalytic domain)	-4.12008		
							Glu903	Tyr-protein kinase (catalytic domain)	-2.26633		
							Tyr904	Tyr-protein kinase (catalytic domain)	-5.50754		
							Leu905	Tyr-protein kinase (catalytic domain)	-12.1934		
							Gly908	Tyr-protein kinase (catalytic domain)	-1.32869		
							Cys909	Tyr-protein kinase (catalytic domain)	-0.389102		
							Leu956	Tyr-protein kinase (catalytic domain): active site (PROSITE pattern)	-11.8097		
							Ala966	Tyr-protein kinase (catalytic domain)	-4.46084		
							Asp967	Tyr-protein kinase (catalytic domain)	-8.06463		
MLCK	***Ferulic acid***	target	-0.016612	3.58347	O (14)	Gly114	Leu112	Protein kinase domain: ATP binding site	-11.3077	-7.0	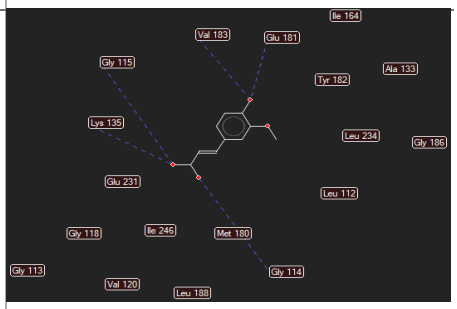
		target	-0.61673	3.25957	O (13)	Gly115	Gly113	Protein kinase domain: ATP binding site	-4.93206		
		target	-0.731165	2.94101	O (13)	Lys135	Gly114	Protein kinase domain: ATP binding site	-2.66587		
		ligand	-2.5	3.02163	O (6)	Glu181	Gly115	Protein kinase domain: ATP binding site	-3.60319		
		target	-1.83815	3.17565	O (6)	Val183	Gly118	Protein kinase domain: ATP binding site	-0.461835		
							Val120	Protein kinase domain: ATP binding site	-7.92989		
							Ala133	Protein kinase domain: ATP binding site	-2.2211		
							Lys135	Protein kinase domain: ATP binding site	-5.26166		
							Ile164	Protein kinase domain	-3.94931		
							Met180	Protein kinase domain	-2.84847		
							Glu181	Protein kinase domain	-4.69027		
							Tyr182	Protein kinase domain	-5.08338		
							Val183	Protein kinase domain	-8.57903		
							Gly186	Protein kinase domain	-0.39823		
							Leu188	Protein kinase domain	-2.85422		
							Glu231	Protein kinase domain: Ser/Thr-protein kinase (active site	-0.516769		
							Leu234	Protein kinase domain: Ser/Thr-protein kinase (active site	-5.34382		
							Ile246	Protein kinase domain	-14.2058		
p38β	***Ferulic acid***	target	-1.74543	3.15179	O (6)	Lys53	Tyr35	Protein kinase domain: ATP binding site	-3.47938	-7.4	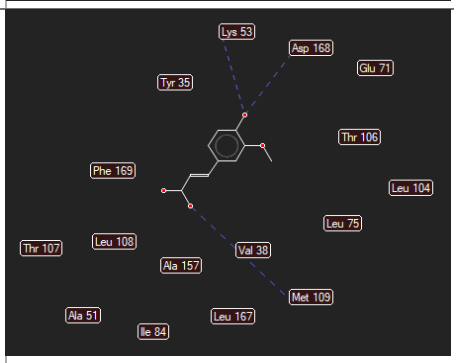
		target	-2.5	3.03162	O (14)	Met109	Val38	Protein kinase domain: ATP binding site	-5.92623		
		ligand	-2.5	2.99261	O (6)	Asp168	Ala51	Protein kinase domain: ATP binding site	-2.40556		
							Lys53	Protein kinase domain: ATP binding site	-7.80963		
							Glu71	Protein kinase domain: Mitogen-activated protein (MAP) kinase, conserved site	-1.44468		
							Leu75	Protein kinase domain: Mitogen-activated protein (MAP) kinase, conserved site	-0.657765		
							Ile84	Protein kinase domain: Mitogen-activated protein (MAP) kinase, conserved site	-6.53897		
							Leu104	Protein kinase domain: Mitogen-activated protein (MAP) kinase, conserved site	-0.317307		
							Thr106	Protein kinase domain: Mitogen-activated protein (MAP) kinase, conserved site	-4.65628		
							Thr107	Protein kinase domain: Mitogen-activated protein (MAP) kinase, conserved site	-2.69625		
							Leu108	Protein kinase domain: Mitogen-activated protein (MAP) kinase, conserved site	-5.28779		
							Met109	Protein kinase domain: Mitogen-activated protein (MAP) kinase, conserved site	-7.86754		
							Ala157	Protein kinase domain: Mitogen-activated protein (MAP) kinase, conserved site	-2.32137		
							Leu167	Protein kinase domain	-12.1546		
							Asp168	Protein kinase domain	-7.62261		
							Phe169	Protein kinase domain	-15.1884		
	Hippuric acid	target	-2.5	2.92987	O (13)	Ser32	Val30	Protein kinase domain: ATP binding site	-0.738123	-7.1	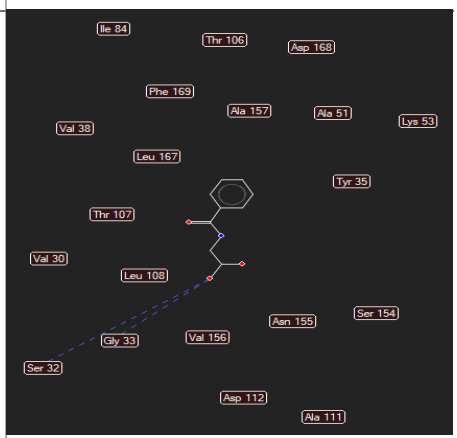
		target	-0.436909	3.05264	O (13)	Gly33	Ser32	Protein kinase domain: ATP binding site	-5.85536		
							Gly33	Protein kinase domain: ATP binding site	-2.7515		
							Tyr35	Protein kinase domain: ATP binding site	-4.43439		
							Val38	Protein kinase domain: ATP binding site	-5.04828		
							Ala51	Protein kinase domain: ATP binding site	-1.8803		
							Lys53	Protein kinase domain: ATP binding site	-1.15227		
							Ile84	Protein kinase domain	-3.79686		
							Thr106	Protein kinase domain: Mitogen-activated protein (MAP) kinase, conserved site	-2.96228		
							Thr107	Protein kinase domain: Mitogen-activated protein (MAP) kinase, conserved site	-0.586252		
							Leu108	Protein kinase domain: Mitogen-activated protein (MAP) kinase, conserved site	-0.391025		
							Ala111	Protein kinase domain: Mitogen-activated protein (MAP) kinase, conserved site	-2.06044		
							Asp112	Protein kinase domain: Mitogen-activated protein (MAP) kinase, conserved site	-5.37423		
							Ser154	Protein kinase domain: Mitogen-activated protein (MAP) kinase, conserved site	-2.2229		
							Asn155	Protein kinase domain: Mitogen-activated protein (MAP) kinase, conserved site	-0.322758		
							Val156	Protein kinase domain: Mitogen-activated protein (MAP) kinase, conserved site	-1.05801		
							Ala157	Protein kinase domain: Mitogen-activated protein (MAP) kinase, conserved site	-3.8809		
							Leu167	Protein kinase domain	-13.4209		
							Asp168	Protein kinase domain	-1.70321		
							Phe169	Protein kinase domain	-16.6541		
	PCA	target	-1.74708	3.10962	O (6)	Lys53	Tyr35	Protein kinase domain: ATP binding site	-2.90708	-6.3	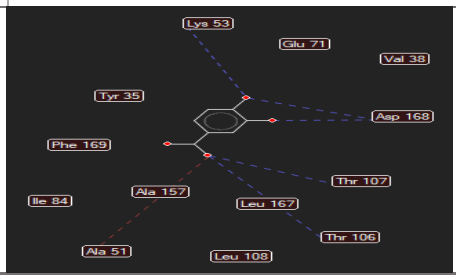
		either	-0.46772	2.99203	O (12)	Thr107	Val38	Protein kinase domain: ATP binding site	-5.00382		
		ligand	-1.98139	3.01518	O (12)	Thr107	Ala51	Protein kinase domain: ATP binding site	-1.81706		
		ligand	-2.3468	3.13064	O (6)	Asp168	Lys53	Protein kinase domain: ATP binding site	-6.1784		
		ligand	-2.5	3.07181	O (8)	Asp168	Glu71	Protein kinase domain	-0.30562		
							Ile84	Protein kinase domain	-6.24366		
							Thr106	Protein kinase domain: Mitogen-activated protein (MAP) kinase, conserved site	-4.20513		
							Thr107	Protein kinase domain: Mitogen-activated protein (MAP) kinase, conserved site	-3.60769		
							Leu108	Protein kinase domain: Mitogen-activated protein (MAP) kinase, conserved site	-0.877834		
							Ala157	Protein kinase domain: Mitogen-activated protein (MAP) kinase, conserved site	-0.582068		
							Leu167	Protein kinase domain	-12.8966		
							Asp168	Protein kinase domain	-9.77978		
							Phe169	Protein kinase domain	-15.1579		

Supplementary Table 6. *(Continued)*

Target	Ligand	Hydrogen bonding					Steric interactions			BA (kcal/mol)	Ligand map H-bonds: blue dashed lines Strong steric interactions: red dashed lines (if present) Weak steric interactions: not figured (only the corresponding AAs are presented)
		Energy donor	Bonding energy (KJ/mol)	H-bond length (Å)	Ligand contribution with atom type (no.)	Target contribution	AA residue	Localisation	EPair (KJ/mol)*		
b-Raf	*PCA*	target	-2.5	2.98147	O (8)	Leu577	His574	Ser-Thr/Tyr-protein kinase, catalytic domain: active site (PROSITE pattern)	-0.914093	-7.1	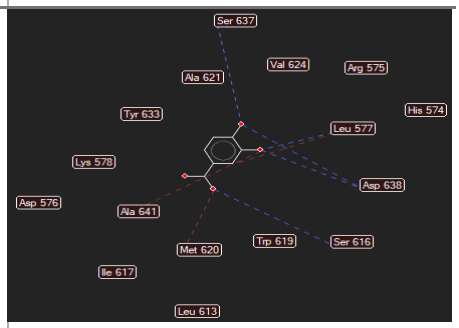
		ligand	-1.13197	3.18683	O (12)	Ser616	Arg575	Ser-Thr/Tyr-protein kinase, catalytic domain: active site (PROSITE pattern)	-11.4905		
		either	-2.5	2.96425	O (6)	Ser637	Asp576	Ser-Thr/Tyr-protein kinase, catalytic domain: active site (PROSITE pattern)	-9.8462		
		ligand	-1.60628	3.27874	O (6)	Asp638	Leu577	Ser-Thr/Tyr-protein kinase, catalytic domain: active site (PROSITE pattern)	-10.5461		
		ligand	-2.5	2.88301	O (8)	Asp638	Lys578	Ser-Thr/Tyr-protein kinase, catalytic domain: active site (PROSITE pattern)	-2.45119		
							Leu613	Ser-Thr/Tyr-protein kinase, catalytic domain	-6.29863		
							Ser616	Ser-Thr/Tyr-protein kinase, catalytic domain	-3.1669		
							Ile617	Ser-Thr/Tyr-protein kinase, catalytic domain	-0.776705		
							Trp619	Ser-Thr/Tyr-protein kinase, catalytic domain	-12.2616		
							Met620	Ser-Thr/Tyr-protein kinase, catalytic domain	-9.47326		
							Ala621	Ser-Thr/Tyr-protein kinase, catalytic domain	-0.964415		
							Val624	Ser-Thr/Tyr-protein kinase, catalytic domain	-3.50425		
							Tyr633	Ser-Thr/Tyr-protein kinase, catalytic domain	-5.20433		
							Ser637	Ser-Thr/Tyr-protein kinase, catalytic domain	-8.21781		
							Asp638	Ser-Thr/Tyr-protein kinase, catalytic domain	-10.8485		
							Ala641	Ser-Thr/Tyr-protein kinase, catalytic domain	-3.81597		

Supplementary Figure 1. *Heat map representation of BA for all targets and ligand. Each column presents different examined ligand and each line different target. Lighter shades of blue present lower BA, i.e. stronger binders.*

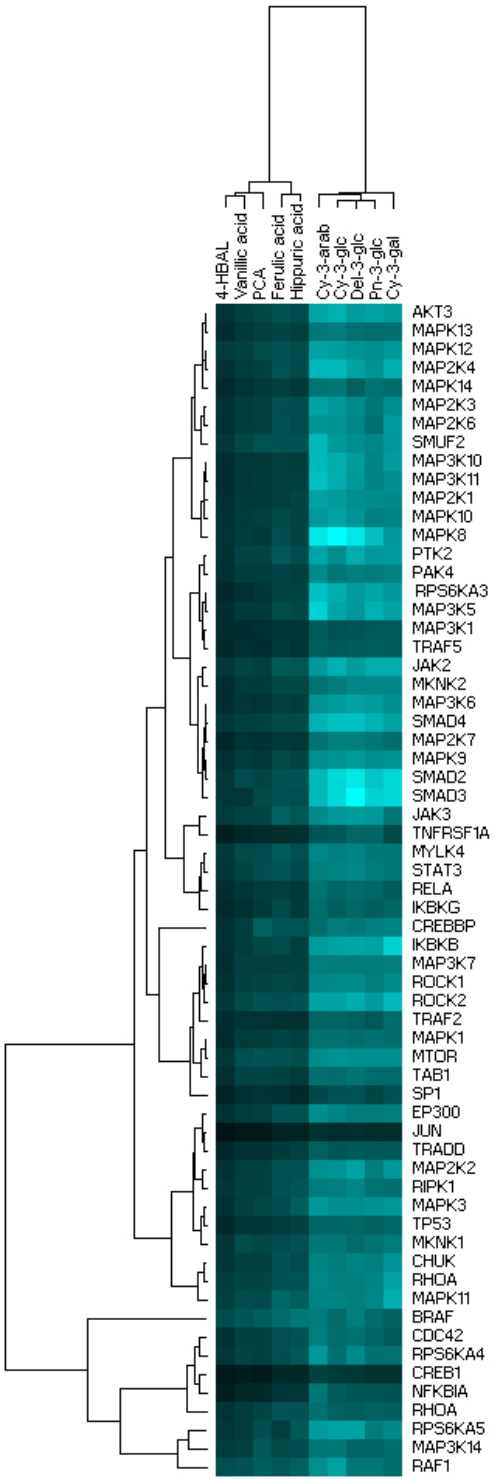

BIOGRAPHY

Irena Krga was born on November 21, 1989 in Belgrade, Serbia, where she finished elementary school and IX Belgrade gymnasium “Mihailo Petrovic Alas”. In 2012, she graduated from the Faculty of Biology at the University of Belgrade, with a grade point average (GPA) 9.63/10. The following year she finished master's programme in ecology at the same faculty, with a GPA 10/10. Her master’s thesis was entitled: "Determination of shikimate content in selected plant species, as a response to stress caused by glyphosate herbicide". During the master’s studies, she volunteered at the Institute for Plant Protection and Environment in Belgrade. In November 2014, she enrolled in the international doctoral program in nutritional sciences between the Faculty of Biology, the University of Belgrade and the Faculty of Medicine, the University of Clermont Auvergne in Clermont-Ferrand, France. She performed the experimental part of her thesis at the Centre of Research Excellence in Nutrition and Metabolism in Belgrade and the National Institute of Agricultural Research in Theix, France. Since April 02, 2018, she is employed at the Centre of Research Excellence in Nutrition and Metabolism, Institute for Medical Research in Belgrade, as the research trainee. She is an active member of European Cooperation in Science and Technology (COST) action FA1403, entitled: “Interindividual variation in response to consumption of plant food bioactives and determinants involved (POSITIVe)”. Within the COST’s short scientific mission programme, she visited the Proteinchemistry, Proteomics & Epigenetic Signaling research institute in Antwerp, Belgium. During her studies, she was awarded a French government grant for the co-tutoring doctorate as well as the scholarship of Young Talents Fund of the Ministry of Youth and Sports of the Republic of Serbia. She is the author of five papers of which four are published in international journals and one in the national journal. She is also the author of 8 publications from international and national scientific conferences.

Published and presented results of this PhD project

Publications:

Research articles

- I. Krga, L.E. Monfoulet, A. Konic-Ristic, S. Mercier, M. Glibetic, C. Morand, D. Milenkovic, Anthocyanins and their gut metabolites reduce the adhesion of monocyte to TNFα-activated endothelial cells at physiologically relevant concentrations, *Arch. Biochem. Biophys*. 599 (2016) 51-59 (IF_{2016}: 3.165).
- I. Krga, N. Vidovic, D. Milenkovic, A. Konic-Ristic, F. Stojanovic, C. Morand, M. Glibetic, Effects of anthocyanins and their gut metabolites on adenosine diphosphate-induced platelet activation and their aggregation with monocytes and neutrophils, *Arch. Biochem. Biophys*. 645 (2018) 34-41(IF_{2016}: 3.165).

Review articles

- I. Krga, D. Milenkovic, C. Morand, L.E. Monfoulet, An update on the role of nutrigenomic modulations in mediating the cardiovascular protective effect of fruit polyphenols, *Food Funct*. 7 (2016) 3656–3676.
- D. Milenkovic, I. Krga, H.H. Aung, C. Leroux, Molecular Nutrition and Epigenetics, *Reference Module in Food Science*, 2018.

Presentations:

Oral presentations

- I. Krga, S. Mercier, R. Tamaian, C. Boby, L-E. Monfoulet, C. Morand, D. Milenkovic. Anthocyanins and their gut metabolites attenuate monocyte adhesion and transendothelial migration through nutrigenomic mechanisms regulating endothelial cell permeability. 8th International Conference on Polyphenols and Health, 3rd-6th October 2017, Quebec City, Canada.
- I. Krga. Effect of anthocyanins and their metabolites on endothelial and platelet function. Proteinchemistry, Proteomics & Epigenetic Signaling (PPES), University of Antwerp, 17th March 2017, Antwerp, Belgium.
- I. Krga. Effect of physiologically relevant concentrations of anthocyanins and their gut metabolites on adhesion of monocyte to TNFα-activated endothelial cells. XIX Days of Doctoral school of Biological science, health, agriculture and environment, 2nd- 3rd June 2016, Clermont-Ferrand, France, p.30.

- I. Krga, S. Mercier, L-E. Monfoulet, C. Morand, A. Konic-Ristic, D. Milenkovic. Effect of physiologically-relevant concentrations of anthocyanins and their gut metabolites on monocyte adhesion to endothelial cells. 2nd Interregional annual conference on Nutrition and metabolism, Rhône-Alpes-Auvergne, 4th-5th November 2015, Saint Galmier, France, p.33.

Poster presentations

- I. Krga, N. Kardum, F. Stojanovic, A. Konic-Ristic, D. Milenkovic M. Glibetic. Effects of physiologically-relevant concentrations of anthocyanins and their gut metabolites on adenosine diphosphate-induced platelet activation and aggregation. 8th International Conference on Polyphenols and Health, 3rd-6th October 2017, Quebec City, Canada.
- I. Krga, R. Tamaian, C. Boby, S. Mercier, C. Morand, D. Milenkovic. Anthocyanins and their gut metabolites reduce monocyte adhesion and migration across TNFα-activated endothelial cells through nutrigenomic mechanisms regulating endothelial integrity. 3rd Scientific Workshop: "Omics breakthroughs in the health effects of plant food bioactive", 20th-21st September 2017, Thessaloniki, Greece, *best poster award*, p.20.
- I. Krga, A. Konic-Ristic, N. Kardum, D. Milenkovic, M. Glibetic. Effects of physiologically-relevant concentrations of anthocyanins and their metabolites on adenosine diphosphate-induced platelet activation and aggregation. 1st Congress of Molecular Biologists of Serbia (CoMBoS) with international participation. 20th-22nd September 2017, Belgrade, Serbia, p.144.
- I. Krga, C. Morand, C. Boby, L.E. Montfoulet, M. Glibetic, D. Milenkovic. Mixtures of anthocyanins and their gut metabolites attenuate monocyte adhesion and transendothelial migration through nutrigenomic mechanisms regulating endothelial cell permeability. 1st Congress of Molecular Biologists of Serbia (CoMBoS) with international participation. 20th-22nd September 2017. Belgrade, Serbia, p.50.
- I. Krga, L.E. Monfoulet, A. Konic-Ristic, S. Mercier, M. Glibetic, C. Morand, D. Milenkovic. Effect of anthocyanins and their gut metabolites on monocyte adhesion to endothelial cells at physiologically-relevant concentrations. 7th International Conference on Polyphenols and Health, 27th-30th October 2015, Tours, France, p.220.

Прилог 1.

Изјава о ауторству

Потписани-а Ирена Крга

број индекса 3010/2014

Изјављујем

да је докторска дисертација под насловом

„Утицај антоцијана и њихових метаболита на функцију ендотелних ћелија и тромбоцита човека *in vitro*”

- резултат сопственог истраживачког рада,
- да предложена дисертација у целини ни у деловима није била предложена за добијање било које дипломе према студијским програмима других високошколских установа,
- да су резултати коректно наведени и
- да нисам кршио/ла ауторска права и користио интелектуалну својину других лица.

Потпис докторанда

У Београду, 24.03.2018

_____

Прилог 2.

Изјава о истоветности штампане и електронске верзије докторског рада

Име и презиме аутора Ирена Крга

Број индекса Б3010/2014

Студијски програм Биологија

Наслов рада „Утицај антоцијана и њихових метаболита на функцију ендотелних ћелија и тромбоцита човека *in vitro*"

Ментор др Марија Глибетић, научни саветник, Универзитет у Београду-Институт за медицинска истраживања
др Драган Миленковић, научни саветник, Национални институт за агрономска истраживања, Клермон-Феран/Те, Француска

Потписани/а Ирена Крга

Изјављујем да је штампана верзија мог докторског рада истоветна електронској верзији коју сам предао/ла за објављивање на порталу **Дигиталног репозиторијума Универзитета у Београду.**

Дозвољавам да се објаве моји лични подаци везани за добијање академског звања доктора наука, као што су име и презиме, година и место рођења и датум одбране рада.

Ови лични подаци могу се објавити на мрежним страницама дигиталне библиотеке, у електронском каталогу и у публикацијама Универзитета у Београду.

Потпис докторанда

У Београду, 24.03.2018

Прилог 3.

Изјава о коришћењу

Овлашћујем Универзитетску библиотеку „Светозар Марковић“ да у Дигитални репозиторијум Универзитета у Београду унесе моју докторску дисертацију под насловом:

„Утицај антоцијана и њихових метаболита на функцију ендотелних ћелија и тромбоцита човека *in vitro*”

која је моје ауторско дело.

Дисертацију са свим прилозима предао/ла сам у електронском формату погодном за трајно архивирање.

Моју докторску дисертацију похрањену у Дигитални репозиторијум Универзитета у Београду могу да користе сви који поштују одредбе садржане у одабраном типу лиценце Креативне заједнице (Creative Commons) за коју сам се одлучио/ла.

1. Ауторство

2. Ауторство – некомерцијално (CC BY-NC)

(3.) Ауторство – некомерцијално – без прерада (CC BY-NC-ND)

4. Ауторство – некомерцијално – делити под истим условима

5. Ауторство – без прераде

6. Ауторство – делити под истим условима

(Молимо да заокружите само једну од шест понуђених лиценци, кратак опис лиценци дат је на полеђини листа).

Потпис докторанда

У Београду, 24.03.2018

1. Ауторство - Дозвољавате умножавање, дистрибуцију и јавно саопштавање дела, и прераде, ако се наведе име аутора на начин одређен од стране аутора или даваоца лиценце, чак и у комерцијалне сврхе. Ово је најслободнија од свих лиценци.

2. Ауторство – некомерцијално. Дозвољавате умножавање, дистрибуцију и јавно саопштавање дела, и прераде, ако се наведе име аутора на начин одређен од стране аутора или даваоца лиценце. Ова лиценца не дозвољава комерцијалну употребу дела.

3. Ауторство - некомерцијално – без прераде. Дозвољавате умножавање, дистрибуцију и јавно саопштавање дела, без промена, преобликовања или употребе дела у свом делу, ако се наведе име аутора на начин одређен од стране аутора или даваоца лиценце. Ова лиценца не дозвољава комерцијалну употребу дела. У односу на све остале лиценце, овом лиценцом се ограничава највећи обим права коришћења дела.

4. Ауторство - некомерцијално – делити под истим условима. Дозвољавате умножавање, дистрибуцију и јавно саопштавање дела, и прераде, ако се наведе име аутора на начин одређен од стране аутора или даваоца лиценце и ако се прерада дистрибуира под истом или сличном лиценцом. Ова лиценца не дозвољава комерцијалну употребу дела и прерада.

5. Ауторство – без прераде. Дозвољавате умножавање, дистрибуцију и јавно саопштавање дела, без промена, преобликовања или употребе дела у свом делу, ако се наведе име аутора на начин одређен од стране аутора или даваоца лиценце. Ова лиценца дозвољава комерцијалну употребу дела.

6. Ауторство - делити под истим условима. Дозвољавате умножавање, дистрибуцију и јавно саопштавање дела, и прераде, ако се наведе име аутора на начин одређен од стране аутора или даваоца лиценце и ако се прерада дистрибуира под истом или сличном лиценцом. Ова лиценца дозвољава комерцијалну употребу дела и прерада. Слична је софтверским лиценцама, односно лиценцама отвореног кода.